

139149

GEODYN SYSTEM
VOLUME 1 (Wolf Research and
Corp.) 395 p HC \$10.25

N75-11415

CSCL 08E

Unclass

G3/43

03461

VOLUME I
GEODYN SYSTEM DESCRIPTION

Contract No.: NAS 5-11735 MOD 65
PCN 550W-72416

Prepared By:

M.M. Chin
C.C. Goad
T.V. Martin

Wolf Research and Development Corporation
Riverdale, Maryland

For
Goddard Space Flight Center
Greenbelt, Maryland

30 September 1972



August 11, 1973

DIRECTIONS FOR GEODYN VOL. I CHANGES

<u>NEW PAGES</u>	<u>REPLACE OLD PAGES</u>	<u>INSERT AFTER PAGE</u>	<u>DESCRIPTION</u>
Table of Contents	Table of Contents		
Table of Contents (Cont.)	Table of Contents (Cont. 3 and 4)		
4.0-2	4.0-2		The equation of $F_4(s)$ has been corrected.
5.4-3	5.4-3		Added new section number.
5.4-6 to } 5.4-10 }		5.4-5	Inserted a new section.
7.5-3	7.5-3		Added a "-" on equation (4)
7.5-4	7.5-4		Corrected the explanation of n_s .
8.1-2	8.1-2		Line 7: "differential" added.
8.2-8	8.2-8		Line 3: "DENSTY" changed to "D71, D650"
8.6-2	8.6-2		Changed the sign on equation (2).
8.6-3	8.6-3		Line 3: "DENSTY" changed to "D71, D650"

REPRODUCIBILITY OF THE ORIGINAL PAGE IS POOR

August 11, 1973

<u>NEW PAGES</u>	<u>REPLACE OLD PAGES</u>	<u>INSERT AFTER PAGE</u>	<u>DESCRIPTION</u>
8.7-1	8.7-1		Added a new section.
8.7-2 to } 8.7-33 }	8.7-2 to } 8.7-33 }	(Note: keep 8.7-16, 8.7-18 to 8.7-27)	Changed "DENSTY" to "D71" and/or changed section number.
8.7-34 to } 8.7-57 }		8.7-33	Added new section.
10.1-3	10.1-3		Equation (3) and (4) have been corrected.
10.1-4	10.1-4		Equation (5) and (6) have been corrected.
10.1-6	10.1-6		Equation (9), (11), and (12) have been corrected.
10.2-1	10.2-1		Equation (1) has been changed.
11.4-6	11.4-6		Function F has been corrected.
12.0-5 } 12.0-6 }	12.0-5		Added new references on section 8.
12.0-7	12.0-5		Page number changed.
A-1	A-1		"DENSTY" changed to "D71, D650"

REPRODUCIBILITY OF THE
ORIGINAL PAGE IS POOR

TABLE OF CONTENTS

	<u>Page</u>
1.0 THE GEODYN PROGRAM	1.0-1
2.0 THE ORBIT AND GEODETIC PARAMETER ESTIMATION PROBLEM	2.0-1
2.1 THE ORBIT PREDICTION PROBLEM	2.1-1
2.2 THE PARAMETER ESTIMATION PROBLEM	2.2-1
3.0 THE MOTION OF THE EARTH AND RELATED COORDINATE SYSTEMS	3.0-1
3.1 THE TRUE OF DATE COORDINATE SYSTEM	3.2-1
3.2 THE INERTIAL COORDINATE SYSTEM	3.2-1
3.3 THE EARTH-FIXED COORDINATE SYSTEM	3.4-1
3.4 TRANSFORMATION BETWEEN EARTH-FIXED AND TRUE OF DATE COORDINATES	3.4-1
3.5 COMPUTATION OF θ_g	3.5-1
3.6 PRECESSION AND NUTATION	3.6-1
3.6.1 Precession	3.6-4
3.6.2 Nutation	3.6-8
4.0 LUNI-SOLAR-PLANETARY EPHEMERIDES	4.0-1
5.0 THE OBSERVER	5.0-1
5.1 GEODETIC COORDINATES	5.1-1
5.2 TOPOCENTRIC COORDINATE SYSTEMS	5.2-1
5.3 TIME REFERENCE SYSTEMS	5.3-1
5.3.1 Time System Transformations	5.3-2
5.4 POLAR MOTION	5.4-1
5.4.1 EFFECT ON THE POSITION OF STATION	5.4-3
5.4.2 PARTIAL DERIVATIVES	5.4-6

TABLE OF CONTENTS (Cont.)

	<u>Page</u>
8.0 FORCE MODEL AND VARIATIONAL EQUATIONS	8.1-1
8.1 EQUATIONS OF MOTION	8.1-1
8.2 THE VARIATIONAL EQUATIONS	8.2-1
8.3 THE EARTH'S POTENTIAL	8.3-1
8.3.1 Spherical Harmonic Expansion	8.3-2
8.3.2 Surface Density Layers	8.3-17
8.3.2.1 Mathematical Representation of Surface Densities	8.3-17
8.3.2.2 Surface Height Computation	8.3-21
8.3.2.3 Layer Model Quadrature Errors	8.3-21
8.3.2.4 Constraints	8.3-22
8.4 SOLAR AND LUNAR GRAVITATIONAL PERTURBATIONS	8.3-1
8.5 SOLAR RADIATION PRESSURE	8.5-1
8.6 ATMOSPHERIC DRAG	8.6-1
8.7 ATMOSPHERIC DENSITY	8.7-1
8.7.1 Jacchia 1971 Density Model	8.7-1
8.7.1.1 The Assumption of the Model	8.7-2
8.7.1.2 Variations in the Thermosphere and Exosphere	8.7-4
8.7.1.3 Polynomial Fit of Density Tables	8.7-15
8.7.1.4 The Density Computation	8.7-28
8.7.1.5 Density Partial Derivatives	8.7-29
8.7.2 Jacchia 1965 Density Model	8.7-34
8.7.2.1 The Assumptions of the Model	8.7-35
8.7.2.2 The Exospheric Temperature Computations	8.7-39

REPRODUCIBILITY OF THE
ORIGINAL PAGE IS POOR

TABLE OF CONTENTS (Cont.)

	<u>Page</u>
8.7.2.3 The Density Computation	8.7-48
8.7.2.4 Density Partial Derivatives	8.7-51
8.8 TIDAL POTENTIAL	8.8-1
9.0 INTEGRATION AND INTERPOLATION	9.1-1
9.1 INTEGRATION	9.1-1
9.2 THE INTEGRATOR STARTING SCHEME	9.3-1
9.3 INTERPOLATION	9.3-1
10.0 THE STATISTICAL ESTIMATION PROCEDURE	10.0-1
10.1 BAYESIAN LEAST SQUARES ESTIMATION	10.1-1
10.2 THE PARTITIONED SOLUTION	10.2-1
10.3 DATA EDITING	10.3-1
10.4 ELECTRONIC BIAS	10.4-1
11.0 GENERAL INPUT/OUTPUT DISCUSSION	11.1-1
11.1 INPUT	11.1-1
11.2 OUTPUT	11.2-1
11.3 COMPUTATIONS FOR RESIDUAL SUMMARY	11.3-1
11.4 KEPLER ELEMENTS	11.4-1
11.4.1 Node Rate and Perigee Rate	11.4-14
11.4.2 Period Decrement and Drag Rate	11.4-16
12.0 REFERENCES	12.0-1
APPENDIX A INDEX OF SUBROUTINE REFERENCES FOR GEODYN PROGRAM	A-1

REPRODUCIBILITY OF THE
ORIGINAL PAGE IS POOR

GLOSSARY OF SYMBOLS

<u>Symbol</u>	<u>Description</u>	<u>Page First Used</u>
A	Matrix partition of $U_{2C} + D_r$ associated with position partials.	9.1-3
A	Matrix partition of $(B^T WB + V_A^{-1})$ associated with \underline{a}	10.2-4
\bar{A}_D	Acceleration of satellite due to drag	3.1-2
A_k	Matrix partition of $(B^T WB + V_A^{-1})$ accounting for effects between \underline{a} and \underline{k}	10.2-4
\bar{A}_R	Acceleration of satellite due to solar radiation pressure	8.1-2
A_r	Matrix partition of A associated with the r^{th} arc	10.2-6
A_{rk}	Matrix partition of A_k associated with the r^{th} arc	10.2-7
A_z	Azimuth of satellite (measurement type)	6.2-1
a	Semi-major axis of reference ellipsoid	5.1-2
a	Semi-major axis of orbit	11.4-1
\bar{a}	Acceleration of satellite produced by the surface density potential	8.3-20

GLOSSARY OF SYMBOLS (Cont.)

<u>Symbol</u>	<u>Description</u>	<u>Page First Used</u>
\underline{a}	Vector of parameters associated with individual arcs, partition of \underline{x}	10.2-2
\bar{a}_d	Acceleration of satellite due to a third body potential	8.5-1
a_e	Earth's mean equatorial radius	6.1-4
\bar{a}_{SD}	Surface density acceleration	8.3-28
\underline{a}_r	Partition of \underline{a} associated with the r^{th} arc	10.2-6
a_{ij}	Polynomial coefficients used to fit the density table	8.7-31
B	Matrix partition of $U_{2C} + D_r$ associated with velocity partials	9.1-3
B	Matrix of partial derivatives of computed measurements with respect to the parameters being determined	10.1-4
B_e	Matrix of partial derivatives of the measurement with respect to the biases	10.4-2
b	A constant measurement bias	6.0-2

REPRODUCIBILITY OF THE
ORIGINAL PAGE IS POOR

GLOSSARY OF SYMBOLS (Cont.)

<u>Symbol</u>	<u>Description</u>	<u>Page First Page</u>
C	Molecular mass of Helium divided by Avogadro's number	8.7-14
b_{ej}	Electronic bias	11.3-1
b_{ij}	A set of appropriate coefficients for the Helium number of density tables	8.7-31
C_D	Satellite drag factor	8.2-2
C_R	Satellite emissivity factor	8.2-2
C_a	Matrix partition of $B^T W \underline{dm}$ + $V_A^{-1} (\underline{x}^{(n)} - \underline{x}_A)$ associated with \underline{a}	10.2-4
C_i	Computed measurement value corresponding to O_i	2.2-1
C_k	Matrix partition of $(B^T W \underline{dm} + V_A^{-1} (\underline{x}^{(n)} - \underline{x}_A))$ associated with \underline{k}	10.2-4
C_{nm}	Gravitational harmonic coefficient of degree n, order m	6.3-2
C'_{nm}	The cosine coefficient of surface density constraint equations	8.3-25

GLOSSARY OF SYMBOLS (Cont.)

<u>Symbol</u>	<u>Description</u>	<u>Page First Used</u>
C_r	Matrix partition of C_a associated with the i^{th} arc	10.2-7
$C_{t+\Delta t}$	The computed observation at time $t+\Delta t$	6.0-1
c	Velocity of light	7.6-1
c_i	Interpolation coefficients	9.3-1
c_i	Interpolation coefficients	9.3-2
D	Mean elongation of the Moon from the Sun	3.6-11
D_r	Matrix containing $\frac{\partial \bar{A}_D}{\partial \bar{x}_t}$	8.2-6
dO_i	Error of observation associated with O_i	2.2-1
\underline{da}	Partition of $dx^{(n+1)}$ associated with \underline{a} (correction vector for arc parameters)	10.2-4
\underline{da}_r	Partition of \underline{da} associated with the r^{th} arc (correction vector for the r^{th} arc parameters).	10.2-8
\underline{da}'_r	Correction vector to r^{th} arc parameters not including common parameter solution effects	11.4-1

GLOSSARY OF SYMBOLS (cont.)

<u>Symbols</u>	<u>Description</u>	<u>Page First Used</u>
dE	Element of surface area	8.3-18
<u>dk</u>	Partition of $\underline{dx}^{(n+1)}$ associated with the common parameters \underline{k}	10.2-4
<u>dm</u>	Vector of residuals (O-C) from the n^{th} approximation to $\hat{\underline{x}}$ (same as $\underline{d}_z^{(n)}$)	10.2-1
<u>dx</u> ⁽ⁿ⁺¹⁾	Vector of corrections to the parameters \underline{x}	10.1-6
<u>dz</u> ⁽ⁿ⁾	Vector of residuals (O-C) from the n^{th} approximation (same as <u>dm</u>)	10.1-6
d_1	The transponder delay in the relay satellite	6.4-3
d_2	The transponder delay in the tracked satellite	6.4-3
E	Eccentric anomaly of the orbit	11.4-1
\hat{E}	East baseline vector in the topocentric horizon coordinate system	5.2-1
E ()	Expected value	11.3-5
E_M	Input multiplier for editing criterion	10.3-2

REPRODUCIBILITY OF THE
ORIGINAL PAGE IS POOR

GLOSSARY OF SYMBOLS (Cont.)

<u>Symbols</u>	<u>Description</u>	<u>Page First Used</u>
E_R	Weighted RMS of previous outer iteration Input for first outer iteration	10.3-2
E_ℓ	Elevation of the satellite (measurement type)	6.2-1
e	Eccentricity of the reference ellipsoid	5.1-2
e	Eccentricity of the orbit	11.4-1
\bar{e}	Constant of integration - a vector of a magnitude equal to the eccentricity of the orbit and pointing toward perihelion	11.4-6
F	Mean angular distance of the Moon from Sun	3.6-11
F	Matrix containing $\frac{\partial \ddot{\mathbf{r}}}{\partial \mathbf{E}}$ (same as $\ddot{\mathbf{Y}}$)	8.2-6
F_B	Base frequency for Doppler measurements	7.6-1
F_M	Measured frequency for Doppler observa- tions	7.6-1
$F_{10.7}$	Mean of the 10.7 cm. solar flux values for a given day	8.7-6
$F_{10.7}$	Average 10.7 cm. flux strength over 3 solar rotations	8.7-6

GLOSSARY OF SYMBOLS (Cont.)

<u>Symbols</u>	<u>Description</u>	<u>Page First Used</u>
f	Flattening of the Earth	5.1-1
f	Transmitter frequency	6.6-3
f	Matrix containing the direct partial derivatives of \bar{x}_t with respect to $\bar{\beta}$	8.2-6
f	Back value of acceleration	9.3-2
f	The true anomaly of the orbit	11.4-1
f.	The geometric relationship defined by the observation type at time t.	6.0-1
G	The universal gravitational constant	6.3-2
g	Mean anomaly of the Moon	3.6-11
g'	Mean anomaly of the Sun	3.6-11
H	Hour angle of the Sun	8.7-7
H _{alt}	Altimeter height (measurement type)	6.1-3
h	Spheroid height	5.1-2
h	Integrator step size	9.3-2
h _s	Local hour angle measured in the westward direction from the station to the satellite	7.4-2

GLOSSARY OF SYMBOLS (Cont.)

<u>Symbols</u>	<u>Directions</u>	<u>Page First Used</u>
I	Identity matrix	9.1-3
i	Inclination of the orbit	11.4-1
J	Julian Ephemeris Date of desired nututation calculation	3.6-10
J_0	Julian Ephemeris Date corresponding to 1900 January 0.5 Ephemeris Time	3.5-10
K	Partition of $(B^T WB + V_A^{-1})$ associated with <u>k</u>	10.2-4
K_p	The 3-hourly planetary geomagnetic index	8.7-9
<u>k</u>	Vector of parameters common to all arcs; partition of <u>x</u>	10.2-2
k_2	Tidal coefficient of degree 2 called the 'Love Number'	8.8-1
l	Direction cosine (measurement type)	6.1-7
l	Distance from a point on the earth's surface to the point at which the po- tential is to be computed	8.3-18
M	Mass of the Earth	6.3-2

REPRODUCIBILITY OF THE
ORIGINAL PAGE IS POOR

GLOSSARY OF SYMBOLS (Cont.)

<u>Symbols</u>	<u>Description</u>	<u>Page First Used</u>
M	Number of blocks on the Earth's surface	8.3-20
M	Number of parameters in \underline{x}	10.1-1
M	Mean anomaly of the orbit	11.4-1
M_e	Mass of the Earth	8.8-1
M_d	Mass of the disturbing body	8.8-1
M_o	Number of unadjusted densities	8.3-29
M'	Number of constraint equations	8.3-27
m	Direction cosine (measurement type)	6.1-7
m_d	Mass of the disturbing body for third body perturbations	8.4-1
m_i	Computed equivalent of the i^{th} measurement (see C_i and $C_{t+\Delta t}$)	10.2-2
m_s	Mass of the satellite	8.5-4
N	Number of observations in \underline{z}	10.1-1
N'	Maximum degree coefficient unaffected by the surface density layer	8.3-27

GLOSSARY OF SYMBOLS (Cont.)

<u>Symbols</u>	<u>Description</u>	<u>Page First Used</u>
\hat{N}	North baseline unit vector in the topocentric horizon coordinate system	5.2-1
N_{bj}	Residuals contributing to the bias computation	11.3-1
n	Direction cosine (measurement type)	6.1-7
n	Number of residuals	11.3-1
n_b	Number of electronic biases	11.3-1
n_s	Surface index of refraction	7.5-3
O_i	The i^{th} observed measurement value	2.2-1
P	Vector of parameters to be determined	2.2-1
$P_m^n ()$	Legendre polynomial	6.3-2
P_s	Solar radiation pressure in the vicinity of the Earth	8.5-4
$p(\underline{x})$	Joint probability density function \underline{x}	10.1-1
$p(\underline{z})$	Joint probability density function for \underline{z}	10.1-1
$p(\underline{x} \underline{z})$	Joint conditional probability density function for \underline{x} , given that \underline{z} has occurred	10.1-1

GLOSSARY OF SYMBOLS (Cont.)

<u>Symbols</u>	<u>Description</u>	<u>Page First Used</u>
$p(z x)$	Joint conditional probability density function for z given that x has occurred	10.1-1
q	Parallactic angle in radians	7.5-1
R_e	Mean earth radius	8.8-1
R_d	Third body disturbing potential	8.4-1
R_d	Distance from center of mass of the earth to the center of mass of the disturbing body	8.8-1
$R_g(t)$	Range vector from the center of the earth to the ground station at time t	6.4-3
R_i	Residual value (dm_i)	11.3-1
\hat{R}_d	Unit vector from center of mass of the earth to the center of mass of the disturbing body	8.8-1
$R_s(t)$	Range sum measurement at time t	6.4-1
$R_1(t)$	Range vector from the center of the earth to the relay satellite at time t	6.4-3
$R_2(t)$	Range vector from the center of the earth to the tracked satellite at time t	6.4-3

GLOSSARY OF SYMBOLS (Cont.)

<u>Symbols</u>	<u>Description</u>	<u>Page First Used</u>
R_{1d}	Down-link range from the relay satellite to the ground	6.4-3
R_{1u}	Up-link range from the ground to the relay satellite	6.4-1
R_{2d}	Relay satellite - tracked satellite range	6.4-1
R_{2u}	Tracked satellite - relay satellite range	6.4-3
\dot{R}_s	Time derivative of R_s	6.4-8
\dot{R}_{1u}	Time derivative of R_{1u}	6.4-8
\dot{R}_{2d}	Time derivative of R_{2d}	6.4-8
r	Distance from the point of interest to the center of mass of the earth	8.3-18
r	Distance from center of mass of the earth to satellite	8.3-1
\bar{r}	Geocentric satellite position vector	5.1-10
\bar{r}	True of date position vector of the satellite	8.7-29
\bar{r}_d	True of date position vector of third body for third body gravitational effects	8.4-1

GLOSSARY OF SYMBOLS (Cont.)

<u>Symbols</u>	<u>Description</u>	<u>Page First Used</u>
\bar{r}_{ob}	Geocentric position vector of a tracking station	2.2-4
\hat{r}	Unit vector from center of mass of the Earth to the satellite	8.8-1
\hat{i}_s	True of date unit vector pointing to the Sun	8.5-4
S	The cosine of the enclosed angle between \bar{r} and \bar{r}_d	8.4-1
S	Surface of the Earth	8.3-18
S_1	The first sum carry along by the integrator	9.3-1
S_2	The second sums carry along by the integrator	9.3-1
S_{nm}	Gravitational harmonic coefficient of degree n, order m	8.2-2
S'_{nm}	The sine coefficient of surface density constraint equations	8.3-25
s^2	Sample variance	11.3-1
T	A sample layer distributed on the surface of the Earth	8.3-25

GLOSSARY OF SYMBOLS (Cont.)

<u>Symbols</u>	<u>Description</u>	<u>Page First Used</u>
T	Exospheric temperature	8.7-15
T_e	Exospheric temperature	8.7-7
T_c	Nighttime minimum global exospheric temperature for a given day	8.7-6
T_{∞}	Average nighttime minimum global exospheric temperature for a given period	8.7-5
U	Geopotential field of the Earth	6.4-3
U	Spherical harmonics part of total earth potential	8.3-18
U_{2C}	Matrix containing the second partial derivatives of the gravitational potentials with respect to the true of date position coordinates	8.2-6
u	Central angle between the satellite vector and a vector pointing toward the ascending node of the orbit	11.4-7
\hat{u}	Unit vector in the direction of $\bar{\rho}$	8.1-2
V	Covariance matrix of \hat{x}	10.1-5
\hat{v}	Unit local vertical at the station	7.5-2

GLOSSARY OF SYMBOLS (Cont.)

<u>Symbols</u>	<u>Description</u>	<u>Page First Used</u>
V_A	<u>a priori</u> covariance matrix associated with \bar{x}_A ; same as Σ_A^{-1}	10.2-1
V_a	Matrix partition of V_A ; <u>a priori</u> covariance matrix associated with <u>a</u>	10.2-3
V_k	Matrix partition of V_A ; <u>a priori</u> covariance matrix associated with <u>k</u>	10.2-3
V_r	Matrix partition of V_a associated with the r^{th} arc	10.2-6
W	Weighting matrix for observations; same as Σ_2^{-1}	10.2-1
W	Total potential of the Earth	8.3-18
X	Coordinate system direction:	2.1-3
	a) Direction in the equatorial plane pointing toward the Greenwich meridian (Earth-fixed system)	
	b) In the direction of the true equinox of date at o.o of the epoch day (inertial system)	
	c) In the direction of the true equinox of date (true of date system)	

GLOSSARY OF SYMBOLS (Cont.)

<u>Symbols</u>	<u>Description</u>	<u>Page First Used</u>
$X(t+\Delta t)$	Position partial at time t	9.3-1
$\dot{X}(t+\Delta t)$	Velocity partial at time t	9.3-2
X_a	The X angle of the satellite (measurement type)	6.1-7
X_e	Earth-fixed position component	3.4-1
X_i	True of date position component	3.4-1
X_m	Matrix containing the variational partials	8.2-6
X_{1i}	Inertial cartesian position coordinates of the relay satellite	6.4-6
X_{2i}	Inertial cartesian position coordinates of the tracked satellite	6.4-6
\dot{X}_{1i}	Time derivative of X_{1i}	6.4-8
\dot{X}_{2i}	Time derivative of X_{2i}	6.4-8
x	True of date X position component of the satellite	2.2-4
x	Rotation angle for polar motion	5.4-5

GLOSSARY OF SYMBOLS (Cont.)

<u>Symbols</u>	<u>Description</u>	<u>Page First Used</u>
\underline{x}	Vector of M parameters	10.1-1
$\hat{\underline{x}}$	The "best" estimate of \underline{x}	10.1-2
$\hat{\underline{x}}^{(n)}$	The n th approximation to $\hat{\underline{x}}$	10.1-2
\underline{x}_A	The <u>a priori</u> estimate of \underline{x}	10.1-2
$\bar{\underline{x}}_t$	The vector describing the true of date position and velocity of the satellite	2.2-4
Y	Coordinate system direction (associated with the X and Z directions)	2.1-3
Y	Partition of X_m ; a matrix containing $\frac{\partial \underline{r}}{\partial \underline{\beta}}$	9.1-3
\dot{Y}	Partition of X_m ; a matrix containing $\frac{\partial \dot{\underline{r}}}{\partial \underline{\beta}}$	9.1-3
\ddot{Y}	Matrix containing $\frac{\partial \ddot{\underline{r}}}{\partial \underline{\beta}}$; same as matrix F	9.1-3
Y_a	The Y angle of the satellite (measurement type)	6.1-7
Y_e	Earth-fixed position component	3.4-1

GLOSSARY OF SYMBOLS (Cont.)

<u>Symbols</u>	<u>Description</u>	<u>Page First Used</u>
Y_i	True of date position component	3.4-1
y	True of date Y position component of the satellite	2.2-4
y	Rotation angle for polar motion	5.4-5
Z	Direction of the spin axis of the Earth for Z direction of coordinate systems. (Taken at 0^h of epoch day for inertial coordinate system.) Compare X	2.1-2
\hat{z}	The zenith baseline unit vector in the topocentric horizon coordinate system	5.2-1
Z_e	Earth-fixed component; same as z	5.1-5
Z_o	Observed zenith angle	7.5-1
z	True of date Z position coordinate of the satellite	2.2-4
z	A precession angle	3.1-1
\underline{z}	A vector of N independent observations	10.1-1

GLOSSARY OF SYMBOLS (Cont.)

<u>Symbols</u>	<u>Description</u>	<u>Page First Used</u>
α	Topocentric right ascension of the satellite (measurement type)	6.1-5
α'	Observed declination of the satellite	7.4-2
$\bar{\alpha}$	The set of parameters not affecting the dynamics of satellite motion	2.2-3
$\bar{\beta}$	The set of parameters affecting the dynamics of satellite motion	2.2-3
γ	Parameter of differential corrections for epoch element and force model parameter errors	6.4-6
β_p, β_p^* γ_p, γ_p^*	Cowell integration scheme coefficients	9.1-2
ΔE_i	Area of the surface density block	3.3-18
Δl	Correction to measurement of direction cosine l	7.5-5
Δm	Correction to measurement of direction cosine m	7.5-5
ΔR	Differential refraction	7.5-1

GLOSSARY OF SYMBOLS (Cont.)

<u>Symbols</u>	<u>Description</u>	<u>Page First Used</u>
ΔT_{ω}	Geomagnetic heating correction to T_{ω}	8.7-9
Δt	Measurement timing bias	6.0-2
Δt_{1u}	Transit time for the range R_{1u}	6.4-3
Δt_{1d}	Transit time for the range R_{1d}	6.4-3
Δt_{2d}	Transit time for the range R_{2d}	6.4-3
Δt_{2u}	Transit time for the range R_{2u}	6.4-3
ΔX_a	Correction to measured X angle	7.6-1
ΔY_a	Correction to measured Y angle	7.6-1
$\Delta \alpha$	Equation of the equinoxes	3.5-2
$\Delta \alpha$	Right ascension measurement correction	7.4-1
$\Delta \delta$	Declination measurement correction	7.4-1
$\Delta \epsilon$	Nutation in obliquity	3.6-11
$\Delta \rho$	Correction to range measurement	7.3-1
$\Delta \rho_n$	Correction to CNES laser range measurement	7.5-2
$\Delta \psi$	Nutation in longitude	3.6-8

GLOSSARY OF SYMBOLS (Cont.)

<u>Symbols</u>	<u>Description</u>	<u>Page First Used</u>
δ	Topocentric declination of satellite (measurement type)	6.1-5
δ'	Observed declination of the satellite	7.5-1
δ_{\odot}	Declination of the Sun	8.7-8
δ_{om}	Kronecker delta	8.3-5
ϵ	The measurement noise vector	10.4-2
ϵ_T	True obliquity of date	3.6-8
ϵ_M	Mean obliquity of date	3.6-8
ζ	Precision angle	3.6-6
θ	Precession angle	3.6-6
θ_g	Greenwich hour angle	2.1-3
λ	East longitude	5.1-1
λ	Sub-satellite longitude	8.7-29
μ_c	Mean of residuals	11.3-1

GLOSSARY OF SYMBOLS (Cont.)

<u>Symbol</u>	<u>Description</u>	<u>Page First Page</u>
v	Satellite eclipse factor	8.5-4
v_F	VLBI fringe rate measurement	6.6-3
\bar{p}	The station-satellite vector	6.1-2
ρ_D	Atmospheric density at the satellite position	8.5-6
ρ_D	Atmospheric density in Kg/m^3	8.7-22
ρ_{DT}	Atmospheric density in g/cm^3	8.7-15
ρ_S	Specular reflectivity of the satellite	8.5-5
ρ_i	the i^{th} station-satellite range	6.6-1
$\dot{\rho}_i$	Time derivative of ρ_i	6.6-3
ρ_T	Transmitter-satellite range	6.7-1
ρ_R	Satellite-receiver range	6.7-1
$\dot{\rho}$	Average range rate measurement	6.7-1
Σ_A	<u>a priori</u> covariance matrix associated with the <u>a priori</u> parameter vector \underline{x}_A	10.1-3
Σ_z	Covariance matrix associated with the observations \underline{z}	10.1-2

GLOSSARY OF SYMBOLS (Continued)

<u>Symbols</u>	<u>Description</u>	<u>Page First Page</u>
σ	Standard deviation	11.3-3
\underline{u}	Vector of noise on the observations \underline{z}	10.1-1
τ_g	VLBI time delay measurement	6.6-3
τ_i	Light time for the i^{th} station	6.6-1
ϕ	Geodetic latitude	5.1-1
ϕ	Sub-satellite latitude	8.7-29
ϕ'	Geodetic longitude	5.1-1
ϕ''	Geocentric latitude of the station	7.4-1
Ω	Longitude of the ascending node of the Moon's orbit	3.6-11
Ω	Longitude of the ascending node of a satellite orbit	11.4-1
ω	Angular velocity of the earth	8.3-18
ω	Argument of perigee of a satellite orbit	11.4-1
X	Surface density (kg/m^2 multiplied by G)	8.3-18
A_{ji}	Surface integrals	8.3-27
A_{ji}^{-1}	Inverse array of A_{ji}	8.3-28

GLOSSARY OF SYMBOLS (Continued)

<u>Symbols</u>	<u>Description</u>	<u>Page First Page</u>
•	Geocentric longitude of the sun in the the ecliptic plane	7.4-1
$\log_{10}n(\text{He})$	Helium number density	8.7-31

SECTION 1.0
THE GEODYN PROGRAM

GEODYN was written for GSFC by WOLF in 1971 and has been operational since January of 1972. A merger of the Multi-Arc NONAME program and the GEOSTAR program, GEODYN is greatly improved in overall capability, accuracy, and versatility over its parent programs.

GEODYN is one of the most widely used orbit and geodetic parameter estimation programs in the world. It is currently operational at GSFC on the IBM 360 '95, '91, and '75; at Ohio State University on the IBM 370/155; and will shortly be operational at Wallops Island on the GE 635. Additionally the GEODYN parent program, Multi-Arc NONAME is operational at the Goddard Institute for Space Studies in New York on an IBM 360/95 and at the Institut für Physik and Plasmaphysik, Garching, West Germany on an IBM 360/91.

GEODYN has been used for

- determination of definitive orbits
- tracking instrument calibration
- satellite operational predictions
- geodetic parameter estimation

and many other items relating to applied research in satellite geodesy using virtually all types of satellite tracking data.

SECTION 2.0

THE ORBIT AND GEODETIC PARAMETER ESTIMATION PROBLEM

The purpose of this section is to provide an understanding of the relationship between the various elements in the solution of the orbit and geodetic parameter estimation problem. As such, it is a general statement of the problem and serves to coordinate the detailed solutions to each element in the problem presented in the sections which follow.

The problem is divided into two parts:

- the orbit prediction problem, and
- the parameter estimation problem.

The solution to the first of these problems corresponds to GEODYN's orbit generation mode. The solution to the latter corresponds to GEODYN's data reduction mode and of course is based on the solution to the former.

The reader should note that there are two key choices which dramatically affect the GEODYN solution structure:

- Cowell's method for integrating the orbit, and
- a Bayesian least squares statistical estimation procedure for the parameter estimation problem.

2.1 The Orbit Prediction Problem

There are a number of approaches to orbit prediction. The GEODYN approach is to use Cowell's method, which is the direct numerical integration of the satellite equations of motion in rectangular coordinates. The initial conditions for these differential equations are the epoch position and velocity; the accelerations of the satellite must be evaluated.

The acceleration producing forces which are currently modelled in GEODYN are the effects of

- o the geopotential,
- o surface densities,
- o the luni-solar potentials,
- o planetary potentials of Venus, Mars, Jupiter and Saturn,
- o Radiation pressure,
- o earth tidal potential, and
- o atmospheric drag

Perhaps the most outstanding common feature of these forces is that they are functions of the position of the satellite relative to the Earth, Sun, Moon, or Planets and of the Sun and Moon relative to the Earth. Only atmospheric drag is a function of any additional quantity,* specifically, the relative velocity of the satellite with respect to the atmosphere.

*Not to be confused with the "fixed" parameters in the models.

The accurate evaluation of the acceleration of a satellite therefore involves the solution to two concomitant problems:

- o the accurate modeling of each force on the satellite - Earth - Sun - Moon - Planet relationship, and
- o The precise modeling of the motions of the Earth, Sun, Moon, and Planets.

The specific details for each model in these solutions are given elsewhere in Sections 3, 4, and 8. The question of how these models fit together is in effect the question of appropriate coordinate systems.

The key factor in the selection of coordinate systems for the satellite orbit prediction problem is the motion of the Earth. For the purposes of GEODYN, this motion consists of:

- o precession and nutation, and
- o rotation.

We are considering here the motion of the solid body of the Earth, as versus the slippage in the Earth's crust (polar motion) which just affects the position of the observer.

The precession and nutation define the variation in

- o the direction of the spin axis of the Earth (+ Z), and

- o the direction of the true equinox of date (+ X).

These directions define the (geocentric) true of date coordinate system.

The rotation rate of the Earth is the time rate of change of the Greenwich hour angle θ_g between the Greenwich meridian and the true equinox of date. Thus the Earth-fixed system differs from the true of date system according to the rotation angle θ_g .

The equations of motion for the satellite must be integrated in an inertial coordinate system. The GEODYN inertial system is defined as the true of date system corresponding to 0^h.0 of a reference epoch.

The coordinate systems in which the accelerations due to each physical effect are evaluated should be noted. The geopotential effects are evaluated in the Earth-fixed system, and then transformed to true of date to be combined with the other effects. The others are evaluated in the true of date system. The total acceleration is then transformed to the reference inertial system for use in the integration procedure.

The integration procedure used in GEODYN is a predictor-corrector type with a fixed time step. There is an optional variable step procedure. As the integration algorithms used provide for output on an even step, an interpolation procedure is required.

2.2 The Parameter Estimation Problem

Let us consider the relationships between the observations O_i , their corresponding computed values C_i and \bar{P} , the vector of parameters to be determined. These relationships are given by

$$O_i - C_i = \sum_j \frac{\partial C_i}{\partial P_j} dP_j - dO_i \quad (1)$$

where

i denotes the i^{th} observation or association with it,

dP_j is the correction to the j^{th} parameter, and

dO_i is the error of observation associated with the i^{th} observation.

The basic problem of parameter estimation is to determine a solution to these equations.

The role of data preprocessing is quite apparent from these equations. First, the observation and its computed equivalent must be in a common time and spatial reference system. Second, there are certain physical effects such as atmospheric refraction which do not significantly vary by any likely change in the parameters represented by \bar{P} .

These computations and corrections may equally well be applied to the observations as to their computed

values. Furthermore, the relationship between the computed value and the model parameters \bar{P} is, in general, nonlinear, and hence the computed values may have to be evaluated several times in the estimation procedure. Thus a considerable increase in computational efficiency may be attained by applying these computations and corrections to the observations; i.e., to preprocess the data.

The preprocessed observations used by GEODYN are directly related to the position and/or velocity of the satellite relative to the observer at the given observation time. These relationships are geometric, hence computed equivalents for these observations are obtained by applying these geometric relationships to the computed values for the positions and velocities of the satellite and the observer at the desired time.

Associated with each measurement from each observing station is a (known) statistical uncertainty. This uncertainty is a statistical property of the noise on the observations. This uncertainty is the reason a statistical estimation procedure is required for the GEODYN parameter determination.

It should be noted that dO_i , the measurement error, is not the same as the noise on the observations. The dO_i account for all of the discrepancy $(O_i - C_i)$ which is not accounted for by the corrections to the parameters \bar{P} . These dO_i represent both

- the contribution from the noise on the observation, and
- the incompleteness of the mathematical model represented by the parameters \bar{P} .

By this last we mean either that the parameter set being determined is insufficient or that the functional form of the model is inadequate.

GEODYN has two different ways of dealing with these errors of observation:

1. The measurement model includes both a constant bias and a timing bias which may be determined.
2. There is an automatic editing procedure to delete bad (statistically unlikely) measurements.

The nature of the parameters to be determined has a significant effect on the functional structure of the solution. In GEODYN, these parameters are:

- the position and velocity of the satellite at epoch. These are the initial conditions for the equations of motion.
- force model parameters. These affect the motion of the satellite.
- station positions and biases for station measurement types. These do not affect the motion of the satellite.

Thus, the parameters to be determined are implicitly partitioned into a set $\bar{\alpha}$, which are not concerned with the dynamics of the satellite motion and a set $\bar{\beta}$ which are.

The computed value C_i for each observation O_i is a function of

\bar{r}_{ob} the Earth-fixed position vector of the station, and

\bar{x}_t the true of date position and velocity vector of the satellite $\{x, y, z, \dot{x}, \dot{y}, \dot{z}\}$

at the desired observation time. When measurement biases are used, C_i is also a function of B , the biases associated with the particular station measurement type.

Let us consider the effect of the given partitioning on the required partial derivatives in the observational equations. The $\frac{\partial C_i}{\partial P}$ become

$$\frac{\partial C_i}{\partial \alpha} = \left(\frac{\partial C_i}{\partial \bar{r}_{ob}}, \frac{\partial C_i}{\partial B} \right) \quad (2)$$

$$\frac{\partial C_i}{\partial \beta} = \frac{\partial C_i}{\partial \bar{x}_t} \frac{\partial \bar{x}_t}{\partial \beta} \quad (3)$$

The partial derivatives $\frac{\partial \bar{x}_t}{\partial \beta}$ are called the variational partials. While the other partial derivatives on the right-hand side of the equations above are computed from the measurement model at the given time, the variational partials must be obtained by integrating the variational equations. As will be shown in Section 8, these equations are similar to the equations of motion.

The need for the above mentioned variational partials obviously has a dramatic effect on any solution to the observational equations. In addition to integrating the equations of motion to generate an orbit, the solution requires that the variational equations be integrated.

We have heretofore discussed the elements of the observational equations; we shall now discuss the solution of these equations; i.e., the statistical estimation scheme.

There are a number of estimation schemes that can be used. The method used in GEODYN is a batch scheme that uses all observations simultaneously to estimate the parameter set. The alternative would be a sequential scheme that uses the observations sequentially to calculate an updated set of parameters from each additional observation. Although batch and sequential schemes are essentially equivalent, practical numerical problems often occur with sequential schemes, especially when processing highly accurate observations. Therefore, a batch scheme was chosen.

The particular method selected for GEODYN is a partitioned Bayesian least squares method as detailed in Section 10. A Bayesian method is selected because such a scheme utilizes meaningful a priori information. The partitioning is such that the arrays which must be simultaneously in core are arrays associated with parameters common to all satellite arcs, and arrays pertaining to the arc being processed. Its purpose is to dramatically reduce the core storage requirements of the program without any significant cost in computation time.

There is an interesting aside related to the use of a priori information in practice. The use of a priori information for the parameters guarantees that the estimation procedure will mechanically operate (but not necessarily converge). The user must ensure that his data contains information relating to the parameters he wishes determined.

REPRODUCIBILITY OF THE
ORIGINAL PAGE IS POOR

SECTION 3.0

THE MOTION OF THE EARTH AND RELATED COORDINATE SYSTEMS

The major factor in satellite dynamics is the gravitational attraction of the Earth. Because of the (usual) closeness of the satellite and its primary, the Earth cannot be considered a point mass, and hence any model for the dynamics must contain at least an implicit mass distribution. The concern of this section is the motion of this mass distribution and its relation to coordinate systems.

We will first consider the meaning of this motion of the Earth in terms of the requisite coordinate systems for the orbit prediction problem.

The choice of appropriate coordinate systems is controlled by several factors:

- In the case of a satellite moving in the Earth's gravitational field, the most suitable reference system for orbit computation is a system with its origin at the Earth's center of mass, referred to as a geocentric reference system.
- The satellite equations of motion must be integrated in an inertial coordinate system.
- The Earth is rotating at a rate $\dot{\theta}_g$, which is the time rate of change of the Greenwich hour angle. This angle is the hour angle of the true equinox of date with respect to the Greenwich meridian as measured in the equatorial plane.

PRECEDING PAGE BLANK NOT FILMED

- The Earth both precesses and nutates, thus changing the directions of both the Earth's spin axis and the true equinox of date in inertial space.

The motions of the Earth referred to here are of course those of the "solid body" of the Earth, the motion of the primary mass distribution. The slippage of the Earth's crust is considered elsewhere in Section 5.2 (polar motion).

3.1 The True of Date Coordinate System

Let us consider that at any given time, the spin axis of the Earth (+ Z) and the direction of the true equinox of date (+ X) may be used to define a right-handed geocentric coordinate system. This system is known as the true of date coordinate system. The coordinate systems of GEODYN will be defined in terms of this system.

3.2 The Inertial Coordinate System

REPRODUCIBILITY OF THE
ORIGINAL PAGE IS POOR

The inertial coordinate system of GEODYN is the true of date coordinate system defined at 0^h:0 of the reference day for each satellite. This is the system in which the satellite equations of motion are integrated.

This is a right-handed, Cartesian, geocentric coordinate system with the X axis directed along the true equinox of 0^h:0 of the reference day and with the Z axis directed along the Earth's spin axis toward north at the same time. The Y axis is of course defined so that the coordinate system is orthogonal.

PRECEDING PAGE BLANK NOT FILMED

It should be noted that the inertial system differs from the true of date system by the variation in time of the directions of the Earth's spin axis and the true equinox of date. This variation is described by the effects of precession and nutation.

3.3 The Earth-fixed Coordinate System

The Earth-fixed coordinate system is geocentric, with the Z axis pointing north along the axis of rotation and with the X axis in the equatorial plane pointing toward the Greenwich meridian. The system is orthogonal and right-handed; thus the Y axis is automatically defined.

This system is rotating with respect to the true of date coordinate system. The Z axis, the spin axis of the Earth, is common to both systems. The rotation rate is equal to the Earth's angular velocity. Consequently, the hour angle θ_g of the true equinox of date with respect to the Greenwich meridian (measured westward in the equatorial plane) is changing at a rate $\dot{\theta}_g$ equal to the angular velocity of the Earth.

3.4 Transformation Between Earth-fixed and True of Date Coordinates

The transformation between Earth-fixed and true of date coordinates is a simple rotation. The Z axis is common to both systems. The angle between X_i , the true of date X component vector, and X_e , the Earth-fixed component vector, is θ_g , the Greenwich hour angle. The Y component vectors are similarly related. These transformations for X_e, Y_e, X_i, Y_i which are accomplished in

XEFIX
YEFIX
XINERT
YINERT
GRHRAN

GEODYN by the functions XEFIX, YEFIX, XINERT, and YINERT GRHRAN
are:

- $X_e = X_i \cos \theta_g + Y_i \sin \theta_g$ XEFIX
- $Y_e = X_i \sin \theta_g + Y_i \cos \theta_g$ YEFIX
- $X_i = X_e \cos \theta_g - Y_e \sin \theta_g$ XINERT
- $Y_i = X_e \sin \theta_g + Y_e \cos \theta_g$ YINERT

The transformation of velocities requires taking into account the rotational velocity, $\dot{\theta}_g$, of the Earth-fixed system with respect to the true of date reference frame. The following relationships should be noted:

$$\frac{\partial X_e}{\partial \theta_g} = Y_e \quad \frac{\partial Y_e}{\partial \theta_g} = -X_e \quad (1)$$

$$\frac{\partial X_i}{\partial \theta_g} = -Y_i \quad \frac{\partial Y_i}{\partial \theta_g} = X_i \quad (2)$$

The velocity transformations are then

OBSDOT

PREDCT

$$\dot{X}_e = [\dot{X}_i \cos \theta_g + \dot{Y}_i \sin \theta_g] + Y_e \dot{\theta}_g$$

$$\dot{Y}_e = [-\dot{X}_i \sin \theta_g + \dot{Y}_i \cos \theta_g] - X_e \dot{\theta}_g$$

$$\dot{X}_i = [\dot{X}_e \cos \theta_g - \dot{Y}_e \sin \theta_g] - Y_i \dot{\theta}_g$$

$$\dot{Y}_i = [\dot{X}_e \sin \theta_g + \dot{Y}_e \cos \theta_g] + X_i \dot{\theta}_g$$

The brackets denote the part of each transform which is a transformation identical to its coordinate equivalent.

These same transformations are used in the transformation of partial derivatives from the Earth-fixed system to true of date. For the k^{th} measurement, C_k , the partial derivative transformations are explicitly:

PREDCT

$$\frac{\partial C_k}{\partial X_i} = \left[\frac{\partial C_k}{\partial X_e} \cos \theta_g - \frac{\partial C_k}{\partial Y_e} \sin \theta_g \right] + \left[\frac{\partial C_k}{\partial X_e} \sin \theta_g + \frac{\partial C_k}{\partial Y_e} \cos \theta_g \right] \dot{\theta}_g \quad (3)$$

PREDCT

$$\frac{\partial C_k}{\partial Y_i} = \left[\frac{\partial C_k}{\partial X_e} \sin \theta_g + \frac{\partial C_k}{\partial Y_e} \cos \theta_g \right] \quad (4)$$

$$+ \left[\frac{\partial C_k}{\partial X_e} \cos \theta_g - \frac{\partial C_k}{\partial Y_e} \sin \theta_g \right] \dot{\theta}_g$$

$$\frac{\partial C_k}{\partial X_i} = \left[\frac{\partial C_k}{\partial X_e} \cos \theta_g - \frac{\partial C_k}{\partial Y_e} \sin \theta_g \right] \quad (5)$$

$$\frac{\partial C_k}{\partial Y_i} = \left[\frac{\partial C_k}{\partial X_e} \sin \theta_g + \frac{\partial C_k}{\partial Y_e} \cos \theta_g \right] \quad (6)$$

The brackets have the same meaning as before.

These above transforms are used or computed using the functions XEFIX, YEFIX, XINERT, or YINERT in three GEODYN subroutines: GRHRAN, OBSDOT, and PREDCT.

XEFIX
 YEFIX
 XINERT
 YINERT
 GRHRAN
 OBSDOT
 PREDCT

3.5 Computation of θ_g

The computation of the Greenwich hour angle is quite important because it provides the orientation of the Earth relative to the true of date system. The additional effects; i.e., to transform from true of date to inertial, of precession and nutation are sufficiently small that early orbit analysis programs neglected them. Thus, this angle is the major variable in relating the Earth-fixed system to the inertial reference frame in which the satellite equations of motion are integrated.

GRHRAN

The evaluation of θ_g is discussed in detail in the Explanatory Supplement, Reference 1. θ_g is computed in subroutines GRHRAN and F from the expression:

GRHRAN

F

$$\theta_g = \theta_{g_0} + \Delta t_1 \dot{\theta}_1 + \Delta t_2 \dot{\theta}_2 + \Delta \alpha \quad (1)$$

where

Δt_1 is the integer number of days since January 0.0 UT of the reference year,

Δt_2 is the fractional UT part of a day for the time of interest,

θ_{g_0} is the Greenwich hour angle on January 0.0 UT of the reference year,

$\dot{\theta}_1$ is the mean advance of the Greenwich hour angle per mean solar day,

$\dot{\theta}_2$ is the mean daily rate of advance of Greenwich hour angle ($2\pi + \dot{\theta}_1$), and

$\Delta \alpha$ is the equation of equinoxes (nutations in right ascension).

The initial θ_{g_0} is obtained from a table of values containing the Greenwich hour angle on January 0.0 for each year. This table is in Common Block CGEOS and is accessed in JANTHG.

JANTHG

The equation of equinoxes, $\Delta\alpha$, is obtained from subroutine EPHEM, which calculates the quantity from the ephemeris tape data according to the Everett fifth-order interpolation scheme.

GRHRAN
F
EPHEM

3.6. Precession and Nutation

EQN
EQUATR
NUTATE
PRECES
REFCOR

The inertial coordinate system of GEODYN, in which the equations of motion are integrated, is defined by the true equator and equinox of date for 0^h.0 of the reference day. However, the Earth-fixed coordinate system is related to the true equator and equinox of date at any given instant. Thus, it is necessary to consider the effects which change the orientation in space of the equatorial plane and the ecliptic plane.

These phenomena are

- the combined gravitational effect of the moon and the sun on the Earth's equatorial bulge, and
- the effect of the gravitational pulls of the various planets on the Earth's orbit.

The first of these affects the orientation of the equatorial plane; the second affects the orientation of the ecliptic plane. Both affect the relationship between the inertial and Earth-fixed reference systems of GEODYN.

The effect of these phenomena is to cause precession and nutation, both for the spin axis of the Earth and for the ecliptic pole. This precession and nutation provides the relationship between the inertial system defined by the true equator and equinox of the reference date and the "instantaneous" inertial system defined by the true equator and equinox of date at any

given instant. Let us consider the effect of each of these phenomena in greater detail.

EQN
EQUATR
NUTATE
PRECES
REFCOR

The luni-solar effects cause the Earth's axis of rotation to precess and nutate about the ecliptic pole. This precession will not affect the angle between the equatorial plane and the ecliptic (the "obliquity of the ecliptic") but will affect the position of the equinox in the ecliptic plane. Thus the effect of luni-solar precession is entirely in celestial longitude. The nutation will affect both, consequently we have nutation in longitude and nutation in obliquity.

The effect of the planets on the Earth's orbit will cause both secular and periodic deviations. However, the ecliptic is defined to be the mean plane of the Earth's orbit. Periodic effects are not considered to be a change in the orientation of the ecliptic; they are considered to be a perturbation of the Earth's celestial latitude. (See Reference 1.)

The secular effect of the planets on the ecliptic plane is separated into two parts: planetary precession and a secular change in obliquity. The effect of planetary precession is entirely in right ascension.

In summary, the secular effects on the orientations of the equatorial plane are:

- luni-solar precession,
- planetary precession, and
- a secular change in obliquity.

EQN
 EQUATR
 NUTATE
 PRECES
 REFCOR

As is the convention, all of these secular effects are considered under the heading, "precession." The periodic effects are

- nutation in longitude, and
- nutation in obliquity.

In terms of the GEODYN system, subroutine PRECES determines the secular effects; i.e., the rotation matrix which will transform coordinates from the mean equator and equinox of date to the mean equator and equinox of 1950.0.

PRECES

Subroutine NUTATE determines the rotation matrix to transform from true equator and equinox of date to mean equator and equinox of date. This accounts for the periodic effects.

NUTATE

GEODYN has two different routines for transforming from one epoch to another. These are EQUATR and REFCOR. EQUATR will take either mean or true coordinate input and will output in either mean or true coordinates. REFCOR will take only true coordinate input and will output only true coordinates. The same general algorithm is used in both:

EQUATR
 REFCOR

- o Rotate from true to mean equator and equinox of input date if required.
- o Rotate from mean of input date to mean of 1950.0. EQUATR
REFCOR
- o Rotate from mean of 1950.0 to mean of output date.
- o Rotate from mean to true of output date if required.

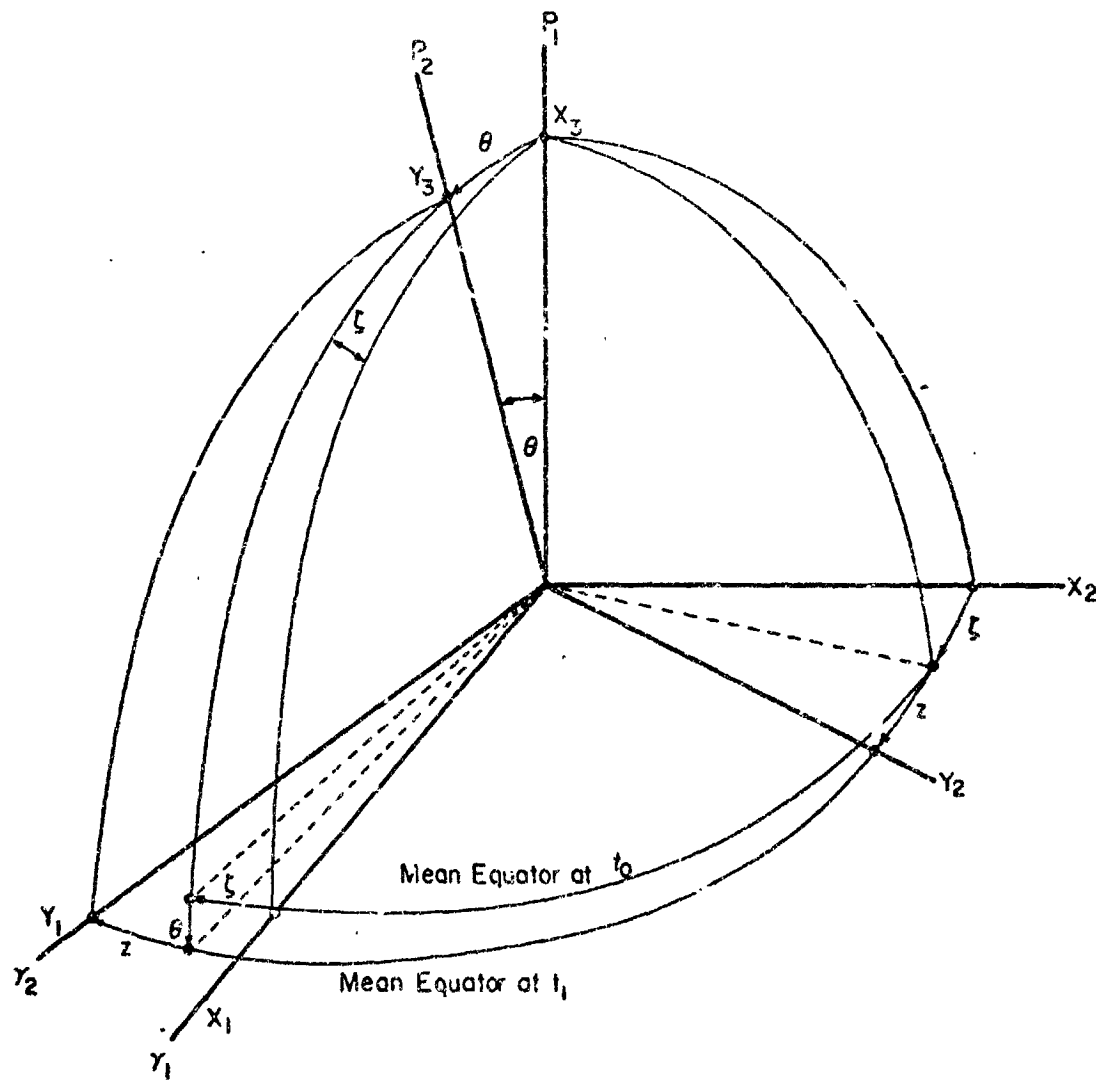
All of these rotations are of course done with rotation matrices.

Subroutine REFCOR will transform between any time of day and 0^h.0 on a given reference day. It performs this transform by interpolating linearly between the rotation matrices for the day of the input and that day plus one. REFCOR

3.6.1 Precession

The precession of coordinates from the mean equator and equinox of one epoch t_0 to the mean equator and equinox of t_1 is accomplished very simply. Examine Figure 1 and consider a position described by the vector \bar{X} in the X_1, X_2, X_3 coordinate system which is PRECES

PRECESSION



- P_1 = Direction of Mean Axis of Motion at t_0
- P_2 = Direction of Mean Axis of Motion at t_1
- Y_1 = Direction of Mean Equinox at t_0 .
- Y_2 = Direction of Mean Equinox at t_1

Fig.1: Rotation Between Mean Equator & Equinox of Epoch t_0
and
Mean Equator & Equinox of Epoch t_1

defined by the mean equator and equinox of t_0 . Likewise, consider the same position as described by the vector Y in the Y_1, Y_2, Y_3 system defined by the mean equator and equinox of t_1 . The expression relating these vectors,

$$Y = R_3 (-z) R_2 (\theta) R_3 (-\zeta) X, \quad (1)$$

follows directly from inspection of Figure 1.

It should be observed that $90^\circ - \zeta$ is the right ascension of the ascending node of the equator of epoch t_0 reckoned from the equinox of t_0 , $90^\circ - z$ is the right ascension of the node reckoned from the equinox of t_1 and θ is the inclination of the equator of t_1 to the epoch of t_0 .

Numerical expressions for these rotation angles z, θ, ζ were derived by Simon Newcomb, based partly upon theoretical considerations but primarily upon actual observation. (See References for the derivations.) The formulae used in GEODYN are relative to an initial epoch of 1950.0:

$$\zeta = .305\ 953\ 204\ 65 \times 10^{-6}d + .109\ 749\ 2 \times 10^{-14}d^2 + .178\ 097 \times 10^{-20}d^3 \quad (2)$$

$$z = .305\ 953\ 204\ 65 \times 10^{-6}d + .397\ 204\ 9 \times 10^{-14}d^2 + .191\ 051 \times 10^{-20}d^3 \quad (3)$$

$$\theta = R.266\ 039\ 997\ 54 \times 10^{-6}d - R.154\ 811\ 8 \times 10^{-14}d^2 \quad (4) \quad \text{PRECES}$$
$$- R.413\ 902 \times 10^{-20}d^3$$

The angles are in radians. The quantity d is the number of elapsed days since 1950.0.

3.6.2 Nutation

NUTATE

The nutation of coordinates between mean and true equator and equinox of date is readily accomplished using rotation matrices. Examine Figure 1 and consider a position described by the vector \bar{X} in the X_1, X_2, X_3 system which is described by the mean equator and equinox of date. Likewise, consider the same position as described by the vector \bar{Z} in the Z_1, Z_2, Z_3 system defined by the true equator and equinox of date. The expression relating these vectors,

$$\bar{Z} = R_1(-\epsilon_T) R_3(-\Delta\psi) R_1(\epsilon_m) \bar{X}, \quad (1)$$

follows directly from inspection of Figure 1.

The definition of these angles are:

ϵ_T - true obliquity of date

ϵ_m - mean obliquity of date

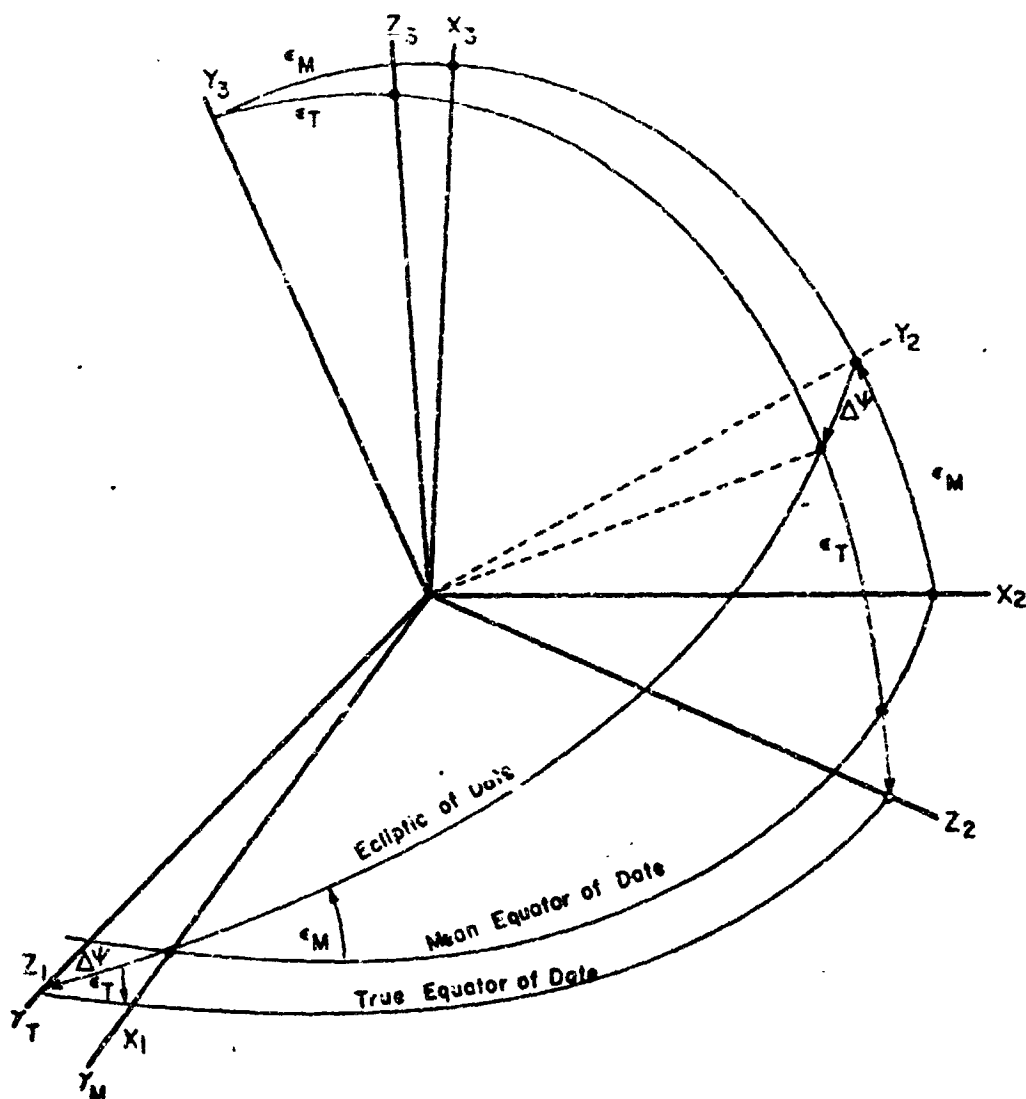
$\Delta\psi$ - nutation in longitude

Note that $\epsilon_T - \epsilon_m$ is the nutation in obliquity.

The remaining problem is to compute the nutations in longitude and obliquity. The algorithm used in GEODYN was developed by Woolard and is coded in subroutine EQN.

NUTATE
EQN

NUTATION



- e_M = Mean Obliquity of Date
- e_T = True Obliquity of Date
- Y_M = Direction of Mean Equinox of Date
- Y_T = Direction of Time Equinox of Date

Figure 1: Rotation Between Mean Equator & Equinox of Date
and
True Equator & Equinox of Date

Woolard's solution as it appears in references 1 through 4 is reproduced in Tables 1a, 1b, and 1c. The periodic terms have been rearranged in descending order of magnitude. The subprogram EQN computes the nutation in longitude and obliquity by using the algorithm in Tables 2a, 2b, and 2c. In Table 2a the angular units of the fundamental arguments have been changed to radians and the time units have been changed to days. Tables 2b and 2c are identical to Tables 1b and 1c often neglecting all periodic terms with coefficients less than .001 and all secular portions of the coefficient which are less than .001. The expressions for true obliquity of date and nutation in right ascension appear in Table 2d.

The definitions of the variables used in these solutions and additional notation are as follows:

- J = Julian Ephemeris Date of desired calculation
- J_0 = 241 5020.5 (Julian Ephemeris Date corresponding to 1900 January 0.5 Ephemeris Time)
- T = $(J - J_0) / 36525$ = Julian ephemeris centuries of 36525 Ephemeris Days elapsed from J_0 to J
- d = $J - J_0$ = Ephemeris Days elapsed from J to J_0

COORDINATE SYSTEM: Geocentric, ecliptic and
mean equinox of date:

EQN:

g = mean anomaly - Moon

g' = mean anomaly - Sun

i = mean angular distance of the Moon from its
ascending node

D = mean elongation of the Moon from the Sun

Ω = longitude of the mean ascending node of the
Moon's orbit

ϵ_M = mean obliquity of date

ϵ_T = true obliquity of date

$\Delta\epsilon$ = nutation in obliquity

$\Delta\psi$ = nutation in longitude

$\Delta\alpha$ = nutation in right ascension
(equation of the equinoxes)

REPRODUCIBILITY OF THE
ORIGINAL PAGE IS POOR

TABLE 1a FUNDAMENTAL ARGUMENTS

g	$= 296^{\circ}06'16''.59 + 1325^T 198^{\circ}50'56''.79 T + 33''.09 T^2 + ''0518 T^3$
g'	$= 3358^{\circ}28'33''.00 + 99^T 359^{\circ}02'59''.10 T - ''59 T^2 - ''0120 T^3$
F	$= 11^{\circ}15'03''.20 + 1342^T 82^{\circ}01'30''.54 T - 11''.56 T^2 - ''0012 T^3$
D	$= 350^{\circ}44'14''.95 + 1236^T 307^{\circ}06'51''.18 T - 5''.17 T^2 - ''0068 T^3$
Ω	$= 259^{\circ}10'59''.79 - 5^T 134^{\circ}08'31''.23 T + 7''.48 T^2 + ''0080 T^3$
ϵ_M	$= 23^{\circ}27'08''.26 - 46''.845T - ''0059T^2 + ''0080 T^3$

TABLE 1b NUTATION IN OBLIQUITY

	Series No.
$\Delta\epsilon = + (+0''.00091 T + 9''.2100) \cos (\quad + \Omega)$	1
$+ (-0''.00029 T + 0.5522) \cos (\quad + 2F - 2D + 2\Omega)$	2
$+ (+0.00004 T - 0.0904) \cos (\quad + 2\Omega)$	3
$+ (-0.00005 T + 0.0884) \cos (\quad + 2F \quad + 2\Omega)$	4
$+ (-0.00006 T + 0.0216) \cos (\quad + g' + 2F - 2D + 2\Omega)$	5
$\quad + 0.0183 \cos (\quad + 2F \quad + \Omega)$	6
$+ (-0.00001 T + 0.0113) \cos (+ g \quad + 2F \quad + 2\Omega)$	7
$+ (+0.00003 T - 0.0093) \cos (\quad - g' + 2F - 2D + \quad)$	8
$\quad - 0.0066 \cos (\quad + 2F - 2D + \Omega)$	9
$\quad - 0.0050 \cos (- g \quad + 2F \quad + 2\Omega)$	10
$\quad - 0.0031 \cos (+ g \quad + \Omega)$	11
$\quad + 0.0030 \cos (- g \quad + \Omega)$	12
$\quad - 0.0024 \cos (-2g \quad + 2F \quad + \Omega)$	13
$\quad + 0.0023 \cos (+ g \quad + 2F \quad + \Omega)$	14
$\quad + 0.0022 \cos (- g \quad + 2F - 2D + 2\Omega)$	15
$\quad + 0.0014 \cos (\quad + 2F + 2D + 2\Omega)$	16
$\quad - 0.0011 \cos (+ g \quad + 2F - 2D + 2\Omega)$	17
$\quad + 0.0011 \cos (+2g \quad + 2F \quad + 2\Omega)$	18
$\quad - 0.0010 \cos (- g \quad + 2F \quad + \Omega)$	19
$\quad + 0.0008 \cos (\quad + g' \quad + \Omega)$	20
$\quad - 0.0007 \cos (- g \quad + D + \Omega)$	21

REPRODUCIBILITY OF THE
ORIGINAL PAGE IS POOR

TABLE 1b (Cont.)

	Series No.
- 0.0007 cos (- g - 2D + Ω)	22
+ 0.0007 cos (+ g + 2g' + 2F - 2D + 2Ω)	23
+ 0.0005 cos (- g' + Ω)	24
+ 0.0005 cos (- g + 2F + 2D + Ω)	25
- 0.0003 cos (+ g' + 2F + 2Ω)	26
+ 0.0003 cos (- g' + 2F + 2Ω)	27
+ 0.0003 cos (+ g + 2F + 2D + 2Ω)	28
+ 0.0003 cos (+ 2D + Ω)	29
+ 0.0003 cos (-2g + 2D + Ω)	30
+ 0.0003 cos (- g' + 2F - 2D + Ω)	31
- 0.0003 cos (+ g + 2F - 2D + Ω)	32
+ 0.0003 cos (- 2D + Ω)	33
+ 0.0003 cos (+ 2F + 2D + Ω)	34
- 0.0002 cos (+2g + 2F - 2D + 2Ω)	35
+ 0.0002 cos (- 2g' + 2F - 2D + Ω)	36
- 0.0002 cos (+2g - 2D + Ω)	37
+ 0.0002 cos (+2g + 2F + Ω)	38
- 0.0002 cos (+ g' + 2F - 2D + Ω)	39
+ 0.0002 cos (-2g + 2F + 2Ω)	40

TABLE 1c NUTATION IN LONGITUDE

	Series No.
$\Delta\psi = + (-0.01737 T - 17.2327) \sin (+ \Omega)$	1
$+ (-0.00013 T - 1.2729) \sin (+ 2F - 2D + 2\Omega)$	2
$+ (+0.00002 T + 0.2008) \sin (+ 2\Omega)$	3
$+ (-0.00062 T - 0.2037) \sin (+ 2F + 2\Omega)$	4
$+ (-0.00031 T + 0.1261) \sin (+ g')$	5
$+ (+0.00001 T + 0.0675) \sin (+ g)$	6
$+ (+0.00012 T - 0.0497) \sin (g' + 2F - 2D + 2\Omega)$	7
$+ (-0.00004 T - 0.0342) \sin (+ 2F + 2\Omega)$	8

REPRODUCIBILITY OF THE
ORIGINAL PAGE IS POOR

TABLE 1c (Cont.)

				Series No.
	-	0.0261	sin (+ g Ω)	9
+ (-0.00005 T	+	0.0214)	sin (- g' + 2F - 2D + 2Ω)	10
	-	0.0149	sin (+ g - 2D)	11
+ (+0.00001 T	+	0.0124)	sin (+ 2F - 2D + Ω)	12
	+	0.0114	sin (- g + 2F + 2Ω)	13
	+	0.0060	sin (+ 2D)	14
	+	0.0058	sin (+ g + Ω)	15
	-	0.0057	sin (- g + Ω)	16
	-	0.0052	sin (- g + 2F + 2D + 2Ω)	17
	+	0.0045	sin (-2g + 2F + Ω)	18
	+	0.0045	sin (+2g - 2D)	19
	-	0.0044	sin (+ g + 2F + Ω)	20
	-	0.0032	sin (+ 2F + 2D + 2Ω)	21
	+	0.0028	sin (+2g)	22
	+	0.0026	sin (+ g + 2F - 2D + 2Ω)	23
	-	0.0026	sin (+2g + 2F + 2Ω)	24
	+	0.0025	sin (+ 2F)	25
	-	0.0021	sin (+ 2F - 2D)	26
	+	0.0019	sin (- g + 2F + Ω)	27
+ (-0.00001 T	+	0.0016)	sin (+ 2g')	28
+ (+0.00001 T	-	0.0015)	sin (+ 2g' + 2F - 2D + 2Ω)	29
	-	0.0015	sin (+ g' + Ω)	30
	+	0.0014	sin (- g + 2D + Ω)	31
	-	0.0013	sin (+ g - 2D + Ω)	32
	-	0.0010	sin (- g' + Ω)	33
	+	0.0010	sin (+2g - 2F)	34
	-	0.0009	sin (- g - 2F + 2D + Ω)	35
	+	0.0007	sin (+ g' + 2F + 2Ω)	36
	-	0.0007	sin (+ g + g - 2Ω)	37
	+	0.0006	sin (+ g + 2D)	38

TABLE 1c (Cont.)

-	0.0006	sin (-	g'	+ 2F	+ 2Ω)	39
-	0.0006	sin (+ g			+ 2F + 2D + 2Ω)		40
+	0.0006	sin (+2g			+ 2F - 2D + 2Ω)		41
-	0.0006	sin (+ 2D + Ω)		42
-	0.0005	sin (-2g			+ 2D + Ω)		43
-	0.0005	sin (-	g'	+ 2F - 2D + Ω)		44
+	0.0005	sin (g			+ 2F - 2D + Ω)		45
-	0.0005	sin (- 2D + Ω)		46
-	0.0005	sin (+ 2F + 2D + Ω)		47
-	0.0004	sin (-	2g'	+ 2F - 2D + Ω)		48

REPRODUCIBILITY OF THE
ORIGINAL PAGE IS POOR

TABLE 2a FUNDAMENTAL ARGUMENTS

g	=	5	168	000	345	745	+	1	228	027	134	939	576	d	+	1	120	251	689	x	10	⁻¹²	d ²	+	5	153	876	x	10	⁻²¹	d ³
g'	=	6	256	583	580	497	+	1	017	201	969	766	646	d	-	1	001	966	037	x	10	⁻¹²	d ²	+	1	193	948	x	10	⁻²¹	d ³
F	=	1	196	365	054	887	+	1	230	895	723	235	372	d	-	1	042	009	958	x	10	⁻¹²	d ²	-	1	119	395	x	10	⁻²¹	d ³
D	=	6	121	523	942	807	+	1	212	768	711	675	140	d	-	1	018	788	191	x	10	⁻¹²	d ²	+	1	676	571	x	10	⁻²¹	d ³
Ω	=	4	523	601	514	852	-	1	000	924	220	294	225	d	+	1	027	182	914	x	10	⁻¹²	d ²	+	1	795	965	x	10	⁻²¹	d ³
ϵ^R	=	1	409	319	755	205	-	1	000	000	006	217	959	d	-	1	000	921	441	x	10	⁻¹²	d ²	+	1	180	087	x	10	⁻²¹	d ³

TABLE 2b NUTATION IN OBLIQUITY

		Series No.
$\Delta\epsilon = + 9''2100 \cos ($	$+ \Omega)$	1
$+ 0.5522 \cos ($	$+ 2F - 2D + 2\Omega)$	2
$- 0.0904 \cos ($	$+ 2\Omega)$	3
$+ 0.0884 \cos ($	$+ 2F + 2\Omega)$	4
$+ 0.0216 \cos ($	$+ g' + 2F - 2D + 2\Omega)$	5
$+ 0.0183 \cos ($	$+ 2F + \Omega)$	6
$+ 0.0113 \cos (+ g$	$+ 2F + 2\Omega)$	7
$- 0.0093 \cos ($	$- g' + 2F - 2D + 2\Omega)$	8
$- 0.0066 \cos ($	$+ 2F - 2D + \Omega)$	9
$- 0.0050 \cos (- g$	$+ 2F + 2\Omega)$	10
$- 0.0031 \cos (+ g$	$+ \Omega)$	11
$+ 0.0030 \cos (- g$	$+ \Omega)$	12
$- 0.0024 \cos (-2g$	$+ 2F + \Omega)$	13
$+ 0.0023 \cos (+ g$	$+ 2F + \Omega)$	14
$+ 0.0022 \cos (- g$	$+ 2F + 2D + 2\Omega)$	15
$+ 0.0014 \cos ($	$+ 2F + 2D + 2\Omega)$	16
$- 0.0011 \cos (+ g$	$+ 2F - 2D + 2\Omega)$	17
$+ 0.0011 \cos (+2g$	$+ 2F + 2\Omega)$	18
$- 0.0010 \cos (- g$	$+ 2F + \Omega)$	19

TABLE 2c NUTATION IN LONGITUDE

	Series No.
$\Delta\lambda = + (-0^m01737 T - 17^m2327) \sin ($	$+ \Omega) 1$
$- 1.2729) \sin ($	$+ 2F - 2D + 2\Omega) 2$
$+ 0.2008) \sin ($	$+ 2\Omega) 3$
$- 0.2037) \sin ($	$+ 2F + 2\Omega) 4$
$+ 0.1261) \sin ($	$+ g') 5$
$+ 0.0675) \sin (+ g$	$) 6$
$- 0.0497) \sin ($	$g' + 2F - 2D + 2\Omega) 7$
$- 0.0342) \sin ($	$+ 2F + 2\Omega) 8$
$- 0.0261 \sin (+ g$	$+ 2F \Omega) 9$
$+ 0.0214) \sin ($	$g' + 2F - 2D + 2\Omega) 10$
$- 0.0149 \sin (+ g$	$- 2D) 11$
$+ 0.0124) \sin ($	$+ 2F - 2D + \Omega) 12$
$+ 0.0114 \sin (- g$	$+ 2F + 2\Omega) 13$
$+ 0.0060 \sin ($	$+ 2D) 14$
$+ 0.0058 \sin (+ g$	$+ \Omega) 15$
$- 0.0057 \sin (- g$	$+ \Omega) 16$
$- 0.0052 \sin (- g$	$+ 2F + 2D + 2\Omega) 17$
$+ 0.0045 \sin (-2g$	$+ 2F + \Omega) 18$
$+ 0.0045 \sin (+2g$	$- 2D) 19$
$- 0.0044 \sin (+ g$	$+ 2F + \Omega) 20$
$- 0.0032 \sin ($	$+ 2F + 2D + 2\Omega) 21$
$+ 0.0028 \sin (+2g$	$) 22$
$+ 0.0026 \sin (+ g$	$+ 2F - 2D + 2\Omega) 23$
$- 0.0026 \sin (+2g$	$+ 2F + 2\Omega) 24$
$+ 0.0025 \sin ($	$+ 2F) 25$
$- 0.0021 \sin ($	$+ 2F - 2D) 26$
$+ 0.0019 \sin (- g$	$+ 2F + \Omega) 27$
$+ 0.0016) \sin ($	$+ 2g') 28$

TABLE 2c (Cont.)

-	0.0015,	sin (+ 2g'	+ 2F	- 2D	+ 2Ω)	29
-	0.0015	sin (+ g'			+ Ω)	30
+	0.0014	sin (- g			+ 2D	+ Ω)	31
-	0.0013	sin (+ g			- 2D	+ Ω)	32
-	0.0010	sin (- g'			+ Ω)	33
+	0.0010	sin (+2g		- 2F)	34

Note: To change time units for coefficient of 1st term, use
 .475 565 $10^{-6}d = .01737 T$

Table 2d: True obliquity of Date and Nutation in right ascension

$$\epsilon_T = \epsilon_M + \Delta\epsilon$$

$$\Delta \alpha = \Delta\psi \cos \epsilon_T$$

SECTION 4.0
LUNI-SOLAR-PLANETARY EPHEMERIS

GEODYN uses precomputed equi-spaced ephemeris data EPHEM
in true of date coordinates for the Moon, the Sun, Venus,
Mars, Jupiter and Saturn. The actual ephemerides are com-
puted using Everett's fifth-order interpolation formula.
The interval between ephemerides; i.e., the tabular interval
h, is 0.5 days for the Moon and the Equation of the equinoxes
and 4.0 days for the other bodies.

The GEODYN ephemeris tape contains all coordinates
in true of date. The quantities on the tape are

- a) geocentric lunar positions and the corresponding
2nd and 4th differences,
- b) solar positions relative to the earth-moon
barycenter and the corresponding 2nd and 4th
differences,
- c) heliocentric positions of Venus, Mars, Jupiter
and Saturn and the corresponding 2nd and 4th
differences,
- d) the equation of the equinoxes and its 2nd and
4th differences.

The format of this tape is presented in Volume III
of the GEODYN documentation.

This ephemeris tape was prepared from a JPL planetary
ephemeris tape corresponding to "JPL Development Ephemeris
Number 69," Reference 1. The program which generates the
GEODYN ephemeris tape is described in Volume IV of the
GEODYN documentation.

The formulation for Everett's fifth-order interpolation is

$$\begin{aligned}
 y(t_j+sh) = & y_j F_0(1-s) + d_j^2 F_2(1-s) & (1) \\
 & + d_j^4 F_4(1-s) \\
 & + y_{j+1} F_0(s) + d_{j+1}^2 F_2(s) \\
 & + d_{j+1}^4 F_4(s)
 \end{aligned}$$

where

EPHEM

$$F_0(s) = s$$

$$F_2(s) = [(s-1)(s)(s+1)]/6$$

$$F_4(s) = [(s-2)(s-1)(s)(s+1)(s+2)]/120$$

The quantity s is of course the fractional interval for the interpolation. The quantities d_j are obtained from the ephemeris tape.

SECTION 5.0
THE OBSERVER

This section is concerned with the position and coordinate systems of the observer. Thus it will cover

- geodetic station position coordinates,
- topocentric coordinate systems,
- time reference systems, and
- polar motion.

The geodetic station position coordinates are a convenient and quite common way of describing station positions. Consequently, GEODYN contains provisions for converting to and from these coordinates, including the transformation of the covariance matrix for the determined Cartesian station positions.

The topocentric coordinate systems are coordinate systems to which the observer references his observations.

The time reference systems are the time systems in which the observer specifies his observations. The transformations between time reference systems are also given. These latter are used both to convert the observation times to A1 time, which is the independent variable in the equations of motion, and to convert the GEODYN output to UTC time, which is the generally recognized system for output.

The positions of the observers in GEODYN are referred to an Earth-fixed system defined by the mean pole of 1900.5 and Greenwich. They are rotated into the Earth-fixed system of date at each observation time by applying "polar motion", which is considered to be slippage of the Earth's crust.

5.1 GEODETIC COORDINATES

Frequently, it is more convenient to define the station positions in a spherical coordinate system. The spherical coordinate system uses an oblate spheroid or an ellipsoid of revolution as a model for the geometric shape of the Earth. The Earth is flattened slightly at the poles and bulges a little at the equator; thus, a cross section of the Earth is approximately an ellipse. Rotating an ellipse about its shorter axis forms an oblate spheroid.

An oblate spheroid is uniquely defined by specifying two dimensions, conventionally, the semi-major axis and the flattening, f , where $f = \frac{a-b}{a}$. (See Figure 1)

This model is used in the GEODYN system. The spherical coordinates utilized are termed geodetic coordinates and are defined as follows:

- ϕ is geodetic latitude, the acute angle between the semi-major axis and a line through the observer perpendicular to the spheroid.

- λ is east longitude, the angle measured eastward in the equatorial plane between the Greenwich meridian and the observer's meridian.
- h is spheroid height, the perpendicular height of the observer above the reference spheroid.

Consider the problem of converting from ϕ , λ , and h to X_e , Y_e , and Z_e , the Earth-fixed Cartesian coordinates.

SQUANT

The geometry for an X-Z plane is illustrated in Figure 1. The equation for this ellipse is

$$x^2 + \frac{z^2}{(1-e^2)} = a^2, \quad (1)$$

where the eccentricity has been determined from the flattening by the familiar relationship

$$e^2 = 1 - (1-f)^2. \quad (2)$$

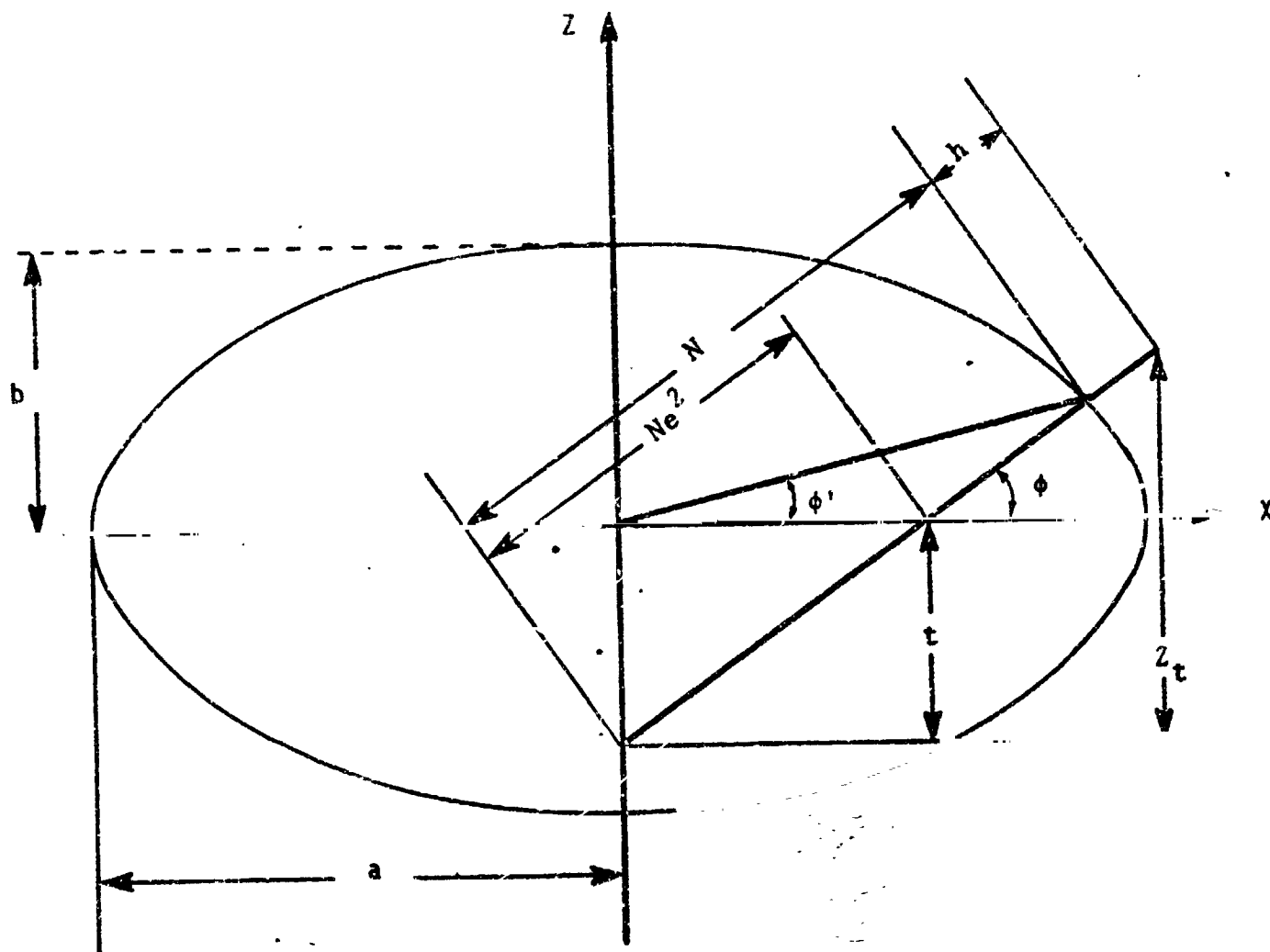


Figure 1: Diagram of Geodetic and Geocentric Latitudes

The equation for the normal to the surface of the ellipse yields

SQUANT

$$\tan \phi = - \frac{dx}{dz} \quad (3)$$

By taking differentials on equation (1) and applying the result in equation (3), we arrive at

$$\frac{z}{x} = (1-e^2) \tan \phi \quad (4)$$

The simultaneous solution of equations (1) and (4) for X yields

$$X = \frac{a \cos \phi}{\sqrt{1-e^2 \sin^2 \phi}} \quad (5)$$

From inspection of Figure 1 we have:

$$\cos \phi = \frac{X}{N} ; \quad (6)$$

and hence, applying equation (5),

$$N = \frac{a}{\sqrt{1-e^2 \sin^2 \phi}} \quad (7)$$

For an observer at a distance h from the reference ellipsoid, the observer's coordinates (X,Z) become

SQUANT

$$X = N \cos \phi + h \cos \phi \quad (8)$$

and

$$Z = N (1-e^2) \sin \phi + h \sin \phi. \quad (9)$$

The conversion of ϕ , λ , and h to X_e , Y_e , and Z_e is then

$$\begin{bmatrix} X_e \\ Y_e \\ Z_e \end{bmatrix} = \begin{bmatrix} (N+h) \cos \phi \cos \lambda \\ (N+h) \cos \phi \sin \lambda \\ (N+h-e^2 N) \sin \phi \end{bmatrix} \quad (10)$$

In the GEODYN system this conversion is performed in subroutine SQUANT.

The problem of converting from X_e , Y_e , and Z_e to ϕ , λ , and h is more complex as we cannot start with a point on the reference ellipsoid. For this reason the determination of accurate values for ϕ and h requires an iterative technique.

Conversion to Geodetic Coordinates

For the problem of converting station coordinates PLHOUT
in X_e , Y_e , and Z_e to ϕ , λ , and h we know that N is on the
order of magnitude of an Earth radius, and h is a few
meters. Hence

$$h \ll N \quad (11)$$

The Earth is approximately a sphere, hence

$$e \ll 1. \quad (12)$$

Therefore, again working in our X-Z plane (see Figure 1),

$$N \sin \phi \approx Z. \quad (13)$$

From Figure 1 (see also equation (9)) we have

$$t \approx Ne^2 \sin \phi, \quad (14)$$

or, for an initial approximation,

$$t \approx e^2 Z. \quad (15)$$

The series of calculations to be performed on each iteration is:

PLHOUT

$$Z_t = Z + t \quad (16)$$

$$N+h = \left(x_e^2 + y_e^2 + z_t^2 \right)^{1/2} \quad (17)$$

$$\sin \phi = z_t / (N+h) \quad (18)$$

$$N = a / \left(1 - e^2 \sin^2 \phi \right)^{1/2} \quad (19)$$

$$t = Ne^2 \sin \phi. \quad (20)$$

When t converges, ϕ and h are computed from $\sin \phi$ and $(N+h)$. The computation of λ is obvious; it being simply

$$\lambda = \tan^{-1} \left(y_e / x_e \right) \quad (21)$$

This procedure for determining ϕ , λ , and h is that coded in subroutine PLHOUT.

There is a different procedure in subroutine PREDCT for computing ϕ , λ , and h for a satellite. This is because the accuracy requirements are less stringent.

DRAG
PREDCT

This different procedure is also used in subroutine DRAG to evaluate the satellite height for subroutine DENSTY.

Because $e \ll 1$, we may write an approximation to equation (9):

$$Z = (N+h) (1-e^2) \sin \phi = Z_e \quad (22)$$

From Figure 1,

$$X = (N+h) \cos \phi = \sqrt{X_e^2 + Y_e^2} \quad (23)$$

and by remembering equation (2),

$$\phi = \tan^{-1} \left[\frac{Z_e}{(1-f)^2 \sqrt{X_e^2 + Y_e^2}} \right] \quad (24)$$

The equation for the ellipse, equation (1), yields the following formula for the radius of the ellipsoid:

DRAG
PREDCT

$$r_{\text{ellipsoid}} = \sqrt{X^2 + Z^2} = \frac{a(1-f)}{\sqrt{1 - (2f-f^2)(1-\sin^2 \phi')}} \quad (27)$$

where ϕ' is the geocentric latitude. After applying the Binomial Theorem, we arrive at

$$r_{\text{ellipsoid}} = a \left[1 - \left(f + \frac{3}{2}f^2\right) \sin^2 \phi' + \frac{3}{2}f^2 \sin^4 \phi' \right] \quad (28)$$

wherein terms on the order of f^3 have been neglected. The (spheroid) height may then be calculated from r , the geocentric radius of the satellite:

$$h = r - r_{\text{ellipsoid}}, \text{ or} \quad (29)$$

$$h = \sqrt{X_e^2 + Y_e^2 + Z_e^2} - a + \left(af + \frac{3}{2}af^2\right) \sin^2 \phi' - \frac{3}{2}af^2 \sin^4 \phi' \quad (30)$$

The sine of the geocentric latitude, $\sin \phi'$, is of course $\frac{Z_e}{r}$.

Subroutine VEVAL also requires the partial derivatives of h with respect to position for the diagonal variational partials computations:

VEVAL

$$\frac{\partial h}{\partial r_i} = \frac{r_i}{r} + 2 \sin \phi' \left[\left(af + \frac{3}{2} af^2 \right) - 3 af^2 \sin^2 \phi' \right] \left[\frac{z_e r_i}{r^3} + \frac{1}{r} \frac{\partial z_e}{\partial r_i} \right] \quad (31)$$

where the

r_i are the Earth-fixed components of \bar{r} ; i.e., $\{X_e, Y_e, Z_e\}$.

In addition to the conversion of the coordinates themselves, GEODYN also converts covariance matrices for the station positions to either the ϕ, λ, h system or the Earth-fixed rectangular system. This is accomplished in INOUP, SQUANT, and PLHOUT by calling VCONV to compute

INOUP
SQUANT
PLHOUT
VCONV

$$V_{OUT} = P^T V_{IN} P \quad (32) \text{ VCONV}$$

where V_{OUT} is the output covariance matrix, V_{IN} is the input covariance matrix, and P is the matrix of partials relating the coordinates in the output system to the coordinates in the input system.

These partial derivatives (in P) which GEODYN requires are for X_e, Y_e, Z_e with respect to ϕ, λ, h and vice versa. These partials are:

PLHOUT

$$\frac{\partial \phi}{\partial X_e} = -X_e Z_e (1-e^2) / ((1-e^2)^2 (X_e^2 + Y_e^2) + Z_e^2) (X_e^2 + Y_e^2)^{\frac{1}{2}}$$

$$\frac{\partial \phi}{\partial Y_e} = -Y_e Z_e (1-e^2) / ((1-e^2)^2 (X_e^2 + Y_e^2) + Z_e^2) (X_e^2 + Y_e^2)^{\frac{1}{2}}$$

$$\frac{\partial \phi}{\partial Z_e} = (X_e^2 + Y_e^2) (1-e^2) / (1-e^2)^2 (X_e^2 + Y_e^2) + Z_e^2 (X_e^2 + Y_e^2)^{\frac{1}{2}}$$

$$\frac{\partial \lambda}{\partial X_e} = -Y_e / (X_e^2 + Y_e^2) \quad (33)$$

$$\frac{\partial \lambda}{\partial Y_e} = X_e / (X_e^2 + Y_e^2)$$

$$\frac{\partial \lambda}{\partial Z_e} = 0$$

$$\frac{\partial h}{\partial X_e} = \frac{\partial \phi}{\partial X_e} (-e^2 a (1-e^2) \sin \phi \cos \phi / (1-e^2 \sin^2 \phi)^{\frac{3}{2}} - Z_e \cos \phi / \sin^2 \phi)$$

$$\frac{\partial h}{\partial Y_e} = \frac{\partial \phi}{\partial Y_e} (-e^2 a (1-e^2) \sin \phi \cos \phi / (1-e^2 \sin^2 \phi)^{\frac{3}{2}} - Z_e \cos \phi / \sin^2 \phi)$$

$$\frac{\partial h}{\partial Z_e} = \frac{\partial \phi}{\partial Z_e} (-e^2 a (1-e^2) \sin \phi \cos \phi / (1-e^2 \sin^2 \phi)^{\frac{3}{2}} - Z_e \cos \phi / \sin^2 \phi)$$

$$+ \frac{1}{\sin \phi}$$

$$\frac{\partial X_e}{\partial \phi} = -\sin \phi \cos \lambda \left[N+h - \frac{Ne^2 \cos^2 \phi}{1-e^2 \sin^2 \phi} \right]$$

SQUANT

$$\frac{\partial X_e}{\partial \lambda} = -(N+h) \cos \phi \sin \lambda$$

$$\frac{\partial X_e}{\partial h} = \cos \phi \cos \lambda$$

$$\frac{\partial Y_e}{\partial \phi} = -\sin \phi \sin \lambda \left[N+h - \frac{Ne^2 \cos^2 \phi}{1-e^2 \sin^2 \phi} \right]$$

$$\frac{\partial Y_e}{\partial \lambda} = (N+h) \cos \phi \cos \lambda$$

(34)

$$\frac{\partial Y_e}{\partial h} = \cos \phi \sin \lambda$$

$$\frac{\partial Z_e}{\partial \phi} = \cos \phi \left[h+N (1-e^2) \left(1 + \frac{e^2 \sin^2 \phi}{1-e^2 \sin^2 \phi} \right) \right]$$

$$\frac{\partial Z_e}{\partial \lambda} = 0$$

$$\frac{\partial Z_e}{\partial h} = \sin \phi$$

The partials for converting from X_e, Y_e, Z_e to ϕ, λ, h are computed in subroutine PLHOUT. Those for converting from ϕ, λ, h to X_e, Y_e, Z_e are computed in subroutine SQUANT.

5.2 TOPOCENTRIC COORDINATE SYSTEMS

The observations of a spacecraft are usually referenced to the observer, and therefore an additional set of reference systems is used for this purpose. The origin of these systems, referred to as topocentric coordinate systems, is the observer on the surface of the earth.

Topocentric right ascension and declination are measured in an inertial system whose Z axis and fundamental plane are parallel to those of the geocentric inertial system. The X axis in this case also points toward the vernal equinox.

The other major topocentric system is the Earth-fixed system determined by the zenith and the observer's horizon plane. This is an orthonormal system defined by \hat{N} , \hat{E} , and \hat{Z} , which are unit vectors which point in the same directions as vectors from the observer pointing north, east, and toward the zenith. Their definitions are:

SQUANT

$$\hat{N} = \begin{bmatrix} -\sin \phi \cos \lambda \\ -\sin \phi \sin \lambda \\ \cos \phi \end{bmatrix} \quad (1)$$

$$\hat{E} = \begin{bmatrix} -\sin \lambda \\ \cos \lambda \\ 0 \end{bmatrix} \quad (2)$$

$$\hat{Z} = \begin{bmatrix} \cos \phi \cos \lambda \\ \cos \phi \sin \lambda \\ \sin \phi \end{bmatrix} \quad (3)$$

where ϕ is the geodetic latitude and λ is the east longitude of the observer (see Section 5.1).

SQUANT
PREDCT
OBSDOT

These \hat{N} , \hat{E} , and \hat{Z} vectors are computed in SQUANT for use in PREDCT and OBSDOT.

This latter system is the one to which such measurements as azimuth and elevation, X and Y angles, and direction cosines are related.

It should be noted that the reference systems for range and range rate must be Earth-fixed, but the choice of origin is arbitrary. In GEODYN, range and range rate are not considered to be topocentric, but rather geocentric.

5.3 TIME REFERENCE SYSTEMS

Three principal time systems are currently in use: ephemeris time, atomic time, and universal time.

Ephemeris time is the independent variable in the equations of motion of the sun; this time is the uniform mathematical time. The corrections that must be applied to universal time to obtain ephemeris time are published in the American Ephemeris and Nautical Almanac or alternatively by BIH, the "Bureau International de l'Heure."

Atomic time is a time based on the oscillations of cesium at zero field. In practice AI time is based on the mean frequency of oscillation of several cesium standards as compared with the frequency of ephemeris time. This is the time system in which the satellite equations of motion are integrated in GEODYN.

Universal time is determined by the rotation of the Earth. UT1, the time reference system used in GEODYN to position the Earth, is universal time that has been corrected for polar motion. UTC is the time of the transmitting clock of any of the synchronized transmitting time signals. The frequency of a UTC clock is pre-set to a predicted frequency of UT2 time, where UT2 time is universal time corrected for observed polar motion and extrapolated seasonal variation in the speed of the earth's rotation.

The reader who is unfamiliar with these time systems should refer to one of the annual reports of PIH.

5.3.1 Time System Transformations

The time system transformations are between any combination of the A1, UT1, UT2, or UTC reference systems. These transformations are computed in the GEODYN system by subroutine TDIF.

TDIF

The time transformation between any input time system and any output time system is formed by simple addition and subtraction of the following set of time differences:

- UT2 - UT1
- A1 - UT1
- A1 - UTC

The following equation is used to calculate (UT2-UT1) for any year:

TDIF

$$\begin{aligned} (UT2-UT1) = & + .5022 \sin 2\pi t - .5012 \cos 2\pi t \\ & - .5006 \sin 4\pi t + .5007 \cos 4\pi t \end{aligned} \quad (1)$$

t = fraction of the tropical year elapsed from the beginning of the Besselian year for which the calculation is made.

(1 tropical year = 365.2422 days)

This difference, (UT2-UT1), is also known by the name "seasonal variation."

The time difference (A1-UT1) is computed by linear interpolation from a table of values. The spacing for the table is every 10 days, which matches the increment for the "final time of emission" data published by the U.S. Naval Observatory in the bulletin, "Time Signals." The differences for this table are determined by

$$(A1 - UT1) = (A1 - UTC) - (UT1 - UTC)$$

The values for (UT1 - UTC) are obtained from "Circular D", BIH. The differences (A1 - UTC) are determined according to the following procedure.

The computation of (A1-UTC) is simple, but not so straightforward. UTC contains discontinuities both in epoch and in frequency because an attempt is made to keep the difference between a UTC clock and a UT2 clock less than $^s.1$. When adjustments are made, by international agreement they are made in steps of $^s.1$ and only at the beginning of the month; i.e., at $o.h.c$ UT of the first day of the month. The general formula which is used to compute (A1-UTC) is

$$(A1-UTC) = a_0 + a_1 (t-t_0) \quad (2)$$

Both a_0 and a_1 are recovered from tables. The values in the table for a_0 are the values of (A1-UTC) at the time of each particular step adjustment. The values in the table for a_1 are the values for the new rates of change between the two systems after each step adjustment.

Values for a_0 and a_1 are published both by the U.S. Naval Observatory and BIH.

5.4 POLAR MOTION

Consider the point P which is defined by the intersection of the Earth's axis of rotation at some time t with the surface of the Earth. At some time $t+\Delta t$, the intersection will be at some point P' which is different than P. Thus the axis of rotation appears to be moving relative to a fixed position on the Earth; hence the term "motion of the pole."

POLE

Let us establish a rectangular coordinate system centered at a point F fixed on the surface of the Earth with F near the point P around 1900, and take measurements of the rectangular coordinates of the point P during the period 1900.0 - 1906.0. It is observed that the point P moves in roughly circular motion in this coordinate system with two distinct periods, one period of approximately 12 months and one period of 14 months. We define the mean position of P during this period to be the point P_0 , the mean pole of 1900.0 - 1906.0.

The average is taken over a six year period in order to average out both the 12 month period and the 14 month period simultaneously (since 6 times 12 months = 72 months and $72/14 = 5$ periods approximately of the 14 month term). The radius of this observed circle varies between 15-35 feet.

In addition to the periodic motion of P about P_0 , by taking six year means of P in the years after 1900 - 1906, called P_m , there is seen to be a secular motion of the mean position of the pole away from its original mean position P_0 in the years 1900 - 1906 at the rate of

approximately $0''0032/\text{year}$ in the direction of the meridian 60°W , and a libration motion of a period of approximately 24 years with a coefficient of about $0''022$. The short periodic motions over a period of six years average about $0''2 - 0''3$.

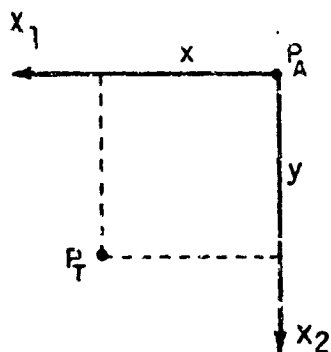
POLE

5.4.1 Effect on the Position of a Station

This motion of the pole means that the observing stations are moving with respect to our "Earth-fixed" coordinate system used in GEODYN. The station positions must be corrected for this effect.

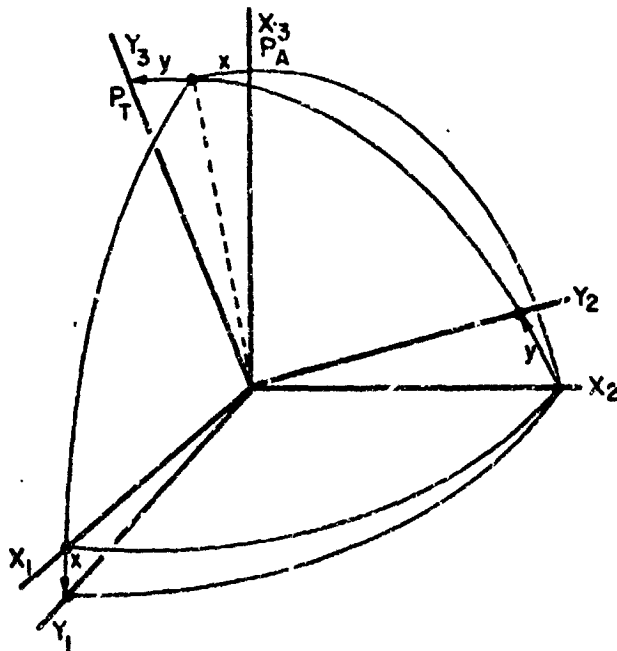
The position of the instantaneous or true pole is computed by linear interpolation in a table of observed values for the true pole relative to the mean pole of 1900 - 1905. The table increment is 10 days; the current range of data is from December 1, 1960 to June 1, 1972. The user should be aware of the fact that this table is expanded as new information becomes available. If the requested time is not in the range of the table, the value for the closest time is used.

The data in the table is in the form of the coordinates of the true pole relative to the mean pole measured in seconds of arc. This data was obtained from "Circular D" which is published by BIH. The appropriate coordinate system and rotation are illustrated in Figures 1 and 2.



- P_A = Center of Coordinate System
 = Adopted Mean Pole
 x_1 = Direction of 1st Principal Axis (along meridian directed to Greenwich)
 x_2 = Direction of 2nd Principal Axis (along 90° West meridian)
 P_T = Instantaneous Axis of Rotation
 x, y = Coordinates of P_T Relative to P_A Measured in seconds of arc

Figure 1: Coordinates of the Instantaneous Axis of Rotation



- x, y = Rectangular Coordinates of P_T Relative to P_A
 $x_1 x_2$ Plane = Mean Adopted Equator Defined by Direction of Adopted Pole P_A
 $y_1 y_2$ Plane = Instantaneous Equator Defined by Direction of Instantaneous Pole P_T

Figure 2: Rotation of Coordinate System from Adopted Mean Pole System to Instantaneous Pole System

Consider the station vector \bar{X} in a system attached to the Earth of the mean pole and the same vector \bar{Y} in the "Earth-fixed" system of GEODYN. The transformation between \bar{Y} and \bar{X} consists of a rotation of x about the X_2 axis and a rotation of y about the X_1 axis; that is

$$\bar{Y} = R_1(y) R_2(x) \bar{X} \quad (1)$$

$$= \begin{bmatrix} 1 & 0 & 0 \\ 0 & \cos y & \sin y \\ 0 & -\sin y & \cos y \end{bmatrix} \begin{bmatrix} \cos x & 0 & \sin x \\ 0 & 1 & 0 \\ \sin x & 0 & \cos x \end{bmatrix} \bar{X}$$

Because x and y are small angles, their cosines are set to 1 and their sines equal to their values in radians. Consequently,

$$\bar{Y} = \begin{bmatrix} 1 & 0 & -x \\ xy & 1 & y \\ x & -y & 1 \end{bmatrix} \bar{X} \quad (2)$$

In the GEODYN system, the position of the true pole is computed by subroutine POLE. The station vectors are referenced to the true pole by subroutine TRUEP.

POLE
TRUEP

5.4.2 Partial Derivatives

The coordinate rotation is defined as

TRUEP

$$\bar{u} = R_1(y) R_2(x) \bar{w}$$

PREDCT
(1)

where

\bar{w} = station vector in a system attached to the Earth of the mean pole.

\bar{u} = station vector in a system attached to the Earth of the true pole.

$R_1(y)$ = matrix of rotation about the X_1 axis

$R_2(x)$ = matrix of rotation about the X_2 axis

August 11, 1973

The rotation matrices are.

$$R_1(y) = \begin{bmatrix} 1 & 0 & 0 \\ 0 & \cos y & \sin y \\ 0 & -\sin y & \cos y \end{bmatrix}$$

$$R_2(x) = \begin{bmatrix} \cos x & 0 & -\sin x \\ 0 & 1 & 0 \\ \sin x & 0 & \cos x \end{bmatrix}$$

Defining

$$\bar{u} = u_1 \hat{i} + u_2 \hat{j} + u_3 \hat{k} \quad (2)$$

$$\bar{w} = w_1 \hat{i} + w_2 \hat{j} + w_3 \hat{k} \quad (3)$$

and performing the matrix multiplications.

$$\begin{aligned} u_1 &= w_1 \cos x - w_3 \sin x \\ u_2 &= w_1 \sin x \sin y + w_2 \cos y + w_3 \cos x \sin y \\ u_3 &= w_1 \sin x \cos y - w_2 \sin y + w_3 \cos x \cos y \end{aligned} \quad (4)$$

The fundamental quantities required for the estimation of polar motion parameters are

$$\frac{\partial m}{\partial x} \quad \text{and} \quad \frac{\partial m}{\partial y}$$

where m is the satellite observation.

Using the chain rule

PREDCT

$$\frac{\partial m}{\partial x} = \frac{\partial m}{\partial u_1} \frac{\partial u_1}{\partial x} + \frac{\partial m}{\partial u_2} \frac{\partial u_2}{\partial x} + \frac{\partial m}{\partial u_3} \frac{\partial u_3}{\partial x}$$

(5)

$$\frac{\partial m}{\partial y} = \frac{\partial m}{\partial u_1} \frac{\partial u_1}{\partial y} + \frac{\partial m}{\partial u_2} \frac{\partial u_2}{\partial y} + \frac{\partial m}{\partial u_3} \frac{\partial u_3}{\partial y}$$

August 11, 1973

The partial derivatives of the satellite observation with respect to the true station coordinates are currently available in GEODYN. The partial derivatives of the station coordinates with respect to the polar motion parameters are:

$$\frac{\partial u_1}{\partial x} = -w_1 \sin x - w_3 \cos x$$

$$\frac{\partial u_1}{\partial y} = 0$$

$$\frac{\partial u_2}{\partial x} = w_1 \cos x \sin y - w_3 \sin x \sin y$$

(6)

$$\frac{\partial u_2}{\partial y} = w_1 \sin x \cos y - w_2 \sin y + w_3 \cos x \cos y$$

$$\frac{\partial u_3}{\partial x} = w_1 \cos x \cos y - w_3 \sin x \cos y$$

$$\frac{\partial u_3}{\partial y} = -w_1 \sin x \sin y - w_2 \cos y - w_3 \cos x \sin y$$

August 11, 1973

Since the angles x and y are small, the following approximations may be made.

$$\begin{aligned}\sin x &= x & \cos x &= 1 \\ \sin y &= y & \cos y &= 1\end{aligned}\tag{7}$$

Substituting equations (7) into equations (6) TRUEP

$$\frac{\partial u_1}{\partial x} = -w_1 x - w_3$$

$$\frac{\partial u_1}{\partial y} = 0$$

$$\frac{\partial u_2}{\partial x} = w_1 y - w_3 x y\tag{8}$$

$$\frac{\partial u_2}{\partial y} = w_1 x - w_2 y + w_3$$

$$\frac{\partial u_3}{\partial x} = w_1 - w_3 x$$

$$\frac{\partial u_3}{\partial y} = -w_1 x y - w_2 - w_3 y$$

SECTION 6.0
MEASUREMENT MODELING AND RELATED DERIVATIVES

The observations in GEODYN are geocentric in nature. The computed values for the observations are obtained by applying these geometric relationships to the computed values for the relative positions and velocities of the satellite and the observer at the desired time.

In addition to the geometric relationships; GEODYN allows for a timing bias and for a constant bias to be associated with a measurement type from a given station. Both of these biases are optional.

The measurement model for GEODYN is therefore

$$C_{t+\Delta t} = f_t(\bar{r}, \dot{\bar{r}}, \bar{r}_{ob}) + b + \dot{f}_t(\bar{r}, \dot{\bar{r}}, \bar{r}_{ob}) \cdot \Delta t \quad (1)$$

where

$C_{t+\Delta t}$ is the computed equivalent of the observation taken at time $t+\Delta t$,

\bar{r} is the Earth-fixed position vector of the satellite,

\bar{r}_{ob} is the Earth-fixed position vector of the station,

$f_t(\bar{r}, \dot{\bar{r}}, \bar{r}_{ob})$ is the geometric relationship defined by the particular observation type at time t ,

b is a constant bias on the measurement, and

Δt is the timing bias associated with the measurement.

The functional dependence of f_t was explicitly stated for the general case. Many of the measurements are functions only of the position vectors and are hence not functions of the satellite velocity vector $\dot{\bar{r}}$. We will hereafter refer to f_t without the explicit functional dependence for rotational convenience.

As was indicated earlier in Section 2.2, we require the partial derivatives of the computed values for the measurements with respect to the parameters being determined (see also Section 10.1). These parameters are:

- the true of date position and velocity of the satellite at epoch. These correspond to the inertial position and velocity which are the initial conditions for the equations of motion,
- force model parameters,
- the Earth-fixed station positions,
- measurement biases.

These parameters are implicitly divided into a set $\bar{\alpha}$ which are not concerned with the dynamics of satellite motion, and a set $\bar{\beta}$ which are,

The partial derivatives associated with the parameters $\bar{\alpha}$; i.e., station positions and measurement biases are computed directly at the given observation times. The partial derivatives with respect to the parameters $\bar{\beta}$; i.e., the epoch position and velocity and the force model parameters, must be determined according to a chain rule:

$$\frac{\partial C_{t+\Delta t}}{\partial \bar{\beta}} = \frac{\partial C_{t+\Delta t}}{\partial \bar{x}_t} \frac{\partial \bar{x}_t}{\partial \bar{\beta}} \quad (2)$$

where

\bar{x}_t is the vector which describes the satellite position and velocity in true of date coordinates.

The partial derivatives $\frac{\partial C_{t+\Delta t}}{\partial \bar{x}_t}$ are computed directly at the given observation times, but the partial derivatives $\frac{\partial \bar{x}_t}{\partial \bar{\beta}}$ may not be so obtained. These latter relate the true of date position and velocity of the satellite at the given time to the parameters at epoch through the satellite dynamics.

The partial derivatives $\frac{\partial \bar{x}_t}{\partial \bar{\beta}}$ are called the variational partials and are obtained by direct numerical integration of the variational equations. As will be shown in Section 8.2, these equations are analogous to the equations of motion.

Let us first consider the partial derivatives of the computed values associated with the parameters in $\bar{\beta}$. We have

$$\frac{\partial C_{t+\Delta t}}{\partial \bar{\beta}} = \frac{\partial f_t}{\partial \bar{x}_t} \frac{\partial \bar{x}_t}{\partial \bar{\beta}} \quad (3)$$

Note that we have dropped the partial derivative with respect to $\bar{\beta}$ of the differential product $f_t \Delta t$. This is because we use first order Taylor series approximation in our error model and hence higher order terms are assumed negligible. This linearization is also completely consistent with the linearization assumptions made in the solution to the estimation equations (Section 10.1).

The partial derivatives $\frac{\partial f_t}{\partial \bar{x}_t}$ are computed by transforming the partial derivatives $\frac{\partial f_t}{\partial \bar{r}}$ and $\frac{\partial f_t}{\partial \bar{r}}$ from the Earth-fixed system to the true of date system (see Section 3.4). These last are the partial derivatives of the geometric relationships given later in this section (6.2).

In summary, the partial derivatives required for computing the $\frac{\partial C_{t+\Delta t}}{\partial \bar{B}}$, the partial derivatives of the computed value for a given measurement, are the variational partials and the Earth-fixed geometric partial derivatives.

The partial derivatives of the computed values with respect to the station positions are simply related to the partial derivatives with respect to the satellite position at time t :

$$\frac{\partial C_{t+\Delta t}}{\partial \bar{r}_{ob}} = \frac{\partial f_t}{\partial \bar{r}_{ob}} = - \frac{\partial f_t}{\partial \bar{r}} \quad (4)$$

where \bar{r} is of course the satellite position vector in Earth-fixed coordinates. This simple relationship is a direct result of the symmetry in position coordinates. The function f is a geometric function of the relative position; i.e., the differences in position coordinates which will be the same in any coordinate system.

The partial derivatives with respect to the biases are obvious:

$$\frac{\partial C_{t+\Delta t}}{\partial b} = 1 \quad (5)$$

$$\frac{\partial C_{t+\Delta t}}{\partial (\Delta t)} = \dot{f}_t \quad (6)$$

In the remainder of this section, we will be concerned with the calculation of the geometric function f_t and its derivatives. These derivatives have been shown above to be the partial derivatives with respect to satellite position and velocity at time t and the time rate of change of the function, \dot{f}_t .

The subroutine breakdown for the calculation of these quantities in GEODYN is as follows: The geometric relationships and the geometric partial derivatives are implemented in subroutine PREDCT. The time rates of change are coded in subroutine OBSDOT.

PREDCT
OBSDOT

The data preprocessing also requires some use of these formulas for computing measurement equivalents. These are then also implemented in subroutine PROCES.

PROCES

6.1 THE GEOMETRIC RELATIONSHIPS

The basic types of observation in GEODYN are:

- right ascension and declination
- range
- range rate
- l and m direction cosines
- X and Y angles
- azimuth and elevation
- altimeter height and rate

The geometric relationship which corresponds to each of these observations is presented below. It should be noted that in addition to the Earth-fixed or inertial coordinate systems, some of these utilize topocentric coordinate systems. These last are presented in Section 5.2.

Range:

Consider the station-satellite vector:

GRHRAN

$$\bar{\rho} = \bar{r} - \bar{r}_{ob} \quad (1)$$

where

\bar{r} is the satellite position vector (x,y,z) in the geocentric Earth-fixed system, and

\bar{r}_{ob} is the station vector in the same system.

The magnitude of this vector, ρ , is the (slant) range, which is one of the measurements.

Range rate:

The time rate of change of this vector $\bar{\rho}$ is

GRHRAN

$$\dot{\bar{\rho}} = \dot{\bar{r}} \quad (2)$$

PREDCT

OBSDOT

as the velocity of the observer in the Earth-fixed system is zero. Let us consider that

$$\bar{\rho} = \rho \hat{u} \quad (3)$$

where

\hat{u} is the unit vector in the direction of $\bar{\rho}$.

Thus we have

GRHRAN
PREDCT
OBSDOT

$$\dot{\rho} = \hat{\rho} \dot{u} + \rho \dot{\hat{u}} \quad (4)$$

The quantity $\dot{\rho}$ in the above equation is the computed value for the range rate and is determined by

$$\dot{\rho} = \hat{u} \cdot \dot{\hat{r}} \quad (5)$$

Altimeter height:

The altimeter height and rate are unique in that the satellite is making the observation. While these are actually measurements from the satellite to the surface of the Earth, they are taken to be measurements of the spheroid height and the time rate of change of that quantity for obvious reasons. Using the formula for spheroid height previously determined in Section 5.1. we have:

PREDCT

$$H_{alt} = r - a_e - \frac{3}{2} a_e f^2 \left(\frac{z}{r}\right)^4 + (a_e f + \frac{3}{2} a_e f^2) \left(\frac{z}{r}\right)^2 \quad (6)$$

where

PREDCT

a_e is the Earth's mean equatorial radius,

f is the Earth's flattening, and

z is r_3 , the z component of the Earth-fixed satellite vector.

Altimeter rate:

The altimeter rate is determined by a chain rule:

PREDCT

$$\dot{H}_{alt} = \nabla H_{alt} \cdot \dot{\mathbf{r}} \quad (7)$$

The required partial derivatives are given in the section on geometric partials.

Right ascension and declination:

PREDCT

The topocentric right ascension α and declination δ are inertial coordinate system measurements as illustrated in Figure 1. GEODYN computes these angles from the components of the Earth-fixed station-satellite vector and the Greenwich hour angle θ_g .

$$\alpha = \tan^{-1} \left(\frac{\rho_2}{\rho_1} \right) + \theta_g \quad (8)$$

$$\delta = \sin^{-1} \left(\frac{\rho_3}{\rho} \right) \quad (9)$$

The remaining measurements are in the topocentric horizon coordinate system. These all require the \hat{N} , \hat{Z} , and \hat{E} (north, zenith, and east base line) unit vectors which describe the coordinate system.

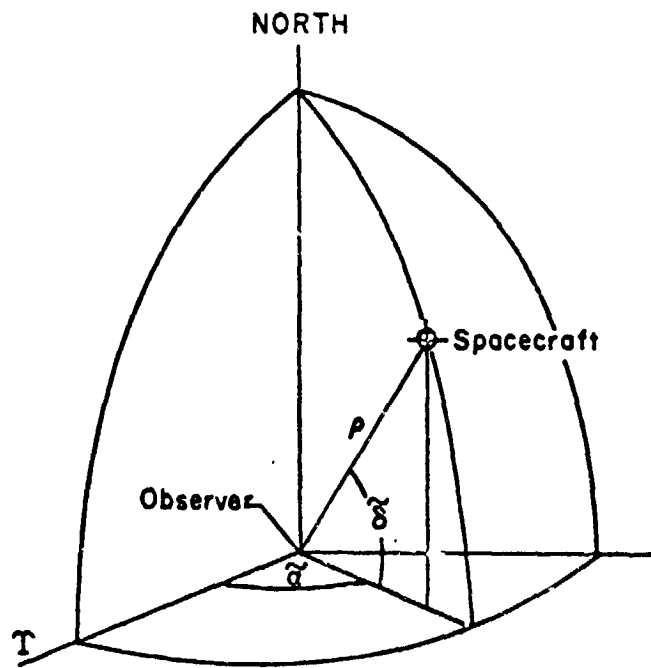


FIGURE 1. Topocentric right ascension & declination angles

Direction cosines:

There are three direction cosines associated with the station-satellite vector in the topocentric system. These are: PREDCT

$$l = \hat{u} \cdot \hat{E} \quad (10)$$

$$m = \hat{u} \cdot \hat{N}$$

$$n = \hat{u} \cdot \hat{Z}$$

The l and m direction cosines are observation types for GEODYN.

X and Y angles:

The X and Y angles are illustrated in Figure 2. They are computed by

$$X_a = \tan^{-1} \left(\frac{l}{n} \right) \quad (11)$$

$$Y_a = \sin^{-1} (m) \quad (12)$$

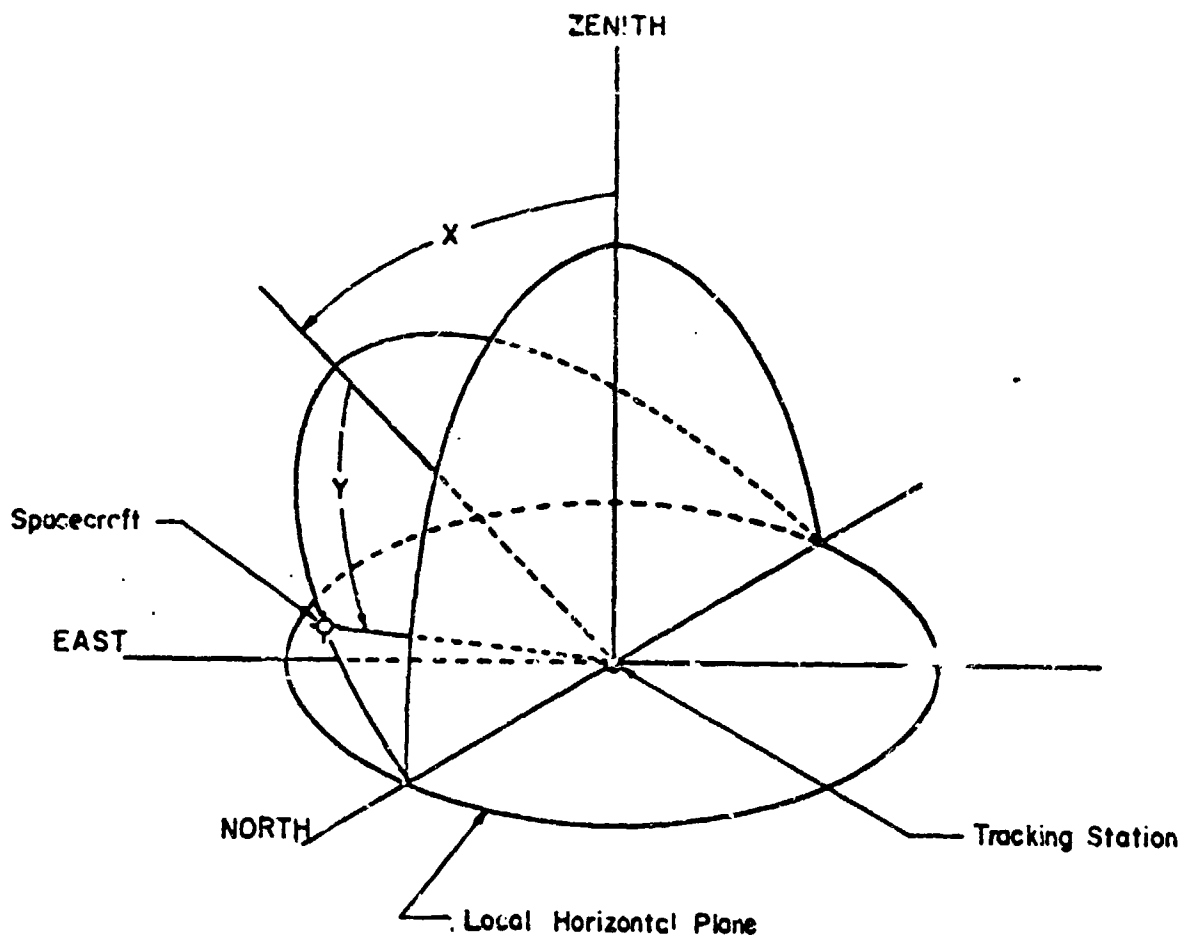


FIGURE 2. X and Y Angles

Figure 3 illustrates the measurements of azimuth and elevation. These angles are computed by:

PREDCT

$$A_z = \tan^{-1} \frac{l}{m} \quad (13)$$

$$E_l = \sin^{-1} (n) \quad (14)$$

6.2 THE GEOMETRIC PARTIAL DERIVATIVES

PREDCT

The partial derivatives for each of the calculated geometric equivalents with respect to the satellite positions and velocity are given here. All are in the geocentric, Earth-fixed system. (The r_i refer to the Earth-fixed components of \bar{r} .)

Range:

$$\frac{\partial \rho}{\partial r_i} = \frac{\rho_i}{\rho} \quad (1)$$

Range rate:

$$\frac{\partial \dot{\rho}}{\partial r_i} = \frac{1}{\rho} \left[\dot{r}_i - \frac{\dot{\rho} \rho_i}{\rho} \right] \quad (2)$$

$$\frac{\partial \dot{\rho}}{\partial \dot{r}_i} = \frac{\rho_i}{\rho} \quad (3)$$

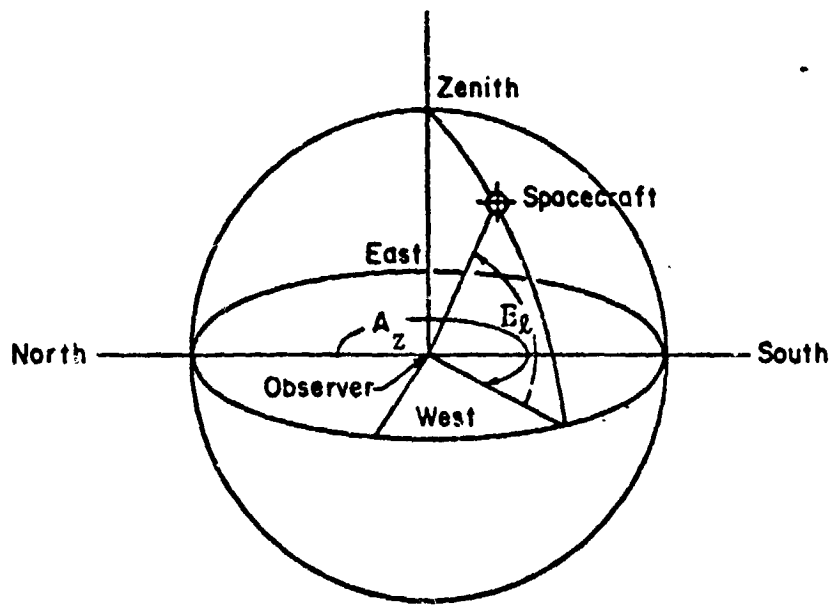


FIGURE 3. Azimuth and Elevation Angles

Altimeter range:

$$\frac{\partial H_{alt}}{\partial r_i} = \frac{r_i}{r} + \frac{1}{r} \left[\left(2 a_e f + 3 a_e f^2 \right) \left(\frac{z}{r} \right) \right. \quad (4)$$

$$\left. - 6 a_e f^2 \left(\frac{z}{r} \right)^3 \right] \times$$

$$\left[\frac{\partial z}{\partial r_i} - \frac{z x_i}{r^2} \right]$$

Altimeter Range Rate:

$$\frac{\dot{\partial H}_{alt}}{\partial r_i} = \frac{\partial}{\partial r_i} \left(\nabla H_{alt} \right) \cdot \dot{\bar{r}} \quad (5)$$

$$\frac{\partial^2 H_{alt}}{\partial r_i \partial r_j} = \frac{1}{r} \left[\frac{\partial r_i}{\partial r_j} - \frac{r_i r_j}{r^2} \right] \quad (6)$$

$$+ \left[\left(2 a_e f + 3 a_e f^2 \right) \left(\frac{z}{r} \right) - 6 a_e f^2 \left(\frac{z}{r} \right)^3 \right] \times$$

$$\left[\frac{1}{r^2} \left(\frac{-r_j}{r} \frac{\partial z}{\partial r_i} - \frac{r_i}{r} \frac{\partial z}{\partial r_j} + \frac{3 z r_i r_j}{r^3} \right. \right.$$

$$\left. \left. - \frac{z}{r} \frac{\partial r_i}{\partial r_j} \right) \right] +$$

PREDCT

$$\left[\left(2 a_e f + 3 a_e f^2 \right) - 18 a_e f^2 \left(\frac{z}{r} \right)^2 \right] \chi$$

$$\left[\frac{1}{r} \frac{\partial z}{\partial r_i} - \frac{z r_i}{r^3} \right] \left[\frac{1}{r} \frac{\partial z}{\partial r_j} - \frac{z r_j}{r^3} \right]$$

$$\frac{\partial \dot{H}_{alt}}{\partial r_i} = \frac{\partial H_{alt}}{\partial r_i}$$

Right Ascension:

$$\frac{\partial \alpha}{\partial r_1} = \frac{-\rho_2}{\sqrt{\rho_1^2 + \rho_2^2}} \quad (7)$$

$$\frac{\partial \alpha}{\partial r_2} = \frac{\rho_1}{\sqrt{\rho_1^2 + \rho_2^2}} \quad (8)$$

$$\frac{\partial \delta}{\partial r_3} = 0 \quad (9)$$

Declination:

$$\frac{\partial \delta}{\partial r_1} = \frac{-\rho_1 \rho_3}{\rho_1^2 \sqrt{\rho_1^2 + \rho_2^2}} \quad (10)$$

$$\frac{\partial \delta}{\partial r_2} = \frac{-\rho_2 \rho_3}{\rho \sqrt{\rho_1^2 + \rho_2^2}} \quad (11) \text{ PREDCT}$$

$$\frac{\partial \delta}{\partial r_3} = \frac{\sqrt{\rho_1^2 + \rho_2^2}}{\rho^2} \quad (12)$$

Direction Cosines:

$$\frac{\partial l}{\partial r_i} = \frac{1}{\rho} \left[E_i - \rho u_i \right] \quad (13)$$

$$\frac{\partial m}{\partial r_i} = \frac{1}{\rho} \left[N_i - \rho u_i \right] \quad (14)$$

$$\frac{\partial n}{\partial r_i} = \frac{1}{\rho} \left[Z_i - \rho u_i \right] \quad (15)$$

X and Y Angles:

PREDCT

$$\frac{\partial X_a}{\partial r_i} = \frac{nE_i - \ell Z_i}{\rho(1-m^2)} \quad (16)$$

$$\frac{Y_a}{\partial r_i} = \frac{N_i - \mu_i}{\rho\sqrt{1-m^2}} \quad (17)$$

Azimuth and Elevation:

$$\frac{\partial A_z}{\partial r_i} = \frac{mE_i - \ell N_i}{\rho\sqrt{1-n^2}} \quad (18)$$

$$\frac{\partial E_\ell}{\partial r_i} = \frac{Z_i - \nu_i}{\rho(1-n^2)} \quad (19)$$

6.3 THE TIME DERIVATIVES

OBSDOT

The derivatives of each measurement type with respect to time is presented below. All are in the Earth-fixed system.

Range:

$$\dot{\rho} = \hat{u} \cdot \dot{\mathbf{r}} \quad (1)$$

Range Rate:

The range rate derivative deserves special attention. Remembering that

$$\dot{\hat{p}} = \dot{\mathbf{r}}, \quad (2)$$

We write

$$\dot{\rho} = \hat{u} \cdot \dot{\hat{p}} \quad (3)$$

Thus

$$\ddot{\rho} = \hat{u} \cdot \ddot{\hat{p}} + \dot{\hat{u}} \cdot \dot{\hat{p}} \quad (4)$$

Because

OBSDOT

$$\dot{\vec{\rho}} = \frac{d}{dt} (\rho \hat{u}) = \rho \dot{\hat{u}} + \dot{\rho} \hat{u} \quad (5)$$

we may substitute in Equation 4 above for $\dot{\hat{u}}$:

$$\ddot{\vec{\rho}} = \frac{1}{\rho} (\dot{\vec{\rho}} \cdot \dot{\vec{\rho}} - \dot{\rho} \hat{u} \cdot \dot{\vec{\rho}}) + \hat{u} \cdot \ddot{\vec{\rho}} \quad (6)$$

or, as

$$\dot{\vec{\rho}} = \hat{u} \cdot \dot{\vec{\rho}} \quad (7)$$

we may write

$$\ddot{\vec{\rho}} = \frac{1}{\rho} (\dot{\vec{\rho}} \cdot \dot{\vec{\rho}} - \dot{\rho}^2 + \dot{\rho} \cdot \ddot{\vec{\rho}}) \quad (8)$$

In order to obtain $\ddot{\vec{\rho}}$, we use the limited gravity potential (see Section 8.3).

$$U = \frac{GM}{r} \left(1 - \frac{C_{20} a^2 e^2}{r^2} P_2^0(\sin \phi) \right) \quad (9)$$

The gradient of this potential with respect to the Earth-fixed position coordinates of the satellite is the part of $\ddot{\rho}$ due to the geopotential:

OBSDOT

$$\frac{\partial U}{\partial r_i} = -\frac{GM}{r^3} \left[1 - \frac{3 a_e^2 C_{20}}{2 r^2} \left(5 \sin^2 \phi - 1 - 2 \frac{z}{r_i} \right) \right] r_i \quad (10)$$

We must add to this the effect of the rotation of the coordinate system. (The Earth-fixed coordinate system rotates with respect to the true of date coordinates with a rate $\dot{\theta}_g$, the time rate of change of the Greenwich hour angle.)

The components of $\ddot{\rho}$ are then

$$\ddot{\rho}_1 = \frac{\partial U}{\partial r_1} + [\dot{x} \cos \theta_g + \dot{y} \sin \theta_g] \dot{\theta}_g + \dot{r}_2 \dot{\theta}_g \quad (11)$$

$$\ddot{\rho}_2 = \frac{\partial U}{\partial r_2} + [-\dot{x} \sin \theta_g + \dot{y} \cos \theta_g] \dot{\theta}_g - \dot{r}_1 \dot{\theta}_g \quad (12)$$

$$\ddot{\rho}_3 = \frac{\partial U}{\partial r_3} = \frac{\partial U}{\partial z} \quad (13)$$

The bracketed quantities above correspond to the coordinate transformations coded in subroutines XEFIX and YEFIX. These transforms are used on the true of date satellite velocity components \dot{x} and \dot{y} . The interested reader should refer to Section 3.4 for further information on transformations between Earth-fixed and true of date coordinates.

OBSDOT
XEFIX
YEFIX

It should be noted that all quantities in this formula, with the exception of those quantities bracketed, are Earth-fixed values. (The magnitude r is invariant with respect to the coordinate system transformations.)

The remaining time derivatives are tabulated here:

$$\text{Right ascension: } \dot{\alpha} = \frac{u_1 \dot{r}_2 - u_2 \dot{r}_1}{\rho (1 - u_3^2)} \quad (14)$$

$$\text{Declination: } \dot{\delta} = \frac{\dot{r}_3 - \rho \dot{u}_3}{\rho \sqrt{1 - u_3^2}} \quad (15)$$

$$\text{Direction Cosines: } \dot{l} = \frac{\dot{\rho} \cdot \hat{E} - l \dot{\rho}}{\rho} \quad (16)$$

$$\dot{m} = \frac{\dot{\rho} \cdot \hat{N} - m \dot{\rho}}{\rho} \quad (17)$$

X and Y angles: $\dot{X}_a = \frac{\dot{\rho} \cdot (n \hat{E} - \ell \hat{Z})}{\rho (1-m^2)}$ (18) OBSDOT

$$\dot{Y}_a = \frac{\dot{\rho} \cdot \hat{N} - m \dot{\rho}}{\rho \sqrt{1-m^2}} \quad (19)$$

Azimuth: $\dot{A}_z = \frac{\dot{\rho} \cdot (m \hat{E} - \ell \hat{N})}{\rho (1-m^2)}$ (20)

Elevation: $\dot{E}_\ell = \frac{\dot{\rho} \cdot \hat{Z} - m \dot{\rho}}{\rho \sqrt{1-m^2}}$ (21)

6.4 SATELLITE-SATELLITE TRACKING

The fundamental satellite-satellite measurement used by the GEODYN program is shown in Figure 1. A signal is transmitted from a ground tracking station to one satellite where it is then relayed to a second satellite. The second satellite in turn relays the signal back to the first satellite where it is relayed to the original ground station. The fundamental measurement made is the transit time for this relay process. Properly corrected for various time delays, this measurement can be transformed into the sum of the range from the ground station to the first satellite and the range from the first satellite to the second satellite. The time rate of change of this measurement is also handled by the GEODYN program.

6.4.1 Satellite-Satellite Tracking Measurement Calculations

TWOSTA

Given the ephemerides of the two satellites, the range sum type measurement can be calculated in a rather straightforward manner. The most important aspect of the calculation is to insure that the correct times are used for the satellites and ground station. That is, transit times and transponder delays must be correctly accounted for.

To see the times needed for the range sum calculation, refer to Figure 1. Let

- $R_s(t)$ = the range sum measurement at time t
- R_{1u} = the up-link range from the ground to the relay satellite
- R_{2d} = the relay satellite-tracked satellite range

REPRODUCIBILITY OF THE
ORIGINAL PAGE IS POOR

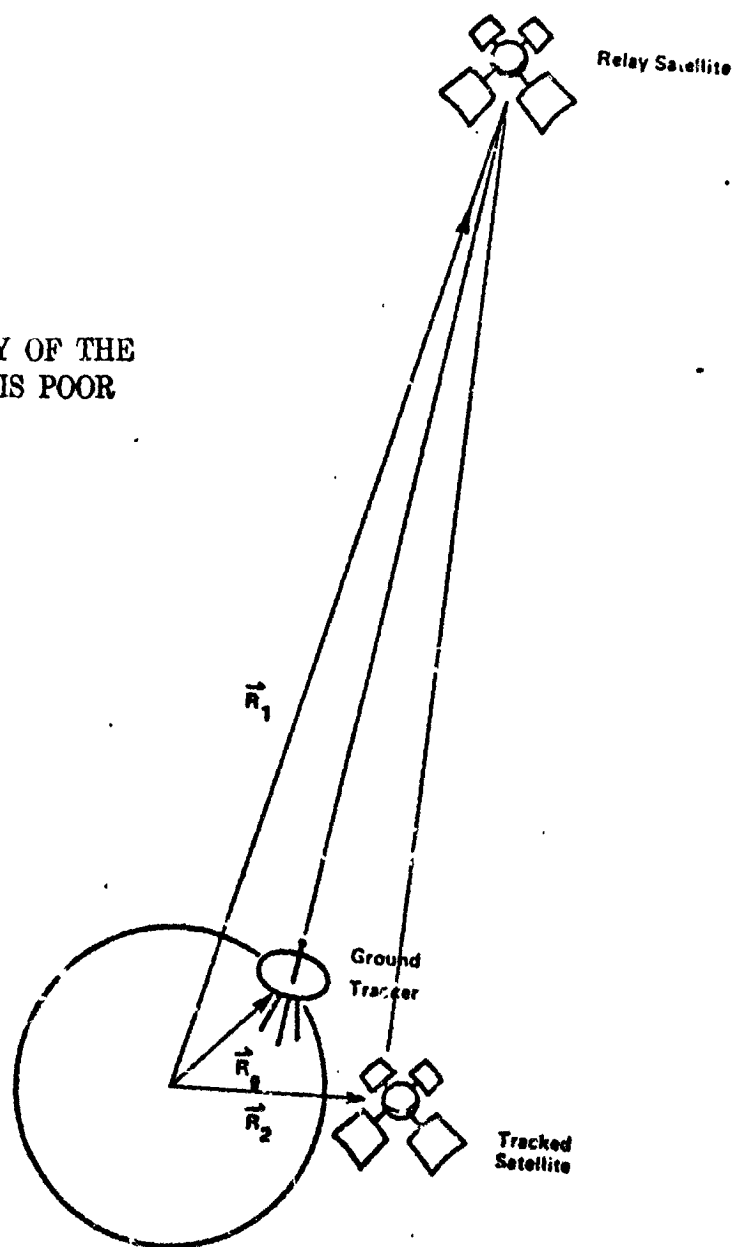


Figure 1. Geometry for Satellite-Satellite Tracking

- R_{2u} = the tracked satellite-relay satellite range
 R_{1d} = the down-link range from the relay satellite to the ground
 $R_g(t), R_1(t), R_2(t)$ = the range vector from the center of the earth to the ground station, relay satellite, and tracked satellite, respectively, at time t
 d_1 = the transponder delay in the relay satellite
 d_2 = the transponder delay in the tracked satellite
 Δt_{1u} = the transit time for the range R_{1u}
 Δt_{2d} = the transit time for the range R_{2d}
 Δt_{2u} = the transit time for the range R_{2u}
 Δt_{1d} = the transit time for the range R_{1d}

The range sum measurement is expressed in terms of the range components as

$$2R_s(t) = R_{1u} + R_{2d} + R_{2u} + R_{1d} \quad (1)$$

Each of the ranges on the right hand side is a function of two different times. Expressing the ranges in terms of the range vectors from the center of the earth and explicitly indicating the times, the measurement R_s is expressible as

$$\begin{aligned}
2R_s(t) = & |\bar{R}_1(t - \Delta t_{1d}) - \bar{R}_g(t)| \\
& + |\bar{R}_2(t - \Delta t_{1d} - d_1 - \Delta t_{2u}) - \bar{R}_1(t - \Delta t_{1d} - d_1)| \\
& + |\bar{R}_1(t - \Delta t_{1d} - d_1 - \Delta t_{2u} - d_2 - \Delta t_{2d}) - \bar{R}_2(t - \Delta t_{1d} - d_1 - \Delta t_{2u} - d_2)| \\
& + |\bar{R}_1(t - \Delta t_{1d} - 2d_1 - \Delta t_{2u} - d_2 - \Delta t_{2d}) \\
& \quad - \bar{R}_g(t - \Delta t_{1d} - 2d_1 - \Delta t_{2u} - d_2 - \Delta t_{2d} - \Delta t_{1u})|
\end{aligned}
\tag{2}$$

This expression shows that the ground station and satellite positions must each be known for several different times.

Summarizing:

a. Ground station position needed at times

1. t
2. $t - \Delta t_{1d} - 2d_1 - \Delta t_{2u} - d_2 - \Delta t_{2d} - \Delta t_{1u}$

b. Relay satellite position needed at times

1. $t - \Delta t_{1d}$
2. $t - \Delta t_{1d} - d_1$
3. $t - \Delta t_{1d} - d_1 - \Delta t_{2u} - d_2 - \Delta t_{2d}$
4. $t - \Delta t_{1d} - 2d_1 - \Delta t_{2u} - d_2 - \Delta t_{2d}$

c. Tracked satellite position needed at times

1. $t - \Delta t_{1d} - d_1 - \Delta t_{2u}$
2. $t - \Delta t_{1d} - d_1 - \Delta t_{2u} - d_2$

The transponder delay which is most critical is that of the tracked satellite because, for the planned tracking geometries, the range rate between the relay and tracked satellite is expected to be much higher than the ground-relay satellite range rate. This maximum rate can be only on the order of 5×10^3 m/sec, however, and a 4 μ sec transponder delay would be necessary to introduce a measurement computation error of 1 cm. Since actual S-band transponder delays are generally no longer than this, we may neglect transponder delays in the measurement calculation and still retain accuracies at the centimeter level.

With the neglect of transponder delays, we are left with 2 times for which the ground station position must be computed, 2 times for which the relay satellite position must be computed, and 1 time for which the tracked satellite position must be computed. Eqn. (2) can then be written in the slightly simpler looking form:

$$\begin{aligned}
 2R_s(t) = & |\bar{R}_1(t-\Delta t_{1d}) - \bar{R}_g(t)| \\
 & + |\bar{R}_2(t-\Delta t_{1d}-\Delta t_{2u}) - \bar{R}_1(t-\Delta t_{1d})| \\
 & + |\bar{R}_1(t-\Delta t_{1d}-\Delta t_{2u}-\Delta t_{2d}) - \bar{R}_2(t-\Delta t_{1d}-\Delta t_{2u})| \\
 & + |\bar{R}_1(t-\Delta t_{1d}-\Delta t_{2u}-\Delta t_{2d}) - \bar{R}_g(t-\Delta t_{1d}-\Delta t_{2u}-\Delta t_{2d}-\Delta t_{1u})|
 \end{aligned}
 \tag{3}$$

REPRODUCIBILITY OF THE ORIGINAL PAGE IS POOR

TWOSTA

This is the form used by GEODYN to calculate the range sum measurement. The range sum rate measurement is calculated from the time derivative of this expression. To see how this calculation is performed, note that, e.g., the final down leg range is

$$|\bar{R}_1(t-\Delta t_{1d}) - \bar{R}_g(t)| = \{[\bar{R}_1(t-\Delta t_{1d}) - \bar{R}_g(t)] \cdot [\bar{R}_1(t-\Delta t_{1d}) - \bar{R}_g(t)]\}^{1/2}$$

and that its time derivative is

$$\frac{d}{dt} \left[\bar{R}_1(t - t_{1d}) - \bar{R}_g(t) \right] = \frac{[\dot{\bar{R}}_1(t - \Delta t_{1d}) - \dot{\bar{R}}_g(t)] \cdot [\bar{R}_1(t - \Delta t_{1d}) - \bar{R}_g(t)]}{\{[\bar{R}_1(t - \Delta t_{1d}) - \bar{R}_g(t)] \cdot [\bar{R}_1(t - \Delta t_{1d}) - \bar{R}_g(t)]\}^{1/2}} \quad (4)$$

The calculation thus requires the satellite velocities, and the station inertial velocity, at the same times as were needed for the range sum computation. The satellite velocities are always computed by the GEODYN integrator along with the satellite positions, so only the station inertial velocities are needed as additional input to the range sum rate calculation.

6.4.2 Partial Derivative Calculations for Satellite-Satellite Tracking Measurements

Differential corrections for epoch element and force model parameter errors require the computation of the partial derivatives of the measurements with respect to these adjusted parameters. Let γ be one of these parameters. Then, since the range and range rate measurements are explicit functions of the satellite coordinates only, the partial derivatives of R_s , e.g., can be written from Eqn. (1) as

$$\begin{aligned} \frac{\partial R_s}{\partial \gamma} = & \frac{1}{2} \left[\frac{\partial R_{1u}}{\partial X_{1i}} + \frac{\partial R_{2d}}{\partial X_{1i}} + \frac{\partial R_{2u}}{\partial X_{1i}} + \frac{\partial R_{1d}}{\partial X_{1i}} \right] \frac{\partial X_{1i}}{\partial \gamma} \\ & + \frac{1}{2} \left[\frac{\partial R_{2d}}{\partial X_{2i}} + \frac{\partial R_{2u}}{\partial X_{2i}} \right] \frac{\partial X_{2i}}{\partial \gamma} \end{aligned} \quad (5)$$

where

X_{1i} , X_{2i} are the inertial cartesian position coordinates of the relay and tracked satellite, respectively. Summation over i from 1 to 3 is implied.

REPRODUCIBILITY OF THE
ORIGINAL PAGE IS POOR

Eqn. (5) is shown in a somewhat simplified form, since the different range sum components depend upon the satellite coordinates at slightly different times. For partial derivative computations, however, this slight time difference is negligible. The partial derivatives of the satellite coordinates with respect to the γ parameters are obtained by independently integrating the appropriate variational equations for each satellite in the same manner in which GEODYN integrated these equations for one satellite.

Eqn. (5) can be simplified somewhat by noting that

$$\frac{\partial R_{2d}}{\partial X_{1i}} = - \frac{\partial R_{2d}}{\partial X_{2i}} \quad (6a)$$

$$\frac{\partial R_{2u}}{\partial X_{1i}} = - \frac{\partial R_{2u}}{\partial X_{2i}} \quad (6b)$$

$$\frac{\partial R_{2d}}{\partial X_{1i}} = \frac{\partial R_{2u}}{\partial X_{1i}} \quad (6c)$$

$$\frac{\partial R_{1u}}{\partial X_{1i}} = \frac{\partial R_{1d}}{\partial X_{1i}} \quad (6d)$$

Using (6a) - (6d), Eqn. (5) can be written

TWOSTA

$$\frac{\partial R_s}{\partial \gamma} = \frac{\partial R_{1d}}{\partial X_{1i}} \frac{\partial X_{1i}}{\partial \gamma} + \frac{\partial R_{2d}}{\partial X_{1i}} \left(\frac{\partial X_{1i}}{\partial \gamma} - \frac{\partial X_{2i}}{\partial \gamma} \right) \quad (7)$$

and is a sufficiently accurate form for the range sum partial derivative calculation.

The partial derivatives of the range sum rate measurements are calculated in a similar manner, except that velocity

partials must now be included. Thus, if down leg rate partials are approximately equal to up leg rate partials,

$$\begin{aligned} \frac{\partial \dot{R}_s}{\partial \gamma} &= \frac{\partial \dot{R}_{1u}}{\partial X_{1i}} \frac{\partial X_{1i}}{\partial \gamma} + \frac{\partial \dot{R}_{1u}}{\partial \dot{X}_{1i}} \frac{\partial \dot{X}_{1i}}{\partial \gamma} + \frac{\partial \dot{R}_{2d}}{\partial X_{1i}} \frac{\partial X_{1i}}{\partial \gamma} + \frac{\partial \dot{R}_{2d}}{\partial \dot{X}_{1i}} \frac{\partial \dot{X}_{1i}}{\partial \gamma} \\ &+ \frac{\partial \dot{R}_{2d}}{\partial X_{2i}} \frac{\partial X_{2i}}{\partial \gamma} + \frac{\partial \dot{R}_{2d}}{\partial \dot{X}_{2i}} \frac{\partial \dot{X}_{2i}}{\partial \gamma} \end{aligned} \quad (8)$$

As can be seen from Eqn. (4), relations comparable to Eqn. (5) hold also for the rates, and Eqn. (8) can be written

$$\begin{aligned} \frac{\partial \dot{R}_s}{\partial \gamma} &= \frac{\partial \dot{R}_{1u}}{\partial X_{1i}} \frac{\partial X_{1i}}{\partial \gamma} + \frac{\partial \dot{R}_{1u}}{\partial \dot{X}_{1i}} \frac{\partial \dot{X}_{1i}}{\partial \gamma} + \frac{\partial \dot{R}_{2d}}{\partial X_{1i}} \left(\frac{\partial X_{1i}}{\partial \gamma} - \frac{\partial X_{2i}}{\partial \gamma} \right) \\ &+ \frac{\partial \dot{R}_{2d}}{\partial X_{1i}} \left(\frac{\partial \dot{X}_{1i}}{\partial \gamma} - \frac{\partial \dot{X}_{2i}}{\partial \gamma} \right) \end{aligned} \quad \text{TWOSTA} \quad (9)$$

6.5 PCE MEASUREMENTS TYPES

PREDCT

The PCE measurement types are sets of elements precisely determined in previous GEODYN orbit determination runs.

The inertial Cartesian elements obtained from interpolation of the integrator output are used as the calculated measurements for PCE types, $x, y, z, \dot{x}, \dot{y}, \dot{z}$.

The partials of these measurements are

$$\begin{pmatrix}
 \frac{\partial x}{\partial x} & \frac{\partial x}{\partial y} & \frac{\partial x}{\partial z} & \frac{\partial \dot{x}}{\partial x} & \frac{\partial \dot{x}}{\partial y} & \frac{\partial \dot{x}}{\partial z} \\
 \frac{\partial y}{\partial x} & \frac{\partial y}{\partial y} & \frac{\partial y}{\partial z} & \frac{\partial \dot{y}}{\partial x} & \frac{\partial \dot{y}}{\partial y} & \frac{\partial \dot{y}}{\partial z} \\
 \frac{\partial z}{\partial x} & \frac{\partial z}{\partial y} & \frac{\partial z}{\partial z} & \frac{\partial \dot{z}}{\partial x} & \frac{\partial \dot{z}}{\partial y} & \frac{\partial \dot{z}}{\partial z} \\
 \frac{\partial \dot{x}}{\partial x} & \frac{\partial \dot{x}}{\partial y} & \frac{\partial \dot{x}}{\partial z} & \frac{\partial \ddot{x}}{\partial x} & \frac{\partial \ddot{x}}{\partial y} & \frac{\partial \ddot{x}}{\partial z} \\
 \frac{\partial \dot{y}}{\partial x} & \frac{\partial \dot{y}}{\partial y} & \frac{\partial \dot{y}}{\partial z} & \frac{\partial \ddot{y}}{\partial x} & \frac{\partial \ddot{y}}{\partial y} & \frac{\partial \ddot{y}}{\partial z} \\
 \frac{\partial \dot{z}}{\partial x} & \frac{\partial \dot{z}}{\partial y} & \frac{\partial \dot{z}}{\partial z} & \frac{\partial \ddot{z}}{\partial x} & \frac{\partial \ddot{z}}{\partial y} & \frac{\partial \ddot{z}}{\partial z}
 \end{pmatrix} = \begin{pmatrix}
 1 & 0 & 0 & 0 & 0 & 0 \\
 0 & 1 & 0 & 0 & 0 & 0 \\
 0 & 0 & 1 & 0 & 0 & 0 \\
 0 & 0 & 0 & 1 & 0 & 0 \\
 0 & 0 & 0 & 0 & 1 & 0 \\
 0 & 0 & 0 & 0 & 0 & 1
 \end{pmatrix}$$

The osculating elements obtained by conversion of the above mentioned Cartesian elements are used as the calculated measurements for PCE types, $a, e, i, \Omega, \omega, M$.

The partials for these measurements are given in Section 11.4.

6.6 VLBI MEASUREMENT TYPES

TWOSTA

The geometry for the VLBI measurements used by the GEODYN program is shown in Figure 1. A signal is transmitted from one satellite to two ground stations.

VLBI Time Delay Measurement Calculation:

$$\tau_g = \tau_2 - \tau_1 \quad (1)$$

$$\tau_1 = \frac{\rho_1}{c}$$

$$\tau_2 = \frac{\rho_2}{c}$$

τ_g - is the time delay measurement.

τ_1 - is the light time for the first ground station.

τ_2 - is the light time for the second ground station.

ρ_1 - is the first station-satellite range.

ρ_2 - is the second station-satellite range.

c - is the velocity of light.

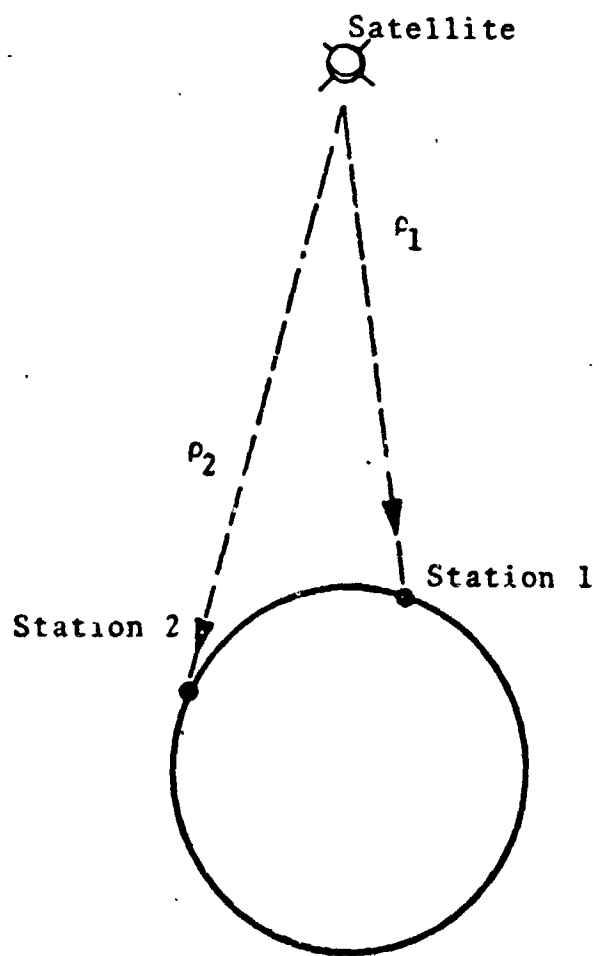


Figure 1. Geometry of VLBI Measurement Type

Partial Derivative:

TWOSTA

$$\frac{\partial \tau_g}{\partial r_i} = \frac{1}{c} \left[\frac{\partial \rho_2}{\partial r_i} - \frac{\partial \rho_1}{\partial r_i} \right] \quad (2)$$

and the partials $\frac{\partial \rho_2}{\partial r_i}$, $\frac{\partial \rho_1}{\partial r_i}$ are given in Section 6.2.

VLBI Fringe Rate Measurement Calculation:

$$v_F = \frac{f}{c} [\dot{\rho}_2 - \dot{\rho}_1] \quad (3)$$

where

f - is transmitter frequency.

$\dot{\rho}_2$ - is the time derivative of ρ_2

$\dot{\rho}_1$ - is the time derivative of ρ_1 .

Partial Derivative:

$$\frac{\partial v_F}{\partial r_i} = \frac{f}{c} \left[\frac{\partial \dot{\rho}_2}{\partial r_i} - \frac{\partial \dot{\rho}_1}{\partial r_i} \right] \quad (4)$$

where the partials $\frac{\partial \dot{\rho}_2}{\partial r_i}$, $\frac{\partial \dot{\rho}_1}{\partial r_i}$ are given in Section 6.2.

6.7 AVERAGE RANGE RATE MEASUREMENT TYPES

Figure 1 illustrates the geometry of the average range rate measurement types. A signal is transmitted from a transmitter to a satellite, then a ground station receives the signal from the satellite, and,

ρ_T - is the transmitter-satellite range

ρ_R - is the satellite-receiver range

\bar{R}_R - is the position vector of the receiver

\bar{R}_T - is the position vector of the transmitter

\bar{R}_S - is the position vector of the satellite.

If t_6 is the recorded time of the end of the doppler counting interval at the receiver and, if T is the length of the counting interval, then the average range rate measurement is

$$\frac{\dot{\rho}}{\rho} = \frac{\rho_R(t_6, t_5) + \rho_T(t_5, t_4) - \rho_R(t_3, t_2) - \rho_T(t_2, t_1)}{2T} \quad (1)$$

Where it is necessary to iterate for the satellite and transmitter times,

$$t_5 = t_6 - \frac{\rho_R(t_6, t_5)}{c}$$

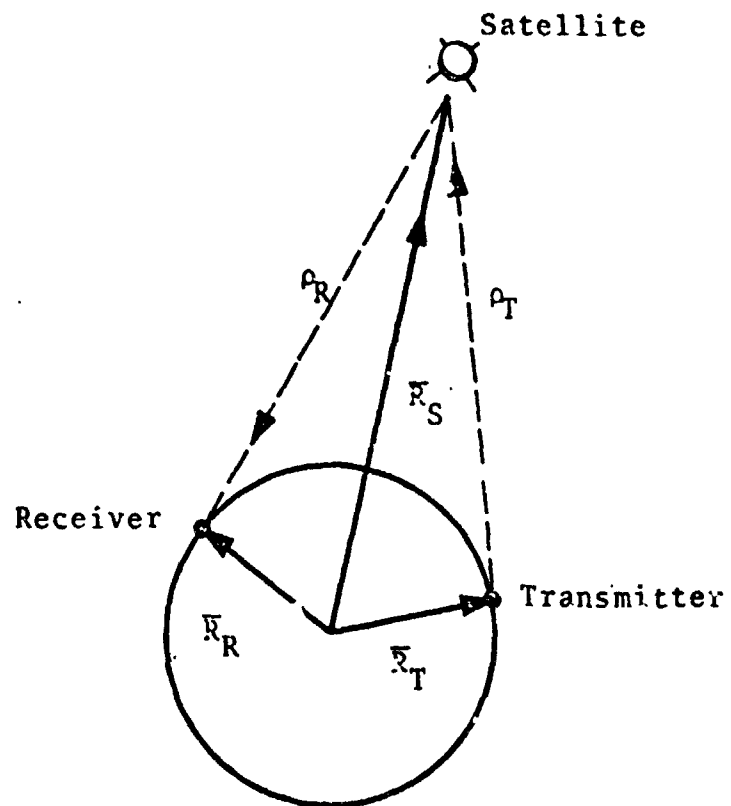


Figure 1. Geometry for Average Range Rate Measurement

$$t_4 = t_5 - \frac{\rho_T(t_5, t_4)}{c}$$

$$t_3 = t_6 - T$$

$$t_2 = t_3 - \frac{\rho_R(t_3, t_2)}{c}$$

$$t_1 = t_2 - \frac{\rho_T(t_2, t_1)}{c}$$

and where

$$\rho_R(t_6, t_5) = |\bar{R}_R(t_6) - \bar{R}_S(t_5)|$$

$$\rho_T(t_5, t_4) = |\bar{R}_T(t_4) - \bar{R}_S(t_5)|$$

$$\rho_R(t_3, t_2) = |\bar{R}_R(t_3) - \bar{R}_S(t_2)|$$

$$\rho_T(t_2, t_1) = |\bar{R}_T(t_1) - \bar{R}_S(t_2)|$$

(2)

A two-way average range rate measurement is a special case of the three-way average range rate measurement (i.e., the receiver and the transmitter are the same). Therefore,

$$\rho_T = \rho_R, \quad \bar{R}_T = \bar{R}_R$$

The Partial Derivatives are

TWOSTA

$$\frac{\partial \dot{\rho}}{\partial r_i} = \frac{1}{2^m} \left[\frac{\partial \rho_R(t_6, t_5)}{\partial r_i} + \frac{\partial \rho_T(t_5, t_4)}{\partial r_i} - \frac{\partial \rho_R(t_3, t_2)}{\partial r_i} - \frac{\partial \rho_T(t_2, t_1)}{\partial r_i} \right]$$

where the partial $\frac{\partial \rho}{\partial r_i}$ is given in Section 6.2.

SECTION 7.0
DATA PREPROCESSING

The function of data preprocessing is to convert and correct the data. These corrections and conversions relate the data to the physical model and to the coordinate and time reference systems used in GEODYN. The data corrections and conversions implemented in GEODYN are to

- transform all observation times to A1 time at the satellite
- refer right ascension and declination observations to the true equator and equinox of date.
- correct range measurements for transponder delay and gating effects
- correct SAC right ascension and declination observations for diurnal aberration
- correct for refraction
- convert TRANET Doppler observations into range rate measurements.

These conversions and corrections are applied to the data on the first iteration of each arc. Each of these preprocessing items is considered in greater detail in the subsections which follow.

7.1 TIME PREPROCESSING

The time reference system used to specify the time of each observation is determined by a time identifier on the data record. This identifier also specifies whether the time recorded was the time at the satellite or at the observing station.

The preprocessing in GEODYN transforms all observations to A1 time in either GEOSRD or DODSRD. If the time recorded is the time at the station, it is converted to time at the satellite. This conversion is applied in subroutine PROCES using a correction equal to the propagation time between the spacecraft and the observing station. The station-satellite distance used for this correction is computed from the initial estimate of the trajectory.

DODSRD
GEOSRD
PROCES

There is special preprocessing for right ascension and declination measurements from the GEOS satellites when input in National Space Science Data Center format. If the observation is passive, the image recorded is an observation of light reflected from the satellite and the times are adjusted for propagation delay as above. If the observation is active, the image recorded is an observation of light transmitted from the optical beacon on the satellite. The beacons on the GEOS satellites are programmed to produce a sequence of seven flashes at four second intervals starting on an even minute. For the active observations, the times are set equal to the programmed flash time with a correction applied for known clock errors (Reference 1), plus half a millisecond, the time allowed for flash buildup.

GEOSRD

The corrections for the active observations are applied in GEOSRD, which calls SATCLC and SATCL2 to evaluate the corrections for GEOS 1 and GEOS 2, respectively. These routines compute the correction by simple linear interpolation in a table of known errors in the satellite on-board clock.

GEOSRD
SATCLC
SATCL2

7.2 REFERENCE SYSTEM CONVERSION TO TRUE OF DATE

DODSRD
EQUATR
GEOSRD

The camera observations, right ascension and declination, may be input referred to the mean equator and equinox of date, to the true equator and equinox of date, or to the mean equator and equinox of some standard epoch. The GEODYN system transforms these observations to the true equator and equinox of date in subroutines GEOSRD and DODSRD. The necessary precession and nutation is performed by subroutine EQUATR.

7.3 TRANSPONDER DELAY AND GATING EFFECTS

The range observations may be corrected for transponder delay or gating errors. If requested, the GEODYN subroutine PROCES applies the corrections.

PROCES

The transponder delay correction is computed as a polynomial in the range rate:

$$\Delta\rho = a_0 + a_1 \dot{\rho} + a_2 (\dot{\rho})^2 \quad (1)$$

where a_0 , a_1 , and a_2 depend on the characteristics of the particular satellite.

A gating error is due to the fact that actual range measurements are either time delays between transmitted and received radar pulses or the phase

shifts in the modulation of a received signal with respect to a coherent transmitted signal. Thus there is the possibility of incorrectly identifying the returned pulse or the number of integral phase shifts. The difference between the observed range and the computed range on the first iteration of the arc is used to determine the appropriate correction. The correction is such that there is less than half a gate, where the gate is the range equivalent of the pulse spacing or phase shift. The appropriate gate of course depends on the particular station.

PROCES

7.4 ABERRATION

PROCES

Optical measurements may require corrections (Reference 2) for the effects of annual aberration and diurnal aberration.

Annual Aberration

The corrections to right ascension and declination measurements for annual aberration effects are given by

$$\alpha = \alpha' - \frac{20''.5 (\cos \alpha' \cos \epsilon \cos \epsilon_T + \sin \alpha' \sin \epsilon)}{\cos \delta'}$$

$$\delta = \delta' - 20''.5 [\cos \epsilon \cos \epsilon_T (\tan \alpha' \cos \delta' - \sin \alpha' \sin \delta') + \cos \alpha' \sin \delta' \sin \epsilon]$$

where

PROCES

α - true right ascension of the satellite

α' - observed right ascension of the satellite

δ - true declination of the satellite

δ' - observed declination of the satellite

ϵ_T - true obliquity of date

\bullet - geocentric longitude of the sun in the ecliptic plane

Diurnal Aberration

The corrections to right ascension and declination measurements for diurnal aberration effects are given by

$$\alpha = \alpha' + 0''.320 \cos \phi' \cos h_s \sec \delta'$$

$$\delta = \delta' + 0''.320 \cos \phi' \sin h_s \sin \delta'$$

where

ϕ' - geocentric latitude of the station

h_s - local hour angle measured in the westward direction from the station to the satellite

α - true right ascension of the satellite

α' - observed right ascension of the satellite

δ - true declination of the satellite

δ' - observed declination of the satellite

7.5 REFRACTION CORRECTIONS

The GEODYN system can apply corrections to all of the observational types significantly affected by refraction. The corrections requested are applied by subroutine PROCES.

PROCES

Right Ascension and Declination:

Optical measurements may require corrections (References 3, 4, 5) for the effects of parallactic refraction. These corrections are given by

$$\alpha = \alpha' - \Delta R \sin q / \cos \delta$$

$$\delta = \delta' - \Delta R \cos q$$

where the change in the zenith angle, ΔR , in radians is given by

$$\Delta R = - \frac{0.435 (4.84813) \tan Z_0}{\rho \cos Z_0} [1 - e^{(-1.385) 10^{-4} \rho \cos Z_0}]$$

and

α - true right ascension of the satellite

α' - observed right ascension of the satellite

δ - true declination of the satellite

δ' - observed declination of the satellite

Z_0 - observed zenith angle in radians

ρ - range from the station to the satellite in meters

q - parallactic angle in radians

The parallactic angle q is defined by the intersection of two planes represented by their normal vectors \hat{P}_1 and \hat{P}_2 .

$$\hat{P}_1 = \hat{C}_p \times \hat{u}$$

$$\hat{P}_2 = \hat{v} \times \hat{u}$$

where

$$\hat{C}_p = (0, 0, 1)$$

\hat{v} - unit local vertical at the station

\hat{u} - unit vector pointing from the station to the satellite in inertial space.

Therefore, the sine and cosine of the parallactic angle are given by

$$\cos q = \hat{P}_1 \cdot \hat{P}_2$$

$$\sin q = \hat{P}_3 \cdot \hat{P}_2$$

August 11, 1973

where

PROCES

\hat{P}_1 - unit vector in the \bar{P}_1 direction

\hat{P}_2 - unit vector in the \bar{P}_2 direction

and

$$\hat{P}_3 = \frac{\bar{P}_1 \times \hat{u}}{|\bar{P}_1 \times \hat{u}|}$$

The parallactic angle, q , is measured in the clockwise direction about the station-satellite vector (i.e., a left-handed system is used to define this angle). All vectors and vector cross products used in this formulation conform to a right-handed system.

Range:

PROCES

The refraction correction applied to CNES laser range data is

$$\Delta \rho = \frac{\Delta \rho_n}{\sin E_\ell + (\cot E_\ell) 10^{-3}}$$

and the correction applied to range data from all other tracking systems is

$$\Delta \rho = \frac{2.77 n_s}{328.5(0.026 + \sin E_\ell)} \quad (4)$$

August 11, 1973

where

$\Delta \rho_n$ - is that correction associated with a range observation measured along the direction of the satellite zenith, and is provided along with each observation on the data tape.

E_l is the elevation angle computed from the initial estimate of the trajectory

and

n_s PPM deviation from unity of the surface index of refraction; if this value is not specified, it is assumed to be 328.5.

Range Rate:

For range-rate, the correction $\dot{\Delta \rho}$ is derived from the range correction:

$$\dot{\Delta \rho} = \frac{2.77 n_s \cos E_l}{.328.5(0.026 + \sin E_l)^2} \dot{E}_l \quad (5)$$

where

PROCES

\dot{E}_ℓ is the computed rate of change of elevation.

Elevation:

For elevation observations the correction ΔE_ℓ is computed as follows:

PROCES

$$\Delta E_\ell = \frac{n_s 10^3}{16.44 + 930 \tan E_\ell} \quad (6)$$

Azimuth is not affected by refraction.

Direction Cosines:

The corrections $\Delta \ell$ and Δm are derived from the elevation correction:

$$\Delta \ell = -\sin A_z \sin (E_\ell) \Delta E_\ell \quad (7)$$

$$\Delta m = -\cos A_z \sin (E_\ell) \Delta E_\ell \quad (8)$$

where A_z is the azimuth angle computed from the initial estimate of the trajectory.

PROCES

X and Y Angles:

For X and Y angles the corrections ΔX and ΔY are computed as follows:

$$\Delta X_a = - \frac{\sin A_z \Delta E_\ell}{(\sin^2 E_\ell + \sin^2 A_z \cos^2 E_\ell)} \quad (9)$$

$$\Delta Y_a = - \frac{\cos A_z \sin E_\ell \Delta E_\ell}{\sqrt{1 - \cos^2 A_z \cos^2 E_\ell}} \quad (10)$$

Note that these are also derived from the elevation correction.

7.6 TRANET DOPPLER OBSERVATIONS

TRANET Doppler observations are received as a series of measured frequencies with an associated base frequency for each station pass. Using the following relationship, the GEODYN system converts these observations to range rate measurements in subroutine GEOSRD:

GEOSRD

$$\dot{\rho} = \frac{c(F_B - F_M)}{F_M} \quad (1)$$

where

F_M is the measured frequency,

F_B is the base frequency,

and

c is the velocity of light.

7.7 SATELLITE-SATELLITE TRACKING DATA PREPROCESSING

TEOSTA
UP DCK.

The preprocessing on the satellite-satellite tracking involves the determination of all the appropriate transit times. Because of the station-satellite and inter-satellite distances, this process must be performed iteratively. The required times are computed during the first iteration and are then stored for use in subsequent iterations.

The satellite-satellite tracking measurements are also corrected for tropospheric refraction. The corrections made here are identical to those which would be made on range and range rate measurements to the relay satellite only. Although it is theoretically possible for signals from the relay to low altitude satellite to pass through the atmosphere, such tracking would occur at reduced signal intensity and would be equivalent to the low elevation tracking of satellite from ground based stations. Such data is seldom used in orbit estimation.

The standard procedure for transponder delay corrections on satellite-satellite tracking is to use block data constants for each satellite, with a satellite ID used to identify the appropriate block data entries. Since constants for the transponders to be used for satellite-satellite tracking are not presently available the block data entries must be modified appropriately when the data becomes available.

SECTION 8.0
FORCE MODEL AND VARIATIONAL EQUATIONS

A fundamental part of the GEODYN system requires computing positions and velocities of the spacecraft at each observation time. The dynamics of the situation are expressed by the equations of motion, which provide a relationship between the orbital elements at any given instant and the initial conditions of epoch. There is an additional requirement for variational partials, which are the partial derivatives of the instantaneous orbital elements with respect to the parameters at epoch. These partials are generated using the variational equations, which are analogous to the equations of motion.

8.1 EQUATIONS OF MOTION

In a geocentric inertial rectangular coordinate system, the equations of motion for a spacecraft are of the form.

$$\ddot{\bar{r}} = -\frac{\mu\bar{r}}{r^3} + \bar{A} \quad (1)$$

where

\bar{r} is the position vector of the satellite.

μ is GM, where G is the gravitational constant and M is the mass of the Earth.

\bar{A} is the acceleration caused by the asphericity of the Earth, extra-terrestrial gravitational forces, atmospheric drag, and solar radiation.

This provides a system of second order differential equations which, given the epoch position and velocity components, may be integrated to obtain the position and velocity at any other time. This direct integration of these accelerations in Cartesian coordinates is known as Cowell's method and is the technique used in GEODYN's orbit generator. This method was selected for its simplicity and its capacity for easily incorporating additional perturbative forces.

There is an alternative way of expressing the above equations of motion:

F

$$\ddot{\bar{r}} = \nabla U + \bar{A}_D + \bar{A}_R \quad (2)$$

where

U is the potential field due to gravity,

\bar{A}_D contains the accelerations due to drag, and

\bar{A}_R contains the accelerations due to solar radiation pressure.

This is, of course, just a regrouping of terms coupled with a recognition of the existence of a potential field. This is the form used in GEODYN.

The inertial coordinate system in which these equations of motion are integrated in GEODYN is that system corresponding to the true of date system of 0^h0 of the reference day. The complete definitions for these coordinate systems (and the Earth-fixed system) are presented in Section 3.0.

The evaluation of the accelerations for $\ddot{\mathbf{r}}$ is controlled by subroutine F. This evaluation is performed in the true of date system. Thus there is a requirement that the inertial position and velocity output from the integrator be transformed to the true of date system for the evaluation of the accelerations, and a requirement to transform the computed accelerations from the true of date system to the inertial system. These transformations are performed by subroutine REFCOR (which controls the precession and nutation routines, PRECES and NUTATE) and is controlled by subroutine F.

F
REFCOR

8.2 THE VARIATIONAL EQUATIONS

The variational equations have the same relationship to the variational partials as the satellite position vector does to the equations of motion. The variational partials are defined as the $\frac{\partial \bar{\mathbf{x}}_t}{\partial \bar{\mathbf{B}}}$ where $\bar{\mathbf{x}}_t$ spans the true of date position and velocity of the satellite at a given time; i.e.,

VEVAL

$$\bar{x}_t = \{x, y, z, \dot{x}, \dot{y}, \dot{z}\};$$

VEVAL

and $\bar{\beta}$ spans the epoch parameters; i.e.,

x_0, y_0, z_0	the satellite position vector at epoch
$\dot{x}_0, \dot{y}_0, \dot{z}_0$	the satellite velocity vector at epoch
C_D	the satellite drag factor
\dot{C}_D	the time rate of change of the drag factor
C_R	the satellite emissivity factor
C_{nm}, S_{nm}	gravitational harmonic coefficients for each n, m pair being determined.
χ	surface density coefficients

Let us first realize that the variational partials may be partitioned according to the satellite position and velocity vectors at the given time. Thus the required partials are

$$\frac{\partial \bar{r}}{\partial \bar{\beta}}, \frac{\partial \dot{\bar{r}}}{\partial \bar{\beta}} \quad (1)$$

where

VEVAL

\bar{r} is the satellite position vector (x, y, z)
in the true of date system, and

$\dot{\bar{r}}$ is the satellite velocity vector $(\dot{x}, \dot{y}, \dot{z})$
in the same system.

The first of these, $\frac{\partial \bar{r}}{\partial \beta}$, can be obtained by the double
integration of

$$\frac{d^2}{dt^2} \left(\frac{\partial \bar{r}}{\partial \beta} \right) \quad (2)$$

or rather, since the order of differentiation may be
exchanged,

$$\frac{\partial \ddot{\bar{r}}}{\partial \beta} \quad (3)$$

Note that the second set of partials, $\frac{\partial \dot{\bar{r}}}{\partial \beta}$, may be obtained
by a first order integration of $\frac{\partial \ddot{\bar{r}}}{\partial \beta}$. Hence we recognize
that the quantity to be integrated is $\frac{\partial \ddot{\bar{r}}}{\partial \beta}$. Using the second
form given for the equations of motion in the previous
subsection, the variational equations are given by

$$\frac{\partial \ddot{\bar{r}}}{\partial \bar{\beta}} = \frac{\partial}{\partial \bar{\beta}} (\nabla U + \bar{A}_R + \bar{A}_D) \quad \text{VEVAL} \quad (4)$$

where

U is the potential field due to gravitational effects

\bar{A}_R is the acceleration due to radiation pressure

\bar{A}_D is the acceleration due to drag

The similarity to the equations of motion is now obvious.

At this point we must consider a few items:

VEVAL

- The potential field is a function only of position. Thus we have

$$\frac{\partial}{\partial \bar{\beta}} \left(\frac{\partial U}{\partial r_i} \right) = \sum_{m=1}^3 \left(\frac{\partial^2 U}{\partial r_i \partial r_m} \right) \frac{\partial r_m}{\partial \bar{\beta}} \quad (5)$$

- The partials of solar radiation pressure with respect to the geopotential coefficients, the drag coefficient, and the satellite velocity are zero, and the partials, with respect to satellite position, are negligible.
- Drag is a function of position, velocity, and the drag coefficients. The partials, with respect to the geopotential coefficients and satellite emissivity, are zero, but we have

$$\frac{\partial \bar{A}_D}{\partial \bar{\beta}} = \frac{\partial A_D}{\partial \bar{x}_t} \frac{\partial \bar{x}_t}{\partial \bar{\beta}} + \frac{\partial \bar{A}_D}{\partial C_D} \frac{\partial C_D}{\partial \bar{\beta}} + \frac{\partial \bar{A}_D}{\partial C_D} \frac{\partial \dot{C}_D}{\partial \bar{\beta}} \quad (6)$$

Let us write our variational equations in matrix notation. We define

VEVAL

n to be the number of epoch parameters in $\bar{\beta}$

F is a $3 \times n$ matrix whose j^{th} column vectors are $\frac{\partial \ddot{\bar{r}}}{\partial \beta_j}$

U_{2c} is a 3×6 matrix whose last 3 columns are zero and whose first 3 columns are such that the i, j^{th} element is given by $\frac{\partial^2 U}{\partial r_i \partial r_j}$

D_r is a 3×6 matrix whose j^{th} column is defined by $\frac{\partial \bar{A}_D}{\partial x_{tj}}$

X_m is a $6 \times n$ matrix whose i^{th} row is given by $\frac{\partial \bar{x}_t}{\partial \beta_j}$. Note that X_m contains the variational partials.

f is a $3 \times n$ matrix whose first six columns are zero and whose last $n-6$ columns are such that the i, j^{th} element is given by $\frac{\partial}{\partial \beta_j} (\nabla U + \bar{A}_D + \bar{A}_R)$. Note that the first six columns correspond to the first six elements of $\bar{\beta}$ which are the epoch position and velocity. (This matrix contains the direct partials of \bar{x}_t with respect to $\bar{\beta}$.)

We may now write

$$F = [U_{2c} + D_r] X_m + f \quad (7)$$

This is a matrix form of the variational equations.

Note that U_{2c} , D_r , and f are evaluated at the current time, whereas X_m is the output of the integration. Initially, the first six columns of X_m plus the six rows form an identity matrix; the rest of the matrix is zero (for $i=j$, $X_{m,i,j} = 1$; for $i \neq j$, $X_{m,i,j} = 0$).

Because each force enters into the variational equations in a manner which depends directly on its model, the specific contribution of each force is discussed in the section with the force model. We shall, however, note a few clerical details here.

The task of computing these variational equations in the GEODYN system is largely accomplished by subroutine VEVAL. The matrix dimensions given are for notational convenience; empty rows and columns are not programmed.

The above equation is also applied in subroutine PRELCT to "chain the partials back to epoch," that is, to relate the partials at the time of each set of measurements back to epoch.

PRELCT

August 11, 1973

The matrix for $\frac{\partial \bar{x}_t}{\partial \beta}$, X_m above, is initialized in ORBIT
subroutine ORBIT.

The contributions of subroutines D71, D650, DRAG D71
EGRAV, F, SURDEN, and RESPAR will be discussed as part D650
of the following subsections. The matrices U_{2c} and f will f DRAC
be referred to in each subsection as though the particular RESPAR
force being discussed had the only contribution. SURDEN

8.3 THE EARTH'S POTENTIAL

In GEODYN the Earth's potential is described by the combination of a spherical harmonic expansion and a surface density layer. Generally, however, the spherical harmonic expansion is used exclusively and no surface density terms are included.

8.3.1 Spherical Harmonic Expansion

The Earth's potential is most conveniently expressed in a spherical coordinate system as is shown in Figure 1. By inspection:

EGRAV

- ϕ' , the geocentric latitude, is the angle measured from \overline{OA} , the projection of \overline{OP} in the X-Y plane, to the vector \overline{OP} .
- λ , the east longitude, is the angle measured from the positive direction of the X axis to \overline{OA} .
- r is the magnitude of the vector \overline{OP} .

Let us consider the point P to be the satellite position. Thus, \overline{OP} is the geocentric Earth-fixed satellite vector corresponding to \bar{r} , the true of date satellite vector, whose components are (x,y,z). The relationship between the spherical coordinates (Earth-fixed) and the satellite position coordinates (true of date) is then given by

EGRAV

$$r = \sqrt{x^2 + y^2 + z^2} \quad (1)$$

$$\phi' = \sin^{-1} \left(\frac{z}{r} \right) \quad (2)$$

$$\lambda = \tan^{-1} \left(\frac{y}{x} \right) - \theta_g \quad (3)$$

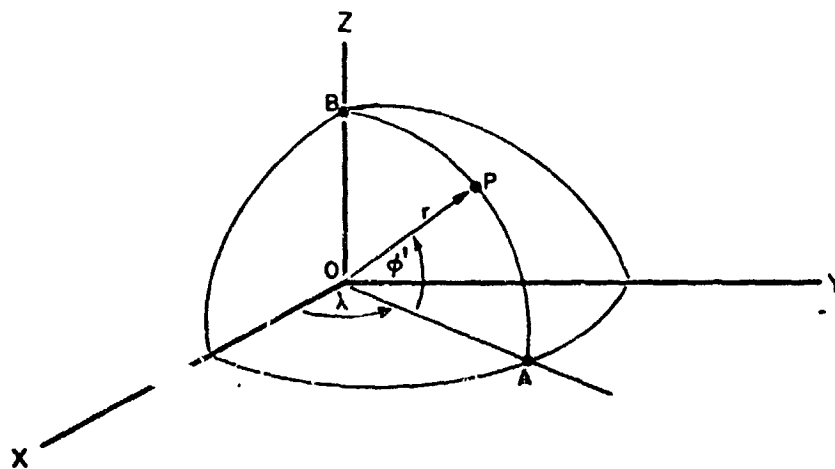


Figure 1: Spherical Coordinates

where θ_g is the rotation angle between the true of date system and the Earth-fixed system (see Section 3.4).

EGRAV

The Earth's gravity field is represented by the normal potential of an ellipsoid of revolution and small irregular variations, expressed by a sum of spherical harmonics. This formulation, used in the GEODYN system, is

$$U = \frac{GM}{r} \left\{ 1 + \sum_{n=2}^{nmax} \sum_{m=0}^n \left(\frac{a_e}{r} \right)^n P_n^m (\sin \phi) \left[C_{nm} \cos m\lambda + S_{nm} \sin m\lambda \right] \right\} \quad (4)$$

where

G is the universal gravitational constant,

M is the mass of the earth,

r is the geocentric satellite distance,

nmax is the upper limit for the summation (highest degree),

a_e is the Earth's mean equatorial radius,

ϕ' is the satellite geocentric latitude,

EGRAV

λ is the satellite east longitude,

$P_n^m(\sin \phi)$ indicate the associated ~~six~~ Legendre functions, and

C_{nm} and S_{nm} are the ~~denormalized~~ ^{unnormalized} gravitational coefficients.

The relationships between the normalized coefficients ($\bar{C}_{nm}, \bar{S}_{nm}$) and the denormalized coefficients are as follows:

DENORM

$$C_{nm} = \left[\frac{(n-m)! (2n+1) (2-\delta_{om})}{(n+m)!} \right]^{1/2} \bar{C}_{nm} \quad (5)$$

where

δ_{om} is the Kronecker delta,

$\delta_{om} = 1$ for $m=0$ and $\delta_{om} = 0$ for $m \neq 0$.

A similar expression is valid for the relationship between \bar{S}_{nm} and S_{nm} . This conversion factor is computed by the GEODYN system function DENORM.

The gravitational accelerations in true of date co-ordinates $(\ddot{x}, \ddot{y}, \ddot{z})$ are computed from the geopotential, $U(r, \phi', \lambda)$, by the chain rule; e.g.,

$$\ddot{x} = \frac{\partial U}{\partial r} \frac{\partial r}{\partial x} + \frac{\partial U}{\partial \phi'} \frac{\partial \phi'}{\partial x} + \frac{\partial U}{\partial \lambda} \frac{\partial \lambda}{\partial x} \quad (6)$$

The accelerations \ddot{y} and \ddot{z} are determined likewise. The partial derivatives of U with respect to r , ϕ' , and λ are given by

$$\frac{\partial U}{\partial r} = \frac{GM}{r^2} \left[1 + \sum_{n=2}^{n_{\max}} \left(\frac{a_e}{r}\right)^n \sum_{m=0}^n (C_{nm} \cos m\lambda + S_{nm} \sin m\lambda) (n+1) P_n^m(\sin \phi') \right] \quad (7)$$

$$\frac{\partial U}{\partial \lambda} = \frac{GM}{r} \sum_{n=2}^{n_{\max}} \left(\frac{a_e}{r}\right)^n \sum_{m=0}^n (S_{nm} \cos m\lambda - C_{nm} \sin m\lambda) m P_n^m(\sin \phi') \quad (8)$$

$$\frac{\partial U}{\partial \phi'} = \frac{GM}{r} \sum_{n=2}^{n_{\max}} \left(\frac{a_e}{r}\right)^n \sum_{m=0}^n (C_{nm} \cos m\lambda + S_{nm} \sin m\lambda) \left[P_n^{m+1}(\sin \phi') - m \tan \phi' P_n^m(\sin \phi') \right] \quad (9)$$

The partial derivatives of r , ϕ , and λ with respect to the true of date satellite position components are

EGRAV

$$\frac{\partial r}{\partial r_i} = \frac{r_i}{r} \quad (10)$$

$$\frac{\partial \phi}{\partial r_i} = \frac{1}{\sqrt{x^2 + y^2}} \left[-\frac{z r_i}{r^2} + \frac{\partial z}{\partial r_i} \right] \quad (11)$$

$$\frac{\partial \lambda}{\partial r_i} = \frac{1}{\sqrt{x^2 + y^2}} \left[\frac{\partial y}{\partial r_i} - \frac{y}{x} \frac{\partial x}{\partial r_i} \right] \quad (12)$$

The Legendre functions are computed via recursion EGRAV
 formulae:

Zonals: $m=0$

$$P_n^0(\sin \phi) = \frac{1}{n} \left[(2n-1) \sin \phi' P_{n-1}^0(\sin \phi) - (n-1) P_{n-2}^0(\sin \phi) \right] \quad (13)$$

$$P_1^0(\sin \phi) = \sin \phi' \quad (14)$$

Tesserals: $m \neq 0$ and $m \leq n$

$$P_n^m(\sin \phi) = P_{n-2}^m(\sin \phi) + (2n-1) \cos \phi' P_{n-1}^{m-1}(\sin \phi) \quad (15)$$

$$P_1^1(\sin \phi) = \cos \phi' \quad (16)$$

Sectorals: $m=n$

$$P_n^m = (2n-1) \cos \phi' P_{n-1}^{n-1}(\sin \phi) \quad (17)$$

The derivative relationship is given by

EGRAV

$$\frac{d}{d\phi'} \left(p_n^m (\sin \phi) \right) = p_n^{m+1} (\sin \phi) - m \tan \phi' p_n^m (\sin \phi) \quad (18)$$

It should also be noted that multiple angle formulas are used for evaluating the sine and cosine of $m\lambda$.

ECRAV

VEVAL

These accelerations on the spacecraft are computed in subroutine EGRAV. Arrays containing certain intermediate data are passed to subroutine VEVAL for use in the computations for the variational equations. These contain the values for:

$$\frac{GM}{r} \left(\frac{a}{r} \right)^n \quad (19)$$

$$p_n^m (\sin \phi')$$

$$\sin m\lambda$$

$$\cos m\lambda$$

$$m \tan \phi'$$

for each m and/or n .

The following discussion relates primarily to the mathematical formulations utilized in subroutine VEVAL.

VEVAL

The variational equations require the computation of the matrix U_{2c} , whose elements are given by

$$(U_{2c})_{i,j} = \frac{\partial^2 U}{\partial r_i \partial r_j} \quad (20)$$

where

$r_i = \{x, y, z\}$, the true of date satellite position.

U is the geopotential.

Because the Earth's field is in terms of r , $\sin \phi$, and λ , we write

$$U_{2c} = C_1^T U_2 C_1 + \sum_{k=1}^3 \frac{\partial U}{\partial e_k} C_{2k} \quad (21)$$

where

e_k range over the elements r , $\sin \phi$, and λ

U_2 is the matrix whose i, j^{th} element is given by $\frac{\partial^2 U}{\partial e_i \partial e_j}$

C_1 is the matrix whose i, j^{th} element is given by $\frac{\partial e_i}{\partial r_j}$

VEVAL

and

C_{2k} is a set of three matrices whose i, j^{th} elements are given by $\frac{\partial^2 e_k}{\partial r_i \partial r_j}$

We compute the second partial derivatives of the potential U with respect to r, ϕ' , and λ :

$$\frac{\partial^2 U}{\partial r^2} = \frac{2GM}{r^3} + \frac{GM}{r^3} \sum_{n=2}^{n_{\max}} (n+1)(n+2) \left(\frac{a_e}{r}\right)^n \sum_{m=0}^n \quad (22)$$

$$(C_{nm} \cos m\lambda + S_{nm} \sin m\lambda) P_n^m(\sin \phi')$$

$$\frac{\partial^2 U}{\partial r \partial \phi'} = -\frac{GM}{r^2} \sum_{n=2}^{n_{\max}} (n+1) \left(\frac{a_e}{r}\right)^n \sum_{m=0}^n (C_{nm} \cos m\lambda \quad (23)$$

$$+ S_{nm} \sin m\lambda) \frac{\partial}{\partial \phi'} (P_n^m(\sin \phi'))$$

$$\frac{\partial^2 U}{\partial r \partial \lambda} = \frac{GM}{r^2} \sum_{n=2}^{n_{\max}} (n+1) \left(\frac{a_e}{r}\right)^n \sum_{m=0}^n m \quad (24)$$

$$(-C_{nm} \sin m\lambda + S_{nm} \cos m\lambda) P_n^m(\sin \phi')$$

VEVAL

$$\frac{\partial^2 U}{\partial \phi^2} = \frac{GM}{r} \sum_{n=2}^{n_{\max}} \left(\frac{a_e}{r}\right)^n \sum_{m=0}^n (C_{nm} \cos m\lambda + S_{nm} \sin m\lambda) \cdot \quad (25)$$

$$\frac{\partial^2}{\partial \phi^2} \left(P_n^m (\sin \phi) \right)$$

$$\frac{\partial^2 U}{\partial \phi \partial \lambda} = \frac{GM}{r} \sum_{n=2}^{n_{\max}} \left(\frac{a_e}{r}\right)^n \sum_{m=0}^n m (-C_{nm} \sin m\lambda + S_{nm} \cos m\lambda) \frac{\partial}{\partial \phi} \left(P_n^m (\sin \phi) \right) \quad (26)$$

$$\frac{\partial^2 U}{\partial \lambda^2} = -\frac{GM}{r} \sum_{n=2}^{n_{\max}} \left(\frac{a_e}{r}\right)^n \sum_{m=0}^n m^2 (C_{nm} \cos m\lambda + S_{nm} \sin m\lambda) P_n^m (\sin \phi) \quad (27)$$

where

$$\frac{\partial}{\partial \phi} \left(P_n^m (\sin \phi) \right) = P_n^{m+1} (\sin \phi) - m \tan \phi P_n^m (\sin \phi) \quad (28)$$

$$\begin{aligned} \frac{\partial^2}{\partial \phi'^2} \left(P_n^m (\sin \phi') \right) &= P_n^{m+2} (\sin \phi') - (m+1) \tan \phi' P_n^{m+1} (\sin \phi') \\ &- m \tan \phi' \left[P_n^{m+1} (\sin \phi') - m \tan \phi' P_n^m (\sin \phi') \right] \\ &- m \sec^2 \phi' P_n^m (\sin \phi') \end{aligned} \quad (29)$$

The elements of U_2 have almost been computed. What remains is to transform from (r, ϕ', λ) to $(r, \sin \phi', \lambda)$. This affects only the partials involving ϕ' :

$$\frac{\partial U}{\partial \sin \phi'} = \frac{\partial U}{\partial \phi'} \frac{\partial \phi'}{\partial \sin \phi'} \quad (30)$$

$$\frac{\partial^2 U}{\partial \sin \phi'^2} = \frac{\partial \phi'}{\partial \sin \phi'} \left(\frac{\partial^2 U}{\partial \phi'^2} \right) \frac{\partial \phi'}{\partial \sin \phi'} + \frac{\partial U}{\partial \phi'} \frac{\partial^2 \phi'}{\partial \sin \phi'^2} \quad (31)$$

where

$$\frac{\partial \phi'}{\partial \sin \phi'} = \sec \phi' \quad (32)$$

$$\frac{\partial^2 \phi'}{\partial \sin \phi'^2} = \sin \phi' \sec^3 \phi' \quad (33)$$

For the C_1 and C_{2k} matrices, the partials of r , $\sin \phi'$, and λ are obtained from the usual formulas:

VEVAL

$$r = \sqrt{x^2 + y^2 + z^2} \quad (34)$$

$$\sin \phi' = \frac{z}{r} \quad (35)$$

$$\lambda = \tan^{-1}\left(\frac{y}{x}\right) - \theta_g \quad (36)$$

We have for C_1 :

$$\frac{\partial r}{\partial r_i} = \frac{r_i}{r} \quad (37)$$

$$\frac{\partial \sin \phi'}{\partial r_i} = \frac{-z r_i}{r^3} + \frac{1}{r} \frac{\partial z}{\partial r_i} \quad (38)$$

$$\frac{\partial \lambda}{\partial r_i} = \frac{1}{x^2 + y^2} \left[x \frac{\partial y}{\partial r_i} - y \frac{\partial x}{\partial r_i} \right] \quad (38)$$

The C_{2k} are symmetric. The necessary elements are given by

VEVAL

$$\frac{\partial^2 r}{\partial r_i \partial r_j} = \frac{r_i r_j}{r^3} + \frac{1}{r} \frac{\partial r_i}{\partial r_j} \quad (39)$$

$$\frac{\partial^2 \sin \phi'}{\partial r_i \partial r_j} = \frac{3z r_i r_j}{r^5} - \frac{1}{r^3} \left[r_j \frac{\partial z}{\partial r_i} + r_i \frac{\partial z}{\partial r_j} + z \frac{\partial r_i}{\partial r_j} \right] \quad (40)$$

$$\frac{\partial^2 \lambda}{\partial r_i \partial r_j} = \frac{-2r_j}{(x^2+y^2)^{3/2}} \left[x \frac{\partial y}{\partial r_i} - y \frac{\partial x}{\partial r_i} \right] \quad (41)$$

$$+ \frac{1}{x^2+y^2} \left[\frac{\partial x}{\partial r_j} \frac{\partial y}{\partial r_j} - \frac{\partial y}{\partial r_j} \frac{\partial x}{\partial r_j} \right]$$

If gravitational constants, C_{nm} or S_{nm} are being estimated, we require their partials in the f matrix for the variational equations computations. These partials are

RESPAR

$$\frac{\partial}{\partial C_{nm}} \left(- \frac{\partial U}{\partial r} \right) = (n+1) \frac{GM}{r^2} \left(\frac{a}{r} \right)^n \cos(m\lambda) P_n^m(\sin \phi') \quad (42)$$

$$\frac{\partial}{\partial C_{nm}} \left(- \frac{\partial U}{\partial \lambda} \right) = m \frac{GM}{r} \left(\frac{a}{r} \right)^n \sin(m\lambda) P_n^m(\sin \phi') \quad (43)$$

$$\frac{\partial}{\partial C_{nm}} \left(-\frac{\partial U}{\partial \phi'} \right) = -\frac{GM}{r} \left(\frac{a_e}{r} \right)^n \cos(m\lambda) \left[P_n^{m+1}(\sin \phi') \right. \\ \left. - m \tan \phi' P_n^m(\sin \phi') \right] \quad \text{RESPAR} \quad (44)$$

The partials for S_{nm} are identical with $\cos(m\lambda)$ replaced by $\sin(m\lambda)$ and with $\sin(m\lambda)$ replaced by $-\cos(m\lambda)$.

These partials are converted to inertial true of date coordinates using the chain rule; e.g.,

$$\frac{\partial}{\partial C_{nm}} \left(-\frac{\partial U}{\partial x} \right) = \frac{\partial}{\partial C_{nm}} \left(\frac{-\partial U}{\partial r} \right) \frac{\partial r}{\partial x} + \frac{\partial}{\partial C_{nm}} \left(\frac{-\partial U}{\partial \lambda} \right) \frac{\partial \lambda}{\partial x} \\ + \frac{\partial}{\partial C_{nm}} \left(\frac{-\partial U}{\partial \phi'} \right) \frac{\partial \phi'}{\partial x} \quad (45)$$

This particular set of computations is performed by subroutine RESPAR. The items which EGRAV computes for VEVAL are also available to RESPAR and are therefore utilized.

8.3.2 Surface Density Layers

The representation of the earth's gravitational field in terms of a simple density layer spread over the surface of the earth was first introduced by Koch [Reference 10] in 1968. Attempts at determining numerical values for surface densities on a global scale have been made using both optical [Reference 6] and Doppler [Reference 7] data. In some cases, the surface densities have been estimated as alternatives to the spherical harmonic expansion, and in other cases the surface densities are a supplementary contribution to a set of "known" low degree and order spherical harmonic coefficients.

The surface densities implemented in the GEODYN program are basically in the nature of a supplementary potential contribution. The spherical harmonic field is retained for representing the geopotential on a global scale and the surface densities can be introduced on either a local or global scale into any number of blocks of constant density. That is, the fineness of representation of the geopotential via surface densities is arbitrarily small, consistent with computer core availability and the existence of data for actually resolving a large number of surface densities. In addition, the capability now exists in the GEODYN program for simultaneously adjusting both spherical harmonic coefficients and surface layer densities. No investigator has apparently yet attempted this. When actually making simultaneous adjustments, the results must be very carefully interpreted. This problem is considered further below in the discussion of constraints.

8.3.2.1 Mathematical Representation of Surface Densities.

The total potential of the earth 'W' can be, somewhat arbitrarily, divided into a spherical harmonic part 'U' and a remainder 'T' to be expressed in some other form

$$W = U + T \quad (1)$$

with

$$U = \frac{GM}{r} \left[1 + \sum_{n=2}^N \sum_{m=0}^n \left(\frac{a_e}{r} \right)^n P_n^m(\sin \phi) \left(C_{nm} \cos m \lambda + S_{nm} \sin m \lambda \right) \right] + 1/2 \omega^2 r^2 \cos^2 \phi \quad (2)$$

where r is the distance from the point of interest to the center of mass of the earth and ϕ and λ are geocentric latitude and longitude. The last term in (2) is omitted if the potential is being computed outside the surface of the earth. In GEODYN, the maximum degree spherical harmonic coefficient is basically arbitrary, normally being limited to the maximum degree for which coefficients are available.

The potential T can be represented as that of a simple layer distributed over the surface of the earth. Mathematically, T is then given by the surface integral

$$T = \int_S \int \chi \, dE / \ell \quad (3)$$

where ℓ is the distance from a point on the surface to the point at which the potential is to be computed, dE is the element of surface area, χ is the surface density (in units of kg/m^2 multiplied by G), and S is the surface of the earth. Figure 1 shows the geometry and a portion of the surface areas. To numerically evaluate the integral in (3), it is necessary to divide the entire surface into blocks of constant density. If there are M such blocks, then (3) can be written

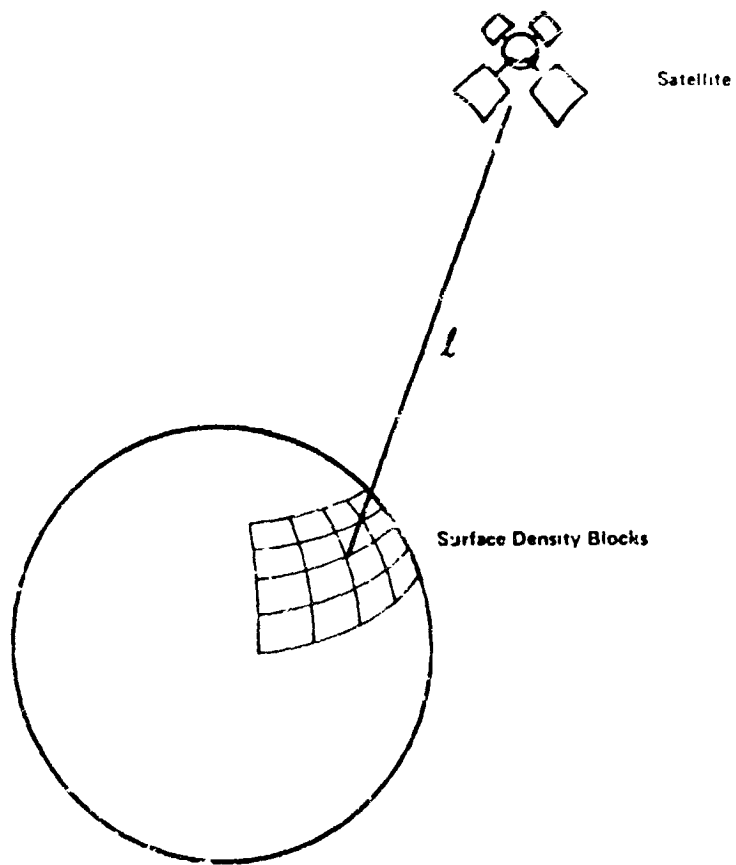


Figure 3. Geometry of Surface Density Blocks
Relative to Perturbed Satellite

$$T = \sum_{i=1}^M \chi_i \iint_{\Delta E_i} \Delta E / \rho \quad (4)$$

where χ_i is now the average density on the i'th block and the integral is to be taken over the area of the i'th block.

The integral in Eqn. (4) must be evaluated numerically. It is evaluated in GEODYN by dividing the area ΔE_i up into four blocks of equal area and taking the kernel, $1/\rho$, to be constant over each of these sub-blocks. This is the division which has been most commonly used for surface density layers and has been shown by Koch [Reference 8] to be a quite good approximation, generally accurate to within a few percent. Results of numerical tests are also given below.

With the division into sub-blocks, the potential due to surface densities is

$$T = \sum_{i=1}^M \chi_i \sum_{j=1}^4 \Delta E_{ij} / \rho_{ij} \quad (5)$$

where ΔE_{ij} is the area of the j'th sub-division of the i'th block and ρ_{ij} is the distance from the center of this sub-division to the point where the potential is to be evaluated. The acceleration produced by the surface density potential is obtained by taking its gradient,

$$\bar{a})_{\text{surface densities}} = \nabla T = \sum_{i=1}^M \chi_i \sum_{j=1}^4 \Delta E_{ij} \nabla (1/\rho_{ij}) \quad (6)$$

SURDEN

The forcing function for integrating the variation equations to obtain the sensitivity of satellite position to a particular surface density block is obtained by differentiating Eqn. (6) with respect to χ_i .

$$\frac{\partial \bar{a}}{\partial x_i} = \sum_{j=1}^4 \Delta E_{ij} \nabla \left(1/r_{ij} \right)$$

(7)
SURDEN

Note that these forcing functions must be computed as part of the computation of the surface density acceleration contribution.

GEOIDH
AVGPOT

8.3.2.2 Surface Height Computation. A number of potential choices are available for locating the surfaces on which the surface densities are to be spread. Such surfaces include the spheroid, the geoid, and the physical surface of the earth. The method which has been implemented in GEODYN is to locate the density layers on the geoid defined by the earth and geopotential model being used in the program. The model presently being employed is the SAO 1969 Standard Earth [Reference 9].

The geoid choice for locating the surface densities is the most natural for use in estimating surface density values in blocks restricted to ocean areas, as might be one of the initial uses of the GEOS-C altimeter data. For complete global density layers, and perhaps incorporating measurements of surface gravity, some other surface may be more convenient.

8.3.2.3 Layer Model Quadrature Errors. The process of approximating the integral over the area of a surface density block by 4 sub-blocks with the kernel estimated at the center introduces some error into the integration of surface density effects on the orbit. Koch [Reference 3] has investigated the error introduced by dividing the blocks into only 4 sub-

blocks, and concluded that errors generally less than a few percent were introduced.

A test was made in GEODYN to determine the effects of different divisions of a $20^\circ \times 20^\circ$ block for a satellite of 500 nm altitude passing directly over the center of the block. The results for a subdivision into 4, 9 and 16 blocks are shown in Figure 2. This Figure shows that the 4-block subdivision does indeed introduce substantial error, but only when the satellite is directly over the center of the block. It should be noted that a 20° block size is much larger than would normally be considered for the fine detail representation of the geopotential. A division into $20^\circ \times 20^\circ$ blocks on a global scale is, of course, a reasonable possibility.

Figure 3 shows the acceleration effects due to the $20^\circ \times 20^\circ$ surface density layer for a complete revolution of the 500 nm satellite. It will be noted that the effects are quite localized, as is indeed one of the advantages of the surface density representation. There is a large perturbation when the satellite is directly over the block. There is a definite but rather small perturbation when the satellite comes over the next revolution about 10° away from the edge of the block. Otherwise, the effects of the blocks are rather constant and small.

GEOIDH
SURDEN
PDEN

8.3.2.4 Constraints. For several reasons, it is necessary to apply certain constraints to the surface density adjustments which are to be allowed. That this is necessary can be seen by noting that the total surface density potential can be expressed in terms of a spherical harmonic series,

Figure 2. X Component of Acceleration of 500 nm Satellite When Passing Over 20°x20° Surface Density Block for Different Block Sub-Divisions

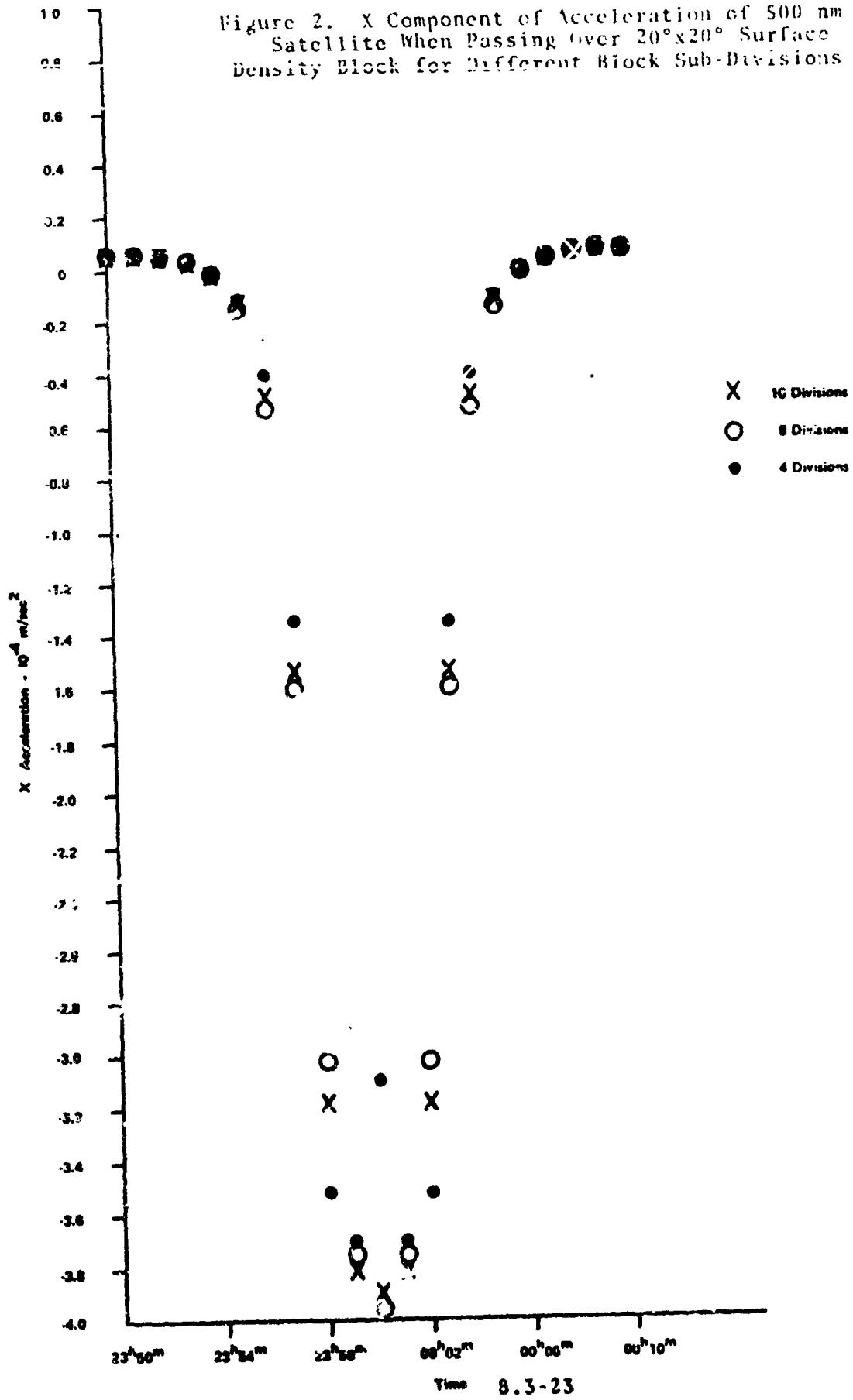
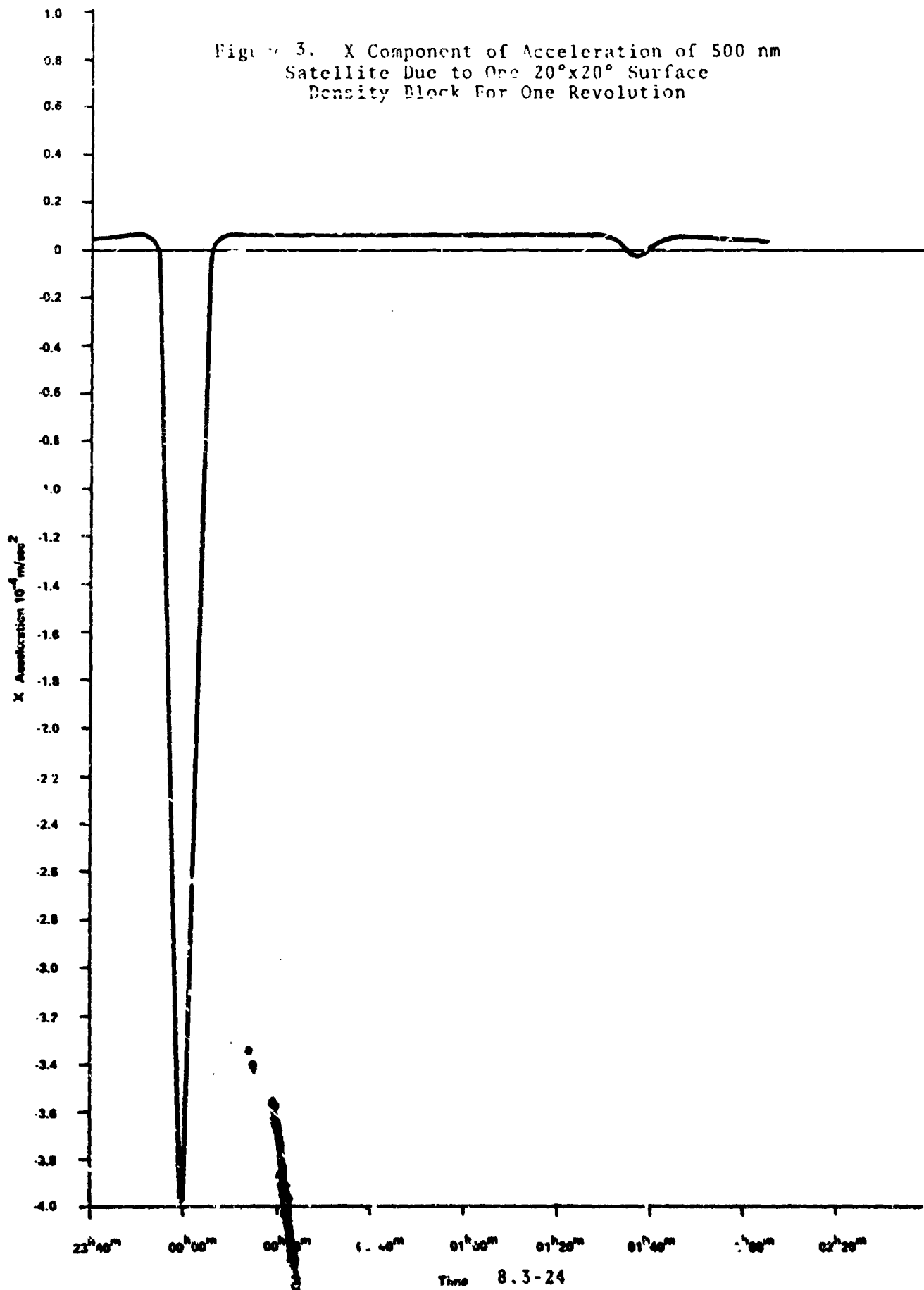


Figure 3. X Component of Acceleration of 500 nm
Satellite Due to One 20°x20° Surface
Density Block For One Revolution



$$T = \frac{GM}{r} \sum_{n=0}^{\infty} \left(\frac{a_e}{r}\right)^n \sum_{m=0}^n P_n^m(\sin \phi) [C'_{nm} \cos m\lambda + S'_{nm} \sin m\lambda] \quad (8)$$

which is of the identical form as the global spherical harmonic expansion given by Eqn. (2), except that the expansion is now infinite. It is most significant, however, that the surface density expansion could actually include the equivalent perturbations of the normal spherical harmonic set of coefficients, and that both numerical and interpretation problems can arise if both spherical harmonic coefficients and surface densities are allowed to adjust simultaneously.

It may also be noted that first degree coefficients in (8) would not, in general, be zero. It is thus necessary to force the distribution of densities to be such that these coefficients are zero in order to avoid moving the center of mass of the earth.

The form which constraints should take can be found by expressing $1/r$ in Eqn. (4) in terms of spherical harmonics and identifying coefficients $P_n^m(\sin \phi) \cos m\lambda$ and $P_n^m(\sin \phi) \sin m\lambda$. Schwarz [Reference 15] has shown that this leads to expressions for C'_{nm} and S'_{nm} of

$$\begin{pmatrix} C'_{nm} \\ S'_{nm} \end{pmatrix} = \frac{(2-\delta_{om})}{GM} \frac{(n-m)!}{(n+m)!} \sum_{i=1}^M$$

$$\chi_i \iiint_{\Delta E_i} \left(\frac{r}{a_e}\right)^n P_n^m(\sin \phi) \begin{pmatrix} \cos m\lambda \\ \sin m\lambda \end{pmatrix} dE \quad (9)$$

where $\delta_{om} = 1$ if $m=0$ and zero otherwise. This set of integrals can be obtained numerically by breaking the area ΔE_i up into sub-blocks as was done for the acceleration calculation.

The constraint equations are obtained by setting C'_{nm} and S'_{nm} equal to zero for every spherical harmonic coefficient to which the surface densities should not contribute. In GEODYN, the default set of zero coefficients has been set to C'_{10} , C'_{11} , S'_{11} . Additional constraints (as, e.g., no contribution to 8th degree or lower degree coefficients) can be imposed upon input option.

The GEODYN implementation of constraints is through the solution for a number of densities equal to the total number of densities adjusted less the number of constraint equations. The normal matrix thus contains only independent densities and core requirements are minimized. The procedure for eliminating densities is seen by writing the constraint equations obtained from (9) as

$$\sum_{i=1}^M \chi_i \iint_{\Delta E_i} \left(\frac{r}{a_e} \right)^n P_n^m(\sin \phi) \cos m\lambda \, dE = 0 \quad (10a)$$

$$\sum_{i=1}^M \chi_i \iint_{\Delta E_i} \left(\frac{r}{a_e} \right)^n P_n^m(\sin \phi) \sin m\lambda \, dE = 0 \quad (10b)$$

for $m \leq n$
 $n \leq N'$

where N' is the maximum degree coefficient unaffected by the surface density layers.

The set of Eqns. (10) can be written formally as

$$\sum_{i=1}^{M'} \Lambda_{ji} \chi_i = 0, \quad j = 1, M' \quad \text{GEOIDH} \quad (11)$$

where the Λ_{ji} are given by the surface integrals in (10), and M' is the number of constraint equations. The number M' is related to N' by

$$M' = N'(N'+2), \quad (12)$$

as follows from the number of C'_{nm} and S'_{nm} coefficients for which $n \leq N'$ and which are not identically zero. On the assumption that $M' < M$, (ii) can be written

$$\sum_{i=1}^{M'} \Lambda_{ji} x_i + \sum_{i=M'+1}^M \Lambda_{ji} x_i = 0. \quad (13)$$

Now let the square array with elements Λ_{ji} and $i \leq j$ possess an inverse whose elements are denoted by Λ'_{ji} . Then this matrix may be used in (13) to solve for the first M' surface densities,

$$x_k = - \sum_{j=1}^{M'} \Lambda'_{kj} \sum_{i=M'+1}^M \Lambda_{ji} x_i, \quad k = 1, M' \quad \text{PDEN} \quad (14)$$

There are thus $M-M'$ independent densities remaining and Eqn. (14) can be used to relate the dependent densities.

The integration of the variational equations to obtain the partials of the trajectory with respect to the independent surface densities requires that the forcing function for the variational equations include both the direct and indirect effects of the independent adjusted densities. If \bar{a}_{SD} is the surface density acceleration, then the required forcing function is

$$\left(\frac{\partial \bar{a}_{SD}}{\partial \chi_i} \right)_{\text{total}} = \frac{\partial \bar{a}_{SD}}{\partial \chi_i} + \sum_{k=1}^{M'} \frac{\partial \bar{a}_{SD}}{\partial \chi_k} \frac{\partial \chi_k}{\partial \chi_i}, \quad i = M' + 1, M \quad (15)$$

SURDEN

with $\frac{\partial \chi_k}{\partial \chi_i}$ to be obtained from Eqn. (14).

It should be noted that GEODYN has the option of adjusting only a portion of the surface densities. This, in effect, means that there are additional constraint equations, but they are quite simple to incorporate. The constraints given by Eqn. (14) are still required to hold with no modification whatsoever. Ordering the densities such that the unadjusted densities are last in the array, then Eqn. (15) is modified only to the extent that i has the range $M'+1$ to $M-M_0$, with M_0 the number of unadjusted densities. If there are more constraint equations than there are densities to be adjusted, GEODYN will terminate upon reading the input deck with the appropriate error message.

8.4 SOLAR, LUNAR, AND PLANETARY GRAVITATIONAL PERTURBATIONS

SUNGRV

The perturbations caused by a third body on a satellite orbit are treated by defining a function, R_d , which is the third body disturbing potential. This potential takes on the following form:

$$R_d = \frac{GMm_d}{r_d} \left[\left(1 - \frac{2r}{r_d} S + \frac{r^2}{r_d^2} \right)^{-1/2} - \frac{r}{r_d} S \right] \quad (1)$$

where

m_d is the mass of the disturbing body.

\bar{r}_d is the geocentric true of date position vector to the disturbing body.

S is equal to the cosine of the enclosed angle between \bar{r} and \bar{r}_d .

\bar{r} is the geocentric true of date position vector of the satellite.

G is the universal gravitational constant, and

M is the mass of the Earth.

The third body perturbations considered in GEOPYN are for the Sun, the Moon, Venus, Mars, Jupiter, and Saturn. All are computed in subroutine SUNGRV by

$$\bar{a}_d = -GMm_d \left[\frac{\bar{d}}{D_d} + \frac{1}{r_d} \left(\frac{\bar{r}_d}{r_d} \right) \right] \quad (2) \quad \text{SUNGRV}$$

where

$$\bar{d} = \bar{r} - \bar{r}_d$$

$$D_d = \left[r_d^2 - 2r r_d S + r^2 \right]^{3/2}$$

These latter quantities, \bar{d} and D as well as $D^{2/3}$ are passed to subroutine VEVAL for the variational equation calculations. VEVAL computes the matrix U_{2C} whose i, j^{th} elements is given by

VEVAL

$$\frac{\partial^2 R_d}{\partial r_i \partial r_j} = - \frac{GMm_d}{D_d} \left[\frac{\partial r_i}{\partial r_j} + \frac{3d_i a_j}{D_d^{2/3}} \right] \quad (3)$$

This matrix is a fundamental part of the variational equations.

8.5 SOLAR RADIATION PRESSURE

The force due to solar radiation can have a significant effect on the orbits of satellites with a large area to mass ratio. The accelerations due to solar radiation pressure are formulated in the

F

GEODYN system as

F

$$\bar{A}_R = -v C_R \frac{A_S P_S}{m_S} \hat{r}_S \quad (1)$$

where

v is the eclipse factor, such that

$v=0$ when the satellite is in the Earth's shadow

$v=1$ when the satellite is illuminated by the Sun

C_R is a factor depending on the reflective characteristics of the satellite,

A_S is the cross sectional area of the satellite;

m_S is the mass of the satellite,

P_S is the solar radiation pressure in the vicinity of the Earth, and

\hat{r}_S is the (geocentric) true of date unit vector pointing to the Sun.

The unit vector \hat{r}_S is determined as part of the luni-solar-planetary ephemeris computations

c-3

The eclipse factor, v , is determined as follows: F
Compute

$$D = \bar{r} \cdot \hat{r}_s \quad (2)$$

where \bar{r} is the true of date position vector of the satellite. If D is positive, the satellite is always in sunlight. If D is negative, compute the vector \bar{P}_R .

$$\bar{P}_R = \bar{r} - D \hat{r}_s \quad (3)$$

This vector is perpendicular to \hat{r}_s . If its magnitude is less than an Earth radius, or rather if

$$\bar{P}_R \cdot \bar{P}_R < a_e^2, \quad (4)$$

the satellite is in shadow.

The satellite is assumed to be specularly reflecting with reflectivity ρ_s ; thus

$$C_R = 1 + \rho_s \quad (5)$$

When a radiation pressure coefficient is being determined; i.e., C_R , the partials for the f matrix

in the variational equations computation must be computed. The i^{th} element of this column matrix is given by

F
VEVAL

$$f_i = -v \frac{A_s}{m_s} P_s r_{s_i} \quad (6)$$

These computations for the effects of solar radiation pressure are done in subroutine F.

8.6 ATMOSPHERIC DRAG

A satellite moving through an atmosphere experiences a drag force. The acceleration due to this force is given by

DRAG

$$\bar{A}_D = -\frac{1}{2} C_D \frac{A_s}{m_s} \rho_D v_r \bar{v}_r \quad (1)$$

where

C_D is the satellite drag coefficient

A_s is the cross-sectional area of the satellite

August 11, 1973

m_s is the mass of the satellite,

DRAG

ρ_D is the density of the atmosphere at the satellite position, and

\bar{v}_r is the velocity vector of the satellite relative to the atmosphere.

Both A_s and C_D are treated as constants in GEODYN. Although A_s depends somewhat on satellite attitude, the use of a mean cross-sectional area does not lead to significant errors for geodetically useful satellites. The factor C_D varies slightly with satellite shape and atmospheric composition. However, for any geodetically useful satellite, it may be treated as a satellite dependent constant.

The relative velocity vector, \bar{v}_r , is computed assuming that the atmosphere rotates with the Earth. The true of date components of this vector are then

$$\dot{x}_r = \dot{x} + \dot{\theta}_g y \quad (2)$$

$$\dot{y}_r = \dot{y} - \dot{\theta}_g x \quad (3)$$

$$\dot{z}_r = \dot{z} \quad (4)$$

as is indicated from Section 3.4, the subsection on transformations between Earth-fixed and true of date systems. The quantities \dot{x} , \dot{y} , and \dot{z} are of course the components of $\dot{\bar{r}}$, the satellite velocity vector in true of date coordinates.

August 11, 1973

The drag accelerations are computed in the GEODYN system by subroutine DRAG, with the atmospheric density ρ_D being evaluated by subroutine D71, D650. In addition, subroutine DRAG computes the direct partials for the f matrix of the variational equations when the drag coefficient C_D is being determined. These partials are given by

DRAG
D71
D650

$$f = - \frac{1}{2} \frac{A_S}{m_S} \rho_D v_r \bar{v}_r \quad (5)$$

When drag is present in an orbit determination run, the D_r matrix in the variational equations must also be computed. This matrix, which contains the partial derivatives of the drag acceleration with respect to the Cartesian orbital elements, is constructed in subroutine VEVAL. We have

VEVAL

$$D_r = - \frac{1}{2} C_D \frac{A_S}{m_S} \left[\rho_D v_r \frac{\partial \bar{v}_r}{\partial \bar{x}_t} + \rho_D \frac{\partial v_r}{\partial \bar{x}_t} \bar{v}_r + \frac{\partial \rho_D}{\partial \bar{x}_t} v_r \bar{v}_r \right] \quad (6)$$

where

\bar{x}_t is $(x, y, z, \dot{x}, \dot{y}, \dot{z})$; i.e., \bar{x}_t spans \bar{r} and $\dot{\bar{r}}$.

$$\frac{\partial \bar{v}_r}{\partial \bar{x}_t} = \begin{bmatrix} 0 & -\dot{\theta}_g & 0 \\ \dot{\theta}_g & 0 & 0 \\ 0 & 0 & 0 \\ 1 & 0 & 0 \\ 0 & 1 & 0 \\ 0 & 0 & 1 \end{bmatrix} \quad \text{VEVAL} \quad (7)$$

$$\frac{\partial v_r}{\partial \bar{x}_t} \bar{v}_r = \frac{1}{v_r} \begin{bmatrix} -\dot{y}_r & \dot{\theta}_g & \dot{x}_r & -\dot{y}_r & \dot{\theta}_g & \dot{y}_r & -\dot{y}_r & \dot{\theta}_g & \dot{z}_r \\ \dot{x}_r & \dot{\theta}_g & \dot{x}_r & \dot{x}_r & \dot{\theta}_g & \dot{y}_r & \dot{x}_r & \dot{\theta}_g & \dot{z}_r \\ & & 0 & & & 0 & & & 0 \\ \dot{x}_r & \dot{x}_r & & \dot{x}_r & \dot{y}_r & & \dot{x}_r & \dot{z}_r & \\ \dot{y}_r & \dot{x}_r & & \dot{y}_r & \dot{y}_r & & \dot{y}_r & \dot{z}_r & \\ \dot{z}_r & \dot{x}_r & & \dot{z}_r & \dot{y}_r & & \dot{z}_r & \dot{z}_r & \end{bmatrix} \quad (8)$$

and

$\frac{\partial \rho_D}{\partial \bar{x}_t}$ is the matrix containing the partial derivatives of the atmospheric density with respect to \bar{x}_t and is partially computed in subroutine DENSITY (see section 8.7.4 on atmospheric density partial derivatives). Because the density is not a function of the satellite velocity, the required partials are $\frac{\partial \rho_D}{\partial \bar{r}}$. DENSITY

August 11, 1973

8.7 ATMOSPHERIC DENSITY

In the computation of drag, it is essential to obtain models of the atmospheric density which will yield realistic perturbations due to drag. The GEODYN program uses the 1971 revised Jacchia Model which considers the densities between 90 km and 2500 km, and the 1965 Jacchia-Nicolet Model which gives densities between 120 km and 1000 km with an extrapolation formula for higher altitudes.

The following discussion will cover primarily the assumptions of the models and empirical formulae used in subroutine D71 and subroutine D650. The procedure for empirically evaluating the density tables which was developed by WOLF will also be included in the discussion.

8.7.1 JACCHIA 1971 DENSITY MODEL

The 1971 revised Jacchia model, as implemented in subroutine D71, is based on Jacchia's 1971 report, "Revised Static Models of the Thermosphere and Exosphere with Empirical Temperature Profiles" (Reference 1). The density computation from the exospheric temperature as well as from variations independent of temperature is based on density data appearing in that report. This data presented in Table 1 shows the density distribution at varying altitudes and exospheric temperatures.

For further detailed development of these empirical formulae, the interested reader should consult the aforementioned report and Jacchia's 1970 report (Reference 2).

8.7.1.1 The Assumptions of the Model

The Jacchia 1971 model (J71) is based on empirically determined formulae with some inherent simplifying assumptions. Such an approach is taken primarily because the various processes occurring in different regions of the atmosphere are complex in nature. Moreover, at present, a thorough comprehension of such processes is lacking. The present J71 model is patterned after the J65a (Jacchia 1965a) model which was based upon previous assumptions by Nicolet (Reference 3). D71

In Nicolet's atmospheric model, temperature is considered as the primary parameter with all other physical parameters such as density and pressure derivable from temperature. This approach was adopted by Jacchia in his J65a model. However, in the J71 model, there are variations modeled by Jacchia which are independent of temperature. They are the semi-annual variations, seasonal-latitudinal variations of the lower thermosphere, and seasonal-latitudinal variations of helium, all of which involve a time dependency. Although in J71 Jacchia mentions variations in hydrogen concentration, he does not attempt any quantitative evaluation of these variations.

Composition

The J71 model has assumed that the only constituents of the atmosphere are nitrogen, oxygen, argon, helium, and hydrogen. This composition is assumed to exist in a state of mixing at heights below 100 km and in a diffusion state at higher altitudes. A further assumption on the composition of the atmosphere is that any variation in the mean molecular mass, M , in the mixing region is the result of oxygen dissociation only. The variation in M has been described by an empirical profile for heights ranging from 90 km to 100 km.

It is also believed that gravitational separation for helium exists at lower height than for the other components. To avoid the cumbersome ordeal of modeling a separate homopause for helium, Jacchia has modified the concentration at sea-level by a certain amount such that at altitudes where helium becomes a substantial constituent, the modeled densities will correspond to the observed densities. Although this will yield a higher helium density below 100 km, the contribution of helium to the overall density will be negligible below this height.

Hydrogen does not become part of the density model until a height of 500 km. At this altitude, hydrogen is assumed to be in the diffusion equilibrium state.

Temperature

The temperature above the thermopause is referred to as the exospheric temperature. Although this temperature is independent of height, it is subject to solar activity, geomagnetic activity, and diurnal and other variations. The J71 model assumes constant boundary conditions of 90 km with a constant thermodynamic temperature of 183° K at this height. From numerous atmospheric conditions it is suggested that the atmospheric conditions at 90 km do indeed vary nominally, and thus, this assumption may be reasonably acceptable (Reference 4). Profiles of the thermodynamic temperature show that it increases with height and reaches an inflection point at 125 km. Above this altitude, this temperature asymptotically attains the value of the exospheric temperature. An analytic model of the atmospheric densities by Roberts (Reference 4) has been constructed based on modifications to Jacchia's 1970 temperature profile between

90 km and 125 km. The J71 model assumes that the basic shape of the temperature profiles remain unchanged during atmospheric heating due to geomagnetic storms. In all likelihood, the profiles at low altitudes become distorted to yield higher temperatures during such occurrences.

D71

Since the J71 model assumes the atmosphere to be in static equilibrium, for any sudden changes in solar activity or in geophysical conditions, which are characteristically dynamic, the model will generally be unable to properly represent the variations in both temperature and density due to this invalid assumption. The priority has been given to the best representation of density.

8.7.1.2 Variations in the Thermosphere and Exosphere

Several types of variations occurring in the different regions of the atmosphere are incorporated in the J71 model. These variations are: solar activity variations, diurnal variations, geomagnetic activity variations, semi-annual variation, seasonal-latitudinal variations of the lower thermosphere, and seasonal-latitudinal variations of helium. Still another variation which is not quantitatively evaluated by J71 is the rapid density fluctuations believed to be associated with gravity waves (Reference 1). Each of the above variations may be modeled empirically from observable data. However, because a static model is used, the various predictions will exhibit different degrees of accuracy for each variation. It is fundamental, however, to note that unless the characteristic time for which these variations occur is much longer than that for the processes of diffusion, conduction, and convection to occur, the predictions will be poor (Reference 1).

Solar Activity

D71

The variations in the thermosphere and exosphere as a result of solar activity are of a dual nature. One type of variation is a slow variation which prevails over an 11-year period as the average solar flux strength varies during the solar cycle. The other type is a rapid day-to-day variation due to the actively changing solar regions which appear and disappear as the sun rotates and as sunspots are formed.

To observe such activities, the 10.7 cm solar flux line is commonly used as an index of solar activity. The National Research Council in Ottawa has made daily measurements on this flux line since 1947. These values appear monthly in the "Solar Geophysical Data (Prompt Reports)" by the National Oceanic and Atmospheric Administration and the Environmental Data Service in Boulder, Colorado (U.S. Department of Commerce).

A linear relationship exists between the average 10.7 cm flux and the average nighttime minimum global exospheric temperature (Jacchia 1971) and may be expressed as:

$$T_{\infty} = 379^{\circ} + 3.24^{\circ} \bar{F}_{10.7} \text{ (}^{\circ}\text{Kelvin)} \quad (1)$$

where

T_{∞} = is the average nighttime minimum global exospheric temperature averaged over three solar rotations (81 days).

$F_{10.7}$ is the average 10.7 cm flux strength over three solar rotations and measured in units of 10^{-22} watts m^{-2} (cycle/sec) $^{-1}$ bandwidth.

D71

Equation (1) expresses the relationship with solar flux when the planetary geomagnetic index, K_p is zero; i.e., for no geomagnetic disturbances.

The nighttime minimum of the global exospheric temperature for a given day (Reference 1) is

$$T_c = T_\infty + 1.3^\circ (F_{10.7} - \bar{F}_{10.7}) \quad (2)$$

where

$F_{10.7}$ is the daily value of the 10.7 cm solar flux in the same units as $\bar{F}_{10.7}$ for one day earlier, since there is a one day lag of the temperature variation response to the solar flux (Roemer 1968).

Thus, Equation (2) models a daily temperature variation about the average nighttime minimum global temperature as determined in Equation 1.

Diurnal Variations

Computations from drag measurements have indicated that the atmospheric density distribution varies from day to night. The densities are at a peak at 2 P.M. local solar time (LST) approximately at the latitude of the sub-solar point, and at a minimum at 3 A.M. (LST) approximately

of the same latitude in the opposite hemisphere. The diurnal variation of density at any point is subject to seasonal changes. By empirical relationships, this variation may be described in terms of the temperature. Again, because a static model is used, the accuracy of this temperature is open to question.

D71

At a particular hour and geographic location, the temperature, T_g , can be expressed in terms of the actual global nighttime minimum temperature, T_c , for the given day (Reference 1). Thus, we may write

$$T_g = T_c (1 + R \sin^m \theta) \left(1 + R \frac{\cos^m \eta - \sin^m \theta}{1 + R \sin^m \theta} \cos^n \frac{\tau}{2} \right) \quad (3)$$

where

$$R = 0.3$$

$$m = 2.2$$

$$n = 3.0$$

$$\tau = H + \beta + p \sin(H + \gamma) \text{ for } (-\pi < \tau < \pi)$$

$$\beta = -37^\circ \text{ (lag of the temperature maximum with the uppermost point of the sun.)}$$

$$p = +6^\circ \text{ (introduces an asymmetry in the temperature curve.)}$$

$$\gamma = +43^\circ \text{ (determines the location of the asymmetry in the temperature curve.)}$$

$$\eta = \frac{1}{2} \text{ ABS } (\phi' - \delta_\odot)$$

$$\theta = \frac{1}{2} \text{ ABS } (\phi' + \delta_\odot)$$

ϕ' = geographic (geocentric) latitude

D'1

δ_{\odot} = declination of the sun

H = hour angle of the sun

(when the point considered, the sun, and the earth's axis are all coplanar, $H=0$. The hour angle is measured westward 0° to 360° .)

The parameter R determines the relative amplitude of the temperature variation. Jacchia and his associates have undertaken investigations of R which reveal indications of its variation in time and with altitude. After consulting 1969-1970 data, Jacchia presently has abandoned any attempt at any definitive conclusions about the variations of R with time or with solar activity (Reference 1). Instead, he believes this evidence to be the result of inherent limitations of the static atmospheric representation. Consequently, in the J71 model, a constant value of $R=0.3$ is maintained.

Geomagnetic Activity

Precise effects of geomagnetic activity cannot be obtained by present measurements from satellite drag, since such techniques can only show averaged values of densities. It is also realized that the consequences of a geomagnetic disturbance in view of the atmospheric temperatures and densities over the global regions are of a complex nature. However, when such disturbances occur, there are indications of increases in temperature and density in the thermosphere above the aurora belt. By the time this atmospheric disturbance reaches the equatorial regions, a period of roughly 7 hours, the effects are damped out considerably. (Reference 1).

A static model description of temperature and density D71 cannot be viewed accurately since the propagation time of the geomagnetic storms is relatively short. Therefore, any empirical formulae used to compute the effects on the parameters yield only a vague picture.

Jacchia et al (1967) have related the exospheric temperature to the 3-hourly planetary geomagnetic index K_p . The quantity K_p is used as a measure of a three-hour variation in the earth's magnetic field. The response of the temperature change to geomagnetic storms lags the variation in K_p by about 6.7 hours. In the following equation (Reference 1) the correction to the exospheric temperature due to geomagnetic activity is

$$\Delta T_{\infty} = 28^{\circ} K_p + 0.03^{\circ} \exp (K_p) \quad (4)$$

for heights above 200 km.

Although this K_p in equation (4) is a three-hour planetary geomagnetic index, in subroutine DENSTY an averaged K_p over a 24-hour period is used to minimize the amount of input data to GEODYN. The loss of accuracy in using the daily average of K_p is minimized, since the above equation is for a smoothed effect of the variations derived from satellite data.

Below 200 km, density predictions from equation (4) prove to be too low. Better results are obtained if the variations were represented as a two-step hybrid formula in which a correction to the density and to the temperature is made. Thus, in J71 the following hybrid formula (Reference 1) is given as

$$(a) P_4 = \Delta \log_{10} \rho = 0.012 K_p + 1.2 \times 10^{-5} \exp (K_p) \quad D71$$

$$(b) \Delta T_{\infty} = 14^{\circ} K_p + 0.02^{\circ} \exp (K_p) \quad (5)$$

where $\Delta \log_{10} \rho$ is the decimal logarithm correction to the density ρ .

The values of a three-hour K_p index are available along with the daily solar flux data in the publication "Solar Geophysical Data" by the N.O.A.A. and E.D.S., Boulder, Colorado (Department of Commerce).

In computing the exospheric temperature, accurate daily values for both the solar and geomagnetic flux must be used. These values are stored in the subroutines FLUXM and FLUXS of GEODYN, and they are updated as new information is received. This information may be updated (subroutine ADFLUX) using the appropriate GEODYN Input Cards. The user should be aware of the fact that these tables are expanded as new information is made available (Reference 3).

FLUXM
FLUXS
ADFLUX

At the beginning of each run, a file is generated for JANTHG each satellite arc which contains the required flux data for the time period indicated. Subroutine JANTHG sets up the flux tables as well as averaging the daily values of solar flux over three solar rotation periods. This enables the releasing of vast computer storage required for daily flux values over 14 years. The selected data is stored in common block FLXBLK.

A midpoint point average is used to compute the six solar rotation flux values $F_{10.7}$.

Semiannual Variation

The semiannual variation at present is least understood of the atmospheric variations. In past models, J65, attempts at empirically relating the temperature to this variation seemed appropriate in the range of heights, 250 to 650 km, for which data was available. However, with the availability of new data for a wider range of altitudes, larger discrepancies in the densities appeared. After close scrutiny, Jacchia in 1971 (Reference 1) found that the amplitude of the semiannual density does not appear to be connected with the solar activity. It does, however, show a strong dependence on height and a variation from year to year. Drag analyses from the Explorer 32 satellite have revealed that a primary minimum in July and a primary maximum in October occur for the average density variation (Reference 1).

Jacchia in J71 expresses the semiannual variation as a product function (Reference 1) in which

$$P_2 = \Delta \log_{10} \rho = f(z)g(t) \quad (6)$$

where $f(z)$ is the relationship between the amplitude, i.e., the difference between the primary maximum and minimum, and the height, z , and where $g(t)$ is the average density variation as a function of time for the amplitude normalized to 1. The two expressions for $f(z)$ and $g(t)$ which yield the best fit to the data are

$$f(z) = (5.876 \times 10^{-7} z^{2.331} + 0.06328) \exp(-2.868 \times 10^{-3} z) \quad D71$$

(7)

for z in kilometers;

$$g(t) = 0.02835 + 0.3817[1 + 0.4671 \sin(2\pi t + 4.1370) \sin(4\pi t + 4.259)]$$

(8)

where

$$\tau = \phi + 0.09544 \left\{ [0.5 + 0.5 \sin(2\pi\phi + 6.035)]^{1.650} - 0.5 \right\}$$

$$\phi = (t - 36204) / 365.2422$$

t = time expressed in Modified Julian Days
(M.J.D. = Julian Day minus 2 400 000.5).
M.J.D. = 36204 is for January 1, 1958.

The term ϕ is the phase of the semiannual variation which is the number of days elapsed since January 1, 1958 divided by the number of days for the tropical year.

Seasonal-Latitudinal Variations of the Lower Thermosphere

In the lower thermosphere, from about 90 km to 120 km, there are variations occurring in temperature and density depending on the latitude and the season. Only the density variation is considered because any temperature variation proves to be too tedious to handle. Between the heights from 90 km to 100 km, there is a rapid increase in the amplitude of this variation in density with a maximum amplitude occurring between 105 and 120 km (Reference 1). Above

120 km there is no data on which to base predictions of the seasonal-latitudinal variations. This variation appears to decrease in amplitude to the point where negligible fluctuations exist at 150 km. Therefore, in DENSITY, the seasonal-latitudinal variations are neglected at heights above 160 km.

Jacchia in J71 fits the seasonal variations to an empirical correction to the decimal logarithm of the density (Reference 1) as follows:

$$P_3 = \Delta \log_{10} \rho = S \frac{\phi'}{|\phi'|} P \sin^2 \phi' \quad (9)$$

where

ϕ' = geographic latitude

$S = 0.014 (z-90) \exp [-0.0013(z-90)^2]$

z = height in kilometers

$P = \sin (2\pi\phi + 1.72)$

ϕ = phase as given in equation (8).

seasonal-Latitudinal Variations of Helium

Helium in the atmosphere has been observed to migrate D71 towards the winter pole. The phenomenon of this seasonal shift in the helium concentration in the upper atmosphere is not yet understood. It therefore becomes necessary to perform an empirical fit to drag data from which this seasonal variation is derived. The expression which is used in J71 (Reference 1) to describe the helium variation is

$$Q_2 = \Delta \log_{10} n(\text{He}) = 0.65 \left| \frac{\delta \theta}{\epsilon} \right| \left[\sin^3 \left(\frac{\Pi}{4} - \frac{\phi}{2} \frac{\delta \theta}{|\delta \theta|} \right) - \sin^3 \frac{\Pi}{4} \right] \quad (10)$$

where

- $n(\text{He})$ = number density of helium (number of particles/cm³)
- $\Delta \theta$ = declination of the sun
- ϕ = geographic latitude
- ϵ = obliquity of the ecliptic ($\epsilon = 23.44^\circ$)

The variation of the helium density in subroutine DENSITY is not considered for heights below 500 km. It is also neglected for latitudes whose absolute value is less than 15° between the range of heights from 500 km to 800 km.

The correction to the density due to the seasonal latitudinal variations of helium is then

$$\Delta \rho_D = 10^{\log_{10} n(\text{He})} \left[10^{\Delta \log_{10} n(\text{He})} - 1 \right] C \text{ gm/cm}^3 \quad (11)$$

where

C is the molecular mass of helium divided by Avogadro's Number.

8.7.1.3 Polynomial Fit of Density Tables

The data which appears in Table 1 shows the variation of density with altitude and exospheric temperature which is reproduced from Jacchia's 1971 report (Reference 1). From heights of 90 km to 100 km, the density values were obtained by numerically integrating the barometric equations. The diffusion equation was numerically integrated to obtain values of the density on the altitude range, 100 km. $<Z \leq 2500$ km. In both cases, an empirical temperature profile was used for each exospheric temperature.

In the GEODYN subroutine DENSTY, the atmospheric density is computed based on the data from Table 1 after appropriate corrections are applied to the exospheric temperature. The tabulated densities have been fitted (by WOLF) to various degree polynomials of the form:

$$P_1 = \text{LOG}_{10} \rho_{DT} = \sum_i h^{(i-1)} \sum_j a_{ij} T^{(j-1)} \quad (12)$$

where

ρ_{DT} is the density in g/cm^3

T is the exospheric temperature,

h is the spheroidal height (altitude), and

a_{ij} is a set of appropriate coefficients for the density tables.

third degree fit. The coefficients for the selected polynomials for the total density are shown in Table 2. In Table 3, coefficients of polynomials for the helium number density are presented.

The computed densities from the fitted polynomials show a reasonable percentage error from the densities given in Table 1. For each of the regions and temperature ranges, the maximum errors are given in Table 4. The largest error of 12% occurs in the region between 500 - 1000 km in the temperature range of 500° - 800°K. In the region of 1000- 2500 km with temperatures between 800° - 1900°K, a fourth degree fit to the temperature yields a maximum error of 11.0% in the densities. D71

The helium number density fits are also given in Table 4. As one can see, the values of the number density are quite satisfactorily fitted by the polynomials. The maximum error in the whole range of heights and temperatures is only 2.8%.

Overall, these fits could be improved by either using higher degree polynomials or possibly other functions, or by further sub-dividing the density table. However, these maximum errors appear to be tolerable since they are considered to be within the range of accuracy of the model presently used. Above 2500 km, the density was found to be negligibly small, and therefore, was set to zero.

Table 1 (cont'd.) (Reproduced from Jacchia 1971 Report, Reference 1)

Summary of Log Densities

	550	600	650	700	750	800	850	900	950
620	-16.285	-15.833	-15.600	-15.393	-15.213	-15.055	-14.915	-14.792	-14.682
625	-16.436	-16.048	-15.860	-15.692	-15.492	-15.334	-15.205	-15.092	-14.992
630	-16.555	-16.251	-16.110	-15.976	-15.767	-15.618	-15.495	-15.395	-15.309
635	-16.644	-16.377	-16.270	-16.155	-15.963	-15.815	-15.695	-15.600	-15.525
640	-16.712	-16.480	-16.400	-16.327	-16.163	-16.016	-15.895	-15.800	-15.725
645	-16.755	-16.552	-16.500	-16.441	-16.276	-16.130	-16.015	-15.920	-15.845
650	-16.808	-16.638	-16.600	-16.557	-16.401	-16.265	-16.145	-16.050	-15.975
655	-16.845	-16.701	-16.675	-16.643	-16.497	-16.370	-16.255	-16.160	-16.085
660	-16.878	-17.057	-17.038	-17.016	-16.876	-16.756	-16.645	-16.550	-16.475
665	-16.926	-17.150	-17.135	-17.116	-16.989	-16.879	-16.772	-16.680	-16.605
670	-16.936	-17.215	-17.200	-17.187	-17.069	-16.960	-16.855	-16.765	-16.690
675	-16.962	-17.272	-17.255	-17.242	-17.125	-17.015	-16.910	-16.820	-16.745
680	-16.987	-17.323	-17.303	-17.289	-17.171	-17.060	-16.955	-16.865	-16.790
685	-17.011	-17.369	-17.346	-17.333	-17.213	-17.101	-16.995	-16.905	-16.830
690	-17.034	-17.408	-17.384	-17.371	-17.250	-17.137	-17.030	-16.940	-16.865
695	-17.057	-17.442	-17.417	-17.404	-17.281	-17.167	-17.060	-16.970	-16.895
700	-17.079	-17.472	-17.446	-17.433	-17.308	-17.194	-17.086	-17.000	-16.925
705	-17.100	-17.501	-17.474	-17.461	-17.334	-17.219	-17.110	-17.020	-16.945
710	-17.120	-17.527	-17.499	-17.485	-17.356	-17.239	-17.130	-17.040	-16.965
715	-17.139	-17.553	-17.525	-17.511	-17.379	-17.261	-17.150	-17.060	-16.985
720	-17.157	-17.578	-17.549	-17.534	-17.400	-17.280	-17.168	-17.078	-16.998
725	-17.174	-17.602	-17.571	-17.555	-17.417	-17.294	-17.181	-17.090	-17.010
730	-17.189	-17.625	-17.592	-17.576	-17.435	-17.311	-17.196	-17.105	-17.025
735	-17.203	-17.646	-17.612	-17.595	-17.453	-17.327	-17.210	-17.118	-17.038
740	-17.216	-17.665	-17.629	-17.611	-17.469	-17.341	-17.222	-17.130	-17.050
745	-17.228	-17.682	-17.644	-17.625	-17.483	-17.353	-17.232	-17.140	-17.060
750	-17.239	-17.697	-17.658	-17.638	-17.500	-17.368	-17.245	-17.152	-17.072
755	-17.250	-17.711	-17.671	-17.650	-17.511	-17.378	-17.254	-17.160	-17.080
760	-17.260	-17.723	-17.682	-17.660	-17.520	-17.387	-17.261	-17.166	-17.085
765	-17.269	-17.734	-17.692	-17.669	-17.528	-17.395	-17.266	-17.170	-17.090
770	-17.277	-17.744	-17.701	-17.678	-17.535	-17.402	-17.271	-17.174	-17.095
775	-17.285	-17.753	-17.708	-17.684	-17.541	-17.408	-17.275	-17.178	-17.100
780	-17.292	-17.761	-17.714	-17.689	-17.546	-17.413	-17.278	-17.181	-17.105
785	-17.298	-17.768	-17.719	-17.694	-17.549	-17.416	-17.279	-17.183	-17.107
790	-17.304	-17.774	-17.723	-17.698	-17.552	-17.418	-17.280	-17.184	-17.108
795	-17.309	-17.779	-17.727	-17.701	-17.555	-17.420	-17.281	-17.185	-17.109
800	-17.313	-17.783	-17.730	-17.704	-17.557	-17.421	-17.281	-17.185	-17.109
805	-17.316	-17.786	-17.732	-17.706	-17.558	-17.422	-17.282	-17.186	-17.110
810	-17.318	-17.788	-17.733	-17.707	-17.559	-17.423	-17.282	-17.186	-17.110
815	-17.320	-17.789	-17.734	-17.708	-17.560	-17.424	-17.282	-17.186	-17.110
820	-17.321	-17.790	-17.734	-17.708	-17.560	-17.424	-17.282	-17.186	-17.110
825	-17.322	-17.790	-17.734	-17.708	-17.560	-17.424	-17.282	-17.186	-17.110
830	-17.322	-17.790	-17.734	-17.708	-17.560	-17.424	-17.282	-17.186	-17.110
835	-17.322	-17.790	-17.734	-17.708	-17.560	-17.424	-17.282	-17.186	-17.110
840	-17.322	-17.790	-17.734	-17.708	-17.560	-17.424	-17.282	-17.186	-17.110
845	-17.322	-17.790	-17.734	-17.708	-17.560	-17.424	-17.282	-17.186	-17.110
850	-17.322	-17.790	-17.734	-17.708	-17.560	-17.424	-17.282	-17.186	-17.110
855	-17.322	-17.790	-17.734	-17.708	-17.560	-17.424	-17.282	-17.186	-17.110
860	-17.322	-17.790	-17.734	-17.708	-17.560	-17.424	-17.282	-17.186	-17.110
865	-17.322	-17.790	-17.734	-17.708	-17.560	-17.424	-17.282	-17.186	-17.110
870	-17.322	-17.790	-17.734	-17.708	-17.560	-17.424	-17.282	-17.186	-17.110
875	-17.322	-17.790	-17.734	-17.708	-17.560	-17.424	-17.282	-17.186	-17.110
880	-17.322	-17.790	-17.734	-17.708	-17.560	-17.424	-17.282	-17.186	-17.110
885	-17.322	-17.790	-17.734	-17.708	-17.560	-17.424	-17.282	-17.186	-17.110
890	-17.322	-17.790	-17.734	-17.708	-17.560	-17.424	-17.282	-17.186	-17.110
895	-17.322	-17.790	-17.734	-17.708	-17.560	-17.424	-17.282	-17.186	-17.110
900	-17.322	-17.790	-17.734	-17.708	-17.560	-17.424	-17.282	-17.186	-17.110
905	-17.322	-17.790	-17.734	-17.708	-17.560	-17.424	-17.282	-17.186	-17.110
910	-17.322	-17.790	-17.734	-17.708	-17.560	-17.424	-17.282	-17.186	-17.110
915	-17.322	-17.790	-17.734	-17.708	-17.560	-17.424	-17.282	-17.186	-17.110
920	-17.322	-17.790	-17.734	-17.708	-17.560	-17.424	-17.282	-17.186	-17.110
925	-17.322	-17.790	-17.734	-17.708	-17.560	-17.424	-17.282	-17.186	-17.110
930	-17.322	-17.790	-17.734	-17.708	-17.560	-17.424	-17.282	-17.186	-17.110
935	-17.322	-17.790	-17.734	-17.708	-17.560	-17.424	-17.282	-17.186	-17.110
940	-17.322	-17.790	-17.734	-17.708	-17.560	-17.424	-17.282	-17.186	-17.110
945	-17.322	-17.790	-17.734	-17.708	-17.560	-17.424	-17.282	-17.186	-17.110
950	-17.322	-17.790	-17.734	-17.708	-17.560	-17.424	-17.282	-17.186	-17.110

REPRODUCIBILITY OF THE ORIGINAL PAGE IS POOR

Table 1 (cont'd.) (Reproduced from Jacchia 1971 Report, Reference I)

Summary of Log Densities

	1029	1050	1100	1150	1200	1250	1300	1350	1400	1450
85	-8.661	-8.661	-8.661	-8.661	-8.661	-8.661	-8.661	-8.461	-8.461	-8.461
86	-8.621	-8.621	-8.621	-8.621	-8.621	-8.621	-8.621	-8.621	-8.621	-8.621
87	-8.782	-8.782	-8.782	-8.782	-8.782	-8.782	-8.782	-8.782	-8.782	-8.782
88	-8.942	-8.942	-8.942	-8.942	-8.942	-8.942	-8.942	-8.942	-8.942	-8.942
89	-9.102	-9.102	-9.102	-9.102	-9.102	-9.102	-9.102	-9.102	-9.102	-9.102
90	-9.262	-9.262	-9.262	-9.262	-9.262	-9.262	-9.262	-9.262	-9.262	-9.262
91	-9.422	-9.422	-9.422	-9.422	-9.422	-9.422	-9.422	-9.422	-9.422	-9.422
92	-9.582	-9.582	-9.582	-9.582	-9.582	-9.582	-9.582	-9.582	-9.582	-9.582
93	-9.742	-9.742	-9.742	-9.742	-9.742	-9.742	-9.742	-9.742	-9.742	-9.742
94	-9.902	-9.902	-9.902	-9.902	-9.902	-9.902	-9.902	-9.902	-9.902	-9.902
95	-10.062	-10.062	-10.062	-10.062	-10.062	-10.062	-10.062	-10.062	-10.062	-10.062
96	-10.222	-10.222	-10.222	-10.222	-10.222	-10.222	-10.222	-10.222	-10.222	-10.222
97	-10.382	-10.382	-10.382	-10.382	-10.382	-10.382	-10.382	-10.382	-10.382	-10.382
98	-10.542	-10.542	-10.542	-10.542	-10.542	-10.542	-10.542	-10.542	-10.542	-10.542
99	-10.702	-10.702	-10.702	-10.702	-10.702	-10.702	-10.702	-10.702	-10.702	-10.702
100	-10.862	-10.862	-10.862	-10.862	-10.862	-10.862	-10.862	-10.862	-10.862	-10.862
101	-11.022	-11.022	-11.022	-11.022	-11.022	-11.022	-11.022	-11.022	-11.022	-11.022
102	-11.182	-11.182	-11.182	-11.182	-11.182	-11.182	-11.182	-11.182	-11.182	-11.182
103	-11.342	-11.342	-11.342	-11.342	-11.342	-11.342	-11.342	-11.342	-11.342	-11.342
104	-11.502	-11.502	-11.502	-11.502	-11.502	-11.502	-11.502	-11.502	-11.502	-11.502
105	-11.662	-11.662	-11.662	-11.662	-11.662	-11.662	-11.662	-11.662	-11.662	-11.662
106	-11.822	-11.822	-11.822	-11.822	-11.822	-11.822	-11.822	-11.822	-11.822	-11.822
107	-11.982	-11.982	-11.982	-11.982	-11.982	-11.982	-11.982	-11.982	-11.982	-11.982
108	-12.142	-12.142	-12.142	-12.142	-12.142	-12.142	-12.142	-12.142	-12.142	-12.142
109	-12.302	-12.302	-12.302	-12.302	-12.302	-12.302	-12.302	-12.302	-12.302	-12.302
110	-12.462	-12.462	-12.462	-12.462	-12.462	-12.462	-12.462	-12.462	-12.462	-12.462
111	-12.622	-12.622	-12.622	-12.622	-12.622	-12.622	-12.622	-12.622	-12.622	-12.622
112	-12.782	-12.782	-12.782	-12.782	-12.782	-12.782	-12.782	-12.782	-12.782	-12.782
113	-12.942	-12.942	-12.942	-12.942	-12.942	-12.942	-12.942	-12.942	-12.942	-12.942
114	-13.102	-13.102	-13.102	-13.102	-13.102	-13.102	-13.102	-13.102	-13.102	-13.102
115	-13.262	-13.262	-13.262	-13.262	-13.262	-13.262	-13.262	-13.262	-13.262	-13.262
116	-13.422	-13.422	-13.422	-13.422	-13.422	-13.422	-13.422	-13.422	-13.422	-13.422
117	-13.582	-13.582	-13.582	-13.582	-13.582	-13.582	-13.582	-13.582	-13.582	-13.582
118	-13.742	-13.742	-13.742	-13.742	-13.742	-13.742	-13.742	-13.742	-13.742	-13.742
119	-13.902	-13.902	-13.902	-13.902	-13.902	-13.902	-13.902	-13.902	-13.902	-13.902
120	-14.062	-14.062	-14.062	-14.062	-14.062	-14.062	-14.062	-14.062	-14.062	-14.062
121	-14.222	-14.222	-14.222	-14.222	-14.222	-14.222	-14.222	-14.222	-14.222	-14.222
122	-14.382	-14.382	-14.382	-14.382	-14.382	-14.382	-14.382	-14.382	-14.382	-14.382
123	-14.542	-14.542	-14.542	-14.542	-14.542	-14.542	-14.542	-14.542	-14.542	-14.542
124	-14.702	-14.702	-14.702	-14.702	-14.702	-14.702	-14.702	-14.702	-14.702	-14.702
125	-14.862	-14.862	-14.862	-14.862	-14.862	-14.862	-14.862	-14.862	-14.862	-14.862
126	-15.022	-15.022	-15.022	-15.022	-15.022	-15.022	-15.022	-15.022	-15.022	-15.022
127	-15.182	-15.182	-15.182	-15.182	-15.182	-15.182	-15.182	-15.182	-15.182	-15.182
128	-15.342	-15.342	-15.342	-15.342	-15.342	-15.342	-15.342	-15.342	-15.342	-15.342
129	-15.502	-15.502	-15.502	-15.502	-15.502	-15.502	-15.502	-15.502	-15.502	-15.502
130	-15.662	-15.662	-15.662	-15.662	-15.662	-15.662	-15.662	-15.662	-15.662	-15.662
131	-15.822	-15.822	-15.822	-15.822	-15.822	-15.822	-15.822	-15.822	-15.822	-15.822
132	-15.982	-15.982	-15.982	-15.982	-15.982	-15.982	-15.982	-15.982	-15.982	-15.982
133	-16.142	-16.142	-16.142	-16.142	-16.142	-16.142	-16.142	-16.142	-16.142	-16.142
134	-16.302	-16.302	-16.302	-16.302	-16.302	-16.302	-16.302	-16.302	-16.302	-16.302
135	-16.462	-16.462	-16.462	-16.462	-16.462	-16.462	-16.462	-16.462	-16.462	-16.462

REPRODUCIBILITY OF THE ORIGINAL PAGE IS POOR

Table 1 (cont'd) (Reproduced from Jacchia 1971 Report, Reference 1)

Summary of Log Densities

	1000	1050	1100	1150	1200	1250	1300	1350	1400	1450
420	-14.533	-14.494	-14.614	-14.340	-14.273	-14.212	-14.155	-14.102	-14.054	-14.006
440	-14.731	-14.636	-14.550	-14.472	-14.400	-14.335	-14.274	-14.218	-14.165	-14.118
460	-14.877	-14.776	-14.685	-14.601	-14.525	-14.456	-14.391	-14.332	-14.277	-14.225
480	-15.020	-14.914	-14.817	-14.729	-14.648	-14.574	-14.506	-14.443	-14.385	-14.330
500	-15.162	-15.049	-14.947	-14.854	-14.769	-14.691	-14.621	-14.553	-14.491	-14.434
520	-15.301	-15.183	-15.076	-14.978	-14.889	-14.806	-14.731	-14.661	-14.595	-14.535
540	-15.439	-15.315	-15.203	-15.100	-15.006	-14.920	-14.841	-14.767	-14.697	-14.636
560	-15.574	-15.445	-15.328	-15.221	-15.122	-15.032	-14.949	-14.872	-14.801	-14.735
580	-15.708	-15.573	-15.451	-15.340	-15.237	-15.143	-15.056	-14.976	-14.902	-14.832
600	-15.837	-15.699	-15.573	-15.457	-15.351	-15.253	-15.162	-15.079	-15.001	-14.929
620	-15.965	-15.823	-15.693	-15.573	-15.462	-15.361	-15.267	-15.180	-15.099	-15.024
640	-16.090	-15.945	-15.810	-15.677	-15.573	-15.468	-15.370	-15.280	-15.195	-15.113
660	-16.211	-16.063	-15.926	-15.789	-15.682	-15.573	-15.472	-15.379	-15.292	-15.211
680	-16.329	-16.179	-16.039	-15.909	-15.799	-15.677	-15.573	-15.477	-15.387	-15.304
700	-16.442	-16.292	-16.150	-16.017	-15.894	-15.779	-15.673	-15.573	-15.481	-15.395
720	-16.551	-16.400	-16.258	-16.123	-15.997	-15.880	-15.771	-15.669	-15.573	-15.485
740	-16.654	-16.505	-16.362	-16.227	-16.099	-15.979	-15.867	-15.763	-15.665	-15.574
760	-16.753	-16.606	-16.463	-16.327	-16.198	-16.076	-15.962	-15.855	-15.755	-15.661
780	-16.845	-16.702	-16.561	-16.424	-16.294	-16.171	-16.055	-15.945	-15.844	-15.743
800	-16.932	-16.793	-16.654	-16.519	-16.389	-16.264	-16.147	-16.036	-15.922	-15.834
820	-17.012	-16.878	-16.745	-16.609	-16.480	-16.355	-16.236	-16.124	-16.009	-15.913
840	-17.087	-16.959	-16.827	-16.696	-16.568	-16.443	-16.324	-16.210	-16.103	-16.001
860	-17.157	-17.034	-16.907	-16.779	-16.652	-16.528	-16.409	-16.295	-16.186	-16.077
880	-17.223	-17.104	-16.982	-16.858	-16.733	-16.611	-16.492	-16.377	-16.267	-16.153
900	-17.288	-17.169	-17.049	-16.933	-16.811	-16.690	-16.572	-16.457	-16.347	-16.232
920	-17.355	-17.233	-17.119	-17.003	-16.885	-16.766	-16.649	-16.535	-16.425	-16.314
940	-17.418	-17.296	-17.180	-17.064	-16.945	-16.833	-16.724	-16.610	-16.500	-16.387
960	-17.476	-17.354	-17.237	-17.131	-17.021	-16.908	-16.795	-16.684	-16.574	-16.461
980	-17.529	-17.407	-17.291	-17.184	-17.073	-16.976	-16.864	-16.754	-16.643	-16.539
1000	-17.582	-17.462	-17.340	-17.234	-17.142	-17.037	-16.929	-16.821	-16.714	-16.601
1020	-17.619	-17.495	-17.375	-17.265	-17.173	-17.078	-17.019	-16.977	-16.875	-16.772
1040	-17.652	-17.538	-17.415	-17.305	-17.213	-17.118	-17.019	-16.977	-16.875	-16.772
1060	-17.679	-17.565	-17.443	-17.334	-17.242	-17.146	-17.047	-17.005	-16.903	-16.800
1080	-17.702	-17.587	-17.466	-17.357	-17.265	-17.169	-17.070	-17.028	-16.926	-16.823
1100	-17.722	-17.607	-17.486	-17.377	-17.285	-17.189	-17.090	-17.048	-16.946	-16.843
1120	-17.737	-17.622	-17.501	-17.392	-17.300	-17.204	-17.105	-17.063	-16.961	-16.858
1140	-17.748	-17.634	-17.513	-17.403	-17.311	-17.215	-17.116	-17.074	-16.972	-16.869
1160	-17.755	-17.642	-17.521	-17.411	-17.319	-17.223	-17.124	-17.082	-16.980	-16.877
1180	-17.757	-17.645	-17.524	-17.414	-17.322	-17.226	-17.127	-17.085	-16.983	-16.880
1200	-17.757	-17.645	-17.524	-17.414	-17.322	-17.226	-17.127	-17.085	-16.983	-16.880
1220	-17.757	-17.645	-17.524	-17.414	-17.322	-17.226	-17.127	-17.085	-16.983	-16.880
1240	-17.757	-17.645	-17.524	-17.414	-17.322	-17.226	-17.127	-17.085	-16.983	-16.880
1260	-17.757	-17.645	-17.524	-17.414	-17.322	-17.226	-17.127	-17.085	-16.983	-16.880
1280	-17.757	-17.645	-17.524	-17.414	-17.322	-17.226	-17.127	-17.085	-16.983	-16.880
1300	-17.757	-17.645	-17.524	-17.414	-17.322	-17.226	-17.127	-17.085	-16.983	-16.880
1320	-17.757	-17.645	-17.524	-17.414	-17.322	-17.226	-17.127	-17.085	-16.983	-16.880
1340	-17.757	-17.645	-17.524	-17.414	-17.322	-17.226	-17.127	-17.085	-16.983	-16.880
1360	-17.757	-17.645	-17.524	-17.414	-17.322	-17.226	-17.127	-17.085	-16.983	-16.880
1380	-17.757	-17.645	-17.524	-17.414	-17.322	-17.226	-17.127	-17.085	-16.983	-16.880
1400	-17.757	-17.645	-17.524	-17.414	-17.322	-17.226	-17.127	-17.085	-16.983	-16.880
1420	-17.757	-17.645	-17.524	-17.414	-17.322	-17.226	-17.127	-17.085	-16.983	-16.880
1440	-17.757	-17.645	-17.524	-17.414	-17.322	-17.226	-17.127	-17.085	-16.983	-16.880
1460	-17.757	-17.645	-17.524	-17.414	-17.322	-17.226	-17.127	-17.085	-16.983	-16.880
1480	-17.757	-17.645	-17.524	-17.414	-17.322	-17.226	-17.127	-17.085	-16.983	-16.880
1500	-17.757	-17.645	-17.524	-17.414	-17.322	-17.226	-17.127	-17.085	-16.983	-16.880

REPRODUCIBILITY OF THE ORIGINAL PAGE IS POOR

Table 1 (cont'd) (Reproduced from Jacchia 1971 Report, Reference 1)

Summary of Log Densities

	1950	1600	1650	1700	1750	1800	1850	1900
92	-8.631	-8.651	-8.661	-8.661	-8.661	-8.661	-8.661	-8.651
93	-8.621	-8.621	-8.621	-8.621	-8.621	-8.621	-8.621	-8.621
94	-8.782	-8.782	-8.782	-8.782	-8.782	-8.782	-8.782	-8.782
95	-8.943	-8.944	-8.944	-8.944	-8.944	-8.944	-8.944	-8.944
96	-9.104	-9.104	-9.104	-9.104	-9.104	-9.104	-9.104	-9.104
100	-9.262	-9.262	-9.262	-9.262	-9.262	-9.262	-9.262	-9.262
102	-9.419	-9.419	-9.419	-9.419	-9.419	-9.419	-9.419	-9.419
104	-9.577	-9.577	-9.577	-9.577	-9.577	-9.577	-9.577	-9.577
106	-9.721	-9.721	-9.721	-9.721	-9.721	-9.721	-9.721	-9.721
108	-9.865	-9.865	-9.865	-9.865	-9.865	-9.865	-9.865	-9.865
110	-10.004	-10.004	-10.004	-10.004	-10.004	-10.004	-10.004	-10.004
115	-10.321	-10.321	-10.321	-10.321	-10.321	-10.321	-10.321	-10.321
120	-10.593	-10.593	-10.593	-10.593	-10.593	-10.593	-10.593	-10.593
125	-10.823	-10.823	-10.823	-10.823	-10.823	-10.823	-10.823	-10.823
130	-11.018	-11.018	-11.018	-11.018	-11.018	-11.018	-11.018	-11.018
135	-11.205	-11.205	-11.205	-11.205	-11.205	-11.205	-11.205	-11.205
140	-11.354	-11.354	-11.354	-11.354	-11.354	-11.354	-11.354	-11.354
145	-11.483	-11.483	-11.483	-11.483	-11.483	-11.483	-11.483	-11.483
150	-11.612	-11.612	-11.612	-11.612	-11.612	-11.612	-11.612	-11.612
155	-11.744	-11.744	-11.744	-11.744	-11.744	-11.744	-11.744	-11.744
160	-11.872	-11.872	-11.872	-11.872	-11.872	-11.872	-11.872	-11.872
165	-12.005	-12.005	-12.005	-12.005	-12.005	-12.005	-12.005	-12.005
170	-12.137	-12.137	-12.137	-12.137	-12.137	-12.137	-12.137	-12.137
175	-12.273	-12.273	-12.273	-12.273	-12.273	-12.273	-12.273	-12.273
180	-12.405	-12.405	-12.405	-12.405	-12.405	-12.405	-12.405	-12.405
185	-12.543	-12.543	-12.543	-12.543	-12.543	-12.543	-12.543	-12.543
190	-12.677	-12.677	-12.677	-12.677	-12.677	-12.677	-12.677	-12.677
195	-12.817	-12.817	-12.817	-12.817	-12.817	-12.817	-12.817	-12.817
200	-12.957	-12.957	-12.957	-12.957	-12.957	-12.957	-12.957	-12.957
205	-13.097	-13.097	-13.097	-13.097	-13.097	-13.097	-13.097	-13.097
210	-13.237	-13.237	-13.237	-13.237	-13.237	-13.237	-13.237	-13.237
215	-13.377	-13.377	-13.377	-13.377	-13.377	-13.377	-13.377	-13.377
220	-13.517	-13.517	-13.517	-13.517	-13.517	-13.517	-13.517	-13.517
225	-13.657	-13.657	-13.657	-13.657	-13.657	-13.657	-13.657	-13.657
230	-13.797	-13.797	-13.797	-13.797	-13.797	-13.797	-13.797	-13.797
235	-13.937	-13.937	-13.937	-13.937	-13.937	-13.937	-13.937	-13.937
240	-14.077	-14.077	-14.077	-14.077	-14.077	-14.077	-14.077	-14.077
245	-14.217	-14.217	-14.217	-14.217	-14.217	-14.217	-14.217	-14.217
250	-14.357	-14.357	-14.357	-14.357	-14.357	-14.357	-14.357	-14.357
255	-14.497	-14.497	-14.497	-14.497	-14.497	-14.497	-14.497	-14.497
260	-14.637	-14.637	-14.637	-14.637	-14.637	-14.637	-14.637	-14.637
265	-14.777	-14.777	-14.777	-14.777	-14.777	-14.777	-14.777	-14.777
270	-14.917	-14.917	-14.917	-14.917	-14.917	-14.917	-14.917	-14.917
275	-15.057	-15.057	-15.057	-15.057	-15.057	-15.057	-15.057	-15.057
280	-15.197	-15.197	-15.197	-15.197	-15.197	-15.197	-15.197	-15.197
285	-15.337	-15.337	-15.337	-15.337	-15.337	-15.337	-15.337	-15.337
290	-15.477	-15.477	-15.477	-15.477	-15.477	-15.477	-15.477	-15.477
295	-15.617	-15.617	-15.617	-15.617	-15.617	-15.617	-15.617	-15.617
300	-15.757	-15.757	-15.757	-15.757	-15.757	-15.757	-15.757	-15.757
305	-15.897	-15.897	-15.897	-15.897	-15.897	-15.897	-15.897	-15.897
310	-16.037	-16.037	-16.037	-16.037	-16.037	-16.037	-16.037	-16.037
315	-16.177	-16.177	-16.177	-16.177	-16.177	-16.177	-16.177	-16.177
320	-16.317	-16.317	-16.317	-16.317	-16.317	-16.317	-16.317	-16.317
325	-16.457	-16.457	-16.457	-16.457	-16.457	-16.457	-16.457	-16.457
330	-16.597	-16.597	-16.597	-16.597	-16.597	-16.597	-16.597	-16.597
335	-16.737	-16.737	-16.737	-16.737	-16.737	-16.737	-16.737	-16.737
340	-16.877	-16.877	-16.877	-16.877	-16.877	-16.877	-16.877	-16.877
345	-17.017	-17.017	-17.017	-17.017	-17.017	-17.017	-17.017	-17.017
350	-17.157	-17.157	-17.157	-17.157	-17.157	-17.157	-17.157	-17.157
355	-17.297	-17.297	-17.297	-17.297	-17.297	-17.297	-17.297	-17.297
360	-17.437	-17.437	-17.437	-17.437	-17.437	-17.437	-17.437	-17.437
365	-17.577	-17.577	-17.577	-17.577	-17.577	-17.577	-17.577	-17.577
370	-17.717	-17.717	-17.717	-17.717	-17.717	-17.717	-17.717	-17.717
375	-17.857	-17.857	-17.857	-17.857	-17.857	-17.857	-17.857	-17.857
380	-17.997	-17.997	-17.997	-17.997	-17.997	-17.997	-17.997	-17.997
385	-18.137	-18.137	-18.137	-18.137	-18.137	-18.137	-18.137	-18.137
390	-18.277	-18.277	-18.277	-18.277	-18.277	-18.277	-18.277	-18.277
395	-18.417	-18.417	-18.417	-18.417	-18.417	-18.417	-18.417	-18.417
400	-18.557	-18.557	-18.557	-18.557	-18.557	-18.557	-18.557	-18.557

REPRODUCIBILITY OF THE ORIGINAL PAGE IS POOR

Table 1 (cont'd) (Reproduced from Jacchia 1971 Report, Reference 1)

Summary of Log Densities

	1500	1550	1600	1650	1700	1750	1800	1850	1900
420	-13.946	-13.926	-13.889	-13.854	-13.820	-13.789	-13.759	-13.731	-13.705
440	-14.073	-14.070	-13.991	-13.953	-13.918	-13.885	-13.853	-13.823	-13.794
460	-14.177	-14.152	-14.090	-14.050	-14.013	-13.978	-13.944	-13.912	-13.882
480	-14.280	-14.232	-14.186	-14.146	-14.106	-14.069	-14.033	-14.000	-13.963
500	-14.330	-14.330	-14.293	-14.239	-14.197	-14.158	-14.121	-14.085	-14.052
520	-14.379	-14.427	-14.377	-14.331	-14.287	-14.246	-14.206	-14.169	-14.134
540	-14.477	-14.527	-14.470	-14.421	-14.375	-14.332	-14.291	-14.252	-14.215
560	-14.573	-14.615	-14.561	-14.510	-14.452	-14.416	-14.373	-14.333	-14.294
580	-14.668	-14.708	-14.651	-14.597	-14.547	-14.500	-14.455	-14.413	-14.372
600	-14.751	-14.798	-14.739	-14.686	-14.632	-14.582	-14.536	-14.493	-14.450
620	-14.834	-14.888	-14.827	-14.769	-14.715	-14.664	-14.615	-14.569	-14.525
640	-14.914	-14.977	-14.914	-14.854	-14.797	-14.744	-14.693	-14.646	-14.600
660	-15.030	-15.065	-14.999	-14.937	-14.878	-14.823	-14.771	-14.721	-14.674
680	-15.125	-15.152	-15.084	-15.019	-14.959	-14.902	-14.847	-14.795	-14.747
700	-15.214	-15.238	-15.168	-15.101	-15.038	-14.979	-14.923	-14.870	-14.820
720	-15.291	-15.324	-15.250	-15.172	-15.117	-15.056	-14.998	-14.943	-14.891
740	-15.358	-15.398	-15.322	-15.252	-15.195	-15.132	-15.072	-15.016	-14.962
760	-15.414	-15.458	-15.381	-15.331	-15.272	-15.207	-15.146	-15.083	-15.022
780	-15.468	-15.513	-15.436	-15.389	-15.328	-15.261	-15.218	-15.159	-15.112
800	-15.517	-15.565	-15.483	-15.446	-15.374	-15.305	-15.270	-15.229	-15.170
820	-15.564	-15.615	-15.527	-15.498	-15.424	-15.355	-15.320	-15.289	-15.239
840	-15.609	-15.665	-15.573	-15.549	-15.473	-15.408	-15.362	-15.336	-15.286
860	-15.654	-15.713	-15.616	-15.595	-15.517	-15.455	-15.502	-15.456	-15.413
880	-15.699	-15.760	-15.656	-15.737	-15.648	-15.589	-15.543	-15.503	-15.459
900	-15.744	-15.808	-15.697	-15.780	-15.683	-15.628	-15.591	-15.549	-15.507
920	-15.789	-15.856	-15.737	-15.821	-15.726	-15.675	-15.639	-15.597	-15.556
940	-15.834	-15.903	-15.784	-15.869	-15.776	-15.729	-15.694	-15.652	-15.612
960	-15.879	-15.950	-15.823	-15.908	-15.818	-15.775	-15.741	-15.700	-15.660
980	-15.924	-15.997	-15.862	-15.947	-15.860	-15.821	-15.788	-15.747	-15.708
1000	-15.969	-16.044	-15.900	-15.985	-15.900	-15.865	-15.833	-15.792	-15.753
1020	-16.014	-16.090	-15.937	-16.022	-15.939	-15.909	-15.879	-15.839	-15.801
1040	-16.059	-16.136	-15.964	-16.049	-15.968	-15.942	-15.914	-15.875	-15.838
1060	-16.104	-16.182	-16.009	-16.094	-16.015	-15.990	-15.964	-15.925	-15.890
1080	-16.149	-16.228	-16.054	-16.139	-16.058	-16.034	-16.009	-15.970	-15.932
1100	-16.194	-16.274	-16.099	-16.184	-16.106	-16.084	-16.059	-16.020	-15.982
1120	-16.239	-16.319	-16.144	-16.229	-16.148	-16.128	-16.103	-16.064	-16.027
1140	-16.284	-16.364	-16.189	-16.274	-16.196	-16.177	-16.152	-16.113	-16.077
1160	-16.329	-16.409	-16.234	-16.319	-16.238	-16.220	-16.195	-16.156	-16.121
1180	-16.374	-16.454	-16.279	-16.364	-16.286	-16.269	-16.244	-16.205	-16.171
1200	-16.419	-16.499	-16.324	-16.409	-16.329	-16.313	-16.288	-16.249	-16.215
1220	-16.464	-16.544	-16.369	-16.454	-16.376	-16.361	-16.336	-16.297	-16.264
1240	-16.509	-16.589	-16.414	-16.499	-16.421	-16.406	-16.381	-16.342	-16.309
1260	-16.554	-16.634	-16.459	-16.544	-16.466	-16.452	-16.427	-16.388	-16.355
1280	-16.599	-16.679	-16.504	-16.589	-16.511	-16.497	-16.472	-16.433	-16.400
1300	-16.644	-16.724	-16.549	-16.634	-16.561	-16.547	-16.522	-16.483	-16.450
1320	-16.689	-16.769	-16.594	-16.679	-16.606	-16.592	-16.567	-16.528	-16.495
1340	-16.734	-16.814	-16.639	-16.724	-16.656	-16.642	-16.617	-16.578	-16.545
1360	-16.779	-16.859	-16.684	-16.769	-16.696	-16.682	-16.657	-16.618	-16.585
1380	-16.824	-16.904	-16.729	-16.814	-16.746	-16.732	-16.707	-16.668	-16.635
1400	-16.869	-16.949	-16.774	-16.859	-16.791	-16.777	-16.752	-16.713	-16.680
1420	-16.914	-16.994	-16.819	-16.904	-16.836	-16.822	-16.797	-16.758	-16.725
1440	-16.959	-17.039	-16.864	-16.949	-16.881	-16.867	-16.842	-16.803	-16.770
1460	-17.004	-17.084	-16.909	-16.994	-16.926	-16.912	-16.887	-16.848	-16.815
1480	-17.049	-17.129	-16.954	-17.039	-16.966	-16.952	-16.927	-16.888	-16.855
1500	-17.094	-17.174	-16.999	-17.084	-17.016	-17.002	-16.977	-16.938	-16.905
1520	-17.139	-17.219	-17.044	-17.129	-17.061	-17.047	-17.022	-16.983	-16.950
1540	-17.184	-17.264	-17.089	-17.174	-17.106	-17.092	-17.067	-17.028	-16.995
1560	-17.229	-17.309	-17.134	-17.219	-17.151	-17.137	-17.112	-17.073	-17.040
1580	-17.274	-17.354	-17.179	-17.264	-17.196	-17.182	-17.157	-17.118	-17.085
1600	-17.319	-17.399	-17.224	-17.309	-17.241	-17.227	-17.202	-17.163	-17.130
1620	-17.364	-17.444	-17.269	-17.354	-17.291	-17.277	-17.252	-17.213	-17.180
1640	-17.409	-17.489	-17.314	-17.409	-17.346	-17.332	-17.307	-17.268	-17.235
1660	-17.454	-17.534	-17.359	-17.449	-17.386	-17.372	-17.347	-17.308	-17.275
1680	-17.499	-17.579	-17.404	-17.494	-17.431	-17.417	-17.392	-17.353	-17.320
1700	-17.544	-17.624	-17.449	-17.539	-17.476	-17.462	-17.437	-17.398	-17.365
1720	-17.589	-17.669	-17.494	-17.584	-17.521	-17.507	-17.482	-17.443	-17.410
1740	-17.634	-17.714	-17.539	-17.629	-17.566	-17.552	-17.527	-17.488	-17.455
1760	-17.679	-17.759	-17.584	-17.674	-17.611	-17.597	-17.572	-17.533	-17.500
1780	-17.724	-17.804	-17.629	-17.719	-17.656	-17.642	-17.617	-17.578	-17.545
1800	-17.769	-17.849	-17.674	-17.764	-17.701	-17.687	-17.662	-17.623	-17.590
1820	-17.814	-17.894	-17.719	-17.809	-17.746	-17.732	-17.707	-17.668	-17.635
1840	-17.859	-17.939	-17.764	-17.854	-17.791	-17.777	-17.752	-17.713	-17.680
1860	-17.904	-17.984	-17.809	-17.899	-17.836	-17.822	-17.797	-17.758	-17.725
1880	-17.949	-18.029	-17.854	-17.944	-17.881	-17.867	-17.842	-17.803	-17.770
1900	-17.994	-18.074	-17.899	-18.004	-17.941	-17.927	-17.902	-17.863	-17.830
1920	-18.039	-18.119	-17.944	-18.039	-17.976	-17.962	-17.937	-17.898	-17.865
1940	-18.084	-18.164	-17.989	-18.084	-18.021	-18.007	-17.982	-17.943	-17.910
1960	-18.129	-18.209	-18.034	-18.129	-18.066	-18.052	-18.027	-17.988	-17.955
1980	-18.174	-18.254	-18.079	-18.174	-18.116	-18.102	-18.077	-18.038	-18.005
2000	-18.219	-18.299	-18.124	-18.219	-18.161	-18.147	-18.122	-18.083	-18.050

REPRODUCIBILITY OF THE ORIGINAL PAGE IS POOR

TABLE 2.
DENSITY POLYNOMIAL COEFFICIENTS
(For Decimal Logarithm of Density)

	T^0	T^1	T^2	T^3	T^4
90-200KM					
h^0	4.22085	0.98393E-2	-.64952E-5	0.14715E-8	
h^1	-0.20134	-.23412E-3	0.15337E-6	-.34675E-10	
h^2	0.78592E-3	0.16966E-5	-.11060E-8	0.25007E-12	
h^3	-.12087E-5	-.34360E-8	0.22457E-11	-.51069E-15	
200-500KM for 500°-800°K					
h^0	-.12838E+2	0.40709E-2	0.97074E-5	-.10643E-7	
h^1	0.82282E-1	-.31215E-3	0.26543E-6	-.55193E-10	
h^2	-.68951E-3	0.24402E-5	-.27058E-8	0.99003E-12	
h^3	0.11263E-5	-.41807E-8	0.50617E-11	-.20484E-14	
200-500KM for 800°-1900°K					
h^0	-8.4595	-.15000E-3	-.62640E-6	0.24612E-9	
h^1	-.28395E-1	0.17760E-6	0.61398E-8	-.23362E-11	
h^2	0.55998E-5	0.77461E-7	-.59492E-10	0.14921E-13	
h^3	0.39434E-8	-.76435E-10	0.58533E-13	-.14595E-16	
500-100KM for 500°-800°K					
h^0	-.77659E+2	0.167271	-.56570E-4	-.50424E-7	
h^1	0.50638	-.98936E-3	0.74932E-6	-.53178E-10	
h^2	-.38935E-3	0.12973E-5	-.19776E-8	0.14191E-12	
h^3	0.15962E-6	-.54049E-9	0.46709E-12	-.71886E-16	

REPRODUCIBILITY OF THE
ORIGINAL PAGE IS POOR

TABLE 2
DENSITY POLYNOMIAL COEFFICIENTS

	T^0	T^1	T^2	T^3	T^4
500-1000KM for 800°-1900°K					
h^0	0.50081E+2	-.12600	0.83896E-4	-.18276E-7	
h^1	-.30572	0.61706E-3	-.41443E-6	0.91096E-10	
h^2	0.41767E-3	-.88743E-6	0.61040E-9	-.13634E-12	
h^3	-.17955E-6	0.39386E-9	-.27639E-12	0.62649E-16	
1000-2500KM for 500°-800°K					
h^0	0.50532E+2	-.26156	0.41963E-3	-.21661E-6	
h^1	-.48352E-1	0.28801E-3	-.48214E-6	0.27095E-9	
h^2	0.11141E-4	-.7755E-7	0.16042E-9	-.99055E-13	
h^3	-.21059E-10	0.44725E-11	-.14085E-13	0.10443E-16	
1000-2500KM for 800°-1900°K					
h^0	0.52410E+2	-.28651	0.21642E-3	-.90623E-7	0.13054E-10
h^1	-.14335	0.43113E-3	-.46137E-6	0.20179E-9	-.30888E-13
h^2	0.87693E-4	-.27157E-6	0.39745E-9	-.13425E-12	0.21370E-16
h^3	-.15716E-7	0.49631E-10	-.55297E-13	0.25432E-16	-.41304E-20

REPRODUCIBILITY OF THE
ORIGINAL PAGE IS POOR

TABLE 3

 HELIUM DENSITY POLYNOMIAL COEFFICIENTS
 (DECIMAL LOG OF HELIUM NUMBER DENSITY)

	T^0	T^1	T^2	T^3	T^4
500-1000KM for 500°-800°K					
h^0	9.3712	-.52634E-2	0.52983E-5	-.20471E-8	
h^1	-.13141E-1	0.31218E-4	-.32598E-7	0.12573E-10	
h^2	0.26071E-5	-.75730E-8	0.93058E-11	-.40669E-14	
h^3	-.52156E-9	0.19056E-11	-.26578E-14	0.12535E-17	
500-1000KM for 800°-1900°K					
h^0	8.3914	-.16433E-2	0.78032E-6	-.14323E-9	
h^1	-.69049E-2	0.84138E-5	-.44577E-8	0.85627E-12	
h^2	0.10510E-5	-.12663E-8	0.71134E-12	-.14180E-15	
h^3	-.12222E-9	0.14745E-12	-.97658E-16	0.21458E-19	
1000-2500KM for 500°-800°K					
h^0	9.1045	-4.3410E-2	0.40292E-5	-.14522E-8	
h^1	-.12259E-1	0.27951E-4	-.27972E-7	0.10371E-10	
h^2	0.15893E-5	-.35863E-8	0.35476E-11	-.12985E-14	
h^3	-.11829E-9	0.26138E-12	-.25227E-15	0.89714E-19	
100-2500KM for 800°-1900°K					
h^0	8.6120	-.25363E-2	0.18979E-5	-.73696E-9	0.11388E-12
h^1	-.84847E-2	0.14084E-4	-.11386E-7	0.44871E-11	-.69064E-15
h^2	0.11543E-5	-.19884E-8	0.16635E-11	-.67628E-15	0.10706E-18
h^3	-.94521E-10	0.17387E-12	-.15368E-15	0.65402E-19	-.70760E-22

TABLE 4
 PERCENTAGE ERROR OF POLYNOMIAL FITS
 TO THE DENSITIES

Height Range (KM)	Temperature Range (°K)	Maximum Percent Error	
		Total Density	Helium Density
90-200	500-1900	11.0%	-
200-500	500-800	11.6%	-
200-500	800-1900	5.13%	-
500-1000	500-800	12.0%	0.44%
500-1000	800-1900	8.85%	2.8%
1000-2500	500-800	4.1%	1.5%
100-2500	800-1900	11.0%	1.25%

8.7.1.4 The Density Computation

When all of the terms contributing to the atmosphere density are combined D71

$$\rho_D = 10^3 \left[10^{P_1+P_2+P_3+P_4} + 10^{Q_1} (10^{Q_2} - 1) C \right] \quad (14)$$

where

ρ_D = the atmospheric density in Kg/m^3

P_1 is given by equation (12),

P_2 is given by equation (6),

P_3 is given by equation (9),

P_4 is given by equation (5a),

Q_1 is given by equation (13),

Q_2 is given by equation (10), and

C is the molecular mass of Helium divided by Avogadro's Number = $0.6646(10^{-23})$

REPRODUCIBILITY OF THE ORIGINAL PAGE IS POOR

8.7.1.5 Density Partial Derivatives

D71
VEVAL

In addition to the density, GEODYN also requires the partial derivatives of the density with respect to the Cartesian position coordinates. These partials are used in computing the drag contributions to the variational equations.

The spatial partial derivatives of the atmospheric density are

$$\frac{\partial \rho_D}{\partial \bar{r}} = \frac{\partial \rho_D}{\partial \phi} \frac{\partial \phi}{\partial \bar{r}} + \frac{\partial \rho_D}{\partial \lambda} \frac{\partial \lambda}{\partial \bar{r}} + \frac{\partial \rho_D}{\partial h} \frac{\partial h}{\partial \bar{r}} \quad (1)$$

where

h - spheroid height of the satellite

ϕ - sub-satellite latitude

λ - sub-satellite longitude

\bar{r} - true of date position vector of the satellite

Variations in atmospheric density are primarily due to changes in height. Therefore, only height variations are computed by GEODYN and

$$\begin{aligned} \frac{\partial \rho_D}{\partial \phi} &= 0 \\ \frac{\partial \rho_D}{\partial \lambda} &= 0 \end{aligned} \quad (2)$$

and consequently

371

$$\frac{\partial \rho_D}{\partial \bar{r}} = \frac{\partial \rho_D}{\partial h} \frac{\partial h}{\partial \bar{r}} \quad (3)$$

where

$\frac{\partial h}{\partial \bar{r}}$ is presented along with the spheroid height computation in Section 5.1.

The density is given (Section 8.7.4) by

$$\rho_D = 10^3 \left[10^{P_1 + P_2 + P_3 + P_4} + 10^{Q_1} (10^{Q_2} - 1) C \right] \quad (4)$$

where

ρ_D - density in Kg/m³

$$P_1 = \sum_{i=1}^n h^{(i-1)} \sum_{j=1}^m a_{ij} T^{(j-1)} \quad (5)$$

$$P_2 = g(t) [5.876(10^{-7}) h^{2.351} + 0.06528] \exp [-2.368(10^{-3})h] \quad (6)$$

$$P_3 = 0.014(h-90) P \frac{\phi'}{|\phi'|} \sin^2 \phi' \exp [-0.0015(h-90)^2] \quad (7)$$

$$P_4 = 0.012 K_p + 1.2(10^{-5}) \exp (K_p) \quad (8)$$

$$Q_1 = \sum_{i=1}^n r^{(i-1)} \sum_{j=1}^m b_{ij} T^{(j-1)} = \log_{10} n(\text{He}) \quad (9)$$

$$Q_2 = \Delta \log_{10} n(\text{He}) \quad (10)$$

C = the molecular mass of Helium divided by Avogadro's Number.

h = height in Km.

a_{ij} - polynomial coefficients used to fit the density table.

b_{ij} - polynomial coefficients used to fit the Helium number density table.

All other terms are defined in Section 8.7.1.4 and need no further clarification at this point since they are constants in the partial derivative equations.

Defining two basic derivative formulae,

$$\frac{d}{dx} e^{u(x)} = e^{u(x)} \frac{du(x)}{dx} \quad (11)$$

$$\begin{aligned}
 \frac{d}{dx} 10^{u(x)} &= \frac{d}{dx} e^{u(x) \ln 10} \\
 &= \ln 10 e^{u(x) \ln 10} \frac{du(x)}{dx} \\
 &= 10^{u(x)} \ln 10 \frac{du(x)}{dx}
 \end{aligned} \tag{12}$$

And it follows that

$$\frac{\partial}{\partial h} 10^{P_1 + P_2 + P_3 + P_4} = 10^{P_1 + P_2 + P_3 + P_4} \ln 10 \frac{\partial}{\partial h} (P_1 + P_2 + P_3 + P_4) \tag{13}$$

$$\frac{\partial}{\partial h} 10^{Q_1} = 10^{Q_1} \ln 10 \frac{\partial Q_1}{\partial h} \tag{14}$$

Differentiating the components of (13) and (14)

$$\frac{\partial P_1}{\partial h} = \sum_{i=2}^n (i-1) h^{(i-2)} \sum_{j=1}^m a_{ij} T^{(j-1)} \tag{15}$$

$$\begin{aligned}
 \frac{\partial P_2}{\partial h} &= g(t) \left\{ 5.876(10^{-7}) (2.331) h^{1.331} \exp [-2.868(10^{-3})h] \right. \\
 &\quad + [5.876(10^{-7}) h^{2.331} + 0.06328] (-2.868) (10^{-3}) \\
 &\quad \left. \exp [-2.868(10^{-3}) h] \right\} \tag{16}
 \end{aligned}$$

$$\frac{\partial P_3}{\partial h} = 0.014 P \frac{\phi'}{|\phi'|} \sin^2 \phi' \exp [-0.0013(h-90)^2] \left\{ 1 + 2(h-90)^2 (-0.0013) \right\} \quad (17)$$

$$\frac{\partial P_4}{\partial h} = c \quad (18)$$

$$\frac{\partial Q_1}{\partial h} = \sum_{i=2}^n (i-1) h^{(i-2)} \sum_{j=1}^m a_{ij} \tau^{(j-1)} \quad (19)$$

The resulting partials are in the units of $(\text{Kg}/\text{m}^3)/\text{Km}$ and must therefore be multiplied by 10^{-3} .

VEVAL

$$\frac{\partial \rho_D}{\partial h} = \frac{\partial}{\partial h} 10^{P_1+P_2+P_3+P_4} + (10^{Q_2} - 1) c \frac{\partial}{\partial h} 10^{Q_1} \quad (20)$$

The units of (20) are then

(Kg/m^4) .

8.7.2 JACCHIA 1965 Density Model

D650.

The Jacchia 1965 Density Model, as implemented in subroutine D650, is based on Jacchia's 1965 report, "Static Diffusion Models of the Upper Atmosphere with Empirical Temperature Profiles" (Reference 12). The formulae for computing the exospheric temperature have in some cases been modified according to Jacchia's later papers. The density computation from the exospheric temperature is based on density data provided in that report, reproduced herein as Table 5, which presents density distribution versus altitude and exospheric temperature.

The reader who is interested in the development of these empirical formulas and the reasoning behind them should consult the above mentioned report and Jacchia's later papers. For the convenience of this interested reader, the references 13 for this section from a reasonable comprehensive bibliography.

**REPRODUCIBILITY OF THE
ORIGINAL PAGE IS POOR**

August 11, 1975

8.7.2.1 The Assumptions of the Model

D650

The Jacchia-Nicolet model is based on certain simplifying assumptions and on empirically determined formulae. This is primarily due to the complexity and varied nature of the processes occurring in different regions of the atmosphere and the general lack of anything resembling a complete understanding of the fundamental mechanisms involved. The actual derivation of the model is based upon assumptions first proposed by Nicolet (see Reference 14); Jacchia selected the Nicolet approach to generate a model suitable for satellite dynamics.

The model of the atmosphere proposed by Nicolet considers that the fundamental parameter is the temperature. Other physical parameters such as the pressure and density were derived from the temperature. Thus the first concern is the temperature variation in the atmosphere.

This temperature variation is controlled by the following conditions:

1. Above the thermopause, the temperature of the atmosphere does not vary with altitude. The thermopause varies with solar activity (and the time of day), ranging between about 220 km to 400 km. The temperature above the thermopause is called the exospheric temperature and is directly responsive to solar effects.

D650

REPRODUCIBILITY OF THE
ORIGINAL PAGE IS POOR

August 11, 1973

D650

2. At an altitude of 120 km, the temperature, density, and atmospheric conditions are independent of time. This is an obvious simplification. However, the variations of these parameters above 120 km are considerably larger than those occurring at 120 km, and, considering the other assumptions, this assumption represents a reasonably good approximation.
3. The atmosphere is assumed to be in static equilibrium. With the large day-to-night temperature variations, having a period of the same order of magnitude as the conduction time in the lower thermosphere, and with the occasional occurrence of severe magnetic storms which give rise to fairly rapid and large temperature variations the validity of this assumption is open to question. The best argument for this assumption is its relative simplicity. It should be anticipated, however, that in times of rapid change of the solar or geophysical parameters the predictions of this model will be in error due to the invalidity of this assumption.

The atmosphere is considered to be in diffusive equilibrium above 120 km; that is, the density distributions of each atmospheric constituent with height are

August 11, 1973

governed independently by gravity and temperature. The governing equations are the hydrostatic law, relating the pressure variation with height to the acceleration of gravity, and the perfect gas law, which relates the pressure, density and temperature.

D650

With this approach, Nicolet showed that above 250 km the observed density profiles were reproduced satisfactorily if the (exospheric) temperature was assumed to be a different constant. He also indicated that the problem of representing the density between 120 km and the thermopause was largely a problem of deducing the vertical distribution of temperature.

The contribution of Jacchia to the so-called Jacchia-Nicolet model is largely the development of empirical formulas to compute both the exospheric temperature and vertical temperature distribution as a function of exospheric temperature. These formulae are based on satellite observations coupled with physical reasoning. In addition, Jacchia has updated the boundary conditions of Nicolet. Thus in effect Jacchia has provided all but the basic assumptions behind the model.

The fundamental parameter of the model is therefore the exospheric temperature. This temperature, together with the boundary conditions, implies a particular vertical temperature profile. These three items - exospheric temperature, boundary conditions, and temperature profile - define the density at any altitude over 120 km through the diffusive equilibrium equation.

REPRODUCIBILITY OF THE
ORIGINAL PAGE IS POOR

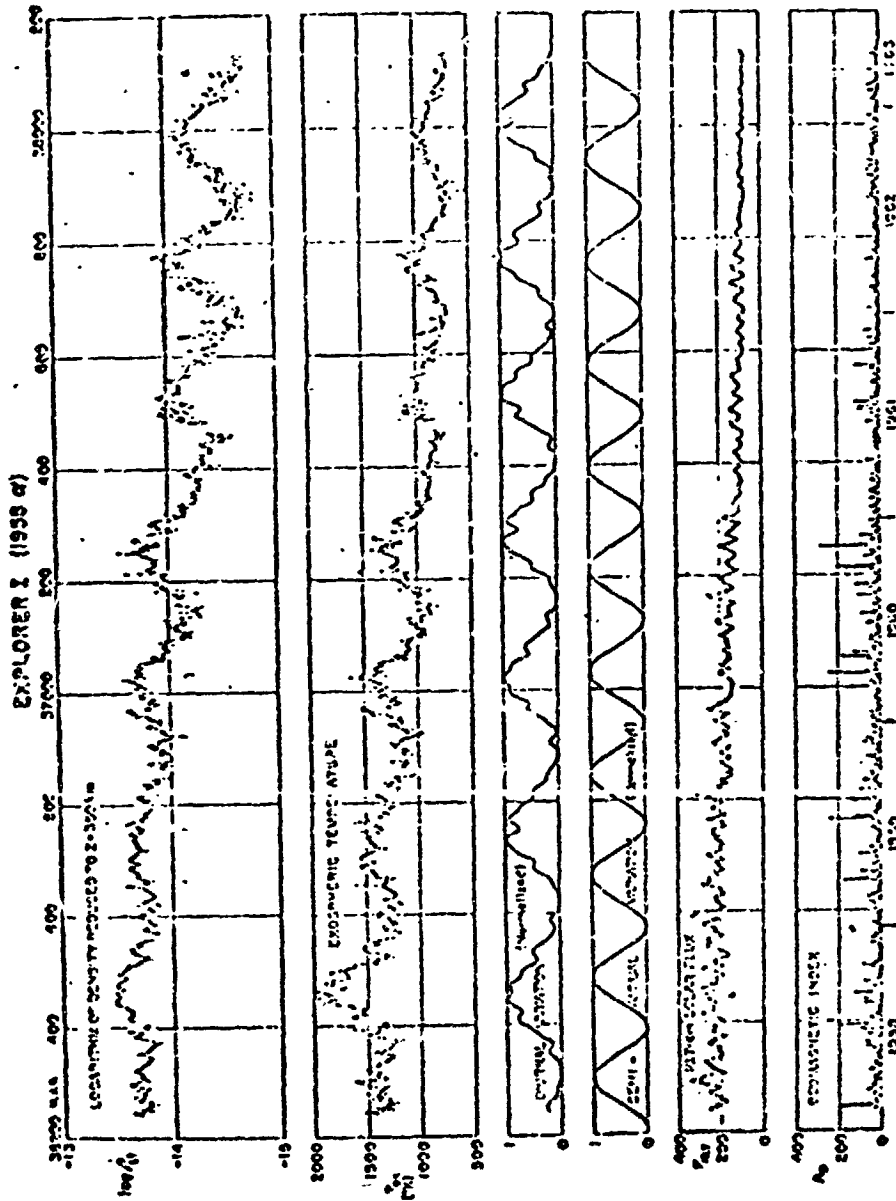


Figure 1. Densities and temperatures derived from the drag of the Explorer I satellite (1958 a), compared with solar and geomagnetic parameters. Notice the decrease in density and temperature which paralleled the decrease in the 10.7-cm solar flux during the five years covered by the diagram. The regular oscillations with a period of about 250 days are caused by the motion of the satellite perigee in and out of the diurnal bulge. Visible are also the 27-day oscillations in phase with those of the 10.7-cm flux and a few perturbations caused by major magnetic storms. Schematic curves of the diurnal and of the semiannual variations are added to aid the eye in recognizing them in the plots of satellite data. The wiggles in the theoretical diurnal-variation curve are caused by the rapid variations in latitude of the satellite perigee. See also the abstract in the Modified Julian Day (MJD) minus 54000.5). (Reproduced from Ref. 14)

REPRODUCIBILITY OF THE ORIGINAL PAGE IS POOR

Figure 5, which was taken from Reference 14, shows a comparison of density and exospheric temperatures derived from observations of Explorer I satellite with solar and geomagnetic parameters. Note the correspondence between the exospheric temperature and the density. D650

8.7.2.2 The Exospheric Temperature Computations

To calculate the fundamental parameter, the exospheric temperature, Jacchia considered four factors which could cause variations:

1. Solar activity variation
2. Semi-annual variation
3. Diurnal variation
4. Geomagnetic activity variation

REPRODUCIBILITY OF THE
ORIGINAL PAGE IS POOR

Each of these variations was determined to be related to one or more observable parameters (see Figure 1). The given empirical formulae are based on these parameters.

Solar Activity

There are many indices of solar activity but the one whose variations most closely parallel those of atmospheric density is the 10.7 cm. (2800 Mc.) solar flux line. The intensity of this line has been measured continuously since 1947, by the National Research Council in Ottawa on a daily basis. The values of the 10.7 cm. flux line are published

August 11, 1975

monthly in the "Solar-Geophysical Data Reports" of the D650
Environmental Science Services Administration in Boulder,
Colorado (U.S. Department of Commerce).

Most of the time solar activity is much more intense in one solar hemisphere than the other so that the flux line appears to vary with the rotation period of the sun, 27 days. This periodicity frequently persists for a year or longer. In addition, there is a variation in the average flux strength with a period of about 11 years which is related to the solar cycle.

From satellite drag data a linear relation between the average 10.7 cm. flux and the average global nighttime minimum exospheric temperature has been obtained (Reference 12) and is expressed as

$$T_0 = 357^\circ + 3.60^\circ F_{10.7} \quad (1)$$

where

REPRODUCIBILITY OF THE
ORIGINAL PAGE IS POOR

$F_{10.7}$ is the average 10.7 cm. flux strength over 2 or 3 solar rotations measured in units of 10^{-22} watts/m²/cycle/sec. bandwidth.

T_0 is the average global nighttime minimum temperature averaged over the same period.

This formula gives the relationship for absolutely quiet geomagnetic conditions; i.e., when a_p is zero.

The variation within one solar rotation is expressed (Reference 12) by

$$T_0' = \bar{T}_0 + 1.8^\circ (F_{10.7} - \bar{F}_{10.7}) \quad (2)$$

where

$F_{10.7}$ is the mean of the 10.7 cm solar flux for a given day in the same units as $\bar{F}_{10.7}$ and

T_0' is the global nighttime minimum for the same day.

This formula accounts (approximately) for the day to day temperature variation superimposed on the average global nighttime minimum temperature determined by the previous formula.

There is some indication that the coefficient 1.8° actually varies from sunspot maximum to sunspot minimum. The indicated range of variation is from about 2.4° down to 1.5°.

REPRODUCIBILITY OF THE ORIGINAL PAGE IS POOR

Semi-Annual Variation

The semi-annual variation is the least understood of the several types of variation in the upper atmosphere. Yearly, the atmospheric density above 200 km reaches a deep minimum in July followed by a high maximum in October-November, a secondary minimum in January, and a secondary maximum in April. Jacchia

August 11, 1973

(Reference 15) found that the observed density variations D650 could be explained by temperature variations in the thermopause, and are roughly proportional to the 10.7 cm flux line. It has been noted that the height of the ionospheric F₂ layer shows a semi-annual variation almost exactly in phase with the observed density variations. Another suggestion by F.S. Johnson (Reference 16) concerning the cause of the semi-annual variation, involves convective transfer at ionospheric levels from the summer pole to the northern pole. This, as yet, does not seem to account correctly for all the details of this variation. The semi-annual variation is not as stable a feature as the diurnal variation. Jacchia (Reference 12) accounted for this feature in 1965 but has, with the recent information of drag data from six satellites, updated his empirical formula (Reference 6) as follows:

$$T_0 = T_0^1 + 2.41 + F_{10.7} [0.349 + 0.296 \sin(2\pi\tau + 226.5^\circ)] \quad (3)$$

$$\sin(4\pi\tau + 247.6^\circ)$$

where

$$\tau = d/Y + 0.1145 \left(\frac{1 + \sin[2\pi(d/Y) + 342.3^\circ]}{2} \right)^{2.16} - 0.5 \quad (4)$$

d = day of the year counted from January 1.

D620

Y = the tropical year in days.

T_0 = global nighttime minimum temperature for that day corrected for semi-annual variation.

Jacchia, Sloney, and Campbell (Reference 17) have more clearly defined this variation. As expected, the relationship between the temperature and the 10.7 cm flux line cannot be considered accurate. It was concluded that the observed density variations are the result of temperature variations at essentially the same level as in the case of the solar effect. However, a variable altitude shows that the semi-annual variation affects the whole atmosphere in the same manner, irrespective of latitude.

**REPRODUCIBILITY OF THE
ORIGINAL PAGE IS POOR**

August 11, 1973

Diurnal Variation

D650

The most regular of the variations is the diurnal variation. One can picture the density distribution as an atmospheric bulge with its peak 30° east of the sub-solar point, degrading nearly symmetrically on all sides, but a little steeper on the morning side. The density peaks at 2 P.M. local solar time and the minimum occurs at 4 A.M. The ratio of the maximum temperature at the center of the bulge to the minimum in the opposite hemisphere remains constant throughout the solar cycle; the ratio is 1.28 in Jacchia's model atmosphere. The cause of the heating is in dispute. Some investigators believe it is due entirely to extreme ultra-violet (EUV) radiations; others, to ion drift; and still others, to a combination of the two.

The temperature, T , at a given hour and geographic location, can be computed in terms of the correct global nighttime minimum temperature for that day, T_0 , using the following formula which approximates a mathematical description of the atmospheric bulge (Reference 12):

$$T = T_0(1+R \sin^m \theta) \left(1 + \frac{R(\cos^m \eta - \sin^m \theta)}{1+R \sin^m \theta} \cos^n \frac{\tau}{2} \right) \quad (5)$$

REPRODUCIBILITY OF THE
ORIGINAL PAGE IS POOR

August 11, 1975

where

D650

$$R = 0.26$$

$$n = m = 2.5$$

$$\tau = H + B + p \sin (H + \gamma) \quad (-\pi < \tau < \pi)$$

$$B = -45^\circ$$

$$p = 12^\circ$$

$$\gamma = 45^\circ$$

$$\bar{n} = \text{ABS}[(\phi - \delta_0)/2]$$

$$\theta = \text{ABS}[(\phi + \delta_0)/2]$$

ϕ = geographic latitude

δ_0 = declination of the sun

REPRODUCIBILITY OF THE
ORIGINAL PAGE IS POOR

H = hour angle of the sun

(H = 0 occurs when the point considered,
the sun, and the earth's axis are coplanar.

H is measured westward 0° to 360°)

Based on satellite information, Jacchia (Reference 18) assumes a maximum day temperature 28% higher than the corresponding nighttime minimum. The variation is represented by R in the above equation. However, further investigation by Jacchia, Slawey, and Campbell (Reference 17), revealed that the diurnal-variation factor (R) is somewhat variable. A value of 32% is considered valid for dates

August 11, 1973

prior to February 1963, and from August 1963, onward, 26% variation is considered valid. Between these dates, R is made to decrease linearly.

D650

Although in these equations the exponents m and n , which determine the mode of the longitudinal and latitudinal temperature variations respectively, are kept distinct, it was found in practice that $m = n$. These values are not really known accurately and could be as small as 2.0.

The constant B determines the lag of the temperature maximum with respect to the uppermost point of the sun; p introduces an asymmetry in the temperature curve whose location is determined by γ .

Geomagnetic Activity

To the temperature, T , which is calculated above, a correction must be added which accounts for atmospheric heating related to changes in the Earth's magnetic field. The heating probably occurs in the E layer of the ionosphere, but the mechanism involved is not well understood. The temperature correction, ΔT , is given by Jacchia, Slowey, and Campbell (Reference 17):

$$\Delta T = 1.0^\circ a_p + 100^\circ [1 - \exp(-0.03a_p)] \quad (6)$$

where

a_p is the three-hourly planetary geomagnetic index.

August 11, 1973

The quantity a_p is a measure of the variation in the earth's magnetic field in a given three hour period.

D650

During magnetic storms the temperature changes generally lag behind the variations in a_p by about five hours, due to conduction. There is some evidence of larger temperature changes for given values of a_p as one proceeds to higher geomagnetic latitudes. However, the amount of data indicating this is negligible at this time.

The D650 subroutine allows for the magnetic heating effects with one modification. To minimize the input data for GEODYN, the 3-hourly index (a_p) is replaced by a 24-hourly or daily index (A_p). Generally, magnetic storms last for 2 or 3 days so that the temperature calculation using A_p will reflect a daily change, but not the 3-hourly fluctuations which occur with a_p .

The quantity A_p and the solar flux data is available from E.S.S.A., Boulder, Colorado. The publication is, "Solar Geophysical Data, Part I."

Accurate daily values for both the solar and geomagnetic flux are required for the computation of the exospheric temperature. In GEODYN, these values are input via a BLOCK DATA routine, INPT. This information may be updated (cf subroutine ADFLUX) using the appropriate GEODYN Input Cards. The user should be aware of the fact that these tables are expanded as new information becomes available.

FLUXS
FLUXA?

August 11, 1973

At the beginning of each run, a file is generated for each satellite arc which contains the required flux data for the time span indicated. Subroutine JANTHG is the routine which sets up the flux tables, including averaging the daily values of solar flux over two solar rotation periods. The reason for this is to free the large amount of computer storage required for daily flux values over six years. As a matter of reference, the associated COMMON BLOCK is PRIORI. JANTHG

8.7.2.3 The Density Computation

The density computation in GEODYN subroutine D650 is based on the density distribution versus altitude and exospheric temperature presented in Table 12, which is reproduced from Jacchia's 1965 paper (Reference). This data was obtained by numerical integration of the diffusion equation using an empirical temperature profile for each indicated exospheric temperature. D650

This vast quantity of information was fitted (by WOLF) to various degree polynomials of the form:

$$\text{LOG}_{10} \rho_D = \sum_i \sum_j a_{ij} T^{(j-1)} h^{(i-1)} \quad (7)$$

where

ρ_D is the density,

August 11, 1973

T is the exospheric temperature,

D650

h is the spheroid height of the satellite (altitude), and

a is a set of appropriate coefficients

Unfortunately, a single polynomial of the type presented is not completely descriptive. An examination of Table 1 reveals that density is nearly independent of temperature for low altitudes, but becomes increasingly dependent for heights above 160 km. Accordingly, appropriate polynomials were chosen to account for the varying dependency of the variables. This necessitated the separation of Table 1 into three parts.

The lower region (120 km - 160 km) is expressed as a second degree polynomial which is solely a function of altitude. This is due to the fact that density is not appreciably dependent on temperature in this region. The remaining regions of 160 km to 420 km and 420 km to 1000 km are described by polynomials of fourth degree in both temperature and altitude.

The coefficients for the selected polynomials are presented in Table 6. These coefficients have been modified to compute the natural log rather than the decimal log of the density.

REPRODUCIBILITY OF THE ORIGINAL PAGE IS POOR

August 11, 1973

The densities produced by these fitted polynomials differ from the densities in Table 1 by an RMS of 3.7 percent. However, the fit does vary in different regions of the table. In the region of worst fit, where the temperature is relatively low (700-1000° K) and the altitude varies from 620-840 km, the RMS is somewhat greater being about 8.5 percent. The largest percent difference between densities is 13.2 percent and falls within the region described.

The fits above could be improved by either going to higher degree polynomials or by additional segmentation of the table. However, these fits are considered to be as accurate as the model being used.

For satellite altitudes above 1000 km, the density is computed according to the extrapolation formula given by Jacchia (Reference 12):

$$\rho_D = \rho_\infty + (\rho_{1000} - \rho_\infty) e^{[b(h-1000)]} \quad (8)$$

where

REPRODUCIBILITY OF THE
ORIGINAL PAGE IS POOR

b = $\frac{d}{dh} (\ln \rho_D)$ as evaluated at 1000 km.

ρ_∞ - is a limiting value for the density.
This is zero in subroutine DENSITY.

h - is the spheroid height.

ρ_{1000} - is the density evaluated at 1000 km.

ρ_D - is the desired density at altitude h .

8.7.2.4 Density Partial Derivatives

D650
VEVAL

In addition to the density, GEODYN also requires the partial derivatives of the density with respect to the Cartesian position coordinates. These partials are used in computing the drag contribution to the variational equations.

As demonstrated above, the density is given by

$$\rho_D = \exp (C_0 + C_1 h + C_2 h^2 + C_3 h^3) \quad (1)$$

where

h is the spheroid height, and the C_i are coefficients which are polynomials in temperature.

We then have

REPRODUCIBILITY OF THE
ORIGINAL PAGE IS POOR

$$\frac{\partial \rho_D}{\partial \bar{r}} = \rho_D (C_1 + 2 C_2 h + 3 C_3 h^2) \frac{\partial h}{\partial \bar{r}} \quad (2)$$

where

\bar{r} is the true of date position vector of the satellite (x, y, z) . The partial derivatives $\frac{\partial h}{\partial \bar{r}}$ are presented along with the computation of spheroid height in Section 2.5.1.

August 11, 1973

The partial derivatives $\frac{\partial r_D}{\partial r}$ are computed in subroutine
VEVAL. The quantities h , p_D , and the C_i are computed
in D650 and passed through COMMON BLOCK DRCEBK.

REPRODUCIBILITY OF THE
ORIGINAL PAGE IS POOR.

Table 5 (continued)

	1850	1300	1250	1200	1150	1100	1050	1000	950	900	850	800	750	700	650
550	-15.045	-15.033	-15.019	-15.011	-15.014	-15.027	-15.052	-15.740	-15.740	-15.740	-16.105	-16.293	-16.472	-16.662	-16.859
570	-15.035	-15.110	-15.276	-15.311	-15.476	-15.593	-15.718	-15.859	-16.011	-16.177	-16.357	-16.541	-16.728	-16.918	-17.111
580	-15.021	-15.104	-15.245	-15.314	-15.455	-15.578	-15.704	-15.835	-16.000	-16.147	-16.315	-16.472	-16.637	-16.807	-16.982
590	-15.143	-15.211	-15.301	-15.391	-15.470	-15.549	-15.628	-15.707	-15.786	-15.865	-15.944	-16.023	-16.102	-16.181	-16.260
610	-15.246	-15.322	-15.410	-15.504	-15.598	-15.691	-15.785	-15.879	-15.972	-16.066	-16.159	-16.252	-16.345	-16.438	-16.531
620	-15.348	-15.377	-15.454	-15.550	-15.644	-15.738	-15.832	-15.926	-16.020	-16.114	-16.208	-16.302	-16.396	-16.490	-16.584
630	-15.449	-15.429	-15.518	-15.615	-15.710	-15.804	-15.898	-15.992	-16.086	-16.180	-16.274	-16.368	-16.462	-16.556	-16.650
640	-15.548	-15.493	-15.582	-15.679	-15.773	-15.867	-15.961	-16.055	-16.149	-16.243	-16.337	-16.431	-16.525	-16.619	-16.713
650	-15.646	-15.541	-15.629	-15.726	-15.820	-15.914	-16.008	-16.102	-16.196	-16.290	-16.384	-16.478	-16.572	-16.666	-16.760
660	-15.743	-15.638	-15.726	-15.823	-15.917	-16.011	-16.105	-16.199	-16.293	-16.387	-16.481	-16.575	-16.669	-16.763	-16.857
670	-15.839	-15.734	-15.822	-15.919	-16.013	-16.107	-16.201	-16.295	-16.389	-16.483	-16.577	-16.671	-16.765	-16.859	-16.953
680	-15.935	-15.830	-15.918	-16.015	-16.109	-16.203	-16.297	-16.391	-16.485	-16.579	-16.673	-16.767	-16.861	-16.955	-17.049
690	-16.031	-15.926	-16.014	-16.111	-16.205	-16.299	-16.393	-16.487	-16.581	-16.675	-16.769	-16.863	-16.957	-17.051	-17.145
700	-16.127	-16.022	-16.110	-16.207	-16.301	-16.395	-16.489	-16.583	-16.677	-16.771	-16.865	-16.959	-17.053	-17.147	-17.241
710	-16.223	-16.118	-16.206	-16.303	-16.397	-16.491	-16.585	-16.679	-16.773	-16.867	-16.961	-17.055	-17.149	-17.243	-17.337
720	-16.319	-16.214	-16.302	-16.399	-16.493	-16.587	-16.681	-16.775	-16.869	-16.963	-17.057	-17.151	-17.245	-17.339	-17.433
730	-16.415	-16.310	-16.398	-16.495	-16.589	-16.683	-16.777	-16.871	-16.965	-17.059	-17.153	-17.247	-17.341	-17.435	-17.529
740	-16.511	-16.406	-16.494	-16.591	-16.685	-16.779	-16.873	-16.967	-17.061	-17.155	-17.249	-17.343	-17.437	-17.531	-17.625
750	-16.607	-16.502	-16.590	-16.687	-16.781	-16.875	-16.969	-17.063	-17.157	-17.251	-17.345	-17.439	-17.533	-17.627	-17.721
760	-16.703	-16.598	-16.686	-16.783	-16.877	-16.971	-17.065	-17.159	-17.253	-17.347	-17.441	-17.535	-17.629	-17.723	-17.817
770	-16.800	-16.695	-16.783	-16.880	-16.974	-17.068	-17.162	-17.256	-17.350	-17.444	-17.538	-17.632	-17.726	-17.820	-17.914
780	-16.896	-16.791	-16.879	-16.976	-17.070	-17.164	-17.258	-17.352	-17.446	-17.540	-17.634	-17.728	-17.822	-17.916	-18.010
790	-16.992	-16.887	-16.975	-17.072	-17.166	-17.260	-17.354	-17.448	-17.542	-17.636	-17.730	-17.824	-17.918	-18.012	-18.106
800	-17.088	-16.983	-17.071	-17.168	-17.262	-17.356	-17.450	-17.544	-17.638	-17.732	-17.826	-17.920	-18.014	-18.108	-18.202
810	-17.184	-17.079	-17.167	-17.264	-17.358	-17.452	-17.546	-17.640	-17.734	-17.828	-17.922	-18.016	-18.110	-18.204	-18.298
820	-17.280	-17.175	-17.263	-17.360	-17.454	-17.548	-17.642	-17.736	-17.830	-17.924	-18.018	-18.112	-18.206	-18.300	-18.394
830	-17.376	-17.271	-17.359	-17.456	-17.550	-17.644	-17.738	-17.832	-17.926	-18.020	-18.114	-18.208	-18.302	-18.396	-18.490
840	-17.472	-17.367	-17.455	-17.552	-17.646	-17.740	-17.834	-17.928	-18.022	-18.116	-18.210	-18.304	-18.398	-18.492	-18.586
850	-17.568	-17.463	-17.551	-17.648	-17.742	-17.836	-17.930	-18.024	-18.118	-18.212	-18.306	-18.400	-18.494	-18.588	-18.682
860	-17.664	-17.559	-17.647	-17.744	-17.838	-17.932	-18.026	-18.120	-18.214	-18.308	-18.402	-18.496	-18.590	-18.684	-18.778
870	-17.760	-17.655	-17.743	-17.840	-17.934	-18.028	-18.122	-18.216	-18.310	-18.404	-18.498	-18.592	-18.686	-18.780	-18.874
880	-17.856	-17.751	-17.839	-17.936	-18.030	-18.124	-18.218	-18.312	-18.406	-18.500	-18.594	-18.688	-18.782	-18.876	-18.970
890	-17.952	-17.847	-17.935	-18.032	-18.126	-18.220	-18.314	-18.408	-18.502	-18.596	-18.690	-18.784	-18.878	-18.972	-19.066
900	-18.048	-17.943	-18.031	-18.128	-18.222	-18.316	-18.410	-18.504	-18.598	-18.692	-18.786	-18.880	-18.974	-19.068	-19.162
910	-18.144	-18.039	-18.127	-18.224	-18.318	-18.412	-18.506	-18.600	-18.694	-18.788	-18.882	-18.976	-19.070	-19.164	-19.258
920	-18.240	-18.135	-18.223	-18.320	-18.414	-18.508	-18.602	-18.696	-18.790	-18.884	-18.978	-19.072	-19.166	-19.260	-19.354
930	-18.336	-18.231	-18.319	-18.416	-18.510	-18.604	-18.698	-18.792	-18.886	-18.980	-19.074	-19.168	-19.262	-19.356	-19.450
940	-18.432	-18.327	-18.415	-18.512	-18.606	-18.700	-18.794	-18.888	-18.982	-19.076	-19.170	-19.264	-19.358	-19.452	-19.546
950	-18.528	-18.423	-18.511	-18.608	-18.702	-18.796	-18.890	-18.984	-19.078	-19.172	-19.266	-19.360	-19.454	-19.548	-19.642
960	-18.624	-18.519	-18.607	-18.704	-18.798	-18.892	-18.986	-19.080	-19.174	-19.268	-19.362	-19.456	-19.550	-19.644	-19.738
970	-18.720	-18.615	-18.703	-18.800	-18.894	-18.988	-19.082	-19.176	-19.270	-19.364	-19.458	-19.552	-19.646	-19.740	-19.834
980	-18.816	-18.711	-18.800	-18.896	-18.990	-19.084	-19.178	-19.272	-19.366	-19.460	-19.554	-19.648	-19.742	-19.836	-19.930
990	-18.912	-18.807	-18.896	-18.992	-19.086	-19.180	-19.274	-19.368	-19.462	-19.556	-19.650	-19.744	-19.838	-19.932	-20.026
1000	-19.008	-18.903	-18.992	-19.088	-19.182	-19.276	-19.370	-19.464	-19.558	-19.652	-19.746	-19.840	-19.934	-20.028	-20.122

REPRODUCIBILITY OF THE ORIGINAL PAGE IS POOR

August 11, 1973

TABLE 6
 DENSITY POLYNOMIAL COEFFICIENTS
 (FOR NATURAL LOG OF DENSITY)

	h^0	h^1	h^2	h^3
420-1000 KM				
T^0	61.5177	48.60687	6.87280	0.305394
T^1	-173.970	93.4870	-14.1203	0.651270
T^2	111.908	-60.34177	9.349784	-0.440330
T^3	-23.3864	12.64406	-1.989456	0.0950336
160-420 KM				
T^0	0.514627	-26.4622	6.28711	-0.664854
T^1	-36.8741	37.5137	-9.994692	1.00192
T^2	22.6334	-23.9095	6.780537	-0.695452
T^3	-4.47654	4.83017	-1.41853	0.148026
120-160 KM				
	1.1335948	-31.858566	8.7827269	

REPRODUCIBILITY OF THE
 ORIGINAL PAGE IS POOR

The gravitational potential originating from solid earth tides caused by a single disturbing body is given (Reference 11).

$$\begin{aligned}
 U_D(r) &= \frac{k_2}{2} \frac{GM_d}{R_d^3} \frac{R_e^5}{r^3} \left[3 (\hat{R}_d \cdot \hat{r})^2 - 1 \right] \\
 &= \frac{k_2}{2} \frac{GM_e}{R_e} \left(\frac{M_d}{M_e} \right) \left(\frac{R_e}{R_d} \right)^3 \left(\frac{R_e}{r} \right)^3 \left[3 (\hat{R}_d \cdot \hat{r})^2 - 1 \right] \quad (1)
 \end{aligned}$$

and the resultant acceleration on a satellite due to this potential is

$$\nabla U_D = \frac{k_2}{2} \frac{GM_d}{R_d^3} \frac{R_e^5}{r^4} \left\{ [3 - 15 (\hat{R}_d \cdot \hat{r})^2] \hat{r} + 6 (\hat{R}_d \cdot \hat{r}) \hat{R}_d \right\} \quad (2)$$

where

k_2 is the tidal coefficient of degree 2 called the "Love Number."

G is the universal gravitational constant

M_e is the mass of the earth.

R_e is the mean earth radius.

M_d is the mass of the disturbing body.

TIDAL

M_e is the mass of the earth.

R_d is the distance from COM_e^* to COM_d^{**} .

r is the distance from COM_e to the satellite.

\hat{R}_d is the unit vector from COM_e to COM_d .

\hat{r} is the unit vector from COM_e to satellite.

* Center of mass of the earth.

**Center of mass of the disturbing body.

SECTION 9.0
INTEGRATION AND INTERPOLATION

GEODYN uses Cowell's Sum method for direct numerical integration of both the equations of motion and the variational equations to obtain the position and velocity and the attendant variational partials at each observation time. The integrator output is not required at actual observation times; it is output on an even integration step. GEODYN uses an interpolation technique to obtain values at the actual observation time. The specific numerical methods used in GEODYN for this integration and interpolation are presented below. These procedures are controlled by subroutine ORBIT.

ORBIT

9.1 INTEGRATION

Let us first consider the integration of the equations of motion. These equations are three second order differential equations in position, and may be formulated as six first order equations in position and velocity if a first order integration scheme were used for their solution. For reasons of increased accuracy and stability, the position vector \bar{r} is obtained by a second order integration of the accelerations $\ddot{\bar{r}}$, whereas the velocity vector $\dot{\bar{r}}$ is obtained as the solution of a first order system. These are both multi-step methods requiring at least one derivative evaluation on each step.

COWELL

The integration scheme is equivalent to the inter- COWELL
polator with arguments 1 and 0 for predictor and corrector
respectively.

To integrate the position components, the predictor

$$\bar{r}_{n+1} = (S_2 + \sum_{p=0}^q \gamma_p^* \ddot{r}_{n-p})h^2 \quad (1)$$

is applied, followed by a Cowell corrector:

$$\bar{r}_{n+1} = (S_2 + \sum_{p=0}^q \gamma_p^* \ddot{r}_{n-p+1})h^2 \quad (2)$$

The velocity components are integrated using the
predictor;

$$\dot{r}_{n+1} = (S_1 + \sum_{p=0}^{q+1} \beta_p^* \ddot{r}_{n-p})h \quad (3)$$

followed by an Adams-Moulton corrector;

$$\dot{r}_{n+1} = (S_1 + \sum_{p=0}^{q+1} \beta_p \ddot{r}_{n-p+1})h \quad (4)$$

In these integration formulae, h is the integration step
size, q has the value ORDER-2, and γ_p , γ_p^* , β_p and β_p^* are co-
efficients whose values are obtained from subroutine COWCOF.*

*Published numbers are in Reference 1.

Under certain conditions, a reduced form of this solution is used. It can be seen from the variational and observation equations that if drag is not a factor and there are no range rate, doppler, or altimeter rate measurements, the velocity variational partials are not used. There is then no need to integrate the velocity variational equations. This represents a significant time saving. In the integration algorithm, the B matrix is zero and (I-H) is reduced to a three by three.

PRECEDING PAGE BLANK NOT FILMED

A detailed description of the H matrix and the X_n and V_n vectors can be found in pages 16, 17 of Reference 2.

Backwards integration involves only a few simple modifications to these normal or forward integration procedures. These modifications are to negate the step size, and invert the time completion test.

The above integration procedures are implemented in GEODYN in the subroutine COWELL. The inversions for backwards integration are performed by COWELL and ORBIT. The matrix inversion is performed by subroutine DNVERT.

COWELL
DNVERT

The default step size for these integration procedures is selected on the basis of perigee height and the eccentricity of the orbit. The default step size selection is explained in detail in the Operations Manual, Volume III of the GEODYN System Documentation. This may be reset to some other fixed value on input. (See the STEP control card description in the above manual.)

Variable Step Mode

There is an optional variable step mode which is the default mode for high eccentricity orbits. The selection of this mode of operation, its default initial step size, halving error bound, and doubling error bound, or variable increase or decrease of step size are also explained in Volume III with the STEP control card.

In the variable step mode, the local error is compared against upper and lower error bounds to determine whether the step size should be increased or decreased. This local error is computed as the difference between the predicted and corrected values of position. Both the increasing and decreasing procedures require the table of back values of accelerations to be modified so as to be compatible with the new step size. The decreasing requires the interpolation for mid-points. This interpolation is of course on the back position, velocity and acceleration values. The increasing is achieved by discarding every other time point in the table of back values and then the refinement using the decreasing algorithm.

COWELL

REARG

REARG

It should be noted that $2(\text{ORDER}-1)-1$ of back values are saved when GEODYN is operating in variable step mode. Increasing of the step size is disabled for the following $\text{ORDER}-2$ steps after a step size change; i.e., until the table of back values is again filled.

These increasing and decreasing procedures are contained in subroutine REARG.

9.2 THE INTEGRATOR STARTING SCHEME

The predictor-corrector combination employed to proceed with the main integration is not self-starting. That is, each step of the integration requires the knowledge of past values of the solution that are not available at the start of the integration. The method presented here is that implemented in the GEODYN subroutine START.

START

A Taylor series approximation is used to predict initial values of position and velocity. With these starting values, the Sum array is evaluated using epoch positions and velocities. Now the loop is closed by interpolations for the positions and velocities not at epoch and their accelerations evaluated. The Sums are now again evaluated, this procedure continues until the Sums converge to the desired accuracy.

9.3 INTERPOLATION

GEODYN uses interpolation for two functions. The first is the interpolation of the orbit elements and variational partials to the observation times; the second is the interpolation for mid-points when the integrator is decreasing the step size.

INTRP
COEF

The formulas used by INTRP are:

$$X(t+\Delta t) = (S_2(t) + \left(\frac{\Delta t}{h} - 1\right) S_1(t) + \sum_{i=1}^n C_i (\Delta t) f_{n-i}) h^2 \quad (1)$$

for positions and

$$\dot{X}(t + \Delta t) = (S_1(t) + \sum_{i=0}^n C_i' (\Delta t) f_{n-i})h \quad (2)$$

for velocities.

S_1 and S_2 are the first and second sums carried along by the integrator, f 's are the back values of acceleration, h the step size, and C_i, C_i' are the interpolation coefficients computed in subroutine COEF. A detailed description of the interpolation formulae can be found on pages 4, 5 of Reference 3.

SECTION 10.0
THE STATISTICAL ESTIMATION SCHEME

The basic problem in orbit determination is to calculate, from a given set of observations of the spacecraft, a set of parameters specifying the trajectory of a spacecraft. Because there are generally more observations than parameters, the parameters are overdetermined. Therefore, a statistical estimation scheme is necessary to estimate the "best" set of parameters.

The estimation scheme selected for GEODYN is a partitioned Bayesian least squares method. The complete development of this procedure is presented in this section.

It should be noted that the functional relationships between the observations and parameters are in general non-linear; thus an iterative procedure is necessary to solve the resultant non-linear normal equations. The Newton-Raphson iteration formula is used to solve these equations.

10.1 BAYESIAN LEAST SQUARES ESTIMATION*

Consider a vector of N independent observations \underline{z} whose values can be expressed as known functions of N parameters denoted by the vector \underline{x} . The following non-linear regression equation holds:

$$\underline{z} = \underline{f}(\underline{x}) + \underline{g}, \quad (1)$$

where \underline{g} is the N vector denoting the noise on the observations. Given \underline{z} , the functional form of \underline{f} , and the statistical properties of \underline{g} , we must obtain the estimate of \underline{x} that is "best" in some sense.**

Bayes theorem in probability holds for probability density functions and can be written as follows:

$$p(\underline{x}|\underline{z}) = \frac{p(\underline{x})}{p(\underline{z})} p(\underline{z}|\underline{x}). \quad (2)$$

where

$p(\underline{x}|\underline{z})$ is the joint conditional probability density function for the parameter vector \underline{x} , given that the data vector \underline{z} has occurred -

*Vector notation in this section is that used by statisticians; i.e., an underscore denotes a vector. The symbol " $\hat{\quad}$ " denotes the "best" estimate of the superscripted quantity.

**For a complete discussion of the properties of estimators see Maurice G. Kendall and Alan Stuart, Reference 1.

$p(\underline{x})$ is the joint probability density function for the vector \underline{x} ;

$p(\underline{z})$ is the joint probability density function for the vector \underline{z} ;

and

$p(\underline{z}|\underline{x})$ is the joint conditional density function for the vector \underline{z} given that \underline{x} has occurred;

$p(\underline{x})$ is often referred to as the a priori density function of \underline{x} , and $p(\underline{x}|\underline{z})$ is referred to as the a posteriori conditional density function. In any Bayesian estimation scheme, we must determine this a posteriori density function and from this function determine a "best" estimate of \underline{x} , which can be denoted $\hat{\underline{x}}$.

To obtain the a posteriori conditional density function, we must make an assumption concerning the statistical properties of the noise on the observations: the noise vector \underline{g} has a joint normal distribution with mean vector $\underline{0}$ and a variance-covariance matrix Σ_z . Σ_z is an $N \times N$ matrix and is assumed diagonal, that is, the observations are considered to be independent and uncorrelated. The "best" estimate of \underline{x} , $\hat{\underline{x}}$, is defined as that vector maximizing the a posteriori density function; this is equivalent to choosing the mean value of this distribution. An estimator of this type has been referred to as the maximum likelihood estimate in the Bayesian sense. (Reference 2)

A further assumption is that the a priori density function $p(\underline{\hat{x}})$ is a joint normal distribution and is written as follows:

$$p(\underline{\hat{x}}) = \left[\frac{\text{Det}(\Sigma_A^{-1})}{2\pi^M} \right]^{\frac{1}{2}} \exp \left\{ -\frac{1}{2} (\underline{x}_A - \underline{\hat{x}})^T \Sigma_A^{-1} (\underline{x}_A - \underline{\hat{x}}) \right\} \quad (3)$$

where

\underline{x}_A is the a priori estimate of the parameter vector,

Σ_A is the a priori variance-covariance matrix associated with the a priori parameter vector. Σ_A is an $M \times M$ matrix, which may or may not be diagonal.

The conditional density function $p(\underline{z}|\underline{\hat{x}})$ can be written as follows:

$$p(\underline{z}|\underline{\hat{x}}) = \left[\frac{\text{Det}(\Sigma_z^{-1})}{2\pi^N} \right]^{\frac{1}{2}} \exp \left\{ -\frac{1}{2} [\underline{z} - \underline{f}(\underline{\hat{x}})]^T \Sigma_z^{-1} [\underline{z} - \underline{f}(\underline{\hat{x}})] \right\} \quad (4)$$

It can be shown that maximizing the a posteriori density function $p(\underline{\hat{x}}|\underline{z})$ is equivalent to maximizing the product $p(\underline{\hat{x}})p(\underline{z}|\underline{\hat{x}})$ because the density function $p(\underline{z})$ is a constant valued function. Further, this reduces to minimizing the following quadratic form:

$$\left(\underline{x}_A - \hat{\underline{x}}\right)^T \sum_A^{-1} \left(\underline{x}_A - \hat{\underline{x}}\right) + \left(\underline{z} - f(\hat{\underline{x}})\right)^T \sum_z^{-1} \left(\underline{z} - f(\hat{\underline{x}})\right). \quad (5)$$

This results in the following set of M non-linear equations:

$$B^T \sum_z^{-1} \left(\underline{z} - f(\hat{\underline{x}})\right) + \sum_A^{-1} \left(\underline{x}_A - \hat{\underline{x}}\right) = 0 \quad (6)$$

where B is an NxM matrix with elements

$$B_{NM} = \left. \frac{\partial f_N(\underline{x})}{\partial x_M} \right|_{\underline{x} = \hat{\underline{x}}}$$

REPRODUCIBILITY OF THE ORIGINAL PAGE IS POOR

This equation defines the Bayesian least squares estimation procedure. We have not stated how the a priori parameter vector and variance-covariance matrix were obtained. In practice these a priori values are almost always estimates that have been obtained from some previous data. In these cases the Bayesian estimates are identical to the classical maximum likelihood estimates that would be obtained if all the data were used; in this context the a priori parameters can be considered as additional observations.

The variance-covariance matrix of $\hat{\underline{x}}$, V , is given by the following formula:

$$V = \left[B^T \sum_z^{-1} B + \sum_A^{-1} \right]^{-1} \quad (7)$$

Solution of the Estimation Formula

Equation 6 defines a set of M non-linear equations in M unknowns $\hat{\underline{x}}$; these equations are solved using the Newton-Raphson iteration formula. Equation 6 can be written as follows:

$$\underline{F}(\hat{\underline{x}}) = 0.$$

The iteration formula is

$$\hat{\underline{x}}^{(n+1)} = \hat{\underline{x}}^{(n)} - \left(\frac{\partial \underline{F}(\hat{\underline{x}})}{\partial \hat{\underline{x}}} \right)^{-1} \underline{F} \left(\hat{\underline{x}}^{(n)} \right) \quad (8)$$

where

$\hat{\underline{x}}^{(n)}$ is the n^{th} approximation to the true solution $\hat{\underline{x}}$.

Now

$$F(\hat{\underline{x}}) = B^T \sum_z^{-1} (\underline{z} - \underline{f}(\hat{\underline{x}})) + \sum_A^{-1} (\underline{x}_A - \hat{\underline{x}}) = 0 \quad (9)$$

Then differentiating and neglecting second derivatives,

$$\left(\frac{\partial F(\hat{\underline{x}})}{\partial \hat{\underline{x}}} \right) = \left[\left(B^T \sum_z^{-1} B \right) \right] + \sum_A^{-1} \quad (10)$$

REPRODUCIBILITY OF THE
ORIGINAL PAGE IS POOR

Substituting equation 10 in equation 8 gives

$$\begin{aligned} \hat{\underline{x}}^{(n+1)} - \hat{\underline{x}}^{(n)} = & \left(B^T \sum_z^{-1} B + \sum_A^{-1} \right)^{-1} \left\{ B^T \sum_z^{-1} (\underline{z} - \underline{f}(\hat{\underline{x}})^{(n)}) \right. \\ & \left. + \sum_A^{-1} (\underline{x}_A - \hat{\underline{x}}^{(n)}) \right\} \quad (11) \end{aligned}$$

Now let $\hat{\underline{x}}^{(n+1)} - \hat{\underline{x}}^{(n)}$, the correction to the n^{th} approximation, be denoted by $d\underline{x}^{(n+1)}$, and let $\underline{z} - \underline{f}(\hat{\underline{x}}^{(n)})$, the vector of residuals from the n^{th} approximation, be $d\underline{z}^{(n)}$. Equation 11 becomes

$$d\underline{x}^{(n+1)} = \left(B^T \sum_z^{-1} B + \sum_A^{-1} \right)^{-1} \left\{ B^T \sum_z^{-1} d\underline{z}^{(n)} + \sum_A^{-1} (\underline{x}_A - \hat{\underline{x}}^{(n)}) \right\} \quad (12)$$

In a multi-satellite, multi-arc estimation program such as GEODYN, it is necessary to formulate the estimation scheme in a manner such that the information for all satellite arcs are not in core simultaneously. The procedure used in GEODYN is a partitioned Bayesian Estimation Scheme which requires only common parameter information and the information for a single arc to be in core at any given time. The development of the GEODYN solution is given here.

The Bayesian estimation formula has been developed in the previous section as

$$\underline{dx}^{(n+1)} = \left(B^T W B + V_A^{-1} \right)^{-1} \left[B^T W \underline{dm} + V_A^{-1} \left(\underline{x}_A - \hat{\underline{x}}^{(n)} \right) \right] \quad (1)$$

where

REPRODUCIBILITY OF THE
ORIGINAL PAGE IS POOR

\underline{x}_A is the a priori estimate of \underline{x} .

V_A is the a priori covariance matrix associated with \underline{x}_A .

W is the weighting matrix associated with the observations.

$\underline{x}^{(n)}$ is the n^{th} approximation to \underline{x} .

\underline{dm} is the vector of residuals (O-C) from the n^{th} approximation.

$\underline{dx}^{(n+1)}$ is the vector of corrections to the parameters; i.e.,

ESTIM

$$\underline{x}^{n+1} = \underline{x}^n + \underline{dx}^{(n+1)}$$

B is the matrix of partial derivatives of the observations with respect to the parameters where the i, j^{th} element is given by

$$\frac{\partial m_i}{\partial x_j}$$

The iteration formula given by this equation solves the non-linear normal equations formed by minimizing the sum of squares of the weighted residuals.

We desire a solution wherein \underline{x} is partitioned according to \underline{a} , the vector of parameters associated only with individual arcs; and \underline{k} , the vector of parameters common to all arcs. For geodetic parameter estimation \underline{a} consists of the sets of orbital elements, satellite parameters, and measurement biases associated with each arc, whereas \underline{k} consists of the geopotential coefficients and station coordinates.

As a result of this partitioning, we may write B , the matrix of partial derivatives of the observations, as

$$B = \begin{bmatrix} B_a & B_k \end{bmatrix} \quad (2)$$

where

ESTIM

$$\left[B_a \right]_{i,j} = \frac{\partial m_i}{\partial a_j}$$

and

$$\left[B_k \right]_{i,j} = \frac{\partial m_i}{\partial k_j}$$

We may also write V_A , the covariance matrix of the parameters as

$$V_A = \begin{bmatrix} V_a & 0 \\ 0 & V_k \end{bmatrix} \quad (3)$$

where we have assumed the independence of the a priori information on the arc parameters and common parameters (in practice valid to an extremely high degree).

We may now rewrite our iteration formula:

ESTIM

$$\begin{bmatrix} \underline{da} \\ \underline{dk} \end{bmatrix} = \begin{bmatrix} B_a^T W R_a + V_a & B_a^T W B_k \\ B_a^T W B_k & B_k^T W B_k + V_k \end{bmatrix}^{-1} X \quad (4)$$

$$\begin{bmatrix} B_a^T W d m^{(n)} + V_a (\underline{a}^{(n)} - \underline{a}_A) \\ B_k^T W d m^{(n)} + V_k (\underline{k}^{(n)} - \underline{k}_A) \end{bmatrix}$$

$$= \begin{bmatrix} A & A_k \\ A_k^T & K \end{bmatrix}^{-1} \begin{bmatrix} C_a \\ C_k \end{bmatrix}$$

The required matrix inversion is obtained by partitioning. We write

$$\begin{bmatrix} N_1 & N_2 \\ N_2^T & N_4 \end{bmatrix} \cdot \begin{bmatrix} A & A_k \\ A_k^T & K \end{bmatrix} = I \quad (5)$$

and, solving the resulting equations, determine

$$N_1 = A^{-1} + \begin{bmatrix} A^{-1} & A_k \end{bmatrix} N_4 \begin{bmatrix} A_k^T & A^{-1} \end{bmatrix} \quad (6)$$

$$N_2 = -A^{-1} A_k N_4 \quad (7) \text{ ESTIM}$$

and

$$N_4 = \left[K - A_k^T A^{-1} A_k \right]^{-1} \quad (8)$$

There is no problem associated with inverting A because the existence of the a priori information alone guarantees this property. On the other hand, the inverse of $K - A_k^T A^{-1} A_k$ is not guaranteed to exist. High correlations between the parameters could make the matrix near singular. In practice, however, the use of a reasonable amount of a priori information eliminates any inversion difficulties.

The iteration formula may now be written as

$$\begin{bmatrix} \underline{da} \\ \underline{dk} \end{bmatrix} = \begin{bmatrix} N_1 & N_2 \\ N_2^T & N_4 \end{bmatrix} \begin{bmatrix} C_a \\ C_k \end{bmatrix} \quad (9)$$

or

$$\underline{da} = \left[A^{-1} + (A^{-1} A_k) N_4 (A_k^T A^{-1}) \right] C_a - A^{-1} A_k N_4 C_k \quad (10)$$

$$\underline{dk} = -N_4 A_k^T A^{-1} C_a + N_4 C_k \quad (11)$$

Noting the similarities between \underline{da} and \underline{dk} , we write

ESTIM

$$\underline{da} = A^{-1} C_a - A^{-1} A_k \underline{dk} \quad (12)$$

and rewrite \underline{dk} as

$$\underline{dk} = N_4 (C_k - A_k^T A^{-1} C_a). \quad (13)$$

Note that most of the elements of A are zero because the measurements in any given arc are independent of the arc parameters of any other arc. Also, the covariances between the a priori information associated with each arc is assumed to be zero. Thus both A and V_a are composed of zeroes except for matrices, A_r and V_r , respectively, along the diagonal, where

r is a subscript denoting the r^{th} arc,

e.g., \underline{a}_r

$$\left[A_r \right]_{i,j} = \sum_{\ell} \frac{\partial m_{\ell}}{\partial a_{r_i}} \frac{1}{\sigma_{\ell}^2} \frac{\partial m_{\ell}}{\partial a_{r_j}} + \left[V_r^{-1} \right]_{i,j} \quad (14)$$

where ℓ ranges over the measurements in the r^{th} arc and i, j range over the parameters in the r^{th} arc, \underline{a}_r .

V_r is the partition of V_a associated with the r^{th} arc.

ESTIM

The reader should note that A^{-1} , like A , is composed of zeroes except for matrices A_r^{-1} along the diagonal.

We shall also require the partitions of A_k and C_a according to each arc. These partitions are given by

$$\left[A_{rk} \right]_{i,j} = \sum_{\ell} \frac{\partial m_{\ell}}{\partial a_{r_i}} \frac{1}{\sigma_{\ell}^2} \frac{\partial m_{\ell}}{\partial k_j} \quad (15)$$

$$\left[C_r \right]_i = \sum_{\ell} \frac{\partial m_{\ell}}{\partial a_{r_i}} \frac{1}{\sigma_{\ell}^2} \overline{dm_{\ell}} \quad (16)$$

where the subscript r again denotes the r^{th} arc and ℓ ranges over the measurement partials and residuals in the r^{th} arc.

Let us now investigate the matrix partitions in the solutions for \underline{da} and \underline{dk} . We consider A^{-1} to be a diagonal matrix with diagonal elements A_r^{-1} and C_a to be a column vector with elements C_r . Hence

$$\left[A^{-1} C_a \right]_r = A_r^{-1} C_r \quad \text{ESTIM} \quad (17)$$

is the r^{th} element of the product matrix. A_k is considered to be a column vector with elements A_{rk} , thus

$$\left[A_k^T A^{-1} C_a \right] = A_{rk}^T A_r^{-1} C_r \quad (18)$$

The elements in the product $A^{-1} A_k$ are given by

$$\left[A^{-1} A_k \right]_r = A_r^{-1} A_{rk} \quad \text{REPRODUCIBILITY OF THE ORIGINAL PAGE IS POOR} \quad (19)$$

We also require the product $A_k^T A^{-1} A_k$. Its elements are given by

$$\left[A_k^T A^{-1} A_k \right]_{r,r} = A_{rk}^T A_r^{-1} A_{rk} \quad (20)$$

The solutions for \underline{da} and \underline{dk} may now be rewritten taking into account the partitioning by arc:

$$\underline{da}_r = A_r^{-1} C_r - A_r^{-1} A_{rk} \underline{dk} \quad (21)$$

$$\underline{dk} = N_k \left(C_k - \sum_r A_{rk}^T A_r^{-1} C_r \right) \quad (22)$$

where

ESTIM

$$N_4 = \left[K - \sum_r \Lambda_{rk}^T \Lambda_r^{-1} \Lambda_{rk} \right]^{-1} \quad (23)$$

These solutions form the partitioned Bayesian estimation scheme used in GEODYN.

Additionally, the covariance matrix for the arc parameters must be updated to account for the simultaneous adjustment of the common parameters:

$$\left[N_1 \right]_r = A_r^{-1} + \left(\Lambda_r^{-1} \Lambda_{rk} \right) N_4 \left(\Lambda_{rk}^T \Lambda_r^{-1} \right) \quad (24)$$

Summary

REPRODUCIBILITY OF THE
ORIGINAL PAGE IS POOR

The procedure for computer implementation is illustrated in Figure 1. This procedure is:

1. Integrate through each arc forming the matrices A_r , Λ_{rk} , and C_r ; and simultaneously accumulate into the common parameter matrices K and C_k .
2. At the end of each arc, form

$$\frac{da_r}{dr} = A_r^{-1} C_r \quad (25)$$

and modify the common parameter matrices as follows:

ESTIM

$$K = K - A_{rk}^T A_r^{-1} A_{rk} \quad (26)$$

and

$$C_k = C_k - A_{rk}^T \frac{da'_r}{dr} \quad (27)$$

The matrices $\frac{da'_r}{dr}$, A_{rk} , and A_r^{-1} must also be put in external storage.

3. After processing all of the arcs; i.e., at the end of a global or "outer" iteration, determine \underline{dk} . Note that K has become K_4^{-1} and C_k has been modified so that

$$\underline{dk} = K^{-1} C_k \quad (28)$$

The updated values for the common parameters are of course given by

$$\underline{k}^{(n+1)} = \underline{k}^{(n)} + \underline{dk} \quad (29)$$

The arc parameters are then updated to account for the simultaneous solution of the common parameters. Information for each arc is updated in turn; that is, the previously

stored \underline{da}'_r , A_{rk} , and A_r^{-1} . The correction vector to the updated arc parameters is given by

ESTIM

$$\underline{da}_r = \underline{da}'_r - (A_r^{-1} A_{rk}) \underline{dk} \quad (30)$$

and hence

$$\underline{a}_r^{(n+1)} = \underline{a}_r^{(n)} + \underline{da}_r \quad (31)$$

The covariance matrix for the arc parameters, A_r^{-1} , is updated by

$$A_r^{-1} = A_r^{-1} + (A_r^{-1} A_{rk}) K^{-1} (A_{rk} A_r^{-1}) \quad (32)$$

This completes the global iteration.

It should be noted that if only the arc parameters are being determined, as is the case for "inner" iterations, the solution vector is \underline{da}'_r and hence the updated arc parameters are computed by

$$\underline{a}_r^{(n+1)} = \underline{a}_r^{(n)} + \underline{da}'_r \quad (33)$$

PARTITIONED ESTIMATION PROCEDURE

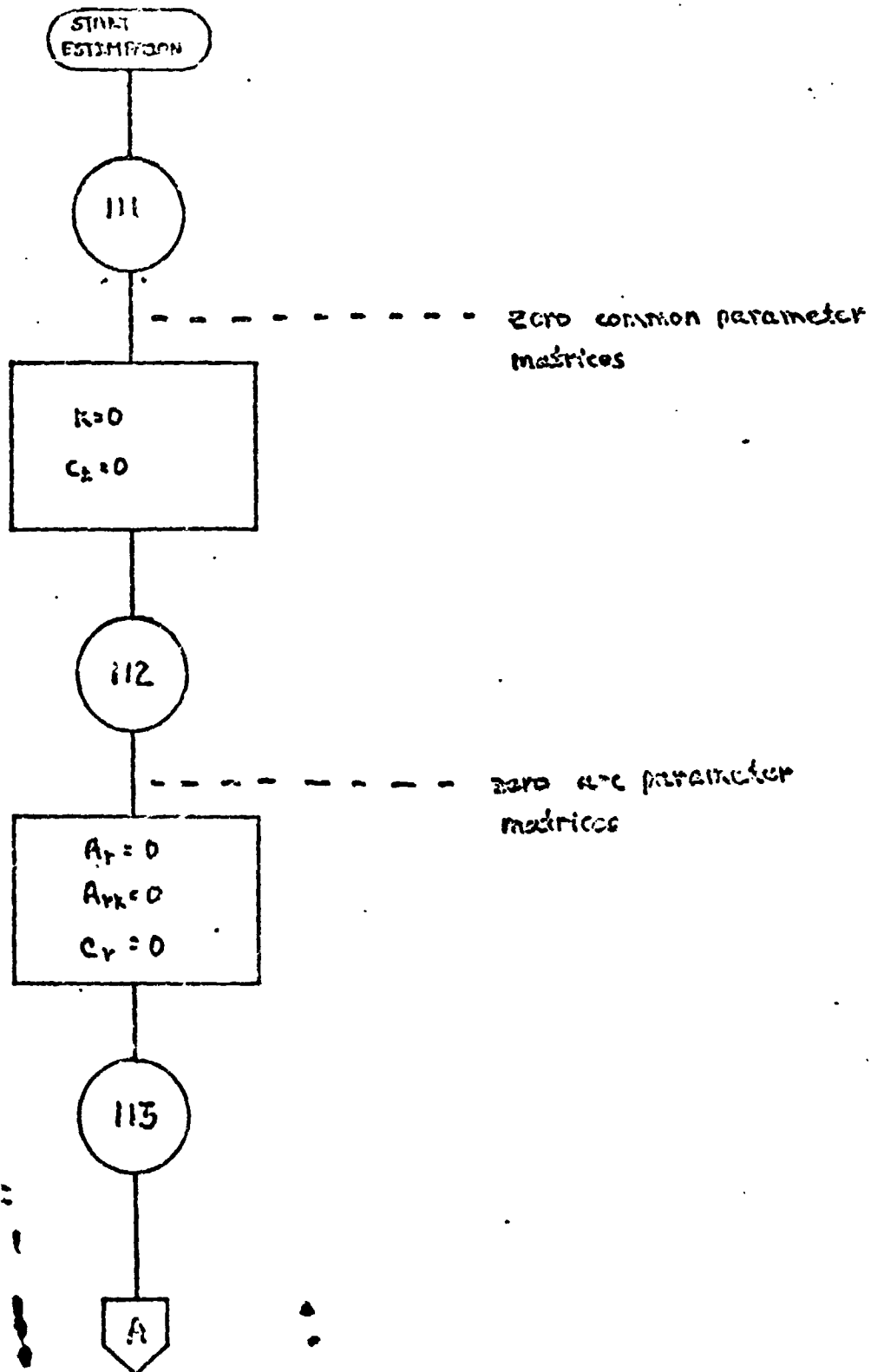
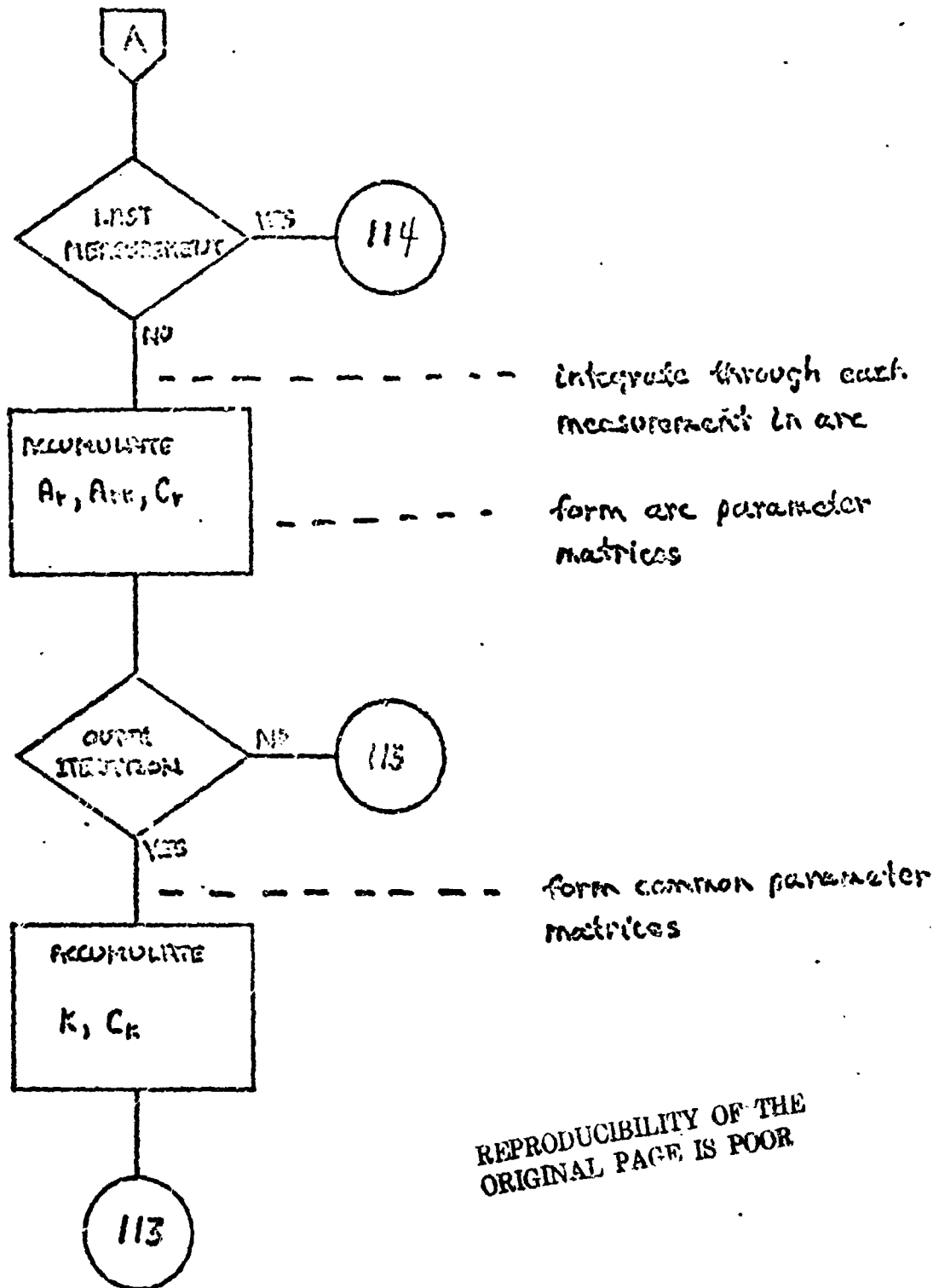
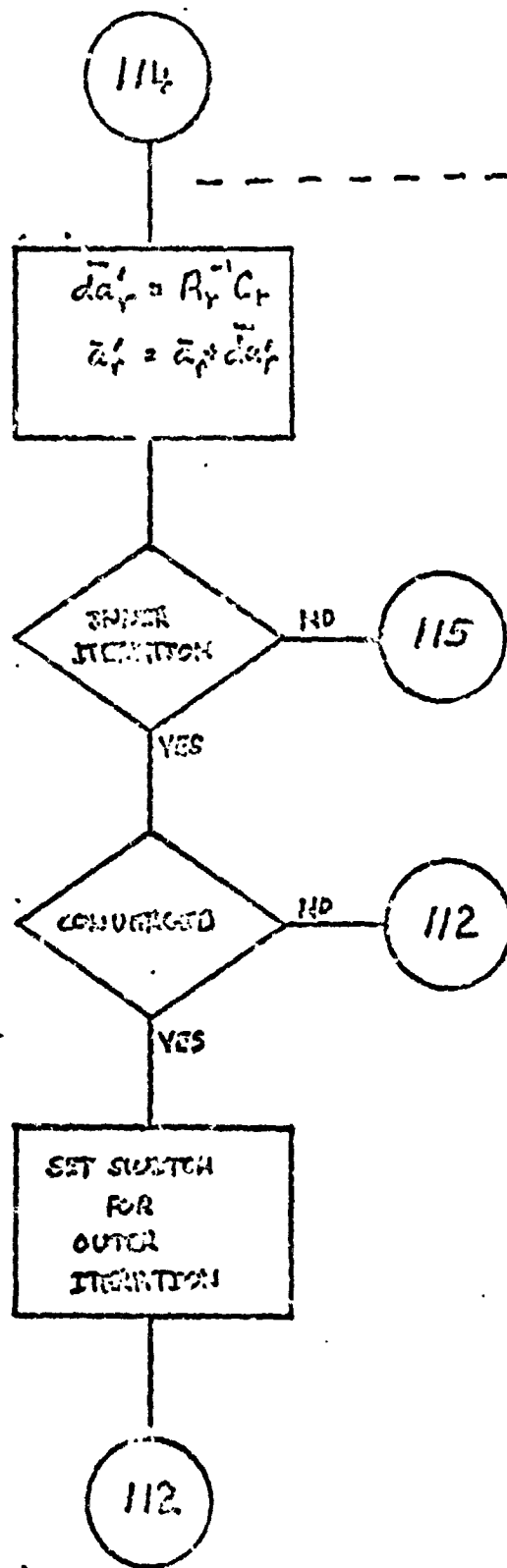


Figure 1: Partitioned Estimation Procedure



REPRODUCIBILITY OF THE ORIGINAL PAGE IS POOR

Figure 1: Partitioned Estimation Procedure (Cont.)



adjust arc elements
(arc parameter effects only)

REPRODUCIBILITY OF THE
ORIGINAL PAGE IS POOR

Figure 1: Partitioned Estimation Procedure (Cont.)

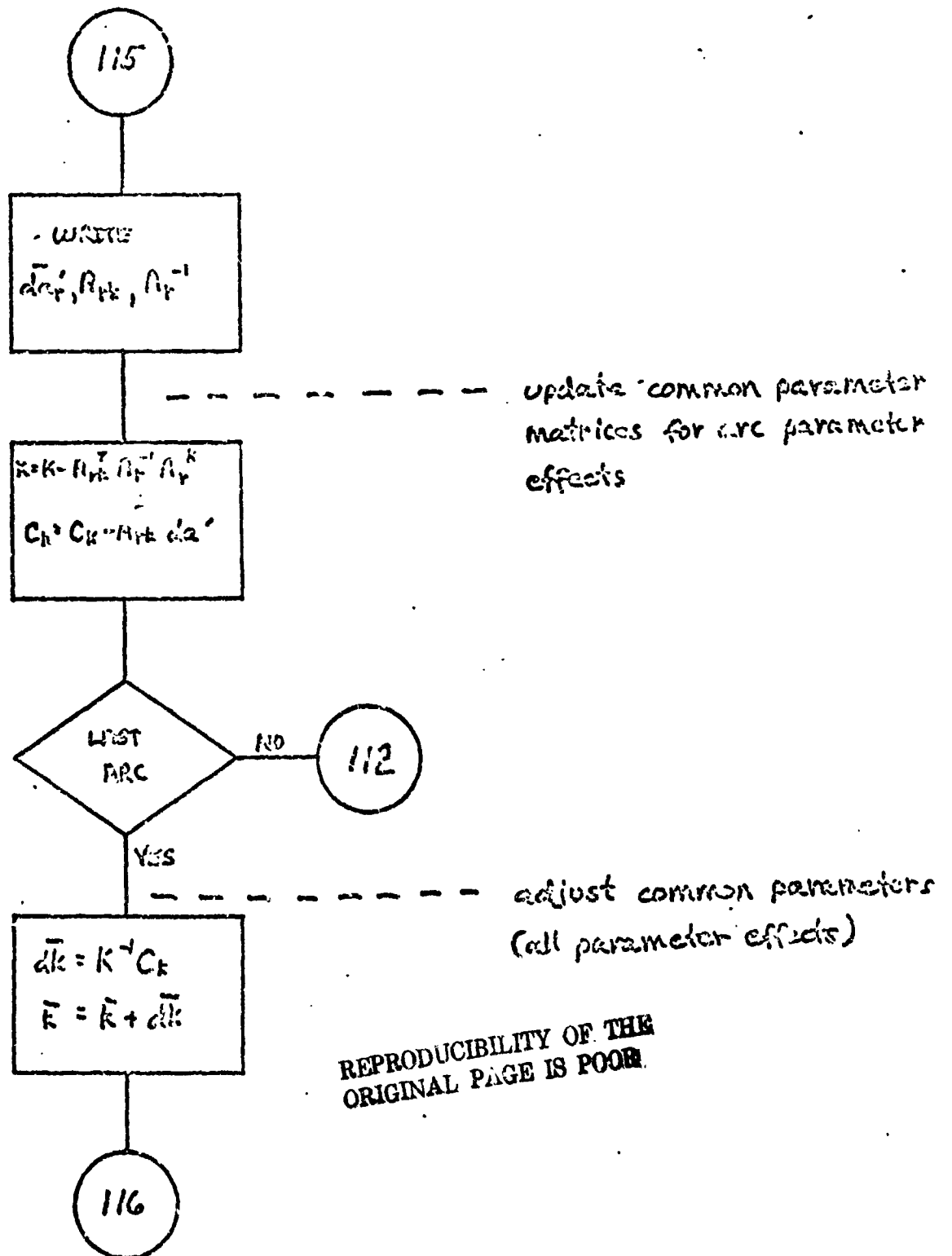


Figure 1: Partitioned Estimation Procedure (Cont.)

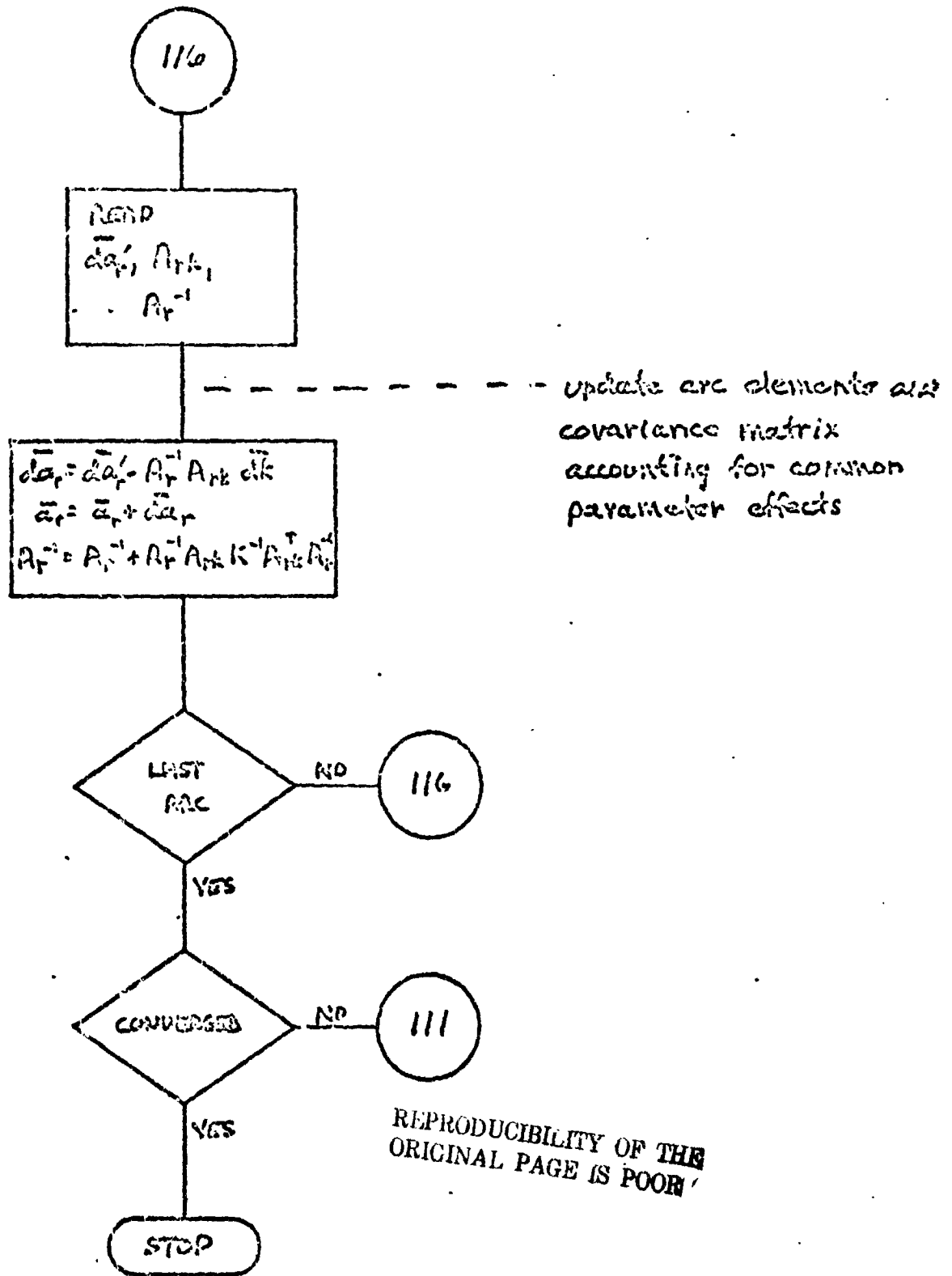


Fig. re 1: Partitioned Estimation Procedure (Cont.)

The common parameter matrix K is carried as a symmetric matrix. It is core-resident throughout the estimation procedure. Its dimension is set by the number of common parameters being determined and remains constant throughout the procedure.

The arc parameter matrices A_r are also carried as symmetric matrices. Their dimensions vary from arc to arc according to the number of arc parameters being determined. Only one arc parameter matrix A_r and the corresponding covariance matrix A_{rk} are resident in core at any given time. These arc parameter matrices are stored on disk during step 2 of the above summary and recovered during step 3.

The a priori covariance matrix V_k is not carried as a full matrix. The correlation coefficients between each coordinate of a given station position are carried. The position coordinates of different stations and the geopotential coefficients are considered to be uncorrelated.

The a priori covariance matrices V_r are also not carried as full matrices. The drag coefficient, radiation pressure coefficient, and each bias are considered to be uncorrelated. The covariance matrix for the epoch elements is carried.

REPRODUCIBILITY OF THE
ORIGINAL PAGE IS POOR

In terms of a subroutine breakdown within GEODYN, this entire section is implemented in subroutine ESTIM with the exception of the matrix inversions. These inversions are done by a routine SYMINV.

ESTIM
SYMINV

10.3 DATA EDITING

The data editing procedures for GEODYN have two forms:

- hand editing using input cards to delete specific points or sets of points, and
- automatic editing depending on the weighted residual as component to a given rejection level.

The hand editing is a simple matching of the appropriate GEODYN control card information with the set of observations. This calling procedure is done in GEODYN subroutines GEOSRD or DODSRD.

GEOSRD
DODSRD

The automatic editing of bad observations from a set of data during a data reduction run is performed in the GEODYN main program. Observations are rejected when

NONAME

$$\left| \frac{C - C}{\sigma} \right| > k$$

(1)

REPRODUCIBILITY OF THE
ORIGINAL PAGE IS POOR

where

NONAME

- O is the observation
- C is the computed observation
- σ is the a priori standard deviation associated with the observation (input)
- k is the rejection level.

The rejection level can apply either for all observations of a given type or for all observations of a given type from a particular station. This rejection level is computed from

$$k = E_M \cdot E_R \quad (2)$$

where

E_M is an input multiplier, and

E_R is the weighted RMS of the previous "outer" or global iteration. The initial value of E_R is set on input.

It should be noted that both E_M and E_R have default values.

For certain types of electronic tracking data (e.g., Doppler data), biases exist which are different from one pass to the next. In many cases, these biases are of no interest per se, although their existence must be appropriately accounted for if the data is to be used in an orbit or geodetic parameter estimation. In addition, a single data reduction may have hundreds of passes of such electronic data, and the complete solution for each bias would require the use of an excessively large amount of computer core for storing the normal matrix for the complete set of adjusted parameters.

The effects of electronic biases can be removed, with the use of only a small amount of additional core, based on the partitioning of the biases from the other parameters being adjusted in the Bayesian least squares estimation. The form which this partitioning takes can be seen from the solution of the basic measurement equation

$$\delta m = B_c \Delta b + B_A X + \epsilon \quad (1)$$

where

- REPRODUCIBILITY OF THE
ORIGINAL PAGE IS POOR
- δm = the vector of residuals (O-C),
- Δb = the set of corrections that should be made to the electronic biases,
- B_c = the matrix of partial derivatives of the measurements with respect to the biases. The elements of this matrix are either 1's or 0's.

Δx = the set of corrections to be made to all the other adjustable parameters,

BSCOM

B = the matrix of partial derivatives of the measurements with respect to the x parameters,

ϵ = the measurement noise vector.

The least squares solution of (1) is

$$\begin{bmatrix} \hat{\Delta b} \\ \hat{\Delta x} \end{bmatrix} = \begin{bmatrix} B_e^T W_e & B_e^T W \delta \\ B^T W B_e & B^T W B \end{bmatrix}^{-1} \begin{bmatrix} B_e^T W \delta m \\ B^T N \delta m \end{bmatrix} \quad (2)$$

with W the weight matrix ($W^{-1} = E(\epsilon \epsilon^T)$), taken to be completely diagonal in CEGDYN. The $\hat{\Delta x}$ part of (2) can be shown to be

$$\begin{aligned} \hat{\Delta x} = & [B^T W B - B^T W B_e (B_e^T W B_e)^{-1} B_e^T W B]^{-1} \\ & \times [B^T W \delta m - B^T W B_e (B_e^T W B_e)^{-1} B_e^T W \delta m] \end{aligned} \quad (3)$$

To effectively remove the electronic bias effects, Eqn (3) states that the normal matrix $B^T W B$ must have $B^T W B_e (B_e^T W B_e)^{-1} B_e^T W B$ subtracted from it and the vector $B^T W \delta m$ must have $B^T W B_e (B_e^T W B_e)^{-1} B_e^T W \delta m$ subtracted from it. Due to the assumed independence of different measurements, it follows that these quantities which must be subtracted are a sum of contributions for different passes,

REPRODUCIBILITY OF THE
ORIGINAL PAGE IS POOR

c 4

$$B^T W B_c (B_e^T W B_c)^{-1} B_e^T W R = \sum_{p=1}^{n_b} B_p^T W_p B_{cp} (B_{ep}^T W_p B_{ep})^{-1} B_{ep}^T W_p B_p \quad (4)$$

$$B^T W \delta_m (B_e^T W \delta_m)^{-1} B_e^T W \delta_m = \sum_{p=1}^{n_b} B_p^T W_p B_{cp} (B_{ep}^T W_p B_{cp})^{-1} B_{ep}^T W_p \delta_{mp} \quad (5)$$

where n_b is the total number of passes with electronic biases and the subscript p denotes an array for measurements of pass p . The computation of the right hand sides of (4) and (5) requires the arrays

$$B_p^T W_p B_p = n_a \times 1 \text{ array}$$

$$B_{ep}^T W_p B_{cp} = 1 \times 1 \text{ array} \quad (6)$$

$$B_{ep}^T W_p \delta_{mp} = 1 \times 1 \text{ array}$$

where n_a is the number of adjusted parameters other than biases affecting the arc in which the biases occur. Thus, $n_a + 2$ storage locations must be assigned for every bias which exists at any one time.

The individual biases may be adjusted, based on the previous iteration orbital elements and force model parameters. This bias can then be used, along with the above accumulated arrays to properly correct the sum of weighted squared residuals upon which the program does dynamic editing. Otherwise, however, it will not be possible for the statistical summaries to incorporate the adjusted values of the electronic biases unless substantial additional core is allocated.

SECTION 11.0
GENERAL INPUT/OUTPUT DISCUSSION

GEODYN is a powerful yet flexible tool for investigating the problems of satellite geodesy and orbit analysis. This same power and flexibility causes extreme variation in both input and output requirements. Consequently, GEODYN contains a great deal of programming associated with input and output.

11.1 INPUT

There are two major functions associated with the input structure:

These are the input of

- Observation data, and
- GEODYN Input Cards.

The observation data utilized by GEODYN includes data from all the major satellite tracking networks. The observational types used to date, together with their originating networks and instrument types, are:

- Right Ascension and Declination

SAO	Baker-Nunn cameras
STADAN	MOTS-cameras

USAF PC-1000 cameras
USC&GS BC-4 cameras
SPEOPT All of above except Baker-Nunn
cameras

• Range

STADAN GRARR S-Band
GSFC Laser
SAO Laser
ANS SECOR
C-Band FPQ-6 Radar
FPS-16 Radar
MSFN S-Band Radar

• Range Rate

STADAN GRARR S-Band
MSFN S-Band Radar

• Frequency Shift

TRANET - Doppler

• Direction Cosines

STADAN Minitrack interferometer

• X and Y Angles

STADAN GRARR
MSFN S-Band Radars

- Azimuth and Elevation Angles

STADAN GSFC Laser
C-BAND FPQ-6 Radar
FPS-16 Radar

- Time Delay and Fringe Rate

C-BAND VLBI Radars

The observations are required to be in either the format specified by the National Space Science Data Center (NSSDC) or the GSFC DODS System.

The NSSDC format includes indicators to identify observation type, instrumentation source, reduction method, coordinate system, and information concerning tropospheric and ionospheric refraction corrections. Data in this format is input via subroutine GEOSRD.

GEOSRD

The DODS format includes indicators to identify observation type, satellite identification, ambiguity corrections, transponder channel when applicable, timing correction, and time reference system information. It also contains flags to indicate the need for transit time correction or other types of pre-processing corrections. Data in this format is input via subroutines DODSRD and DATBSE.

DODSRD
DATBSE

The GEODYN Control Cards are the complete specifications for the problem to be solved including special output requests. Their input, controlled through subroutines ADFLUX and INOUP, consists of data and perhaps variances for

ADFLUX
INOUP

- Cartesian orbital elements
- Satellite drag coefficients

- Satellite emissivity
- Zero set measurement biases to be adjusted
- Station positions
- Geopotential coefficients
- Surface densities
- Earth tidal parameters

ADFLUX
INOIPT

and data for

- Satellite cross-sectional area
- Satellite mass
- Integration times for the orbit
- Epoch time of elements
- Criteria for iteration convergence and data editing
- Solar and geomagnetic flux

Subroutine ADFLUX modifies the program internal data tables of solar and magnetic flux according to the input requests. It also generates the scratch file of flux information to be used with each arc.

Subroutine INOIPT interprets the GEODYN Control Cards and sets the appropriate run parameters. It also generates the GEODYN run description and the descriptions for all arcs.

Subroutine INOUPPT references other routines to set up certain run parameters or to list selected run parameters in a particular format.

INOUPPT

It should be noted that the starting orbital elements for some arcs may be recovered from the DODS Data Base by subroutine DODELM.

DODELM

11.2 Output

Most of the output from GEODYN, not counting the descriptions of the input or run parameters, is produced by the NONAME program. Exceptions to this are the ORB1 tape output, the residual summary and the run summary page.

NONAME

ORB1

SUMMARY

TYPOBB

The printed output consists of a measurement and residual printout, residual summaries, and solution summaries as detailed below.

For each arc:

Measurement and Residual Printout

- Measurement date
- Measurement station
- Measurement type
- Measurement value

- Measurement residual
- Ratio to sigma
- Satellite elevation

Residual Summary by Station and Type

- Station
- Measurement type
- Number of measurements
- Mean of residuals
- Randomness measure
- Residual RMS about zero
- Number of weighted residuals
- Mean ratio to sigma for weighted residuals
- Randomness measure for weighted residuals
- RMS about zero for weighted residuals

Residual Summary by Type

- Measurement type
- Number of weighted residuals
- Weighted RMS about zero
- Weighted RMS about zero for all types together

Element Summary

- a priori Cartesian elements
- Previous Cartesian elements
- Adjusted Cartesian elements
- Adjustment to Cartesian elements (delta)
- Standard deviations of fit (sigmas)
- Position RMS
- Velocity RMS
- a priori Kepler elements
- Previous Kepler elements

- Adjusted Kepler elements
- Adjustment to Kepler elements (delta)
- Double precision adjusted Cartesian elements
(current best elements for arc)

Adjusted Force Model Parameter Summary for Arc

- Drag Coefficients, Solar Radiation Pressure Coefficient, and/or resonant geopotential coefficients.
- a priori coefficient value
- Adjusted coefficient value
- a priori standard deviations for coefficient
- Standard deviation of fit for coefficient

Adjusted Parameter Summary

- Instrument biases - timing bias and/or constant bias
- a priori bias value
- Adjusted bias value
- a priori standard deviation for bias
- Standard deviation of fit for bias

- Time period of coverage

The following items are printed on the last inner iteration of every outer iteration.

- Apogee and perigee heights
- Node rate and perigee rate
- Period of the orbit
- Drag rate and period decrement if drag is being applied
- Updated covariance matrix for Cartesian arc elements
- Adjusted arc parameter correlation coefficients

After all arcs:

Total Residual Summary .

- Total number of weighted measurements for each measurement type
- Total weighted RMS for each measurement type
- Total number of weighted measurements
- Total weighted RMS

Station Summary

- Earth-fixed rectangular coordinates and geodetic (ϕ, λ, h) coordinates
- a priori coordinate values
- a priori standard deviations for coordinate values
- Adjusted coordinate values
- Standard deviation of fit for coordinate values
- Correlations between determined coordinate values

Geopotential Summary

- C_{nm} and S_{nm} coefficients for each n, m set determined
- a priori values
- Adjusted values
- Ratios of adjusted sigma to a priori sigma for each coefficient
- Standard deviations of fit for coefficients

Surface Density Summary

- Surface Density Block Centers
- Block Areas
- a priori values
- adjusted values
- a priori uncertainties
- adjusted uncertainties

Arc Summary for Outer Iteration - For each arc

- Updated Cartesian elements for arc
- Correlation coefficients between individual arc parameters
- Standard deviation of fit for arc parameters
- Correlation coefficients between individual arc parameters and parameters common to all arcs

Common Parameter Correlation Coefficients

- Geopotential coefficients
- Cartesian station positions
- Surface Densities

GEODYN also produces an XYZ and Ground Track listing upon request. This is the normal printout for Orbit Generation Mode. In addition an osculating element printout is provided on option.

The tape output from GEODYN consists of

- the ORB1 tape,
- the XYZ and Ground Track tape,
- a DODS formatted data tape,
- a binary residual tape
- a simulation data tape.

The XYZ and Ground Track tape and the binary residual tapes are used as input to GEODYN support programs.

11.3 Computations for Residual Summary

The residual summary information is computed in subroutine STAINF for printing by the main program. The formulas used in this subroutine for computing each statistic are presented below.

STAINF

The mean is

$$\bar{r}_c = \frac{1}{n} \left[\sum_{i=1}^n R_i - \sum_{j=1}^{n_b} N_{b_j} \bar{r}_{c_j} \right] \quad (1)$$

where

R_i are the residuals

n is the number of residuals

n_b is the number of electronic biases

N_{b_j} are the residuals contributing to the bias computation

b_{e_j} is the value of the electronic bias.

The RMS is the square root of the sample variance:

STAINF

$$\text{RMS} = \sqrt{s^2} \quad (2)$$

where

$$s^2 = \frac{1}{n} \left[\sum_{i=1}^n R_i^2 - \sum_{j=1}^{n_b} N_{b_j} b_{e_j}^2 \right]$$

The expected value of the sample variance differs from the population variance σ^2 :

$$E(s^2) = \sigma^2 - \text{var}(\mu_c) \quad (3)$$

or rather

$$E(s^2) = \sigma^2 \left(1 - \frac{1}{n}\right). \quad (4)$$

Hence we may make a better estimate of σ^2 by computing

$$\sigma^2 = \frac{n}{n-1} s^2 \quad (5)$$

This is known as Bessel's correction. This computed value for the standard deviation, σ , is also called the RMS about zero.

STAINF

The randomness measure used in GEODYN is from a mean square successive difference test. We have

$$\text{RND} = \frac{d^2}{s^2} \quad (6)$$

when

RND is the random normal deviate, our statistic;

s^2 is the unbiased sample variance; and

$$d^2 = \frac{1}{2(n-1)} \sum_{i=1}^{n-1} (R_{i+1} - R_i)^2$$

Note that d^2 is the mean square successive difference.

For each i the difference $R_{i+1} - R_i$ has mean zero and variance $2\sigma^2$ under the null hypothesis that

(R_1, \dots, R_n) is a random sample from a population with variance σ^2 . The expected value of d^2 is then σ^2 .

If a trend is present d^2 is not altered nearly so much as the variance estimate s^2 , which increases greatly.

Thus the critical region RND constant is employed in testing against the alternative of a trend. (Reference 1)

In order to use this test, of course, it is necessary to know the distribution of the RND. It can be shown that in the case of a normal population the expected value is given by

STAINF

$$E (RND) = 1, \quad (7)$$

the variance is given by

$$\text{var} (RND) = \frac{1}{n+1} \left(1 - \frac{1}{n-1} \right), \quad (8)$$

and that the test statistic, RND, is approximately normal for large samples ($n > 20$).

11.4 Kepler Elements

The Kepler elements describe the position of the satellite as referred to an ellipse inclined to the orbit plane. This is shown in Figures 1 and 2. The definitions of these elements are:

- a - semi-major axis of the orbit
- e - eccentricity of the orbit
- i - inclination of the orbit plane
- Ω - longitude of the ascending node
- ω - argument of perigee
- M - mean anomaly
- E - eccentric anomaly
- f - true anomaly

Apogee height and perigee height are sometimes used in place of a and e to describe the shape of the orbit. As can be seen in Figure 1, the radius at perigee is $a(1-e)$ and that at apogee is $a(1+e)$. The heights are determined by subtracting the radius of the reference ellipsoid at the given latitude from the spheroid height of the satellite. The computations of these last are detailed in section 5.1.

APPER

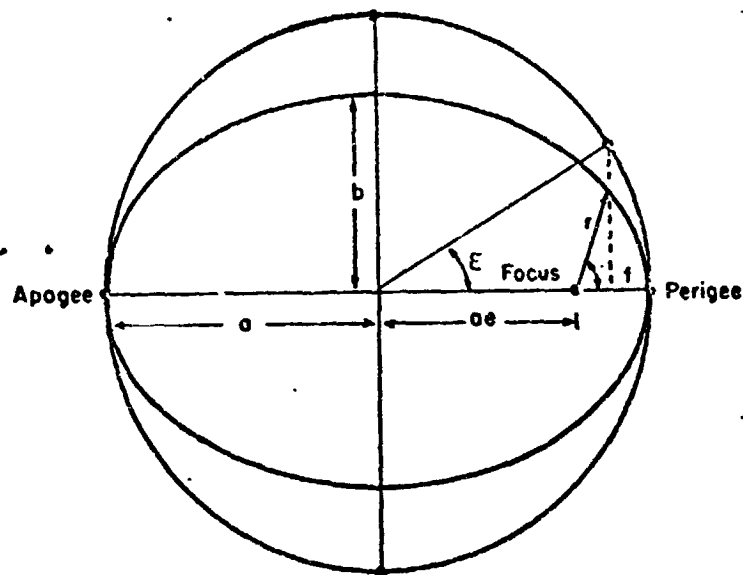


Figure 1: Orbital Ellipse

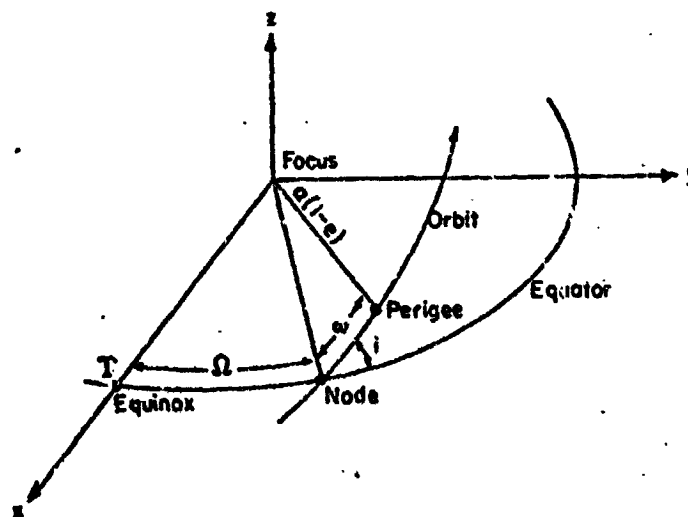


Figure 2: Orbital Orientation

Conversion to Kepler Elements

ELEM

The computation of Kepler elements from the Cartesian positions and velocities $x, y, z, \dot{x}, \dot{y}, \dot{z}$ is as follows:

Compute the angular momentum vector per unit mass:

$$\bar{h} = \bar{r} \times \dot{\bar{r}} \quad (1)$$

where \bar{r} is the position vector and $\dot{\bar{r}}$ is the velocity vector. Note that $v^2 = \dot{\bar{r}} \cdot \dot{\bar{r}}$. The inclination is given by

$$i = \cos^{-1} \left[\frac{h_z}{h} \right] \quad (2)$$

From the vis-viva or energy integral we have

$$v^2 = GM \left(\frac{2}{r} - \frac{1}{a} \right), \quad (3)$$

where G is the universal gravitational constant and M is the mass of the primary about which the satellite is

orbiting. Thus we have

ELEM

$$a = \left[\frac{2}{r} - \frac{v^2}{GM} \right]^{-1} \quad (4)$$

Recalling Kepler's Third Law,

$$h^2 = GM a (1-e^2), \quad (5)$$

we determine

$$e = \left[1 - \left(\frac{h^2}{aGM} \right) \right]^{1/2} \quad (6)$$

The longitude of the ascending node is also determined from the angular momentum vector:

$$\Omega = \tan^{-1} \left(\frac{h_x}{-h_y} \right) \quad (7)$$

The true anomaly, f , is computed next. Note that in integrating

$$\ddot{\mathbf{r}} \times \mathbf{h} = GM \frac{\dot{\mathbf{r}}}{r^3} \quad (8)$$

one arrives at

$$\dot{\bar{r}} \times \bar{h} = GM (\bar{r} + \bar{e}) \quad (9) \quad \text{ELEM}$$

where \bar{e} is a constant of integration of magnitude equal to the eccentricity and pointing toward perihelion.

Thus,

$$\bar{r} \times \bar{e} = re \sin f \left(\frac{-\bar{h}}{h} \right), \quad (10)$$

or, performing a little algebra,

$$\sin f = \frac{a (1-e^2) \bar{r} \cdot \dot{\bar{r}}}{reh} \quad (11)$$

The cosine of the true anomaly comes from

$$r = \frac{a (1-e^2)}{1+e \cos f}, \quad (12)$$

that is .

$$\cos f = \frac{a (1-e^2)}{er} - \frac{1}{e} \quad (13)$$

The true anomaly is then

$$f = \tan^{-1} \left(\frac{\sin f}{\cos f} \right) \quad (14)$$

At this point a decision must be made as to whether the orbit is an ellipse ($1 > e > 0$) or a hyperbola ($1 < e < \infty$). For an elliptic orbit, the eccentric anomaly is computed from the true anomaly:

ELEM

$$\cos E = \frac{\cos f + e}{1 + e \cos f}, \quad (15)$$

$$\sin E = \frac{\sqrt{1-e^2} \sin f}{1 + e \cos f}, \quad (16)$$

and

$$E = \tan^{-1} \left(\frac{\sin E}{\cos E} \right), \quad (17)$$

The mean anomaly is then computed from Kepler's equation:

$$M = E - e \sin E. \quad (18a)$$

In the case of a hyperbolic orbit, we use an equation analogous to Kepler's equation by introducing F , in place of E . The eccentric anomaly is the same as above;

$$F = \tanh^{-1} \left(\frac{\sinh F}{\cosh F} \right)$$

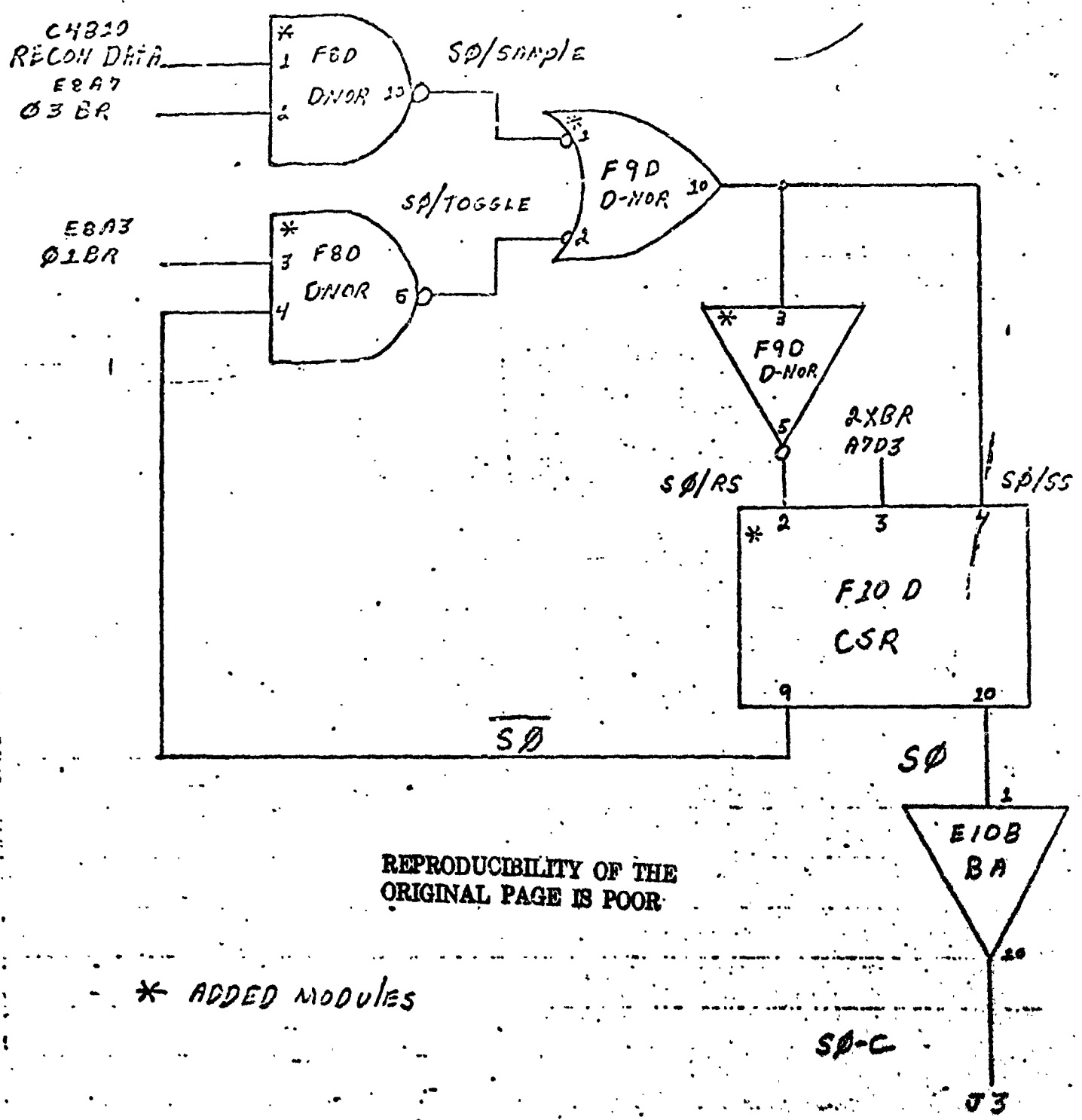
where

$$\sinh F = \frac{\sqrt{1-e^2} \sin f}{1 + e \cos f}$$

$$\cosh F = \frac{\cos f + e}{1 + e \cos f}$$

REPRODUCIBILITY OF THE ORIGINAL PAGE IS POOR

MODIFICATION PROPOSAL #19-194



REPRODUCIBILITY OF THE ORIGINAL PAGE IS POOR.

* ADDED MODULES

Figure 3. Logic Diagram of the Modification.

The mean anomaly is

$$M = e \sinh F - F \quad (18b)$$

where $F = \ln [\sinh F + \cosh F]$

F is computed by using the definition of sinh and cosh

$$\sinh F = \frac{e^F - e^{-F}}{2}$$

$$\cosh F = \frac{e^F + e^{-F}}{2}$$

$$\begin{aligned} (\sinh F + \cosh F) &= \frac{1}{2} (e^F - e^{-F} + e^F + e^{-F}) \\ &= e^F \end{aligned}$$

The central angle u is the angle between the satellite vector and a vector pointing toward the ascending node:

$$\cos u = \frac{x \cos \Omega + y \sin \Omega}{r} \quad (19)$$

$$\sin u = \frac{(y \cos \Omega - x \sin \Omega) \cos i + z \sin i}{r} \quad (20)$$

$$u = \tan^{-1} \left(\frac{\sin u}{\cos u} \right) \quad (21)$$

The argument of perigee is then

$$\omega = u - f \quad (22)$$

PARTIAL DERIVATIVES OF KEPLER ELEMENTS

ELEM

The partial derivatives of Kepler elements with respect to $x, y, z, \dot{x}, \dot{y}, \dot{z}$ are as follows:

P.D.* of inclination:

$$\frac{\partial}{\partial x} i = A[B(\dot{y} \cdot h_z - \dot{z} \cdot h_y) - \dot{y}]$$

$$\frac{\partial}{\partial y} i = A[B(\dot{z} \cdot h_x - \dot{x} \cdot h_z) + \dot{x}]$$

$$\frac{\partial}{\partial z} i = AB(\dot{x} \cdot h_y - \dot{y} \cdot h_x)$$

$$\frac{\partial}{\partial x} i = A[B(\dot{z} \cdot h_y - \dot{y} \cdot h_z) + \dot{y}]$$

$$\frac{\partial}{\partial y} i = A[B(\dot{x} \cdot h_z - \dot{z} \cdot h_x) - \dot{x}]$$

$$\frac{\partial}{\partial z} i = AB(\dot{y} \cdot h_x - \dot{x} \cdot h_y)$$

where

$$A = \frac{1}{h \cdot \sin i}$$

$$B = \frac{\cos i}{h}$$

P.D. of semi-major axis:

$$\frac{\partial}{\partial V} a = \frac{V \cdot 2a^2}{r^3}$$

REPRODUCIBILITY OF THE ORIGINAL PAGE IS POOR

* P.D. - partial derivatives

where

$V = x, y, z$, respectively.

$$\frac{\partial}{\partial V} \frac{1}{a} = \frac{\dot{V} \cdot 2a^2}{GM}$$

where

$\dot{V} = \dot{x}, \dot{y}, \dot{z}$, respectively.

P.D. of eccentricity:

$$\frac{\partial}{\partial x} e = C \left[x \cdot D - \frac{1}{a} (\dot{y} \cdot h_z - \dot{z} \cdot h_y) \right]$$

$$\frac{\partial}{\partial y} e = C \left[y \cdot D - \frac{1}{a} (\dot{z} \cdot h_x - \dot{x} \cdot h_z) \right]$$

$$\frac{\partial}{\partial z} e = C \left[z \cdot D - \frac{1}{a} (\dot{x} \cdot h_y - \dot{y} \cdot h_x) \right]$$

$$\frac{\partial}{\partial x} e = C \left[x \cdot D' - \frac{1}{a} (z \cdot h_y - y \cdot h_z) \right]$$

$$\frac{\partial}{\partial y} e = C \left[y \cdot D' - \frac{1}{a} (x \cdot h_z - z \cdot h_x) \right]$$

$$\frac{\partial}{\partial z} e = C \left[z \cdot D' - \frac{1}{a} (y \cdot h_x - x \cdot h_y) \right]$$

where

$$C = \frac{1}{e \cdot GM}$$

$$D = \frac{1}{r^3}$$

$$D' = \frac{h^2}{GM}$$

P.D. of ascending node:

ELEM

$$\frac{\partial}{\partial x} \Omega = H \cdot z \cdot h_x$$

$$\frac{\partial}{\partial y} \Omega = H \cdot z \cdot h_y$$

$$\frac{\partial}{\partial z} \Omega = -H(y \cdot h_y - x \cdot h_x)$$

$$\frac{\partial}{\partial x} \Omega = -H \cdot z \cdot h_x$$

$$\frac{\partial}{\partial y} \Omega = -H \cdot z \cdot h_y$$

$$\frac{\partial}{\partial z} \Omega = H(y \cdot h_y + x \cdot h_x)$$

where

$$H = \frac{1}{h_x^2 + h_y^2}$$

P.D. of mean anomaly:

$$\frac{\partial}{\partial v} M = \frac{r}{a} S - \sin E \frac{\partial e}{\partial v}$$

where

$$S = \left(\frac{1}{a} \left(\frac{\partial r}{\partial v} - \frac{r}{a} \frac{\partial a}{\partial v} \right) + \cos E \frac{\partial e}{\partial v} \right) / e \sin E$$

v represents x, y, z, \dot{x} , \dot{y} , \dot{z} respectively, and $\frac{\partial r}{\partial x} = \frac{x}{r}$, $\frac{\partial r}{\partial y} = \frac{y}{r}$, $\frac{\partial r}{\partial z} = \frac{z}{r}$.

$$\frac{\partial r}{\partial \dot{x}} = 0, \quad \frac{\partial r}{\partial \dot{y}} = 0, \quad \frac{\partial r}{\partial \dot{z}} = 0$$

P.D. of the argument of perigee:

ELEM

$$\frac{\partial}{\partial v} w = \frac{\partial u}{\partial v} - \frac{\partial f}{\partial v}$$

where

$$\begin{aligned}\frac{\partial u}{\partial v} &= \frac{\partial}{\partial v} \left(\tan^{-1} \frac{\sin u}{\cos u} \right) \\ &= \cos^2 u \frac{\partial u}{\partial v} - \sin u \frac{\partial}{\partial v} \cos u\end{aligned}$$

$$\frac{\partial u}{\partial v} = \frac{-1}{\sin u} \frac{\partial}{\partial v} \cos u$$

and

$$\frac{\partial f}{\partial v} = \frac{\partial}{\partial v} \left(\tan^{-1} \frac{\sin f}{\cos f} \right)$$

similarly

$$\frac{\partial f}{\partial v} = \frac{-1}{\sin f} \frac{\partial}{\partial v} \cos f$$

and

$$\begin{aligned}-\frac{\partial}{\partial x} \cos u &= ((x \sin \Omega - y \cos \Omega) \frac{\partial \Omega}{\partial v} - \cos \Omega \frac{\partial v}{\partial x} - \sin \Omega \frac{\partial v}{\partial y} + \cos \frac{\partial r}{\partial v}) / r \\ -\frac{\partial}{\partial x} \cos f &= \frac{1}{(or)^2} [e(1-e^2) (a \frac{\partial r}{\partial v} - r \frac{\partial \Omega}{\partial v}) - r(r-a(1+e^2)) \frac{\partial}{\partial v} e]\end{aligned}$$

where v and $\frac{\partial r}{\partial v}$ represents the same as above.

In GEODYN, this conversion from $x, y, z, \dot{x}, \dot{y}, \dot{z}$ to $a, e, i, \Omega, \omega, M$ and the partial derivatives are performed by subroutine ELEM.

Conversion From Kepler Elements

The input elements are considered to be $a, e, i, \Omega, \omega,$ and M and the Cartesian elements are required.

POSVEL

An iterative procedure, Newton's method, is used to recover the eccentric anomaly. For an elliptic orbit, the iterative procedure is, from Kepler's equation ($M = E - e \sin E$),

$$E' = E - \frac{E - e \sin E - M}{1 - e \cos E}$$

For a hyperbolic orbit, the iterative procedure is

$$F' = F - \frac{e \sinh F - F - M}{e \cosh F - 1}$$

where $F, \sinh F,$ and $\cosh F$ are defined previously.

This conversion procedure for converting $a, e, i, \Omega, \omega, M$ to $x, y, z, \dot{x}, \dot{y}, \dot{z}$ is performed in the GEODYN system by subroutine POSVEL.

The vectors \bar{A} and \bar{B} are computed. \bar{A} is a vector in the orbit plane directed toward peri center with a magnitude equal to the semi-major axis of the orbit:

$$\bar{A} = a \begin{bmatrix} \cos \omega \cos \Omega - \sin \omega \sin \Omega \cos i \\ \cos \omega \sin \Omega + \sin \omega \cos \Omega \cos i \\ \sin \omega \sin i \end{bmatrix} \quad (23)$$

\bar{B} is a vector in the orbit plane directed 90° counter clockwise from \bar{A} with a magnitude equal to the semi-minor axis of the orbit.

$$\bar{B} = a \sqrt{1-e^2} \begin{bmatrix} -\sin \omega \cos \Omega - \cos \omega \sin \Omega \cos i \\ -\sin \omega \sin \Omega + \cos \omega \cos \Omega \cos i \\ \cos \omega \sin i \end{bmatrix} \quad \text{POSVEL} \quad (24)$$

The position vector \bar{r} is then

$$\bar{r} = (\cos E - e) \bar{A} + (\sin E) \bar{B} \quad (25)$$

The velocity vector is given by

$$\dot{\bar{r}} = \dot{E} \begin{bmatrix} (-\sin E) \bar{A} + (\cos E) \bar{B} \end{bmatrix} \quad (26)$$

where \dot{E} is given by

$$\dot{E} = \frac{\sqrt{\frac{GM}{a^3}}}{1-e \cos E} \quad (27)$$

11.4.1 Node Rate and Perigee Rate

The node rate $\dot{\Omega}$ and perigee rate $\dot{\omega}$ are computed from Lagrange's Planetary Equations. As these are for printout only, GEODYN uses just the Earth oblateness term in the geopotential. From Reference 4, page 39, we have

$$\dot{\Omega} = \left[\frac{3}{2} C_{20} \sqrt{\frac{GM}{a_e^3}} \right] \left(\frac{a}{a_e} \right)^{-3.5} \frac{\cos i}{(1-e^2)^2} \quad (1)$$

$$\dot{\omega} = \left[\frac{3}{4} C_{20} \sqrt{\frac{GM}{a_e^3}} \right] \left(\frac{a}{a_e} \right)^{-3.5} \frac{(1-5 \cos^2 i)}{(1-e^2)^2} \quad (2)$$

in radians per second, or rather

$$\dot{\Omega} = -9.97 \left(\frac{a}{a_e} \right)^{-3.5} \frac{\cos i}{(1-e^2)} \quad (3)$$

$$\dot{\omega} = -4.98 \left(\frac{a}{a_e} \right)^{-3.5} \frac{(1-5 \cos^2 i)}{(1-e^2)^2} \quad (4)$$

in degrees per day. The quantities used in the above equations are defined as:

a_e is the semi-major axis of the Earth

GM is the product of the universal gravitational constant G and the mass of the Earth M

C_{20} is the Earth oblateness term in the geopotential (see Section 8.3).

a semi-major axis of the orbit

e eccentricity of the orbit

i inclination of the orbit

11.4.2 Period Decrement and Drag Rate

The period decrement and the drag rate are determined from the partial derivatives of the position and velocity with respect to the drag coefficient at the final integrator time step in the given arc. These (multiplied by the drag coefficient) represent the sensitivity of the position or velocity to drag effects. Let us define

$$\Delta D = \frac{\partial}{\partial C_D} (\bar{r}) \cdot C_D \quad (1)$$

where

\bar{r} is the satellite (inertial) position vector

C_D is the drag coefficient

We also define

$$\dot{\Delta D} = \frac{\partial}{\partial C_D} (\dot{\bar{r}}) \cdot C_D \quad (2)$$

The (two-body) period of the orbit is

$$P = 2\pi \sqrt{\frac{a^3}{GM}} \quad (3)$$

where

a is the semi-major axis of the orbit

GM is the product of G , the universal gravitational constant, and M , the mass of the Earth.

Thus

$$\Delta P = 3\pi \sqrt{\frac{a}{GM}} \Delta a. \quad (4)$$

The vis viva or energy integral has

$$v^2 = GM \left(\frac{2}{r} - \frac{1}{a} \right), \quad (5)$$

hence

$$a = \frac{1}{\left[\frac{2}{r} - \frac{\dot{\vec{r}} \cdot \dot{\vec{r}}}{GM} \right]} \quad (6)$$

Recognizing that $\Delta(\vec{r})$ is $\Delta \vec{D}$ and $\Delta(\dot{\vec{r}})$ is $\dot{\Delta \vec{D}}$,

$$\Delta a = \frac{2}{\left[\frac{2}{r} - \frac{\dot{\vec{r}} \cdot \dot{\vec{r}}}{GM} \right]^2} \left[\frac{\vec{r} \cdot \Delta \vec{D}}{r^3} + \frac{\dot{\vec{r}} \cdot \dot{\Delta \vec{D}}}{GM} \right] \quad (7)$$

The effect of the drag on the period is then given by

$$\Delta P = \frac{6\pi}{a^2} \sqrt{\frac{a}{GM}} \left[\frac{\bar{r} \cdot \Delta \bar{D}}{r^3} + \frac{\dot{\bar{r}} \cdot \dot{\Delta \bar{D}}}{GM} \right] \quad (8)$$

The daily rate or period decrement is computed as $\Delta P / \Delta t$ where Δt is the elapsed time (in days) between the last integrator time point and epoch.

The drag rate is computed from the along track (actually normal) portion of $\Delta \bar{D}$, that is ΔD_N . We need to construct the unit vector along track, \hat{L} . The velocity vector $\dot{\bar{r}}$ may be resolved into a radial component and a component normal to the radius vector. The magnitude of the normal component is found by the Pythagorean Theorem:

$$A = \sqrt{\dot{\bar{r}} \cdot \dot{\bar{r}} - \left(\frac{1}{r} \bar{r} \cdot \dot{\bar{r}} \right)^2} \quad (9)$$

The unit normal vector \hat{L} is then

$$\hat{L} = \left(\dot{\bar{r}} - \frac{1}{r} \bar{r} \cdot \dot{\bar{r}} \right) / A \quad (10)$$

The normal portion of $\Delta \bar{D}$ is then

$$\Delta D_N = \hat{L} \cdot \Delta \bar{D} \quad (11)$$

This $\overline{\Delta D}_N$ represents the along-track position effect due to drag over the integrated time span. The drag rate is computed as $\Delta D_N / \Delta t$ where Δt is again the elapsed time in days.

SECTION 12.0
REFERENCES

GENERAL:

1. Explanatory Supplement to the Astronomical Ephemeris and the American Ephemeris and Nautical Almanac, Published by Her Majesty's Stationery Office, London, 1961.
2. William M. Kaula. "Theory of Satellite Geodesy," Blaisdell Publishing Company, Waltham, Massachusetts, 1966.

SECTION 3:

1. A Joint Supplement to the American Ephemeris and the British Nautical Almanac, "Improved Lunar Ephemeris 1952-1959," pages IX and X.
2. Astronomical Papers Prepared for the Use of the American Ephemeris and Nautical Almanac, Volume 15, Part 1, page 153, "Theory of the Rotation of the Earth Around its Center of Mass," published by the United States Government Printing Office, Washington, D.C., 1955.
3. Explanatory Supplement to the Astronomical Ephemeris and the American Ephemeris and Nautical Almanac, published by Her Majesty's Stationery Office, London, 1961.

REFERENCES (CONT.)

SECTION 3:

4. S. Newcomb. "A New Determination of the Precessional Constant with the Resulting Precessional Motions," Astronomical Papers prepared for the use of the American Ephemeris, 1897.
5. Edgar W. Woolard. "A Redevelopment of the Theory of Nutation," Astronomical Journal, February 1953, Vol. 58, No. 1, pages 1-3.

SECTION 4:

1. C.J. Devine. "JPL Development Ephemeris Number 19," JPL Technical Report 32-1181, Pasadena, California, November 15, 1967.

SECTION 5:

1. Bernard Guinot and Martine Feissal. "Annual Report for 1967," Bureau International De L'Heure, published for the International Council of Scientific Unions, Paris, 1969.

REFERENCES (CONT.)

SECTION 7:

1. "GEOS-A Clock Calibration for Days 321, 1965 to 50, 1966," Johns Hopkins University Applied Physics Laboratory Report, 1966.
2. TEXT-BOOK ON SPHERICAL ASTRONOMY, W.M. Smart, Cambridge University Press, 1965.
3. George Veis, "Smithsonian Contributions to Astrophysics," Vol. 3, No. 9, 1960.
4. C.A. Lundquist and G. Veis, "Geodetic Parameters for a 1966 Smithsonian Institution Standard Earth," S.A.O. Special Report No. 200, 1966.
5. W. Woolard and G.M. Clemence, "Spherical Astronomy," Academic Press, 1966.

SECTION 8:

1. Jacchia, L.G.
1971 "Revised Static Models of the Thermosphere and Exosphere with Empirical Temperature Profiles," Special Report 332, Smithsonian Institution Astrophysical Observatory (SAO), Cambridge, Massachusetts.
2. 1970 "New Static Models of the Thermosphere and Exosphere with Empirical Temperature Profiles," Special Report 313, SAO.

REFERENCES (CONT.)

3. Gotz, R.
1968 "Density of the Upper Atmosphere," Wolf Research
and Development Corporation, Riverdale, Maryland.
4. Roberts, C.E., Jr.
1970 "An Analytical Model for Upper Atmosphere Densi-
ties Based Upon Jacchia's 1970 Models," Celestial
Mechanics 4 (1971), D. Reidel Publishing Company,
Dordrecht, Holland.
5. Koch, K.R., "Alternate Representation of the Earth's
Gravitational Field for Satellite Geodesy," Boll.
Geofis., 10, 318-325, 1968.
6. Koch, K.R. and F. Morrison, A Simple Layer Model
of the Geopotential from a Combination of Satellite
and Gravity Data," J. Geophys. Res., 75, 1483-1492,
1970.
7. Koch, K.R. and B.U. Witte, Earth's Gravity Field
Represented by a Simple-Layer Potential from
Doppler Tracking of Satellites," J. Geophys. Res.,
76, 8471- 8479, 1971.
8. Koch, K.R., "Errors of Quadrature Connected with
the Simple Layer Model of the Geopotential,"
U.S. Dept. of Commerce Memo NOAA TN NOS 11,
December 1971.
9. Gaposchkin, E.M. and K. Lambeck, 1969 Smithsonian
Standard Earth. Smithsonian Astrophysical Obser-
vatory Special Report No. 315, May 18, 1970.

August 11, 1975

REFERENCES (CONT.)

10. Schwarz, C.R., "Gravity Field Refinement by Satellite to Satellite Doppler Tracking," Ohio State Department of Geodetic Science Report No. 147, December 1970.
11. "Error Models for Solid Earth and Ocean Tidal Effects in Satellite Systems Analysis", Wolf Research and Development Corporation, Contract No. NAS 5-11735-Mod 57. July 1972.
12. Jacchia, L.G., "Static Diffusion Models of the Upper Atmosphere with Empirical Temperature Profiles," Special Report 170, SAO, 1965.
13. U.S. Standard Atmosphere, 1966. Sponsored by National Aeronautics and Space Administration, U.S. Air Force and U.S. Weather Bureau, Washington, D.C. (December).
14. Jacchia, L.G., "Density Variation in the Heterosphere," Special Report 184, SAO (September 20)., 1965
15. Jacchia, L.G., "The Temperature Above the Thermopause," Special Report 150, Smithsonian Institution Astrophysical Observatory (SAO), Cambridge, Massachusetts, 1965.
16. Johnson, F.S., "Circulation at Ionospheric Levels," Southwest Center for Advanced Studies, Report on Contract CWB 10531, (January 30), 1964.
17. Jacchia, L.G., Campbell, I.G., and Slowey, J.W. "Semi-Annual Density Variations in the Upper Atmosphere, 1958 to 1966," Special Report 265, SAO, (January 15), 1968.

REPRODUCIBILITY OF THE
ORIGINAL PAGE IS POOR

18. Jacchia, L.G., "IV. The Upper Atmosphere," Philosophical Transactions of the Royal Society, 1967, A. Vol. 262, pp. 157-171.

SECTION 9:

1. "Cowell Type Numerical Integration as Applied to Satellite Orbit Computations," J.L. Maury, Jr., G.D. Brodsky, GSFC X-553-69-46, Dec. 1969.
2. "Geostar-I, A Geopotential and Station Positions Recovery System," C.E. Velez, G.P. Brodsky, GSFC X-53-69-544, December 1969.
3. "Geostar-II, A Geopotential and Station Position Recovery System," C.E. Velez, G.D. Brodsky, GSFC X-553-70-372, Oct. 1970.

SECTION 10:

1. Maurice G. Kendall and Alan Stuart. "The Advanced Theory of Statistics," Vol. II, London, 1961.
2. Robert C.K. Lee. "Optimal Estimation, Identification and Control," Cambridge, Massachusetts, 1964.
3. "The GEOSTAR Plan for Geodetic Parameter Estimation," Wolf Research and Development Corporation, Contract No. NAS 5-9756-152, November 1968.

**REPRODUCIBILITY OF THE
ORIGINAL PAGE IS POOR**

August 11, 1973

REFERENCES (CONT.)

SECTION 11:

1. B.W. Lindgren. "Statistical Theory," The Macmillan Company, New York, 1968.
2. "Support Activity of the Geodetic Satellite Data Service," National Space Science Data Center Report, Goddard Space Flight Center, November 1965.
3. J. Topping. "Errors of Observation and Their Treatment," Chapman and Hall, Ltd., London, 1965.
4. William M. Kaula. "Theory of Satellite Geodesy," Blaisdell Publishing Company, Waltham, Massachusetts, 1966.

REPRODUCIBILITY OF THE
ORIGINAL PAGE IS POOR

August 11, 1975

APPENDIX A
INDEX OF SUBROUTINE REFERENCES
FOR GEODYN PROGRAM

<u>SUBROUTINE</u>	<u>SECTION</u>
ADFLUX	8.7.2, 11.1
APPER	11.4
AVGPOT	8.3.2.2
BSCOMP	10.4
COEF	9.3
COWELL	9.1
DATBSE	11.1
DENORM	8.3.1
D71	8.2, 8.6, 8.7
D650	8.2, 8.6, 8.7
DNVERT	9.1
DOELM	11.1
DODSRD	7.1, 7.2, 10.3, 11.1
DRAG	5.1, 8.2, 8.6
EGRAV	8.3.1
ELEM	11.4
EPHEM.	3.5, 4.0
EQN	3.6, 3.6.2
EQUATR	3.6, 7.2
ESTIM	10.2
F	3.5, 8.1, 8.2, 8.5
FLUAM	8.7.2
FLUXS	8.7.2
GEOIDH	8.3.2.2, 8.3.2.4
GEOSRD	7.1, 7.2, 7.6, 10.3, 11.1
GRHPAN	3.4, 3.5, 6.1
INOUPY	5.1, 11.1
INTRP	9.3
JANTHG	3.5, 8.7.2
NONAME	10.3, 11.2

REPRODUCIBILITY OF THE
ORIGINAL PAGE IS POOR

<u>SUBROUTINE</u>	<u>SECTION</u>
NUTATE	3.6, 3.6.2
OBSDOT	3.4, 5.2, 6.0, 6.1, 6.3
ORBIT	8.2, 9.0
ORBI	11.2
PDEN	8.3.2.4
PLHOUT	5.1
POLE	5.4
POSVEL	11.4
PRÉCÉS	3.6, 3.6.1
PREDCT	3.4, 5.1, 5.2, 6.0, 6.1, 6.2, 8.2
PROCES	6.0, 7.1, 7.3, 7.4, 7.5
REARG	9.1
REFCOR	3.6, 8.1
REFION	7.5
RESPAR	8.2, 8.3.1
SATCL2	7.1
SATCLC	7.1
TIDAL	8.8
SQUANT	5.1, 5.2
STAINF	11.3
START	9.2
SUMMARY	11.2
SUNGRV	8.4
SURDEN	8.2, 8.3.2.1, 8.3.2.4
SYMINV	10.2
TDIF	5.3.1
TRUEP	5.4
TWOSTA	6.4.1, 6.4.2, 6.5, 6.6, 6.7, 7.7
TYPOBB	11.2
UPDOWN	7.7
VCONV	5.1
VEVAL	5.1, 8.2, 8.3.1, 8.4, 8.5, 8.6, 8.7.5
XFFIX	3.4, 6.3

SUBROUTINE

SECTION

XINERT

3.4

YEFIX

3.4, 6.3

YINEPT

3.4